THE SYNTHESIS OF SOME NATURAL PRODUCTS OF MEDICINAL VALUE USING ORGANOMETALLIC COMPLEXES

BY

TUNMISE TUNRAYO ADEBESIN
B.Sc. Chemical Sciences (ABEOKUTA), M.Sc. Inorganic Chemistry (IBADAN)
MATRIC. No.: 118658

A Thesis in the Department of Chemistry,
Submitted to the Faculty of Science
in partial fulfillment of the requirements for the Degree of

DOCTOR OF PHILOSOPHY

of the

UNIVERSITY OF IBADAN

MARCH 2015

ABSTRACT

The challenge of accomplishing C-C bond formation while protecting sensitive functional groups and overcoming problems of stereo-control has led to the use of transition-metal organometallic compounds in organic compounds synthesis. Nucleophilic additions to cationic dienyliron carbonyl complexes provide a convenient means of C-C bond formation. It is highly regioselective and stereospecific making it useful for the synthesis of natural products and compounds with biological activities. Previous research showed the use of synthetic ligands as nucleophiles but none has used naturally isolated compounds. Therefore, this study was designed to synthesise and characterise new natural products through demetallation of adducts with selected natural products isolated from medicinal plants as nucleophiles. Additionally, to investigate the antimicrobial and electronic properties of these compounds.

The reaction of parent dienylium cations ([1-5-η-(dienyl)Fe$(CO)_3$]BF_4(Dienyl = C_6H_7,2-$MeOC_6H_6$)) with selected natural products were synthesised and their eight adducts were purified using standard procedure. The existing natural products: gedunin, khivorin, polyavolensinol and 7-ketokhivorin were used as nucleophiles. The resulting complexes were demetallated to obtain new products. The synthesised compounds were characterised using Infrared (IR), Nuclear Magnetic Resonance (NMR) and Mass Spectroscopic (MS) techniques. The energy band gap (ΔE) was calculated at Density Functional Theory (DFT) level using hybrid Beckie-3-Lee Yang Parr (B3LYP) functional density with 6-31G (d) and pseudo potential basis sets in gaseous state. The adducts, ligands and the demetallated products were also screened from 2.5 to 405 mg/mL for antimicrobial properties using the disc diffusion method against *Bacillus cereus* ATTC 14579, *Bacillus subtilis* ATTC 33923, *Proteus mirabilis* ATTC 21784, *Salmonella typhi* ATTC 14028 and *Candida albican* MTTC 227. The Minimum Inhibitory Concentrations (MICs) were determined by agar dilution method.

The reaction of dienylium cations with the natural products yielded the corresponding 1,3-diene substituted derivatives. The adducts exhibited strong and intense IR √(CO) bands at 2050 and 1975 cm^{-1} which are characteristic absorptions of neutral tricarbonyl(1,3-diene-substituted) iron derivatives. The complete disappearance of these bands in all the demetallated products confirmed cleavage of the iron tricarbonyl moiety. The ^{1}HNMR spectra of all the products showed overlapping characteristic resonances of the outer and

inner 1,3-diene protons. All the natural products attacked the dienylium cations at $C^{5'}$ via the α-furan and β-indole carbon fragments in their structures. The loss of αβ-unsaturated ketone fragment at m/z 151($C_{10}H_{15}O$) was responsible for the expected absence of the parent peaks in the MS data. There was also loss of M-173 fragment in all the compounds indicating the weakness of the C(diene)-C(natural products) bond and the calculated energy band gap (ΔE) indicated the reactivities of the compounds. The zones of inhibition of the demetallated compounds ranged from 7.5 to 22.5 mm while that of the ligands ranged from 8.0 to 12.5 mm. The adducts show no activity. The MIC values ranged from 0.01 to 29.17 mg/mL.

The demetallation of adducts from nucleophilic addition to dienylium cations provided a convenient method of achieving C-C bond formation and this enabled the synthesis of structurally complex natural products of biological importance. The synthesised compounds could serve as leads in drug development.

Keywords: Dienylium cations, Demetallated adducts, Molecular orbital

Word counts: 496

ACKNOWLEDGEMENTS

My sincere thanks go to my supervisor, Professor T. I. Odiaka for being a father and a mentor. I appreciate you sir for your understanding when the going gets tough and for being there. Thank you for your interest in my intellectual development and for letting me learn from your experience which represent high quality inputs to this work and for believing in me by bringing me into academics to realise my dream of impacting knowledge to others.

I thank the Head of Department of Chemistry- Professor A. A. Adesomoju and the past Heads for the research facilities and support provided during this study. My special gratitude goes to the former Head of Department- Professor O.Osibanjo for his priceless counsel and words of encouragements. My appreciation goes to my Lecturers and colleagues in Inorganic unit, Professor J. A. O Woods for his useful suggestion and kindness, Dr. Aderoju Osowole for the enlightment and useful discussions we had, thank you for teaching me. To my colleagues in the Inorganic Chemistry unit, Dr. Helen Omoregie, Dr. Odola of blessed memory for I will remember you for your kindness, Dr. Temitope Olalekan, Mr. Austin Ozukwe and Dr. Funmi Adekunle for her good nature.

I gratefully acknowledge the MacArthur Foundation for providing fund for the research work. Professor Paul O'brien of the School of Chemistry, University of Manchester, United Kingdom for being my host in the course of my work there. Also for the wonderful people I met there especially Mr. Dayo Oyetunde who taught me how to use most of the equipment, Sister Khadijat for her help and Mr Fred Ajayi for providing me with a good accommodation. I also thank Martins and Dr. Richard Taylor for their friendship.

Special thanks go to Dr. I. A. Oladosu for being there always; he never complained of my incessant presence in his office and has been a good encourager. Thank you sir for your immense contributions and collaborative effort. To Dr. N. Obi-egbedi, I say a big thank you sir for helping out in the computational aspects of this work with great tenacity. I am indebted to you for your kindness and understanding. I acknowledge the assistance of Professor O. Ekundayo, Professor R. A. Oderinde, Professor Adeoye, Professor K. O. Adebowale and Professor E. K Adesogan whom I call Baba. I thank you all for everything. I also appreciate the effort of Dr.Olapeju Aiyelaagbe for her motherly care, thank you ma.

I also thank Professor Toyin Arowolo specially for his care and fatherly love. Thank you sir for your interest and contribution to my life and career and also for believing in me. I

appreciate Professor Adedire, thank you sir for providing help when it was needed. Many thanks go to my pastors: Pastor K. L. Osota for unwavering support, kindness and prayers, Pastor Awofisayo for your love and consistent prayers, Pastor Oladipupo Ayodele for his care and prayers as well Pastor Abiodun and Pastor Odewole for their godly contribution.

To all my friends and colleagues: Dr. N. W. Odozi for her word of encouragement and support, Dr. Abimbola Olatunde for her goodness and kind-heartedness, Dr.O. Olaoluwa, Dr. Kehinde Awokoya for their understanding and encouragement, Dr. Tobi Oluwafemi, thanks for being a good and wonderful friend who cares, Mrs. Odunayo Odule, Dr. Dorcas Moronkola, Dr. G. K. Oloyede, Dr. S. A. Aboaba, Prof. Dayo Olu-Owolabi, Dr. A. H. Alabi, Dr. I. A. Ajayi, Dr. A. A. Adeyi and Dr. Funmilola Ayeni thanks for your useful advice and suggestion and to Barrister Fadare Ademola, I say a big thank you for been there. Also to Dr. Balogun, Dr. Ogundajo, Mr. Abdurazak, Mr. Godwin, Mr. Emmanuel, Dr. Oladimeji, Mr. Toyin, Mr. Adoghe, Mrs. Aderinokun, Mr. Ologun and sister Fatima, I thank you all. It is a pleasure relating with you all. To all my students both undergraduate and postgraduate I say a big thank you.

My sincere, hearty and unalloyed gratitude goes to my only sister Adebesin Kemi. You are special, thanks for your love, support and prayers through these ages. I also thank my mother in-law, Mrs. Sylvester Osoikhia who has been a mother to me.

My devout appreciation goes to my priceless crown, my husband who stood by me. Your patience and confidence keep me focused. You are a friend and will remain constant in my life. Our friendship and admiration for each other has continued to be transcribed and our love will forever be transmitted. Thank you dearest.

I appreciate my lovely daughter Isabella Eugene-Osoikhia. You are a priceless gift and treasure. Thanks for coming when you did and for your understanding of my inadequacies as a mother during this research work. I say thank you. You always make my time with you joyous, enlightening and entertaining.

To my late parents Mr and Mrs James Adebesin, I say a big thank you for serving as vehicles that brought me to life. May your souls rest in perfect peace.

Finally and above all, I am eternally grateful to God Almighty who is the source of all wisdom. You have always been with me Lord and have seen me through thick and thin of life. Thank you for giving me strength, good health, wisdom, understanding, knowledge, favour and help for the absolute success of this programme. You are the Great God and I give you all the glory associated with this programme.

To all of you who have touched my life in one way or the other I say thank you.

CERTIFICATION

I certify that this work was carried out by Tunmise Tunrayo **ADEBESIN** in the Department of Chemistry, University of Ibadan.

.....

Supervisor
T. I. Odiaka
B.Sc., Ph.D. (Wales)., C.Chem., M.R.S.C (London), FICCON.
Professor, Department of Chemistry,
University of Ibadan, Nigeria.

DEDICATION

I dedicate this work to the Almighty God who has been my Everything, Helper, Sustainer and the Lifter of my head. Thank you Lord. This is your doing and it is marvelous in my sight.

ABBREVIATIONS

√	Frequency of absorption
Py	Pyridine
ppm	Parts per million
MeO	Methoxy group
CO	Carbon monoxide or Carbon (II) oxide
BF_4^-	Tetrafluoroborate ion
η	Hapticity of the organic group (Eta)
Me_3NO	Trimethylamine-N-oxide
IR	Infrared
NMR	Nuclear Magnetic Resonance
F.D	Field Desorption
E.I	Electron impact
M.S	Mass Spectrometry
MIC	Minimum Inhibitory Concentration
HOMO	Highest Occupied Molecular Orbital
LUMO	Lowest unoccupied Molecular Orbital
INDO	Intermediate Neglect of Differential Overlap
S_N^1	Unimolecular Nucleophilic Substitution
S_N^2	Bimolecular Nucleophilic Substitution
UV	Ultraviolet
Nu	Nucleophile
k_{obs}	Pseudo-first-order rate constant
INT	Intermediate
DIBAH	Diisobutylaluminium hydride
DFT	Density Functional Theory
QSAR	Quantitative Structure-Activity Relationship
Log P	Partition coefficient

TABLE OF CONTENTS

LIST OF FIGURES

LIST OF TABLES

CHAPTER ONE

INTRODUCTION

1.1 Tricarbonyl (dienylium) iron cations

In 1930, Reihlen and co-workers prepared tricarbonyl (1-4-η-butadiene) iron, the first iron-diene complex (Rheilen *et al.*, 1930). The first complex of a cylic diene, tricarbonyl (1-4-η-cyclohexadiene) iron (1) was synthesised by Pauson and his group (Hallam and Pauson, 1958) by the reaction of cyclohexa-1,4-diene with pentacarbonyliron. Hydride abstraction from (1) using triphenyl methyl tetra fluoroborate yields quantitatively tricarbonyl (1-5-η-cyclohexadienylium) iron tetrafluoroborate (2) (Fischer and Fischer, 1960) as represented below. The hydride abstraction was facilitated by the presence of the metal carbonyl moiety to give the dienylium iron cations with useful electrophilic properties. This discovery by Fischer and Fischer in 1960 was a breakthrough in view of the application of these transition metal complexes in synthetic organic chemistry.

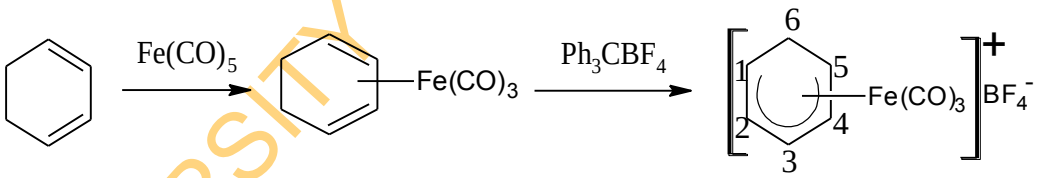

(1) (2)

The metal-stabilised cations obtained by hydride abstraction (2) are stable enough to be isolated, analysed and stored for a long period of time if protected from light and moisture (Bromfield *et al.*, 2009). They are highly reactive towards a wide variety of nucleophiles to form C-C and C-heteroatom bonds. The reaction of these cations is completely stereospecific and regioselective.

The 2-methoxy derivative (3) and 1-methoxy derivative (4) were also made available from methoxybenzenes (Birch, 1950). The presence of methoxy substituent introduces further possibilities of synthetic use.

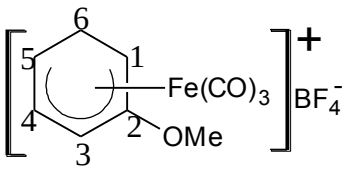

(3)

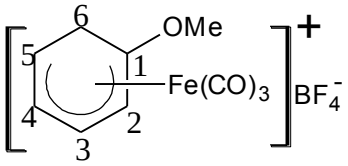

(4)

1.2 Regioselective and Stereospecific nature of the reactions of tricarbonyl dienylium iron cations.

The substitution pattern of the cyclohexadienyl ring will direct the position for nucleophilic attack due to the electronic influence of the groups attached to the cyclic scaffold. An electron donating substituent or group will favour the cationic complex (5), while an electron withdrawing group will show preference for the formation of (6) or (7). This has been aptly summarized by Pearson (Pearson, 1994) and the reason behind this selectivity has been explained by Eisenstein, Butler and Pearson following theoretical studies on these complexes (Eisenstein *et al*., 1984). They showed that stronger HOMO-LUMO interactions between the orbitals of iron and that of the dienyl cation were obtained in certain cases due to a better energy match, resulting in the region-chemical outcome displayed below.

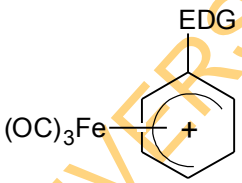

(5)

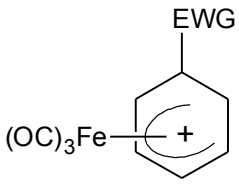

(6)

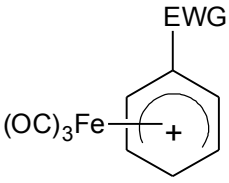

(7)

The nucleophilic attack itself occurs at the terminal position of the delocalized cation i.e the π system and stereopecific on the face opposite to the coordinated iron carbonyl moiety. The bulky tricarbonyliron moiety acts as a stereodirecting group and enforces the incoming nucleophiles on the face opposite to the iron (anti selectivity). The stereospecificity of this reaction will be useful for generating optically active organic compounds, since a number of substituted dienylcomplexes can now be

prepared in optically active form. Moreover, labile diene systems can be protected by the complexation to the tricarbonyliron group because of the pronounced modification of the reactivity of the organic ligand in the coordination sphere of the transition metal (Knolker, 1992).

1.3 Nucleophilic addition to tricarbonyl dienylium iron cations

Metal carbonyl stabilized cationic species (2), despite their stability, are highly reactive towards nucleophiles (Knolker, 1999). The reactivity of the methoxy derivatives with nucleophiles is lower (John and Kane-Maguire, 1979a) compared to that of the unsubstituted dienylium iron cations. This lower reactivity of the methoxy derivatives is in accordance with the mesomeric influence of the methoxide group which has been shown from INDO molecular orbital calculation to decrease the positive charge on the dienyl C^5, the site of nucleophilic attack (Clack *et al*., 1976a).

Leon Kane-Maguire was the first to show that nucleophilic attack on cation (2) can be accomplished with electron-rich heteroaromatic systems such as indole, pyrrole, imidazole, furan, and thiophene (Kane-Maguire and Mansfield, 1973, 1976) as well as with donor-substituted aryl derivatives (Mansfield *et al.*, 1974). Based on this reactivity, cation (3) may be considered as a mild electrophile for aromatic substitution. Tricarbonyl dienylium iron cations react with a wide range of nucleophiles such as: heteroatoms and carbon nucleophiles. Examples of the heteroatoms include: alkoxides, amines, phosphines, and phosphites. Carbon nucleophiles include electron rich aromatics such as malonates, sily enol ethers, tin enolates, enamines, amides, allyl silanes, nitromethane anions, cyanides, and various highly activated carbon species such as diakyl cadmium, and diakyl zinc reagents. Hydride can also be used as a nucleophile in form of sodium borohydride, but it is of less synthetic interest.

However, the synthetic utility of $[(1\text{-}5\text{-}\eta\text{-}(dienyl)Fe(CO)_3]BF_4$(dienyl = C_6H_7 or 2-$MeOC_6H_6$) can also be extended to naturally occurring nucleophiles such as alkaloids, terpenoids, steroids etc bearing in mind that careful treatment of the adducts formed from this nucleophilic addition with appropriate oxidising agents such as Me_3NO leads to cleavage of the tricarbonyl iron moiety, giving rise to new organic derivatives which are otherwise inaccessible by conventional organic techniques. There is no report in the literature on nucleophilic addition of dienylium cations to

natural products except for the work of Odiaka *et al* (Odiaka and Okogun 1985; Odiaka *et al.,* 2007). This work explored the reaction of natural products such as gedunin, khivorin, 7-ketokhivorin and polyavolensinol with the dienylium iron cations (2) and (3) to form new natural product organometallics.

1.3.1 Gedunin as nucleophile towards dienylium iron cations

Gedunin (8) is a tetranortriterpenoid and an active constituent of *Azadirachta indica* A. Juss and *Melia azedarach* (L. Meliaceae) (Akinsanya *et al*., 1961; Khalid *et al*., 1989). It shows a moderate in vitro antimalaria activity against chloroquine resistant *Plasmodium falciparum* (Bray *et al*., 1990) and antifungal properties (Sundarasivarao *et al*., 1977). It also inhibits ovarian cancer cell proliferation (Kamath *et al.,* 2009).

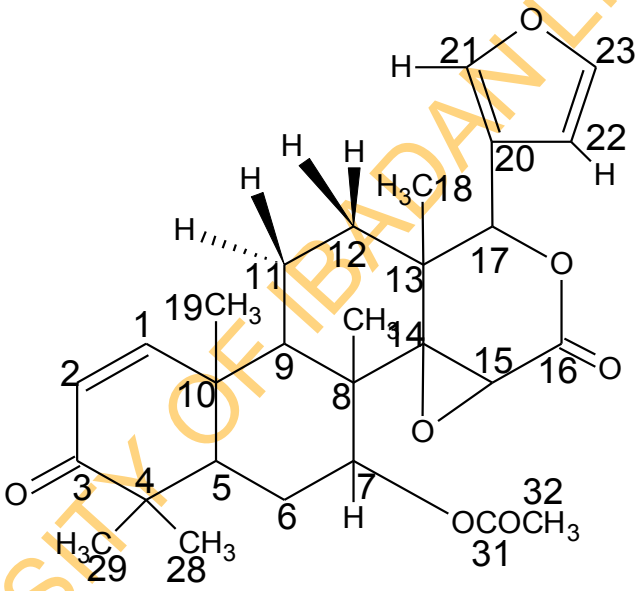

(8)

1.3.2 Khivorin as nucleophile towards dienylium iron cations

Khivorin (9) is also a tetranortriterpenoid isolated from *Khaya ivorensis* (Bevan *et al*., 1962) and possesses a very potent insect antifeedant property (Govindachari and Kumari, 1998). Biogenetically, gedunin is derived from khivorin (Lakshmi and Gupta, 2008).

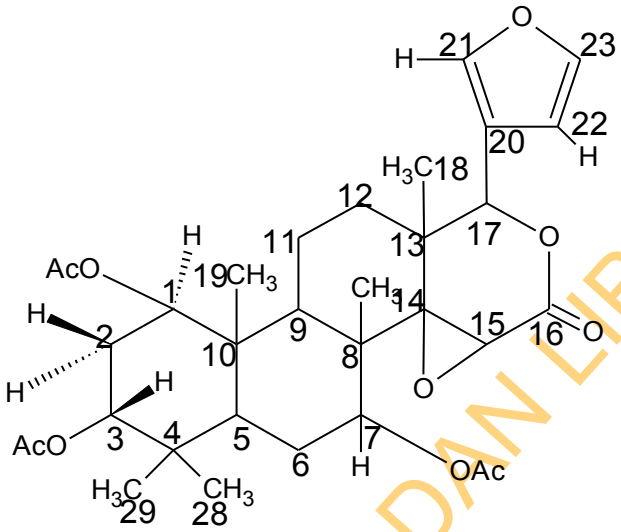

(9)

1.3.3 7-ketokhivorin as nucleophile towards dienylium iron cations

7-ketokhivorin **(**10**)** is derived from khivorin. It is a tetranortriterpenoid isolated from *Khaya ivorensis* (Bevan *et al*., 1962). It also has strong insect antifeedant property (Govindachari and Kumari, 1998).

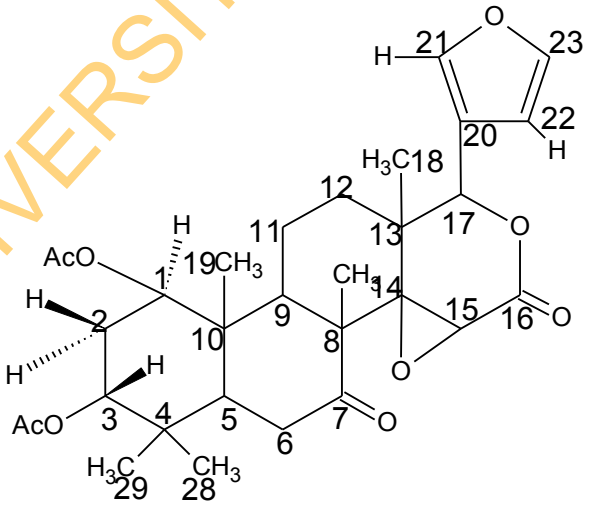

(10)

1.3.4 Polyavolnesinol as nucleophile towards dienylium iron cations

Polyavolensinol (11) is an alkaloid obtained from the stem of *Polyathia suaveolens* (Falshaw *et al*., 1982) a medicinal tree grown in western part of Nigeria and used for treating blackwater fever and stomach disorder (Okorie, 1980, 1981).

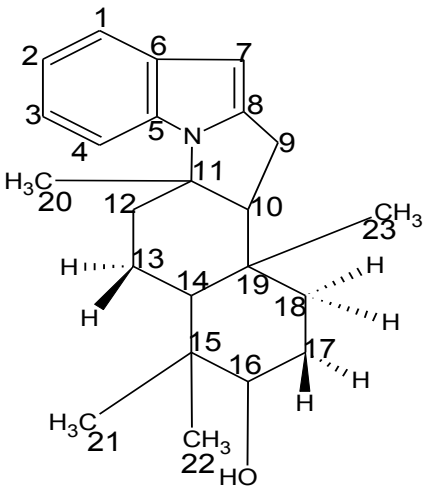

(11)

1.4 Nucleophilic addition to tricarbonyl dienylium iron cations

Nucleophilic attack on cyclohexadienyl transition metal cationic complexes may result in addition to the coordinated organic ligand (Hashimi *et al.*, 1967; Birch *et al.*, 1968, 1979), at the metal (Dauben and Bertelli, 1961), or at the carbonyl group (Cowles *et al.*, 1969). It is a type of S_N1 reaction mechanism which involves the formation of carbonium ion, in this case, dienylium cation followed by the subsequent reaction with the nucleophiles. The site of attack depends on the nucleophile employed. Attack can occur at the organic ring (dienyl ring) to give the ring addition products as given below

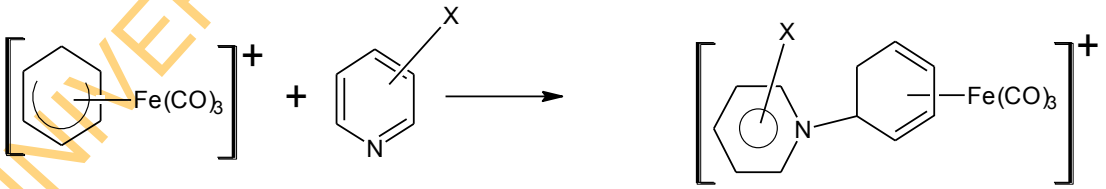

or at the metal to give the carbonyl-displaced product as shown below

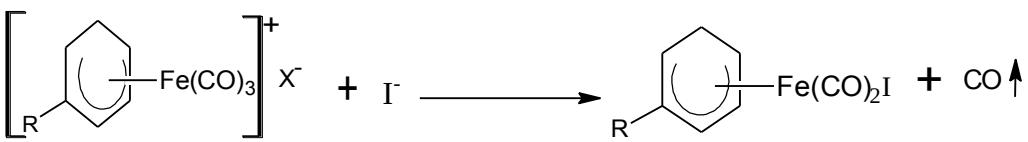

Also, attack at the carbonyl carbon can give the acyl derivative as represented thus

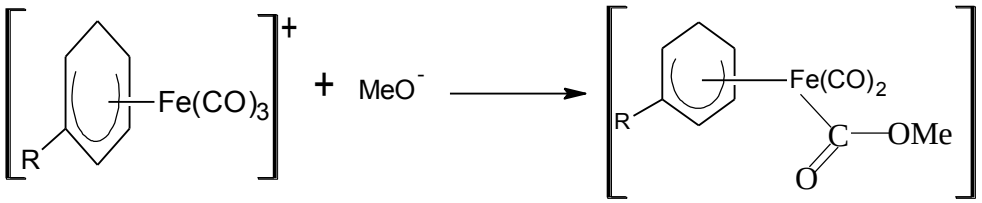

The nature of the product formed will depend on the nature of the organic ring, the metal, the nature of the nucleophile and the solvent used.

1.5 Factors affecting nucleophilic addition to dienylium iron cations

The kinetic result obtained by Odiaka and Kane-Maguire (Odiaka and Kane-Manguire, 1981) on the formation of pyridinium adducts with co-ordinated π-hydrocarbons provide the first quantitative information on the importance of basicity and steric properties in controlling amine nucleophilicity towards co-ordinated π-hydrocarbons. Additions of various pyridines to dienylium cations reveal a very strong dependence on the basicity of amine. This is demonstrated quantitatively by the linear free energy relationship obtained on plotting $\log_{10}K$ versus pKa of the amine conjugate acid in water. Thus, the formation of pyridinium adducts obeys the Bronsted relationship with a slope, (α), of about 1.0. The high slope of 1.0 indicates a very marked dependence of k on nucleophile basicity. However, studies by Hall (Hall, 1957) with other amines indicate that basicities in water and CH_3CN generally show parallel trends.

The high slope contrasts sharply with the very low α values of *ca* 0.05 reported for attack by pyridines (py) and other amines on the very soft Platinium(II) centre in complexes such as trans$[Pt(py)_2Cl_2$ (Cattalini, 1972). Amine attack on moderately soft substrates such as alkyl halides has been reported (Hudson and Loveday, 1962) to give α values of *ca* 0.2. Interestingly, the slope is also somewhat larger than the α values of *ca* 0.5 found for amine addition to free carbonium ion (Ritchie *et al*., 1975). Following the reasoning of Pearson (Pearson *et al*., 1968), these results suggest that the dienyl rings in the $[(\eta^5\text{-dienyl})Fe(CO)_3]^+$ cations (dienyl= C_6H_7,2-$MeOC_6H_6$) are hard species. Assignment of a hard character to the dienyl groups of the dienylium cations is consistent with their frequent representation as stablised carbonium ions, and with the relatively high positive charges calculated (Clack *et al.*, 1976a) to reside

on the ring carbons. A similar strong dependence of k, on nucleophile basicity was also observed for related additions of anilines and phosphines and phosphites to dienylium cations as expected for hard dienyl substrate. Therefore, it can be concluded that reactivity (i.e nucleophilic addition) decreases with decreasing basicity of nucleophiles

Steric effect on nucleophilic addition at dienylium organometallics has been demonstrated using pyridine and its substituted analogues. For example the blocking of the N reaction site by methyl groups caused approximately 10-fold and 10000-fold decrease in rate when compared with the non-sterically hindered pyridines. These results confirm the importance of steric effect in nucleophilic addition (Odiaka and Kane-Maguire, 1981).

The nature of the coordinated organic group also has a dramatic effect on reaction rate. For instance, there is lower reactivity of $[\eta^5\text{-}2\text{-}MeOC_6H_6)Fe(CO)_3]^+$ cation compared with $[\eta^5\text{-}C_6H_7)Fe(CO)_3]^+$ cation towards amines due to the mesomeric influence of the methoxide group present in the former, which has been shown from INDO molecular-orbital calculations to decrease the positive charge on the dienyl C(5) atom, which is the site of nucleophilic addition (Clack *et al*., 1976a, 1976b)

1.6 Bonding in tricarbonyl dienylium iron complexes

A number of treatments with regard to metal- olefin π complexes have evolved from the basic Chatt-Dewar-Duncanson concepts (Chatt and Duncanson, 1953). In particular, the bonding between a transition metal and a conjugated diene, exemplified by the well known tricarbonyl(diene)iron complexes has been treated at a number of levels from simple description in textbook to molecular orbital calculations. All of these treatments involve the donation of electrons from the highest occupied molecular orbital (HOMO) of the diene to the vacant metal d orbitals (or hybrid orbitals) accompanied by a back donation of electrons from a filled metal orbital into the diene lowest unoccupied molecular orbital (LUMO). This should result in a decrease in π-bond order for the terminal C-C bond and an increase for the central C-C bond, compared to the uncomplexed diene and this is confirmed by the growing amount of X-ray crystal structure data where it is found that the central bond is slightly shorter than the terminal bonds (Kruger *et al*., 1977). This is further supported by numerous infra red studies showing a general decrease in the olefin stretching frequency on coordination to the metal centre. The mutual assistance between the π-

orbitals of the olefin and the metal t_2g orbital is known as synergic effect and the result is a decrease or shift of the coordinated C-C infra red band to lower wave number compared to the free C-C band.

1.7 Kinetics and Mechanisms of nucleophilic addition to tricarbonyl iron dienylium cations

Mechanisms of reactions can be derived from detailed kinetic studies. The kinetics give information on the rate at which a reaction will occur while the mechanism describes the various stages that may be encountered before the product is formed.

For fast reaction kinetic runs, this is studied under pseudo-first-order conditions. For a very slow reaction, the kinetics can be monitored using the infrared spectrophotometer or ultraviolet spectrophotometer.

1.7.1 Pseudo-first-order rate runs

The concentration of the organometallic compound is kept constant throughout the kinetic study, while the nucleophile concentration is varied, the least being ten times greater than that of the organometallic complex. A UV study must be carried out to obtain the wavelength of maximum absorption for the reacting species as the product is formed. The least concentrated nucleophile solution is first run over a long wavelength range. This is then followed by the running the solution containing a mixture of the complex and the nucleophile over the same wavelength range to obtain the maximum wavelength of absorption. Then, a plot of absorbance against time is obtained to produce a curve from which a plot of $\log A_t$ versus time (secs) affords the pseudo-first-order rate constant, k_1. From the k_{obs} values obtained for each concentration of nucleophile, an average value is determined for accuracy. The k_{obs} values are plotted against the various concentrations of nucleophile and from this plot, a rate law is obtained and consequently a reaction mechanism is proposed.

If the plot of k_{obs} versus [Nu] gives a straight line which passes through the origin, then slope of the graph is k_1 ($mol^{-1}dm^3s^{-1}$). This suggests that the reaction is irreversible and thus proceeds to completion. A proposed mechanism will be direct addition of the nucleophile on the organometallic complex to form the product in an irreversible manner.

$$\text{Complex} + \text{Nucleophile} \xrightarrow{k_1} \text{Product}$$

When the plot of k_{obs} versus [Nu] gives a straight line with a non –zero intercept (k_{-1}), then k_{-1} is the pseudo-first-order rate constant for the dissociation of the nucleophile from the product to form the starting reacting species. It indicates reversibility of the reaction and consequently the determination of an equilibrium constant from $K_{eqm} = k_1/k_{-1}$. The proposed mechanism is given as:

$$[\text{Complex}] + [\text{Nu}] \underset{k_{-1}}{\overset{k_1}{\rightleftharpoons}} \text{Product}$$

1.7.2 Equimolar rate runs

The concentration of the complex and the nucleophile must be the same. The wavelength of absorption is determined and a stopped-flow study carried out at this wavelength for a fast reaction. The rate expression is given thus: $x/a(a-x) = kt$ where a is the initial concentration of the complex, and x is the concentration of the product at time t. k is the second order rate constantfor the addition of the nucleophile to the complex to form the product. Only second order rate constant, k, can be obtained from an equimolar reaction.

1.7.3 Pre equilibrium mechanism

This assumes the instantaneous formation of an intermediate followed by a slow rate-determining step (k_2), leading to the formation of the product

$$[\text{Complex}] + [\text{Nu}] \underset{\text{fast}}{\overset{k_1}{\rightleftharpoons}} [\text{INT}] \xrightarrow[[\text{Nu}]]{k_2} \text{Product}$$

The pre-equilibrium constant for intermediate formation is given by

$$k_1 = \frac{\text{INT}}{[\text{Complex}][\text{Nu}]}$$

The general rate expression for a pre-equilibrium mechanism is given

$$k_{obs} = \frac{k_2 k_1 [Nu]^2}{1+k_1[Nu]}$$

1.7.4 Steady state mechanism

In the steady state mechanism, we observe the formation of an intermediate whose concentration is nearly zero at any given time. This means that the intermediate disappears as soon as it is formed. The rate of formation of the intermediate is equal to the rate of its disappearance.

Experimentally, we followed the disappearance of both [complex] and [INT] and the final rate of intermediate disappearance is equal to the observed rate of complex disappearance. The general rate expression for a steady state mechanism is given as:

$$k_{obs} = \frac{k_2 k_1 [Nu]^2}{k_{-1}+k_2[Nu]}$$

1.8 Demetallation reaction of dienylium iron adducts

One of the most important applications of organometallics in organic synthesis is the removal of the coordinated metal (iron carbonyl moiety) to afford new organic derivatives. The removal or dislodgement of the metal atom from an organometallic compound is known as demetallation. This can be achieved in the following ways: oxidative, reductive, photolytic and thermolytic methods of demetallation and use of acids or protonic solvents.

1.8.1 Thermolytic method of demetallation

This involves refluxing of the organometallic complex to be decomplexed in an appropriate solvent in the presence or absence of another nucleophile. In some cases, unexpected products are formed. The thermolytic products depend on the nature of the solvent employed in the demetallation process.

For example, in the presence of pyridine as nucleophile and solvent, methoxy benzenechromium tricarbonyl is readily decomplexed to the expected methoxybenzene as shown below (Odiaka, 2004).

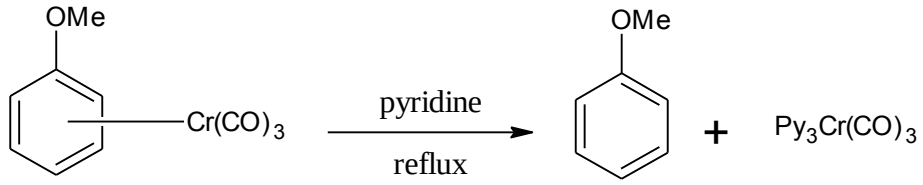

1.8.2 Photolytic method of demetallation

This involves the use of photochemical treatment (hv) of a solution of the organometallic complex in an appropriate solvent. This method is effective in the demetallation of the chromium metal from organometallics. Unexpected products are usually formed with other metals.

1.8.3 Use of acids and protonic solvent

This also involves the gentle refluxing of the organometallic complex under study in an acid which is usually mixed with solvents like water, alcohols, ethers, tetrahydrofuran or dichloromethane. Typical acids used are: HCl, HBr and H_2SO_4. For example, cyclohexadienyl chromium tricarbonyl anions are decomplexed by acid to cyclohexadienes as given below (Odiaka, 2004).

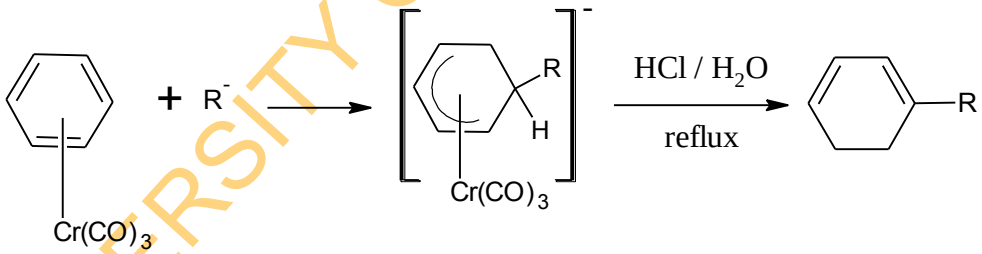

1.8.4 Reductive method of demetallation

In this case, reducing agents are used and these include: H_2/Pd/C, Li/liquid NH_3, organolithium compounds (RLi), di-isobutylaluminium hydride (DIBAH), $NaBH_4$, $LiAlH_4$, Et_3N and H_2. Apart from $NaBH_4$, $LiAlH_4$, Et_3N and H_2 which are active in the decomplexation of palladium complexes, most of the reducing agents in use are active in the decomplexation of chromium complexes.

In most cases, there is a change in the nature of the product formed (Odiaka, 2004) and this can be represented thus:

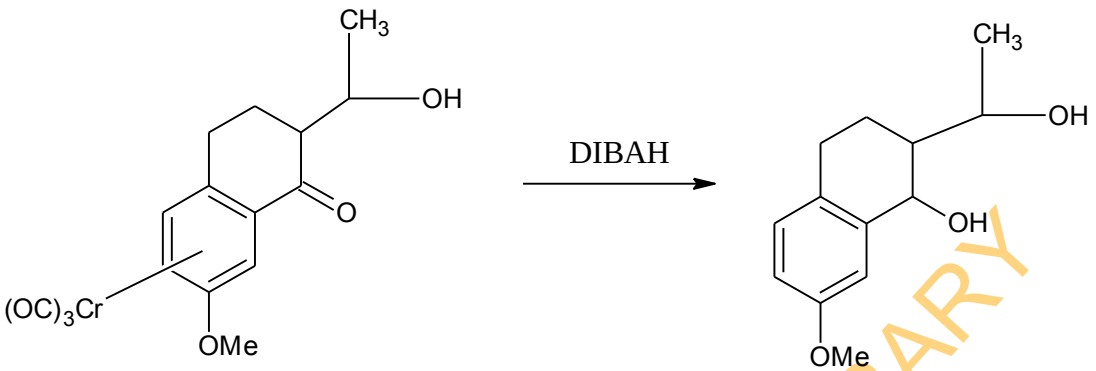

1.8.5 Oxidative method of demetallation

This technique involves the oxidation of the coordinated metal atom usually from its zero oxidation state using $CuCl_2$ (Thompson, 1976), $FeCl_3$ (Emerson *et al.*, 1964), $(NH_4)_2Ce(NO_3)_6$ (Nunn *et al.*, 1988), pyridinium chlorochromate ($C_5H_5NHClCrO_3$) named Collins reagent (Stephenson, 1982) and the ues of amine oxide, trimethylamine- N-oxide (Me_3NO) (Shvo and Hazum, 1974). The latter has been very effective in the removal of the tricarbonyl iron moiety from organometallic adducts.

To achieve its aim, Me_3NO attacks one of the coordinated CO groups on the metal leading to instability of the organometallic adduct and consequently the dislodgement of the coordinated metal as shown below ([1]Odiaka, 1981)

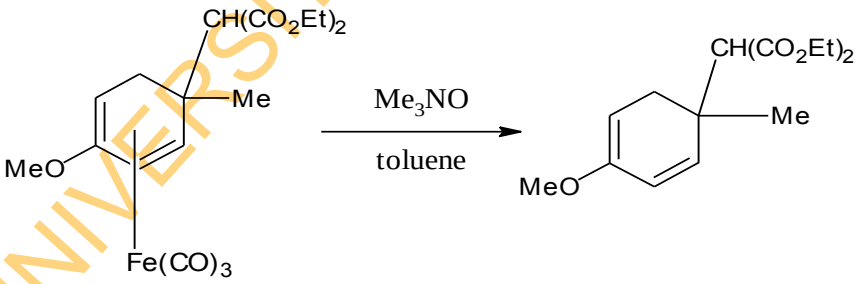

The advantage in the use of Me_3NO is that the reaction conditions are mild and thus compatible with a number of functional groups, although the reaction can take a longer time in some cases.

[1]Odiaka T. I. 1981 Unpublished work

1.9 Aim of the work

Nucleophilic addition to dienylium iron cations provides a convenient means of achieving carbon-carbon bond formation and this enables its application in the synthesis of structurally complex natural products of biological importance.

This work is an extension of the work done by Odiaka *et al* (Odiaka and Okogun, 1985; Odiaka *et al*., 2007) and is designed to synthesise new natural products of biological importance through formation of carbon-carbon bond by the nucleophilic addition of dienylium iron cations 1-5-η-(dienyl)$Fe(CO)_3]BF_4$(Dienyl = C_6H_7, 2-$MeOC_6H_6$) to natural products extracted from Nigerian trees.

1.9.1 Objectives of the work

To synthesise natural products of biological importance through nucleophilic addition of natural products nucleophiles to dienylium iron cations.

To characterise the synthesised compounds using spectroscopic methods

To also investigate the medicinal potential of new compounds synthesised by carrying out antimicrobial studies.

To carry out calculation of the electronic parameters of the synthesised compounds to further explain their reactivities and relate this to their exhibited antimicrobial activities

CHAPTER TWO

LITERATURE REVIEW

2.1 Historical Background

Organometallic compounds are compounds that contain metal-carbon bonds. The first organometallic compound K[Pt (C_2H_4) Cl_3].H_2O was prepared by a German Chemist, Ziese, in 1827 (Love *et al.*, 1975). This was followed by the discovery of the metal carbonyls: $Ni(CO)_4$ (Mond *et al.*, 1890) and $Fe(CO)_5$ (Mond *et al.*, 1891). The first complex of cyclic diene (tricarbonyl (η4-cyclohexadiene) iron was synthesized by Hallam and Pauson (Hallam and Pauson, 1958). The hydride abstraction of the cyclohexadiene was done by Fischer and Fischer in 1960 to give tricarbonyl (cyclohexadienylium) iron cation (Fischer and Fischer, 1960). This discovery by Fischer gave a breakthrough for the use of this cation in organic synthesis.

2.2 Review of nucleophilic addition to tricarbonyl dienylium iron cations

2.2.1 Nucleophilic addition of pyridine and its derivatives to dienylium iron cations

Nucleophilic addition of pyridines and its derivatives in acetonitrile (Odiaka and Kane-Maguire, 1981) to cations [1-5-η-(dienyl)$Fe(CO)_3$]BF_4(dienyl = C_6H_7, 2-$MeOC_6H_6$ or C_7H_9) gave the corresponding cationic tricarbonyl(cyclohexa-1,3-diene) substituted products. The addition of pyridine and its derivatives to the dienyl fragment to give the pyridinium adducts is represented thus:

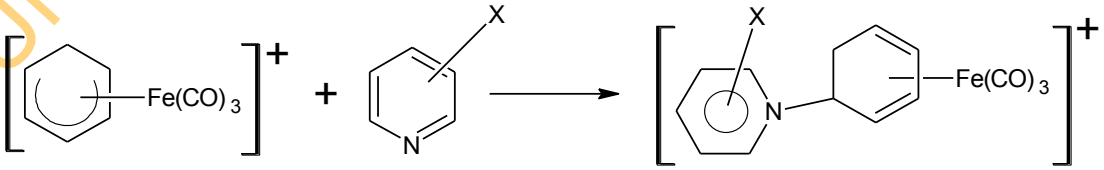

X=H, 2-Me, 3-Me, 4-Me, 2-Cl, 2,6-Me_2 etc **pyridinium adduct**

2.2.2 Nucleophilic addition of anilne and its derivatives to dienylium iron cations

Nucleophilic addition to the dienyl ring of [1-5-η-(C_6H_7)Fe(CO)$_3$]BF_4 by aniline and its derivatives has been reported (Kane-Maguire *et al.*, 1981a, 1981b) to give neutral substituted diene products of the type (1,4-η-5-exo-N-anilinocyclohexa-1,3-diene) tricarbonyliron as shown below. Similar reaction was described with acyclic dienyl cations (Maglio *et al.*, 1971; Maglio and Rosario, 1974). These contrast with the behavior of the analogous cyclopentadienyl complex, [(η-C_5H_5)Fe(CO)$_3$] where nucleophile attack occurs on a carbonyl ligand to give the carboxamido products (Busetto and Angelici, 1968).

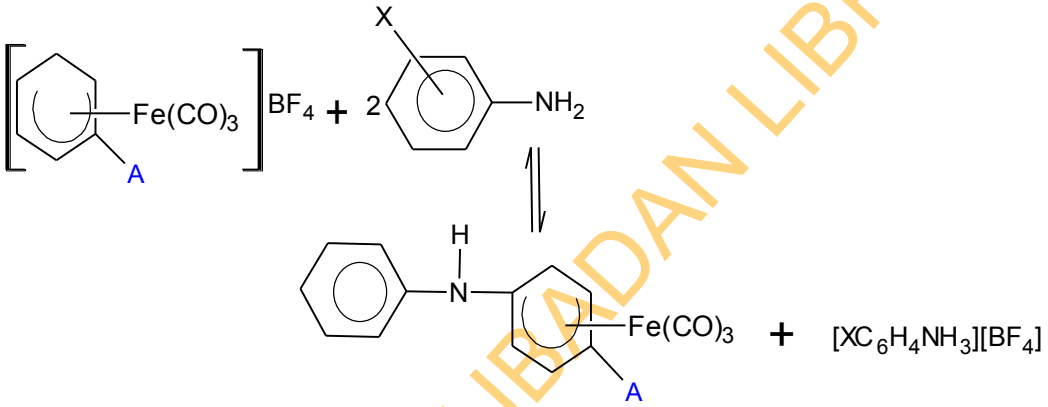

Kinetic results are consistent with direct addition of these nucleophiles to the C^5 atom of the dienyl rings. Similarly, 1,3-diene substituted products are formed from attack on dienylium cations by: N-dimethylaniline (Odiaka and Kane-Maguire, 1979). aryltrimethyl-silanes and stannanes (John *et al.*, 1983), phosphorus nucleophiles (John and Kane-Maguire, 1979b; Birney *et al.*, 1978), β-diketones (Mansfield and Kane-Maguire, 1976), aromatic heterocycles (John *et al.*, 1977) and benzamides (Odiaka and Okogun, 1985; Odiaka and Kane-Maguire, 1985). With alkoxide (Brown *et al.*, 1982), and hydroxide (Atton *et al.*, 1983) as nucleophiles, the kinetically favoured site for initial attack has been shown to be a carbonyl ligand, and under appropriate conditions [(η5-dienyl)Fe(CO)$_2$(COOR)] (R= H, Me, Et) species have been isolated as initial products. These rapid carbonyl additions are reversible and occur at longer reaction times.

2.2.3 Nucleophilic addition of iodide ion to dienylium iron cations

Nucleophilic addition to a carbonyl ligand has been shown to compete with attack at the metal or dienyl ring. In the reactions of $[(\eta^5\text{-}C_6H_7)Fe(CO)_3]^+$ with iodide ion in nitromethane or acetone as solvent, the acyl iodide complex $[(1\text{-}5\text{-}\eta\text{-}C_6H_7)Fe(CO)_2(COI)]^+$ is formed as a major product and some ring adduct, $[(1\text{-}4\text{-}\eta\text{-}IC_6H_7)Fe(CO)_3]$ (John *et al.*, 1986). However, investigation also showed the formation of $[(\eta^5\text{-}C_6H_7)Fe(CO)_2I]^+$ (Siu *et al.*, 1998). Thus, the reaction of I^- ion with $[(1\text{-}5\text{-}\eta\text{-dienyl})Fe(CO)_3]^+$ (dienyl = C_6H_7, 2-$MeOC_6H_6$ or C_7H_9) cations provide a rare example exhibiting each of the possible pathways for attack on a $[(\pi\text{-hydrocarbon})M(CO)_3]^+$ as represented below.

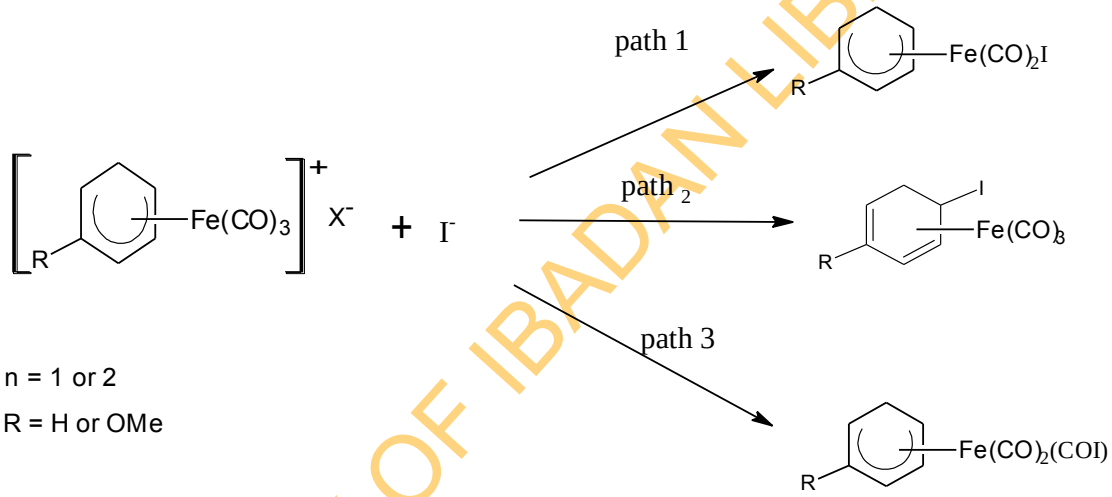

The ratio of the three types of products was found to vary significantly with the nature of the solvent and the dienyl substrate but relatively insensitive to the nature of the iodide salt used. As the solvent changed from nitromethane to acetonitrile to acetone, the ring adduct was the major product. The previously reported carbonyl displaced complex was only a minor product in each case. Acyl iodide product occurred in nitromethane but absent when acetonitrile was used as solvent (Siu *et al.*, 1998) Proportion of the ring adduct decreases down the series C_6H_7>2-$MeOC_6H_6$>>C_7H_9

2.2.4 Nucleophilic addition of tertiary phosphines and phosphites to dienylium iron cations

The reaction of tertiary phosphines and phosphites with dienyl complexes: $[(C_6H_7)Fe(CO)_3][BF_4]$ and $[(2\text{-}MeOC_6H_6)Fe(CO)_3][BF_4]$ provide a general route to phosphonium adducts of the type $[(C_6H_7.PR_3)Fe(CO)_3][BF_4]$ where R=Ph, p-toly, OPh) as well as that of analogous tertiary phosphites. Rate and activation parameters indicate direct addition at the dienyl rings (John and Kane-Maguire, 1979a; Evans *et al.*, 1973; Odiaka, 1985b) as shown thus:

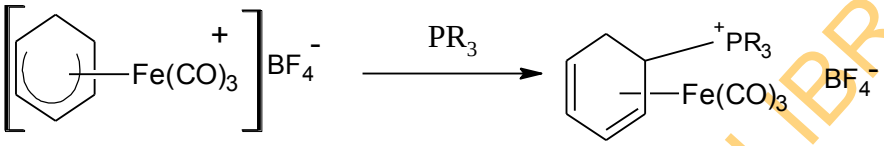

2.2.5 Nucleophilic addition of imidazole to dienylium iron cations

Reaction of imidazole with dienyl iron complexes proceed in two stages giving first the cationic adducts and subsequent deprotonation of the pyrrolic ring nitrogen by excess imidazole, yielding the neutral counterpart. The rate law support direct attack at the dienyl fragment. For attack on C_6H_7 cation, imidazole is about twice as reactive as pyridine as expected from its greater basicity. However, this nucleophilic order is strongly reversed i.e pyridine > imidazole for analoguos attack on $[(2\text{-}MeOC_6H_6)Fe(CO)_3][BF_4]$ (Evans and Kane-Maguire, 1982) This surprising observation suggests some specific rate retarding interaction between the later cation and imidazole such as H-bonding between the imidazole NH and the oxygen of the 2-MeO substituent (Evans and Kane-Maguire, 1982).

2.2.6 Nucleophilic addition of indole and substituted indole to dienylium iron cations

The synthetic utility of cationic organometallic complexes such as $[(C_6H_7)Fe(CO)_3]^+$ as electrophilic reagents towards aromatic substrate such as indole, pyrrole, furan, thiophen and substituted indole have been reported (Kane-maguire and Mansfield, 1973). The reactions can be alternatively regarded as involving nucleophilic addition of the aromatic species to the dienyl cations.

The reaction leads to formation of neutral adducts as given below

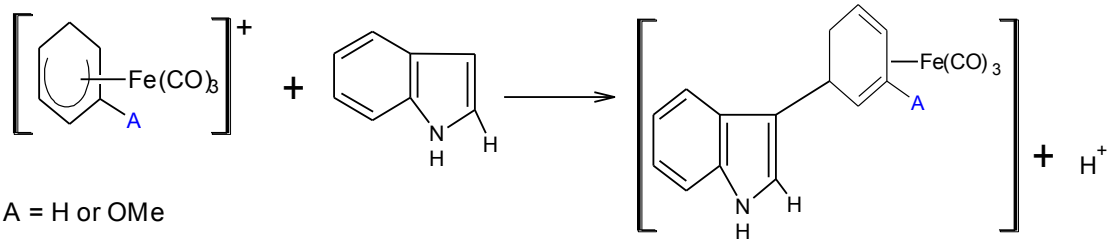

A = H or OMe

The mode of addition of indole gives C- alkylated product for the stereochemistry and support direct electrophilic attack of the dienyl cation at C^3 of indole followed by rapid proton loss (Kane-maguire and Mansfield, 1976). Tetraphenylborate salts of the cations were employed to avoid possible polymerization of the indole substrate by liberated acid during the reaction. Indole is known to be a weak base and also to be converted by acid into dimeric or trimeric species. The tetraphenylborate anion is expected to function as a proton scavenger since it reacts with protons to give benzene and triphenylboron (Cooper and Powell, 1963).

2.2.7 Nucleophilic addition of benzamides and substituted benzamides to dienylium iron cations

X-substituted benzamides (X= H, 2-OH, 4-MeO, 3-MeO, 3,5-$(MeO)_2$, 4-Cl and 2,4-Cl_2) have been shown (Odiaka and Okogun, 1985) to add reversibly to the dienyl rings of the organometallic complex, [1-5-η-(dienyl) $Fe(CO)_3]BF_4$ (dienyl = C_6H_7, 2-$MeOC_6H_6$ or C_7H_9) to give the corresponding cationic tricarbonyl(substituted diene) iron complexes.

2.3 Spectral studies of tricarbonyl dienylium iron cations

2.3.1 Spectra of tricarbonyl (cyclohexadienylium) iron cations

The reaction of cyclohexa-1,4-diene and iron pentacarbonyl in benzene gave a neutral tricarbonyl(cyclohexadiene) iron. This is diamagnetic yellow oil which exhibits strong IR √(CO) bands at 2030-2050 cm^{-1} and 1960-1975cm^{-1}(Birch *et al*., 1968) , but this was given as 2030-2060 cm^{-1} and 1965-1990 cm^{-1} (Odiaka and Kane-Maguire, 1981). The abstraction of a proton from the neutral diene by triphenyl methyltetra fluoroborate gave tricarbonyl(cyclohexadienyl) iron cation **2**, a diamagnetic cation with a characteristic IR √(CO) band at 2100-2120 cm^{-1} and 2040-2070 cm^{-1} (Birch *et al*., 1968) and at 2100-2120 cm^{-1}, 2060-2065 cm^{-1} (Odiaka and Kane-Maguire, 1981). These bands are at higher frequencies than those observed in the neutral diene

counterpart and this is attributed to the presence of positive charge on the dienylium iron cations whose overall effect is to lower back-bonding between the metal and the carbonyl group. The reaction of the dienylium iron cations with most nucleophiles results in the formation of the neutral tricarbonyl (cyclohexadiene) products.

The ^{1}Hnmr data for tricarbonyl (cyclohexadienyl) iron cation **2** showed the different signals as: δ ppm 4.27(1H, t, H^{1}), 5.82(1H, t, H^{2}), 7.22(1H, t, H^{3}), 5.82(1H, t, H^{4}), 4.27(1H, t, H^{5}), 2.57(2H, q, H^{6}) (Birch *et al*., 1968). The quoted values were converted from τ (torr) to δ (chemical shifts in ppm). A comparison of the spectra of the free dienes shows that the inner protons are virtually unchanged from that of the free dienes while the outer protons are moved up to the methylenic region. Methyl protons attached to the inner carbon atoms are deshielded by about 9.5 ppm on complex formation. Methyl protons on the outer carbon atoms are unaffected by complex formation. The methylene protons, H^{6}, appear as an AB quartet (Jones *et al*., 1962). This was interpreted in terms of the non-equivalence of the protons and of the non-coplanarity of the cyclohexadienyl ring.

2.3.2 Spectra of tricarbonyl (2-methoxycyclohexadienylium) iron cations

Tricarbonyl(2-methoxycyclohexadienylium)iron cations have characteristics IR √(CO) bands in chloroform at 2063 and 2000 cm^{-1} and also a strong band at 1663cm^{-1} (Birch *et al*., 1968). ^{1}Hnmr are as follows: δ ppm: 3.90(1H, d, H^{1}), 3.79 (3H, 2, OMe), 6.99(1H, dd, H^{3}), 5.89 (1H, t, H^{4}), 4.22(1H, t, H^{5}), 2.55(2H, q, H^{6}) (Jones *et al*., 1962). There is a close similarity in the ^{1}Hnmr spectral data for tricarbonyl (cyclohexadienyl) iron cations and that of its methoxy derivative only that the methyl protons attached to the inner carbon atoms are deshielded by 9.85 ppm on complex formation compared to the free diene. Similar observation was made for the methylene protons which also appeared as a quartet.

2.4 Spectral studies of natural products used as nucleophiles in this work

2.4.1 Spectral studies of gedunin nucleophile

The IR spectral data for gedunin revealed bands at 1668 cm^{-1}(αβ- unsaturated carbonyl), 1709 (saturated ketone), 1740 cm^{-1}(ester carbonyl); the bands at 875, 1502, and 3150cm^{-1} are characteristic of a β-substituted furan ring. The ^{1}Hnmr in $CDCl_3$ (δ ppm) are: 7.07(1H, d, H^{1}), 5.84(1H, d, H^{2}), 2.12(1H, dd, H^{5}), 1.92(1H, d, H^{6a}), 1.79(1H, t, H^{6b}), 4.52(1H, br, s, H^{7}), 2.46(1H, dd, H^{9}), 2.00(1H, m, H^{11a}), 1.81(1H, m, $H11^{b}$), 1.56(1H, dd, H^{12a}), 1.70(1H, m, H^{12b}), 3.50(1H, s, H^{15}), 5.59(1H, s, H^{17}),

1.22(3H, s, H^{18}), 1.19(3H, s, H^{19}), 7.39(1H, d, H^{21}), 6.31(1H, dd, H^{22}), 7.39(1H, d, H^{23}), 1.03(3H, s, H^{28}), 1.04(3H, s, H^{29}), 1.12(3H, s, H^{30}), 2.07(3H, s, H^{32}) (Khalid *et al*., 1989).

2.4.2 Spectral studies of khivorin and 7-ketokhivorin nucleophiles

The IR spectral data are similar to that of gedunin with the absence of peaks related to the αβ-unsatrurated carbonyl. The ^{1}Hnmr data obtained are 4.5-4.75(m, H^{1}, H^{3}, H^{7}), 3.51(1H, H^{15})*, 5.58(1H, H^{17})*, 7.37(1H, H^{21})*, 7.39(1H, H22)*, 6.31(1H, H^{23}), CMe protons (0.81, 0.92, 1.02, 1.10, 1.25)*, OAc protons(2.02, 2.02, 2.15)* , * = multiplicity not given (Adesogan *et al*., 1967). The ^{1}Hnmr spectra of 7- ketokhivorin is similar to that of khivorin, but H^{17} is shifted upfield δ 5.58 to 5.40 ppm in 7-ketokhivorin due to the presence of ketone in C^{7} position and H^{15} is shifted downfield from δ 3.51 to 3.85 ppm (Lakshmi and Gupta, 2008).

2.4.3 Spectral studies polyavolensinol nucleophile

IR spectral data for polyavolensinol are: 3450cm^{-1}(OH), 1600cm^{-1}(benzene ring), 1450, 1375, 1330, 1300, 1020, 768, 740, 730cm^{-1}. The ^{1}Hnmr data ($CDCl_3$) are: δ ppm 6.93-7.60(4H, m, ArH), 6.17(1H, m, indole β-H), 3.2(1H, t, J= 7.5Hz), 2.80(1H, m, NCH), 0.82(3H, s, CH_3), 1.0(6H, s, $2CH_3$), 1.18(3H, s, CH_3) (Okorie, 1980).

2.5 Review of Spectral studies of products of nucleophilic addition

2.5.1 Spectral studies of pyridinium and substituted pyridinium adducts

The IR spectra of pyridinium adduct exhibit two strong carbonyl bands at 2055 and 1980cm^{-1}. The shift (ca.10cm^{-1}) of IR √(CO) to higher frequency compared with related neutral complexes such as 1,4-η-5-N-anilino-cyclohexa-1,3-diene (tricarbonyl) iron (Odiaka, 1980; Odiaka and Kane-Maguire, 1981) is compatible with cationic species in which the positive charge is largely localised on the nitrogen atom of the pyridine substituent. The ^{1}Hnmr spectra of these adducts are also consistent with their formulation as tricarbonyl (1,4-η-5-N-pyridino-1,3-diene) iron derivatives. The mass spectral data (FD) does not show the expected molecular ion but gave base peak corresponding to [M-pyridine] (Odiaka and Kane-Maguire, 1981).

2.5.2 Spectral studies of anilinium and substituted anilinium adducts

The nature of the reactions between the organometallic complex [1-5-η-(C_6H_7)Fe$(CO)_3$]BF_4 and aniline or substituted anilines has been established by the isolation and characterization of the anilinium adducts. Their IR spectra showed two strong carbonyl bands at 2045 and 1970 cm^{-1} indicating the formation of the neutral complex 1,4-η-5-exo-N-anilinocyclohexa-1,3-diene)iron. The reaction is a reversible one. The ^{1}Hnmr data for the products are consistent with neutral tricarbonyl (substituted-1, 3-diene) iron species (John and Kane-Maguire, 1979b; Odiaka, 1980, 1989).

2.5.3 Spectra studies of iodide adducts

There is complete disappearance of the initial dienyl IR √(CO) bands at 2110 and 2060 cm^{-1} and appearance of four strong bands at 2080, 2040, 2030 and 1967 cm^{-1}. The bands at 2040 and 1967 cm^{-1} are typical of neutral tricarbonyl (diene) iron species and are assigned to the ring adduct [(1-4-η- IC_6H_7)Fe$(CO)_3$] (Brown *et al.*, 1984). The solid product mixture isolated from an analogous preparative procedure exhibited a further medium intensity band at 1735 cm^{-1} (nujol mull). The IR √(CO) bands at 2080, 2030 and 1735 cm^{-1} were assigned to the acyl iodide complex [(1-5-η-C_6H_7) Fe(CO)2(COI)]. The band at 1735 cm^{-1} was specifically assigned to COI ligand (John *et al.*, 1986). The ^{1}Hnmr is characteristic of a ring substituted (η4-1,3-diene)Fe$(CO)_3$ complex (Siu *et al.*, 1998).

2.5.4 Spectral studies of phosphonium adducts

The phosphine adducts exhibited two strong IR carbonyl bands in acetone solution at 2055 and 1985 cm^{-1} which are at slightly higher frequency than those for neutral [Fe (diene)$(CO)_3$] complexes. Their ^{1}Hnmr spectra data are consistent with reported literature values while the mass spectral data (FD) show only single peaks due to the molecular ions (John *et al.*, 1979a).

2.5.5 Spectral studies of imidazolium adducts

The IR √(CO) bands for the cationic adducts in acetone were observed at 2055 and 1985 cm^{-1} which are characteristics of tricarbonyl(diene)iron complexes while those of the neutral adducts were observed at a lower frequency of 2055 and 1979 cm^{-1} (Evans *et al.*, 1996). The ^{1}Hnmr spectra of the cationic adducts are characteristic of 5-substituted 1,3-diene complexes of iron tricarbonyl (Atton *et al.*, 1982). The ^{1}Hnmr of both the cationic and neutral adducts when compared with free imidazole shows that

the imidazole ring protons are shifted appreciably downfield upon the attachment of the [Fe $(CO)_3$(dienyl)]$^+$ to the tertiary nitrogen.

2.5.6 Spectral studies of indole adducts

The adducts showed the expected IR √(CO) band at 2040 and 1970 cm^{-1} in nitromethane which is characteristic of neutral tricarbonyl (diene) iron complexes (Kane-Maguire and Mansfield, 1976). In addition, the IR spectra showed additional presence of N-H stretching band at 3400 cm^{-1} eliminating the possibility of electrophilic substitution at the nitrogen atom. The ^{1}Hnmr spectrum is consistent with the structure in which electrophilic attack by [(dienyl)Fe$(CO)_3$]$^+$ occurred on C^3 of indole. This is in agreement with molecular orbital calculation (Clack *et al*., 1976a) showing C^3 to be the carbon atom of highest π-electron density in the heterocycle.

2.5.7 Spectral studies of amide adducts

The IR √(CO) bands of the adducts was observed at 2055 and 1980 cm^{-1} as expected for cationic 1,3-diene substituted iron complexes. In addition, a strong broad band was also observed at 1060 cm^{-1} which was attributed to the presence of BF_4^- anion (Odiaka and Okogun, 1985).

2.6 Review of kinetics and mechanisms of nucleophilic addition to dienylium organometallics

2.6.1 Kinetics and mechanisms of pyridinium and substituted pyridinium adducts formation.

The kinetic data for the addition of pyridine and substituted pyridines to dienylium iron cations showed a second order rate law. The plots of k_{obs} versus [amine] are linear and pass through the origin. This rate law is most readily explained by one step mechanism in which the second-order rate constants, k_1, refer to direct addition by pyridine nucleophiles to the dienyl rings. The reaction of pyridines is in the order (A) [(1-5-η-C_6H_7)Fe$(CO)_3$]BF_4 > (B) [(1-5-η-2-$MeOC_6H_6$)Fe$(CO)_3$]BF_4 > (C) [(1-5-η-C_7H_9)Fe$(CO)_3$]BF_4. The lower reactivity of (B) compared with (A) is in accordance with the mesomeric influence of the methoxide group, which has been shown from INDO molecular orbital calculation (Clack *et al*., 1976b) to decrease the positive charge on the dienyl C^5 atom, the site of nucleophilic addition. Complex (C) was found to be least reactive due to the more pronounced steric effect of the additional CH_2 group on the dienylium fragment. It exhibited the same k_1 in both acetonitrile and nitromethane indicating the same solvation effects on the dienyl cations and their

corresponding transition states in both solvents. Its reaction also showed strong dependence on amine basicity. Successive blocking of the N reaction site by methyl groups causes approximately 10-fold and 10000-fold decreases in the rate when compared with the non-sterically hindered pyridines, confirming the importance of steric effect in the reactions (Odiaka and Kane-Maguire, 1981)

2.6.2 Kinetics and mechanisms of anilinium and substituted anilinium adducts formation

The kinetic studies of the reversible addition of anilines to the [(1-5-η-dienyl) $Fe(CO)_3$]BF_4 (dienyl = C_6H_7, 2-$MeOC_6H_6$ or C_7H_9) provide detailed information on the influence of steric and electronic effects on the nucleophilicity of amines toward coordinated organic substrates. The plots of k_{obs} versus [amine] are linear with non-zero intercepts, indicating the twoterm rate law. There is also direct addition to the dienyl fragment similar to that of pyridine addition (Odiaka and Kane-Maguire, 1979; Odiaka, 1989)

2.6.3 Kinetics and mechanisms of iodide adducts formation

Detailed kinetic studies of this reaction in various solvents reveal the general second order rate law: rate = k [Fe] [I^-], in each solvent. The rate trend C_6H_7 > 2-$MeOC_6H_6$ > C_7H_9 is consistent with rate determining step of one electron transfer from I^- to the dienyl rings. Concomitant formation of molecular iodine occurs which is converted to I^{3-} in the presence of the large excess of I^- employed. This suggest that a single electron transfer mechanism is operating, involving the transfer of one electron from the I^- to the dienyl cations and the formation of iodine radicals (Siu *et al*., 1998).

2.6.4 Kinetics and mechanisms of phosphonium adducts formation

The rate law, rate = k [Fe][PR_3], is observed for the addition of a range of phosphines and phosphites to dienylium iron cations. The rate and activation parameters indicate direct addition at dienyl rings. The marked dependence of k on the basicity of phosphorus nucleophiles suggests significant bond making in the transition states for adduct formation (John and Kane-Maguire, 1979a).

2.6.5 Kinetics and mechanisms of imidazolium adducts formation

In all cases, the rate law, $k_{obs} = k_1$ [amine] is obeyed and it shows direct addition to the dienyl ring.

2.6.6 Kinetics and mechanisms of indole and substituted indole adducts formation

The kinetic study of the addition of indoles to the dienyl cation [1-5-η-(C_6H_7) $Fe(CO)_3]^+$ and related species in nitromethane obey the rate equation: Rate = k[complex][indole]. This observation together with substituent effects and products stereochemistry supports electrophilic attack of the dienyl cation at C^3 of indole followed by rapid proton loss (Kane-Maguire and Mansfield, 1976).

2.6.7 Kinetics and mechanisms of amide and substituted amides formation

X-substituted benzamides (X = H, 2-OH, 4-MeO, 3-MeO, 3, 5-$(MeO)_2$, 4-Cl and 2,4-Cl_2) have been shown to add reversibly to the dienyl rings of organometallic complex [1-5-η-(dienyl) $Fe(CO)_3]BF_4$ (dienyl = C_6H_7, 2-$MeOC_6H_6$) to give the corresponding cationic tricarbonyl (substituted diene) iron complexes (Odiaka and Okogun, 1985)

2.7 Use of dienylium iron cations in the total synthesis of structurally complex biologically active natural products.

Carbon-carbon bond formation is central to the art and science of organic synthesis (Mathieu and Weill-Raynal, 1973). Any new and wide- ranging methods are therefore important. When employed in organic synthesis, tricarbonyliron complexes (η5-cyclohexadienylium cations) offered a better potential for the formation of C-C and C-heteroatom bonds by reaction with nucleophiles to provide 5-exo-substituted tricarbonyl (η4-cyclohexadiene) iron complexes. Moreover, labile diene systems can be protected by the complexation to the tricarbonyliron group because of the pronounced modification of the reactivity of the organic ligand in the coordination sphere of the transition metal. These features made tricarbonyliron complexes extremely useful and versatile tools for synthetic organic chemistry (Knolker, 1992). The resulting complexes can be converted to the desired organic products by careful removal of the tricarbonyl iron moiety (demetallation) using an appropriate method of demetallation. The use of an oxidizing agent, Me_3NO, is the most preferred because the reaction is mild and compatible with a number of functional groups.

Reaction of tricarbonyl (cyclohexadienylium) iron cations with nucleophiles can lead to formation of N-alkylated or C-alkylated compounds depending on the reaction conditions used and the nucleophile used. Formation of C-heteroatom products is a reversible process which can be converted to the C-alkylation on application of heat.

This process is noteworthy for synthesis of carbazole skeleton for pyrido[4,3-b]carbazole an antitumor agent, ellipticine (Birch *et al.*, 1982), preparation of antibiotics (Knolker *et al*., 1993), Steroids (Minclone *et al*., 1981), alkaloids such as furoclausine A (Knolker, 2004), Limaspermine (Pearson, 1983), Carbobazomycin (Knolker, 1992), sesquiterpene (Hydroazulene) (Genco *et al*., 1976).

2.7.1 Review of important natural products synthesis using tricarbonyl iron dienylium cations

2.7.1.1 Use of dienylium iron cations in the total synthesis of carbazomycins

The reactions of tricarbonyliron complexed cyclohexadienylium cations with arylamines allows region- and stereoselective formation of carbon-carbon and carbon-nitrogen bonds and gives easy access to nitrogen heterocyclic ring systems. Electrophilic aromatic substitution and subsequent oxidative cyclization provides a convergent route to biologically active carbazole alkaloids.

Carbazomycins A and B was isolated by Nakamura and co-workers in 1980 (Sakano and Nakamura, 1980) from microorganisms of the strain *Streptoverticillium ehumense* H 1051-MY 10, which represent the first antibiotics with carbazole skeleton (Sakano *et al.*, 1980, Kaneda *et al.*, 1981). These inhibit the growth of phytopathogenic fungi and have antibacterial and antiyeast properties. The carbazomycins which biogenetically are derived from tryptophan (Yamasaki *et al.*, 1983) exhibit an unusual congested substitution pattern which is tedious to achieve by classical synthetic route (Joule, 1984). This fact and the useful biological activities induced several groups to develop synthetic route to the total synthesis of the carbazomycins. The route to total synthesis of carbazomycins involves consecutive iron-induced C-C and C-N bond formation in a sequence of electrophilic substitution of arylamines by the iron complexed cations and subsequent oxidative cyclization as shown below**.**

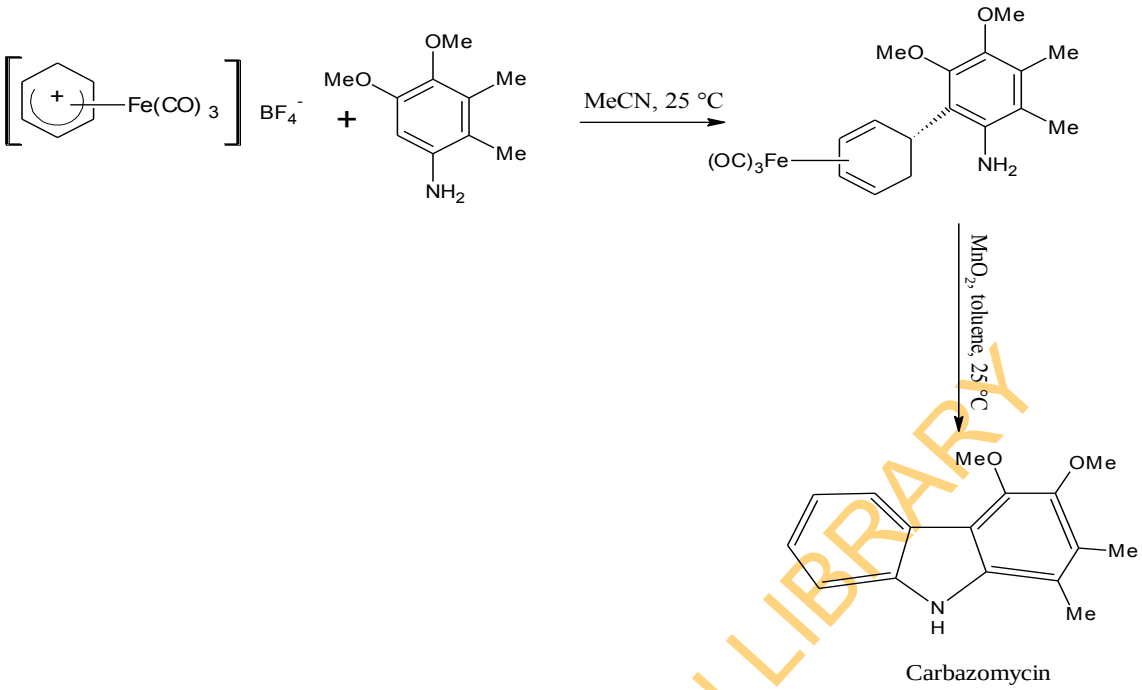

Carbazomycin

2.7.1.2 Use of dienylium iron cations in tota thel synthesis of Clausine K

Total synthesis of Clausine K (12) and Clausine H (13), carbazole alkaloids was achieved using iron mediated arylamine cyclization (Kataeva *et al*., 2005). Clausine K was first isolated from the roots of the plant *Clausena harmandiana* (Yenjai *et al*., 2000) and was found to show antimycobacterial activity against *Mycobacterium tuberculosis* (Sunthikawinsakul *et al*., 2003). Clausine H was first isolated from *Clausena 27xcavate* (Ito *et al*., 1996) and exhibits antiplasmodial activity against *Plasmodium falciparum* (Yenjai *et al*., 2000).

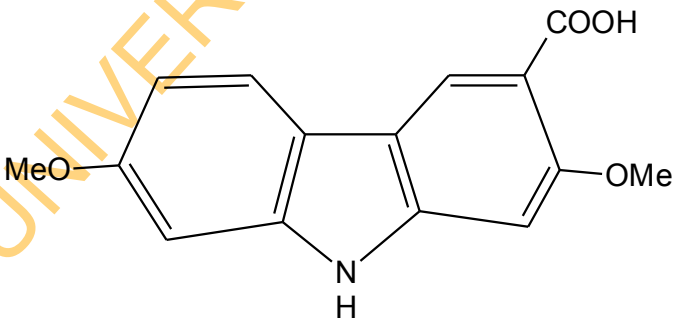

(12)

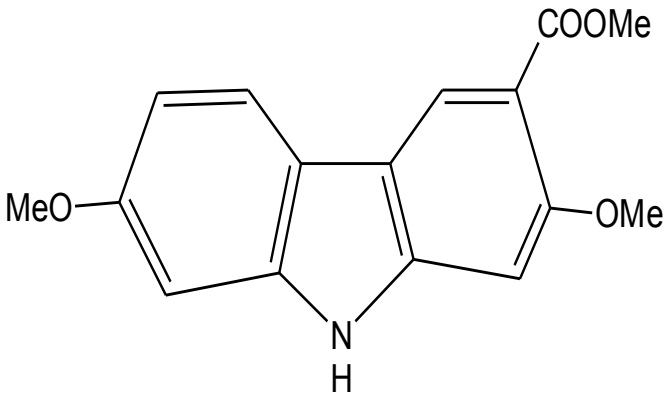

(13)

2.7.1.3 Use of dienylium iron cation in the synthesis of Aspidosperma alkaloids

Limaspermine (14) an Aspidosperma alkaloid with quaternary carbon centre have been synthesized via tricarbonyliron dienylium cation based on the ability of the iron tricarbonyl moiety of the dienylium cation to direct the stereochemistry of C-C formation (Pearson and Rees, 1980, 1982; Pearson, 1983).

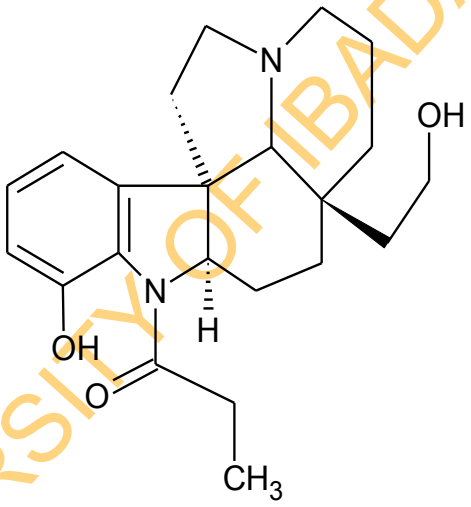

(14)

2.7.1.4 Use of dienylium iron cation in the total synthesis of Furoclausine-A

Furoclausine-A (15) and Furoclausine-B were both isolated from the acetone extract of the root bark of *Clausena excavate* (Wu *et al*., 1997). The extract is used in traditional folk medicine in China for the treatment of various infections and poisonous snake bite. Its first total synthesis was achieved using an iron-mediated construction of the carbazole framework followed with acid catalysed annulations of the furan ring as key steps (Knolker, 2004).

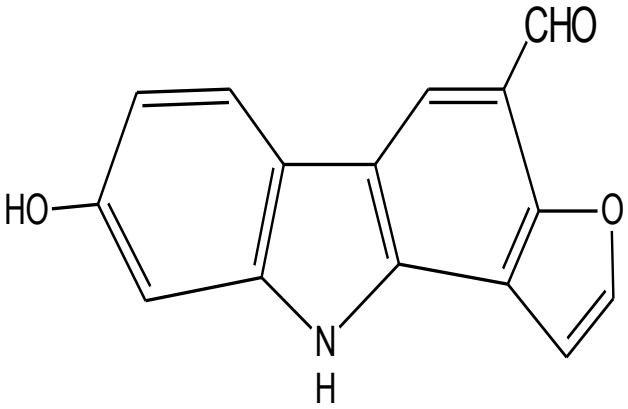

(15)

2.7.1.5 Use of dienylium iron cations in the development of a new synthetic route for Oseltamivir phosphate (Tamiflu)

A novel synthetic route towards oseltamivir (16), an influenza neuraminidase inhibitor used for the treatment of human influenza infection and avian flu virus (Schmidt, 2004) has been achieved by employing a cationic iron carbonyl complex, thereby providing an alternative pathway with potential to access diverse analogues should resistance to Oseltamivir become more prevalent (Moscona, 2005).

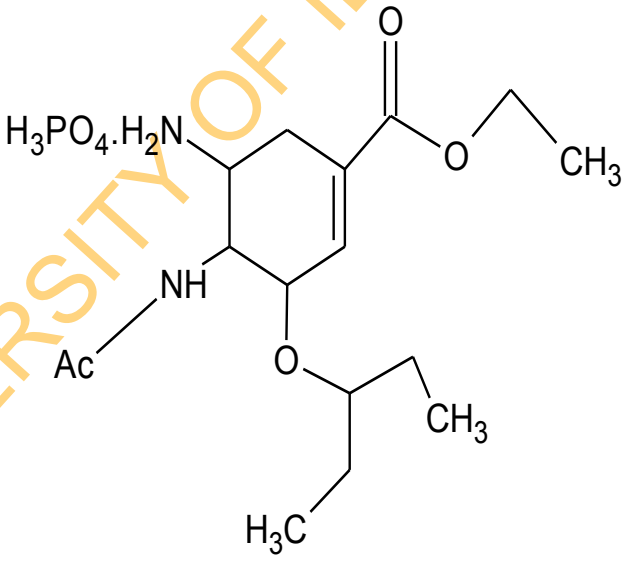

(16)

2.7.1.6 Use of dienylium iron cation in the synthesis of Trichothecene

Trichothecenes (17) are a group of tricyclic sesquiterpenes produced by strains of Fusarium, Trichoderma, Trichothecium and Myrothecium, showing potent antifungal and cytostatic activity and potential anti-Leukemic activity. Trichothecene form the backbone of a number of macrocyclic diesters which are extremely toxic, thus a new method for total synthesis of trichothecenes which will produce analogues with modified activity is of considerable interest. A total synthesis of 12, 13 trichothecenes analogue having oxygenation at C^{14} have been achieved by the use of tricarbonyl (4-methoxy-1-methycyclohexadienylium) iron cations (Pearson and Ong, 1981).

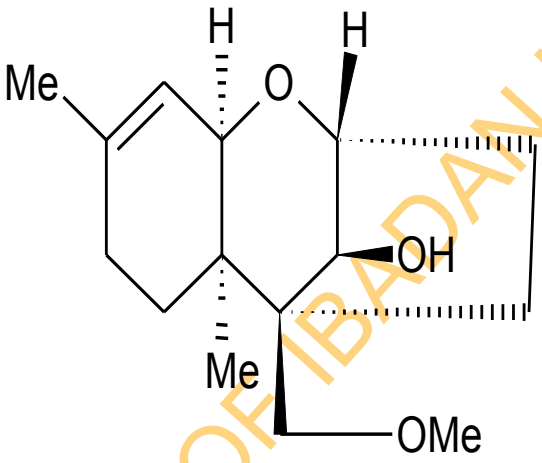

(17)

2.7.1.7 Use of dienylium iron cations in the total synthesis of steroids

Tricarbonyl (4-methoxy-1-methylcyclohexadienylium) iron cation was employed to synthesise a steroidal ring A precursor in total synthesise of steroids (Pearson and Heywood, 1981). This gives a more convenient route.

2.7.1.8 Use of dienylium iron cations in the synthesis of 6-ketosteroids

Tricarbonyl (4-methoxy-1-methylcyclohexadienylium) iron cation was used to synthesis 6-ketosteroids (18) of potential value for the synthesis of β-ecdysone, an insect moulting hormone (Pearson *et al*., 1980)

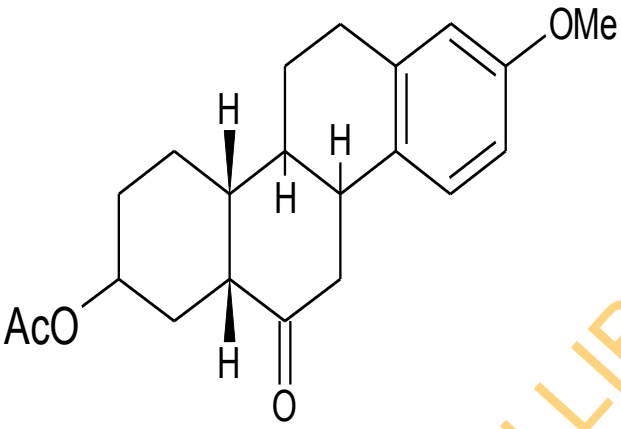

(18)

2.8 Computational chemistry as a tool in understanding the synthesis of organometallic complexes

The relationship between structure and reactivity in a chemical reaction cannot be over-emphasized, and the structure of most organometallic complexes are not well established due to difficulty in growing single crystals for X-ray crystallographic studies (Johnsons *et al*., 1981). Computational Chemistry has recently increased understanding of molecular structures of a wide variety of compounds but this is yet to be extended to organometallic systems (Qu and Bian, 2005). Detailed structural analysis of aniline and pyridine substituted products using semi-empirical method PM3 have been reported by Odiaka (Odiaka *et al*., 2012) and Adejoro (Adejoro *et al*., 2012, 2013, 2014).

2.9 Techniques employed in the characterization of organometallic complexes

Complexes are first purified after synthesis before characterisation. The techniques employed in characterization are as follows: IR (Infrared spectroscopy), ^{1}Hnmr and ^{13}Cnmr (Nuclear magnetic resonance), MS (Mass spectroscopy technique), Microanalysis and X-ray and neutron diffraction.

2.9.1 Infrared spectroscopy

Infrared spectroscopy is a useful tool for the identification of a molecule or a functional group (Emeleus and Sharpe, 1973). Characteristics frequency, shape and intensity of a band are essential elements in such fingerprinting applications, which include structural elucidation of complex molecules (Nakamoto, 1986; Cotton and Monchamp, 1960), bond types and metal-ligand attachment site. However, for complex molecules, it is important to correlate infrared spectra and structures determined by X-ray methods

2.9.2 Nuclear magnetic resonance (^{1}Hnmr and ^{13}Cnmr) spectroscopy

Various types of Nuclear Magnetic Resonance (NMR) spectrometers are now being designed to enable the examination of certain nuclei such as: ^{1}H, ^{13}C, ^{19}F and ^{31}P. The most commonly studied is ^{1}Hnmr and this is closely followed by ^{13}Cnmr. In each case we are looking at the electron density at each nucleus and as well determine the chemical environment of the atom in question and the nature of atoms in the surrounding environment. The nature of other nuclei around the atom under investigation will determine the position of the resonance frequency or chemical shift. Integration of an NMR spectrum enables one to know the number of atoms present in a given signal or peak and their relative intensities (Odiaka, 2004).

Decoupling of a peak due to an atom or atoms at a given frequency enables one to know the atoms that are nearest neighbours to the atom being decoupled. When an atom is decoupled, it becomes non-existent such that the original multiplicity of its nearest neighbours decreases considerably (Odiaka, 2004).

2.9.3 Mass spectrometric techniques

The mass spectrum of a given organometallic complex may be obtained in different forms depending on the information required and the nature of the compound under investigation. Volatile organometallic complexes are best studied by electron impact (EI) mass spectrometry while non-volatile complexes such as salts are studied by other methods of spectrometry: field desorption, electron spray (Odiaka, 2004).

In general the mass spectrometer allows the determination of the formula or the molecular weight of a given compound. In most common spectrometers, the sample under study is bombarded with high energy electrons and the mass per charge ratio (m/e) due to various fragmentations are recorded as a function of their corresponding intensities. Each peak represents an atom or group of atoms that have been knocked off from the compound under study. Such peaks are known as fragmentation patterns and the peak with 100% intensity represent the formular or the molecular weight of the compound. In some organometallic complexes, the added nucleophile may be knocked off in the spectrometer in which case the 100% intensity peak will not correspond to the formula weight of the complex under study (Odiaka, 1980).

2.9.3.1 Field desorption mass spectrometry (FD)

This is suitable for non-volatile compounds such as salts. A clean steel is dipped into a solution of the sample in acetone and the solvent is allowed to evaporate off, leaving the sample under study on the wire. The wire acts as the anode and is placed in an electric field in the mass spectrometer. The walls of the spectrometer acts as the cathode so that a high electric field is generated, causing desorption of the sample as a cation from the wire. The experiment is usually carried out at low temperature ($70^{o}C$) to avoid sample decomposition and ensure little fragmentation.

The desorption of the cation from the wire is automatically recorded on a chart as the parent or base peak. Thus, the fragmentation patterns observed are: P^{+} (Fwt), $(P+1)^{+}$, and $(P+2)^{+}$ ions (John and Kane-maquire, 1979a, 1979b; Games *et al.*, 1975)

2.9.3.2 Electron impact mass spectrometry (Odiaka, 2004)

Here, the sample under study must be volatile if a liquid or sublimable if a solid. The sample is placed in a small steel boat, which is placed in a small compartment designed for it in the spectrometer.

It is then warmed up by gradual increase in temperature until the sample under study becomes gaseous and is hit with high energy electrons. This causes extensive fragmentation. It should be noted here that electron impact may be unsuccessful for some organometallic complexes since increased heating in an attempt to obtain a gaseous sample causes decomposition. However, an electron impact study, if successful enables us to know whether the addition of the nucleophile to the complex occurred in an exo or endo manner. For exo addition, the characteristic peaks observed are M-(CO)-(H_2), M-(2CO)-(H_2) and M-(3CO)-(H_2) where M represents the formula weight of the complex. For endo addition, the hydrogen molecule is not knocked off from the complex so that the characteristics peaks observed are M-(CO), M-(2CO) and M-(3CO).

2.9.3.3 Electrospray mass spectrometry

Mass spectrometry of inorganic and organometallic compounds has often involved volatilising the species prior to forming ions in the gas phase. Most early studies were therefore performed on neutral compounds. The original ionization technique involves electron impact (EI) which led to extensive fragmentation especially for metal carbonyl compounds, although the molecular ion was sometime observed as a low intensity peak. Many efforts have been made to devise softer ionization technique, Fast atom bombardment mass spectrometry has been successful. Electrospray mass spectrometry (ESMS) provides a new method of transferring pre-existing ions from solution to the gas phase. The transfer is very soft and causes minimal fragmentation. It is now a well established technique in the structural analysis of large bimolecules such as proteins. These are protonated with an organic acids and a family of peaks is observed (Ahmed *et al*., 1993).

2.9.4 Microanalysis

The molecular formula of newly synthesized product is predicted from mass spectral measurements and the percentage composition of some elements.such as C, H and N are calculated. The calculated values are compared with the experimental values obtained. If these values are very close to the calculated values, this will suggest that the synthesised compound has the assigned molecular formula.

2.9.5 X-ray and neutron diffraction

A diffractometer is used for X-ray and neutron diffraction studies, although, X-ray diffraction is generally the most direct method for determining the precise geometry or structure of a compound in the solid state. In X-ray studies, the exact picture of the compound under investigation is usually obtained, thus making it an accurate method for structure elucidation. However, the detection of hydride ligands in organometallic compounds by this method is difficult since the intensity of scattered rays is proportional to the atomic number of the scattering atom. The more accurate determination of the hydride position in organometallic compounds can be achieved by means of neutron diffraction after the remainder of the structure has been solved by X-ray diffraction (Odiaka, 2004).

CHAPTER THREE

MATERIALS AND METHODS

3.1. Chemicals, Reagents and Apparatus

The following reagents and solvents were obtained from Sigma-Aldrich, Fluka and the British Drug Houses.

Chemicals and Reagents: Cyclohexa-1,4-diene, iron pentacarbonyl, triphenylmethanol, propionic anhydride, 40% hydrofluoroboric acid, anhydrous ether, dry toluene, alumina, deuterated chloroform, 2-methoxycyclohexa-1,3-diene, deuterated acetonitrile, trimethylamine-N-oxide, Celite 545, dimethysulphoxide, nutrient agar (Mueller Hinton), nutrient broth, nitrogen gas and gentamycin antibiotic and ketocanazole antibiotic, n-hexane, acetone, diethylether, dichloromethane and methylated spirit.

Apparatus: Irradiation apparatus, 125 W mercury lamp, alumina H column, Schlenk line, suction pump, vacuum line, rotary evaporator, autoclave, thermometer, heating mantle, hot plate with magnetic stirrer, all-glass graduated syringe, 1 mm disposable insulin syringe, EDTA bottles, petri dishes, reflux set up.

General procedure

Infra red spectra were run on a Perkin Elmer Spectrum BX FTIR, and ^{1}Hnmr (400M Hz) and ^{13}Cnmr (100 MHz) were run on a Bruker AV 400 Spectrometer while the mass spectral measurements were carried out on a Micromass Platform II Spectrometer at the School of Chemistry, University of Manchester, United Kingdom.

3.2 Preparation of Parent Dienylium Cations

3.2.1: Preparation of tricarbonylcyclohexadiene Iron (1): This was synthesised according to the standard methods of (Birch *et al.*, 1968,) and (Odiaka, 1980). The preparation is represented below:

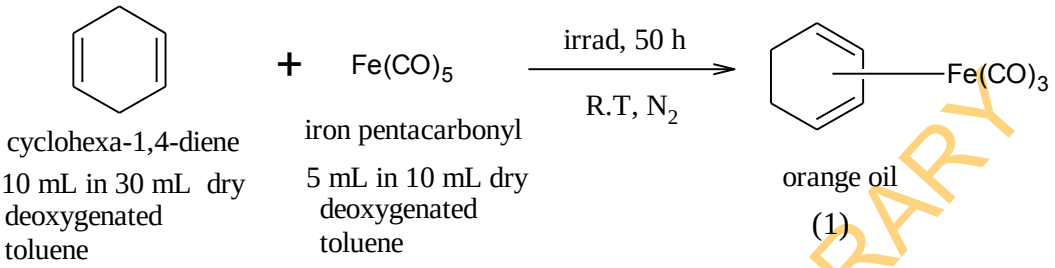

cyclohexa-1,4-diene
10 mL in 30 mL dry deoxygenated toluene

iron pentacarbonyl
5 mL in 10 mL dry deoxygenated toluene

orange oil
(1)

Procedure: 1,4-cyclohexadiene (10 mL) was dissolved in 30 mL dry toluene and 5 mL iron pentacarbonyl in 10 mL dry toluene were introduced into the irradiation apparatus fitted with nitrogen source from the Shlenk line. The mixture was flushed with nitrogen for 5 mins and then irradiated using irradiation tube from 125 W mercury lamp for 50 h at room temperature. The irradiation apparatus was covered with aluminium foil to prevent light as the reaction is a light sensitive reaction. On completion of irradiation, a dark brown solution was obtained; this was allowed to cool down and then filtered under nitrogen in an alumina H column to obtain an orange filtrate. This was concentrated by passing a rapid flush of nitrogen through one side arm of a two necked flask containing the filtrate while the other arm was left open and was heated with a slight warming. This gave brown oil which was dissolved in 50 mL hexane. The solution obtained was again filtered under nitrogen in an alumina H column to give a yellow filtrate. The yellow filtrate was concentrated by rapid flush of nitrogen through one side coupled with a slight warming as explained above. Orange oil was then obtained as reported (Odiaka, 1980).

3.2.2 Abstraction of tricarbonyl cyclohexadiene iron to form tricarbonyl cyclo hexadienylium iron tetrafluoroborate (2)

The reaction is given as follows:

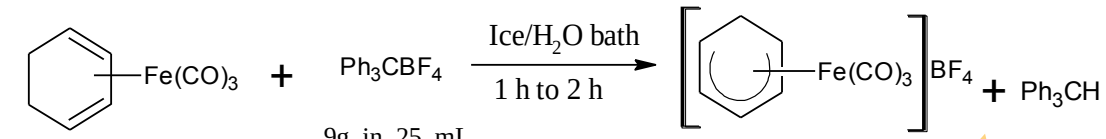

in 25 mL CH_2Cl_2

9g in 25 mL CH_2Cl_2

orange yellow crude

(2)

Procedure: Ph_3CBF_4 (9 g) was weighed and dissolved in 25 mL dichloromethane (CH_2Cl_2).The orange oil synthesized in stage 1 above was separately dissolved in 25 mL dichloromethane. The two solutions were added together in a conical flask and placed in an ice/water bath overnight. There was formation of an orange yellow precipitate which was sucked dry and washed several times with dry ether. This was later recrystalised from hot water to obtain the pure compound. The abstraction of tricarbonylcyclohexadiene iron involves the use of triphenyltetrafluoroborate (Ph_3CBF_4) which was always prepared in-situ as follows:

3.2.3 In-situ preparation of triphenylmethyltetrafluoroborate (Ph_3CBF_4)

Triphenylmethanol (10 g) was weighed. This was dissolved in 100 mL deoxygenated propionic anhydride. The mixture was placed in a water bath for few minutes to allow for complete dissolution, it was then placed in an ice/water bath on a magnetic stirrer. The temperature of the solution was monitored by means of a thermometer. The temperature was brought down to 20^0C. Afterwards, 11 mL of HBF_4 (40% in water) was added in 0.5 mL aliquots at a time and the temperature was maintained at 20^0C throughout the addition with continuous stirring. A greenish yellow precipitate was formed, which was filtered and washed several times with anhydrous ether until a clear washing was obtained and then sucked dried.

3.2.4 Recrystallisation of crude tricarbonyl cyclohexadienyl iron tetrafluoro borate (2)

The crude product was dissolved in 110 mL of distilled water while the temperature was maintained at 80^0C. More than 90% of the crude product dissolved. The hot solution was filtered using a filter paper and the filtrate was left in an ice/water bath for some hours. There was gradual formation of shiny orange crystals and more of this was formed with time. This was recovered by suction filtration and washed several times with cold water. The orange crystal is the pure form of tricarbonylcyclohexadenyl iron tetrafluoroborate. The IR √ (CO) band was observed at 2108 cm^{-1} and 2046 cm^{-1} on Perkin Elmer FTIR and 2108 cm^{-1} and 2047 cm^{-1} on an Alpha P Bruker FTIR. The crystal was stored in a sample vial wrapped with aluminium foil. The ^{1}Hnmr and ^{13}Cnmr studies were carried out using CD_3CN.

3.3 Preparation of tricarbonyl (2-methoxycyclohexadienyl) iron tetrafluoro borate (3):

The method of preparation is similar to that of tricarbonylcyclohexadienyliron tetrafluoroborate. It also involves two stages.

3.3.1 Preparation of tricarbonyl-2-methoxycyclohexadieneiron

The preparation is given thus:

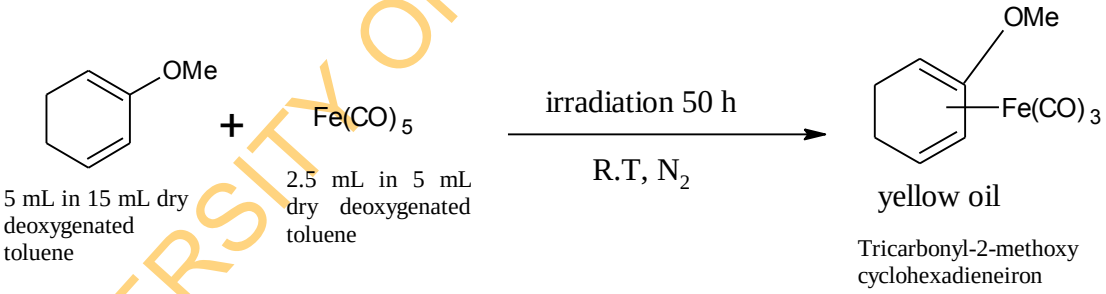

Procedure: 2-methoxy-1,3-cyclohexadiene (5 mL) was dissolved in 15 mL dry toluene and 2.5 mL of iron pentacarbonyl in 5 mL toluene were mixed together in an irradiation flask. The mixture was irradiated under nitrogen for 50 h. A brown solution was obtained at the completion of irradiation. This was followed by a similar work-up as in tricarbonylcyclohexadiene iron above. This gave same yellow oil which was treated with 4.5 g Ph_3CBF_4 in CH_2Cl_2 at 0^oC to give $[(1\text{-}5\text{-}\eta\text{-}2\text{-}MeOC_6H_6)Fe(CO)_3]BF_4$.

3.3.2 Abstraction of tricarbonyl-2-methoxycyclohexadieneiron to give the dienylium compound.

The reaction is as follows:

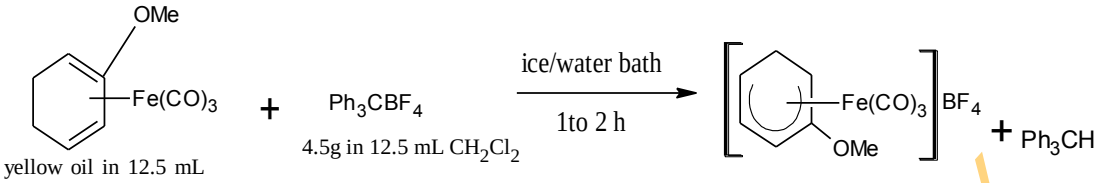

yellow oil in 12.5 mL CH_2Cl_2

Tricarbonyl-2-methoxy cyclohexadieneiron

yellow crude

(3)

A yellow crude precipitate was obtained from the abstraction reaction. It was sucked dry and washed several times with dry ether.The crude product gave √(CO) IR band at 2096 cm^{-1} and 2025 cm^{-1} on a Perkin Elmer FTIR spectrophotometer.

The yellow crude was recrystallized using 50 mL distilled water at 80^0C.The recrystallisation process is similar to that of tricarbonylcyclohexadienyliron tetrafluoroborate. A yellow solution was formed. The hot yellow solution was filtered using a filter paper and the yellow filtrate was placed in an ice/water bath for some hours. There was a gradual formation of yellow crystals which was washed several times with cold water and then obtained by suction filtration through a glass frit. √(CO) IR band was observed at 2046 cm^{-1} and 1963 cm^{-1}.

3.4 Preparation of Adducts

The reaction for the preparation of adducts is given thus:

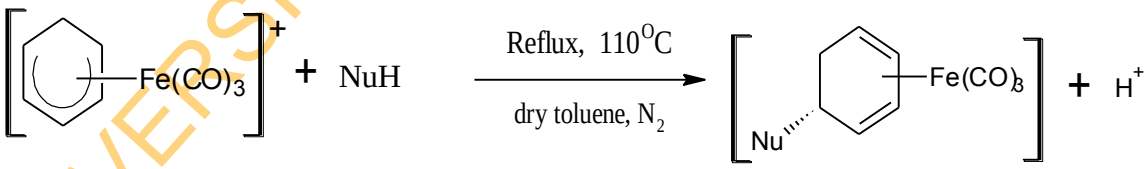

whereNuH=Gedunin/khivorin/7-ketokhivorin/polyavolensinol

Reactions of [(1-5-η-C_6H_7)Fe$(CO)_3$][BF_4] with natural product nucleophiles

3.4.1 Reaction of [(1-5-η-C_6H_7)Fe$(CO)_3$][BF_4] with Gedunin

The reaction for the preparation is given as follows:

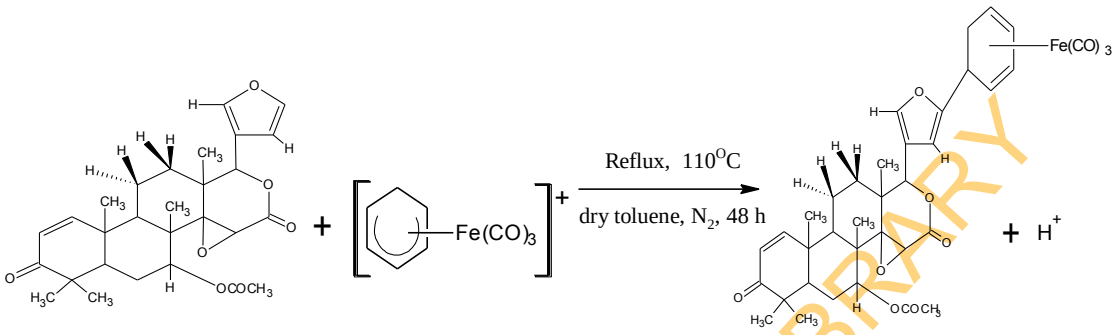

Gedunin (19)

Procedure:

Tricarbonyl[1-4-η-5-(gedunino)cyclohexa-1,3-diene]iron (19**):** [$C_6H_7Fe(CO)_3$]BF_4 **(**0.05 g, 0.1634 mmole) was weighed into a 100 mL quick fit two-necked flask followed by addition of a two-fold molar excess of Gedunin (0.157 g,0.3268 mmoles) in 30 mL dry deoxygenated toluene. The mixture was refluxed at 110^0C for 48 h. At the end of refluxing, the solution was allowed to cool down to room temperature and then rotary evaporated at reduced pressure to give a light yellow solid. This was shaken with 20/20, vol/vol, diethylether/water. The aqeous layer was set aside while the organic layer was rotary evaporated to give a yellow oil. This was dried in a vacuum line for 3 h. The yield of product, 0.04 g was 35%. The IR √ (CO) band was observed at 2041 cm^{-1} and 1964 cm^{-1}.

$C_{37}H_{40}O_{10}Fe$: IR (film) ν_{max} cm^{-1} = 2962 (C-H str of alkanes), 2045 and 1970 (√ (CO) bands of coordinated diene of organometallic moiety), 1738 (C=O str of esters), 1667 (αβ-unsaturated ketone), 1495 (C-C band of C_6H_7), 1368 and 1163 (C-O str of esters), 874 (furan band) and 563 (Fe-C band). **EMS m/z (relative intensity %): MS(700.7),**109(8.1) **[**M-(2CO)-($C_{32}H_{39}O_7$)], 150(1.8) [M-(2CO)-($C_{25}H_{26}O_7Fe$)], 201(1.8)**[**M-(2CO)-($C_{25}H_{31}O_7$)], 257(6.3) **[**M-(2CO)-($C_{23}H_{29}O_5$)-($2H^+$)], 401(63) [M-(2CO)-($C_{12}H_{10}O_2Fe$)-(H^+)], 500(16.3) **[**M-(2CO)-($C_3H_3O_3Fe$)-(H^+)], 505(100) **[**M-(2CO)-(C_5H_5OFe)-($2H^+$)], 547(8.15) [M-(2CO)-(C_2HOFe)], 546(35) [M-(2CO)-(OHFe)-(H^+)], 604(3.1) [M-(2CO)-(C_2HO)+(H^+)].**^{1}Hnmr (**$CDCl_3$, 400 MHz δ ppm) see Table 4.16. **SAMPLE CODE = TUN004**

3.4.2 Reaction of $[(1\text{-}5\text{-}\eta\text{-}C_6H_7)Fe(CO)_3][BF_4]$ with Khivorin. The preparation is as follows:

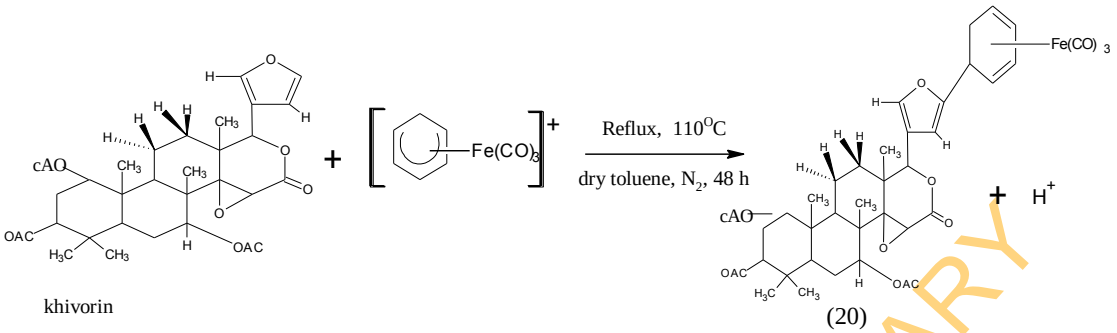

khivorin (20)

Procedure:

Tricarbonyl[1,4-η-5-(khivorino)cyclohexa-1,3-diene] iron (20):

$[C_6H_7Fe(CO)_3]BF_4$ (0.025 g, 0.0817 mmoles) was weighed together with a two-fold molar excess of khivorin (0.096 g, 0.1634 mmoles,). A similar work-up as for Gedunin above produced yellow oil which was dried in a vacuum line for 3 h. The yield of product, 0.024 g was 36%. After drying, the IR spectrum showed √ (CO) bands at 2046 and 1976 cm^{-1}.

$C_{41}H_{48}O_{13}Fe$: Yellow oil, **IR** (film) ν_{max} cm^{-1}= 2962 (C-H str of alkanes), 2050 and 1980 (√ (CO) bands of coordinated diene of organometallic moiety), 1730 (C=O str ester), 1256, 1083 and 1013 (C-O str ester), 873 (furan band), 563 (Fe-C band). **EMS m/z (relative intensity %):MS(804.8),** 173(2.3) [M-(2CO)-($C_{31}H_{41}O_{10}$)-($2H^+$)], 355(1.1) [M-(2CO)-($C_{22}H_{34}O_6$)+(H^+)], 541(5.0) [M-(2CO)-($C_9H_{10}O_2Fe$)-(H^+)], 609(100) [M-(2CO)-(C_5H_5OFe)-($2H^+$)], 625(2.3) [M-(2CO)-(C_4H_3OFe)], 687(1.1) [M-(2CO)-($C_2H_3O_2$)-($2H^+$)]. **^{1}Hnmr (** $CDCl_3$, 400 MHz δ ppm): 4.55(1H, m, H^1), 1.41(2H, dd, $H^{2a\&2b}$), 4.45(1H, m, H^3), 2.12(1H, m, H^5), 2.16(1H, m, H^{6b}), 4.64(1H, m, H^7), 1.38(1H, m, H^{11a}), 1.85(1H, m, H^{11b}), 1.88(1H, m, H^{12a}), 1.57(1H, m, H^{12b}), 1.57(1H, m, H^{12b}), 3.45(1H, s, H^{15}), 1.17(3H, s, H^{18}), 0.74(3H, s, H^{19}), 6.24(1H, s, H^{21}), 5.54(1H, s, H^{22}), 0.85(3H, s, H^{28}), 1.01(3H, s, H^{29}), 0.94(3H, s, H^{30}), 2.08(3H, s, H^{32}), 1.95(3H, s, H^{33}), 1.49(3H, s, H^{34}), 7.33(1H, d, $H^{3'}$), 2.79(1H, m, $H^{2'}$), 1.60(1H, m, $H^{6'a}$) and 2.19(1H, m, $H^{6'b}$).

SAMPLE CODE =TUN005

3.4.3 Reaction of $[(1\text{-}5\text{-}\eta\text{-}C_6H_7)Fe(CO)_3][BF_4]$ with 7-ketokhivorin. The reaction is represented below:

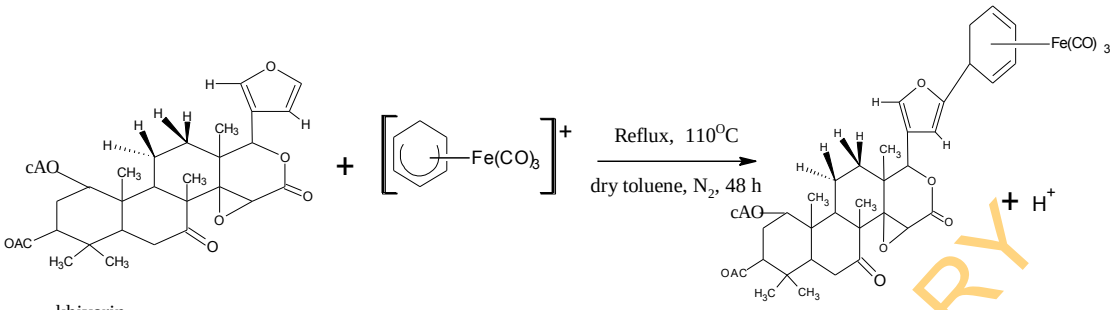

khivorin (21)

Procedure:

Tricarbonyl [1,4-η-5-(7-ketokhivorino)cyclohexa-1,3-diene]iron (21**):** A similar work-up as for Gedunin above using (0.025 g, 0.0817 mmoles) of $[C_6H_7Fe(CO)_3]BF_4$ and a two-fold molar excess of 7-ketokhivorin (0.0907 g, 0.1634 mmoles) produced yellow sticky solid which was dried on a vacuum line for 4 h. The yield of product, 0.028 g was 44%. The IR √ (CO) band was observed at 2047 and 1977 cm^{-1}.

$C_{39}H_{44}O_{12}Fe$: Yellow solid, **IR** (film) ν_{max} cm^{-1}= 2962 (C-H str of alkanes), 2050 and 1980 (√ (CO) band of coordinated diene of organometallic moiety), 1728 (C=O str of ester), 1256, 1084 and 1012 (C-O str of ester), 873 (furan band), 565 (Fe-C band). **EMS m/z (relative intensity %): MS(760.73),**191(1.7) [M-(2CO)-($C_{29}H_{37}O_8$)], 219(2.8) [M-(2CO)-($C_{27}H_{35}$-O_8)+($2H^+$)], 541(4.0) [M-(2CO)-(C_7H_7OFe)], 560(1.7) [M-(2CO)-($C_3H_3O_3Fe$)], 593(4.0) [M-(2CO)-(C_3H_2OFe)-(H^+)], 609(100) [M-(2CO)-(C_2HOFe)+($2H^+$)].

^{1}Hnmr ($CDCl_3$, 400 MHz, δ ppm): 4.65(1H, t, H^1), 1.64(1H, d, H^{2a}), 1.95(1H, d, H^{2b}), 4.55(1H, t, H^3), 2.12(1H, t, H^5), 1.92(1H, t, H^{6a}), 1.55(1H, s, H^{6b}), 4.45(1H, t, H^9), 1.50(1H, s, H^{11a}), 1.88(1H, t, H^{11b}), 2.16(1H, d, H^{12a}), 1.57(1H, t, H^{12b}), 3.45(1H, s, H^{15}), 5.53(1H, s, H^{17}), 0.94(3H, s, H^{18}), 0.74(3H, s, H^{19}), 7.17(1H, s, H^{21}), 7.12(1H, s, H^{22}), 2.08(3H, s, H^{25}), 2.29(3H, s, H^{26}), 1.01(3H, s, H^{28}), 0.85(3H,s, H^{29}), 7.33(1H, m, $H^{1'}$), 7.34(1H, t, $H^{2'}$), 6.24(1H, dd, $H^{3'}$), 2.79(1H, dd, $H^{5'}$), 1.60(1H, d, $H^{6'a}$) and 2.19(1H, d, $H^{6'b}$).

SAMPLE CODE =TUN007

3.4.4 Reaction of $[(1\text{-}5\text{-}\eta\text{-}C_6H_7)Fe(CO)_3][BF_4]$ with polyavolensinol. The reaction is given as follows:

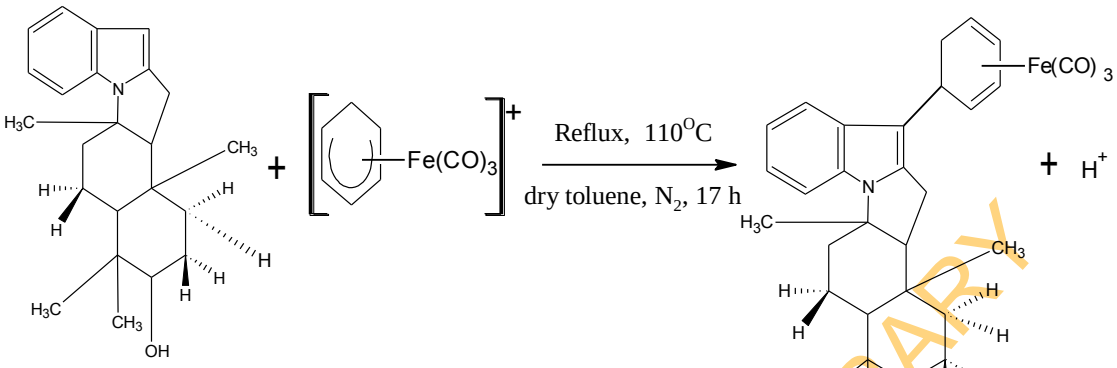

polyavolensinol

(22)

Procedure:

Tricarbonyl [1,4-η-5-(polyavolensinol)cyclohexa-1,3-diene]iron (22**):**

$[C_6H_7Fe(CO)_3]BF_4$ (0.025 g, 0.0817 mmoles) was weighed followed by the addition of a two-fold molar excess of polyavolensinol (0.0551 g, 0.1634 mmoles). A similar work-up as for Gedunin above was followed. A light lilac solid was obtained and dried in a vacuum line for 3 h. The yield of product, 0.024 g was 53%. The IR measurement showed √ (CO) bands at 2042 cm^{-1} and 1963 cm^{-1}.

$C_{32}H_{37}NO_4Fe$: Light lilac solid, **IR** (film) ν_{max} cm^{-1}= 2962 (C-H str of alkanes), 2042 and 1963((√ (CO) bands of coordinated diene of organometallic moiety), 1453 (C-C str aromatic), 1258(CH_3 of alkanes), 1011 (C-O str alcohol), 853 (C-H out of plane), 580 and 561(Fe-C band). **EMS m/z (relative intensity %): MS(555.6),** 207(100) [M-(2CO)-($C_{16}H_{13}ONFe$)-(H^+)], 248(29.4) [M-(2CO)-($C_{16}H_{13}ONFe$)-(H^+)], 279(8.8) [M-(2CO)-($C_{15}H_{26}O$)+($2H^+$)], 338(7.5) [M-(2CO)-(C_7H_7OFe)+($2H^+$)], 390(8.8) [M-(2CO)-(C_3H_2OFe)+(H^+)], 467(12.5) [M-(2CO)-(CH_3OH)], 485(8.8) [M-(2CO)-(CH_2)]. **^{1}Hnmr** ($CDCl_3$, 400 MHz, δ ppm): 7.24(1H, d, H^1), 7.46(1H, t, H^2), 7.26(1H, t, H^3), 7.47(1H, d, H^4), 3.25(1H, d, H^{9a}), 3.23(1H, d, H^{9b}), 3.19(1H, t, H^{10}), 2.63(1H, d, H^{12a}), 1.98(1H, t, H^{12b}), 1.54(1H, t, H^{13a}), 2.29(1H, s, H^{13b}), 2.56(1H, t, H^{14}), 3.22(1H, t, H^{16}), 2.60(1H, d, H^{17a}), 1.49(2H, s, $H^{17b\&20}$), 1.31(1H, t, H^{18a}), 1.37(1H, d, H^{18b}), 0.98(3H, d, H^{21}), 1.14(3H, s, H^{22}), 0.80(3H, s, H^{23}), 6.10(1H, s, OH proton),

6.97(1H, d, $H^{1'}$), 7.00(1H, d, $H^{3'}$), 6.93(1H, t, $H^{4'}$), 2.73(1H, q, $H^{5'}$) and 2.15(1H, dd, $H^{6'b}$).

SAMPLE CODE =TUN006

Reactions of [(1-5-η-2-MeOC$_6$H$_6$)Fe(CO)$_3$][BF$_4$] with Natural Products Nucleophiles

3.5.1 Reaction of [(1-5-η-2-MeOC$_6$H$_6$) Fe(CO)$_3$][BF$_4$] with gedunin. The reaction is represented as follows:

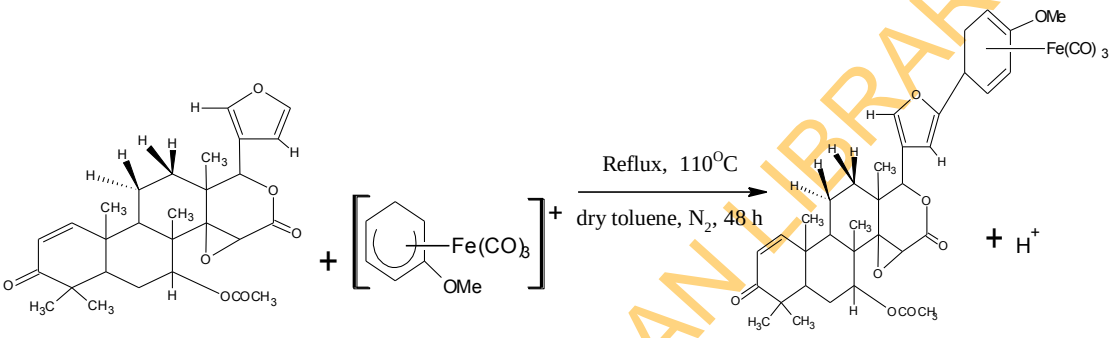

Gedunin (23)

Procedure:

Tricarbonyl [1,4-η-2-methoxy-5-(gedunino)cyclohexa-1,3-diene]iron (23**):**

Following the method for gedunin above, (0.0625 g, 0.01861 mmoles) of [(2-MeOC$_6$H$_6$)Fe(CO)$_3$]BF$_4$ was weighed followed by the addition of a ten-fold molar excess of gedunin (0.1795 g, 0.3723 mmoles). Thick yellow oil was obtained which was dried in a vacuum line for 3 h. The product yield was 46%. This gave √(CO) IR band at 2059 and 1989 cm^{-1}.

C$_{38}$H$_{42}$O$_{11}$Fe: Yellow oil, IR (film) ν_{max} cm^{-1}= 2962(C-H str alkane), 2060 and 1990 (√(CO) band of coordinated diene of organometallic moiety), 1733(C=O str esters), 1667(C=O of αβ-unsat ketone grp), 1368-1163(C-O str esters), 874(furan band), 694 (Fe-C band). **EMS m/z (relative intensity %): MS(730.7),** 107 (1.0) [M-(2CO)-(C$_{29}$H$_{34}$O$_8$Fe)–(H$^+$)], 151 (2.0) [M-(2CO)-(C$_{26}$H$_{28}$O$_8$Fe)-(H$^+$)], 173 (13.0) [M-(2CO)-(C$_{25}$H$_{28}$O$_8$Fe)-(H$^+$)], 412 (1.0) [M-(2CO)-(C$_{16}$H$_{22}$O$_3$)], 467 (3.0) [M(2CO)(C$_9$H$_{11}$O$_2$Fe)] , 505 (100) [M-(2CO)-(C$_6$H$_7$O$_2$Fe)-(2H$^+$)], 506 (20.0) [M-(2CO)-(C$_6$H$_7$O$_2$Fe)-(H$^+$)], 507 (7.0) [M-(2CO)-(C$_6$H$_7$O$_2$Fe)], 537 (16.0) [M-(2CO)-(C$_9$H$_{12}$O)-(H$^+$)], 546 (15.0) [M-(2CO)-(C$_3$H$_3$O$_2$Fe)-(H$^+$)], 547 (4.0) [M-(2CO)-(C$_3$H$_3$O$_2$Fe)], 603 (3.0) [M-(2CO)-(C$_3$H$_4$O$_2$)+(H$^+$)]. **^{1}Hnmr**(CDCl$_3$, 400 MHz, δ ppm): 7.12(1H, d,H^1), 5.82(1H, s, H^2), 5.55(1H, s, H^7), 1.85(1H, d, H^{11b}), 1.75(1H, m,

H^{12b}), 3.5(1H,s, H^{15}), 5.75(1H, s, H^{17}), 1.50(3H, s, H^{18}), 1.25(3H, s, H^{19}), 7.38(1H, s, H^{21}), 6.30(1H, s, H^{22}), 1.00(3H, s, H^{28}), 1.30(3H, s, H^{29}), 1.18(3H, s, H^{30}), 2.03(3H, s, H^{32}), 3.40(3H, q, $H^{33(methoxy)}$), 2.49(1H, dd,$H^{5'}$), 2.32(1H, s, $H^{6'a}$), 2.15(1H, d, $H^{6'b}$).

SAMPLE CODE =TUN009

3.5.2 Reaction of $[(1\text{-}5\text{-}\eta\text{-}2\text{-}MeOC_6H_6)Fe(CO)_3][BF_4]$ with khivorin. The preparation is given thus:

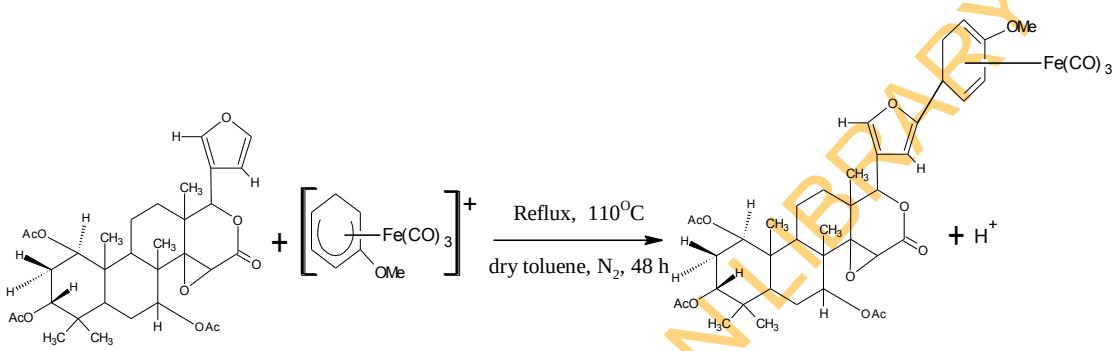

khivorin (24)

Procedure:

Tricarbonyl [1,4-η-2-methoxy-5-(khivorino)cyclohexa-1,3-diene]iron (24**):** $[(2\text{-}MeOC_6H_6)Fe(CO)_3]BF_4$ (0.0125 g, 0.03723 mmoles) and a ten-fold molar excess of khivorin (0.2183 g, 0.3723 mmoles) were weighed. This was followed by the same method for Gedunin above. A yellow flaky solid was obtained and dried in a vacuum line for 3 h. The product yield was 50%. This gave √(CO) IR band at 2060 and 1974 cm^{-1} .

$C_{40}H_{46}O_{13}Fe$: Yellow solid, IR (film) ν_{max} cm^{-1} = 2962 (C-H str alkane), 2060 and 1990 (√ (CO) band of coordinated diene of organometallic moiety), 1727 (C=O str esters), 1376 to1042 (C-O str esters), 801 (furan band), 731 (C-H vibration), 696 (Fe-C band). **EMS m/z (relative intensity %): MS(790.8),** 173(18.0) [M-(2CO)-($C_{29}H_{40}O_{10}Fe$)-(H^+)], 229(3.0) [M-(2CO)-($C_{29}H_{42}O_{10}Fe$)+(H^+)], 257(9.0) [M-(2CO)-($C_{28}H_{39}O_9$)-($2H^+$)], 541(2.0) [M-(2CO)-($C_{10}H_{12}O_3Fe$)-(H^+)], 609(100) [M-(2CO)-($C_6H_7O_2Fe$)-($2H^+$)], 707(2.0) [M-(2CO)-($C_3H_3O_2$)]. **^{1}Hnmr (**$CDCl_3$, 400 MHz, δ ppm): 5.38(1H, m, H^1), 1.18(1H, d, H^{2a}), 1.98(1H, d, H^{2b}), 5.28(1H, m, H^3), 2.44(1H, d, H^5), 3.72(1H, m, H^9), 1.52(1H, s, H^{11a}), 2.45(1H, m, H^{12a}), 2.18(1H, m, H^{12b}), 0.83(3H, s, H^{18}), 1.07(3H, s, H^{19}), 7.17(1H, s, H^{21}), 6.26(1H, m, H^{22}), 2.29(3H, s, H^{31}), 1.89(3H,s, H^{32}), 3,63(3H, s, $H^{33(methoxy)}$), 7.12(1H, d, $H^{3'}$), 7.33(1H, m, $H^{4'}$), 3.40(1H, d, $H^{5'}$), 2.69(1H, m, $H^{6'a}$), 2.65(1H, m, $H^{6'b}$). **SAMPLE CODE =TUN010**

3.5.3 Reaction of [(1-5-η-2-MeOC$_6$H$_6$)Fe(CO)$_3$][BF$_4$] with 7-ketokhivorin. The reaction is shown below:

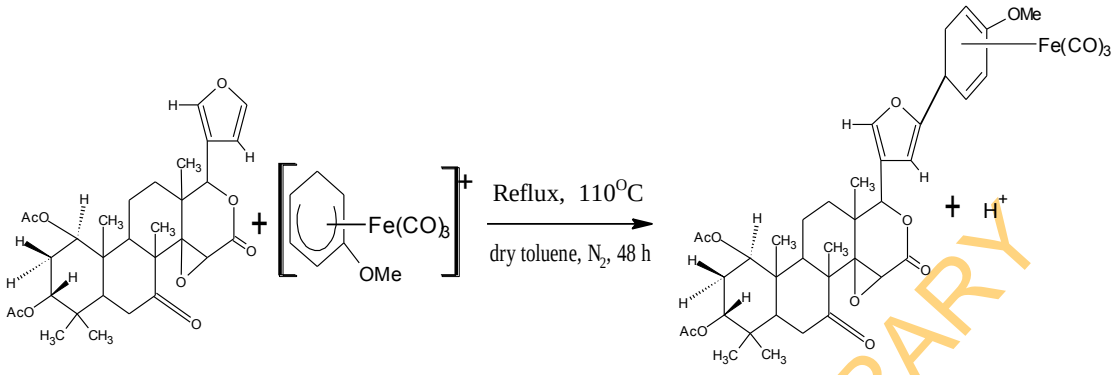

7-ketokhivorin (25)

Procedure:

Tricarbonyl[1,4-η-2-methoxy-5-(7-ketokhivorino)cyclohexa-1,3-diene]iron (25**):** [(2-MeOC$_6$H$_6$)Fe(CO)$_3$]BF$_4$ (0.0125 g, 0.03723 mmoles) and a ten-fold molar excess of 7-ketokhivorin (0.2067 g, 0.3723 mmoles) were weighed followed by the same method as for Gedunin above. A yellow solid was obtained and dried in a vacuum line for 3 h. The yield of product was 45%. This gave √ (CO) IR band at 2060 and 1989 cm^{-1}.

C$_{40}$H$_{46}$O$_{13}$Fe: Yellow solid, IR (film) ν_{max} cm^{-1} = 2962 (C-H str alkane), 2060 and 1990 (√ (CO) band of coordinated diene of organometallic moiety), 1727 (C=O str esters), 1376 to 1042 (C-O str esters), 801 (furan band), 731 (C-H vibration), 696 (Fe-C band). **EMS m/z (relative intensity %): MS(790.8),** 152(5.0) [M-(2CO)-(C$_{33}$H$_{41}$O$_9$)-(H$^+$)], 173(65.0) [M-(2CO)-(C$_{27}$H$_{36}$O$_9$Fe)-(H$^+$)], 205(2.0) [M-(2CO)(C$_{29}$H$_{37}$O$_9$)], 254(3.0) [M-(2CO)-(C$_{24}$H$_{24}$O$_7$Fe)], 383(2.0) [M-(2CO)-(C$_{20}$H$_{30}$O$_5$)-(H$^+$)], 494(3.0) [M-(2CO)-(C$_{13}$H$_{20}$O$_4$)], 541(9.0) [M-(2CO)-(C$_8$H$_9$O$_2$Fe)], 565(100) [M-(2CO)-(C$_6$H$_7$O$_2$Fe)-(2H+)], 581(43.0) [M-(2CO)-(C$_5$H$_5$O$_2$Fe)]. **^{1}Hnmr (**CDCl$_3$, 400 MHz, δ ppm): 5.38(1H, m, H^1), 1.18(1H, d, H^{2a}), 1.98(1H, d, H^{2b}), 5.28(1H, m, H^3), 2.44(1H, d, H^5), 3.72(1H, m, H^9), 1.52(1H, s, H^{11a}), 2.45(1H, m, H^{12a}), 2.18(1H, m, H^{12b}), 0.83(3H, s, H^{18}), 1.07(3H, s, H^{19}), 7.17(1H, s, H^{21}), 6.26(1H, m, H^{22}), 2.29(3H, s, H^{31}), 1.89(3H,s, H^{32}), 3,63(3H, s, H$^{33(methoxy)}$), 7.12(1H, d, H$^{3'}$), 7.33(1H, m, H$^{4'}$), 3.40(1H, d, H$^{5'}$), 2.69(1H, m, H$^{6'a}$), 2.65(1H, m, H$^{6'b}$). **SAMPLE CODE =TUN011**

3.6 Demetallation of Adducts

Demetallation reaction was carried out according to the method of (Shvo and Hazum, 1974) using the oxidizing agent, trimethylamine-N-oxide as given below:

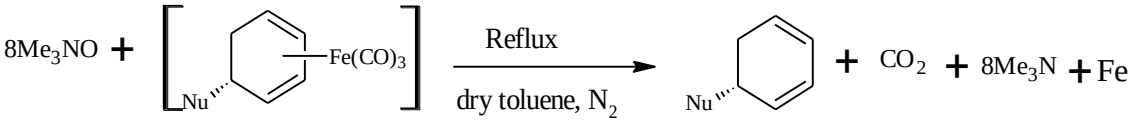

3.6.1 Demetallation of Tricarbonyl [1-4-η-5-(gedunino) cyclohexa-1,3-diene] iron. The reaction is represented thus:

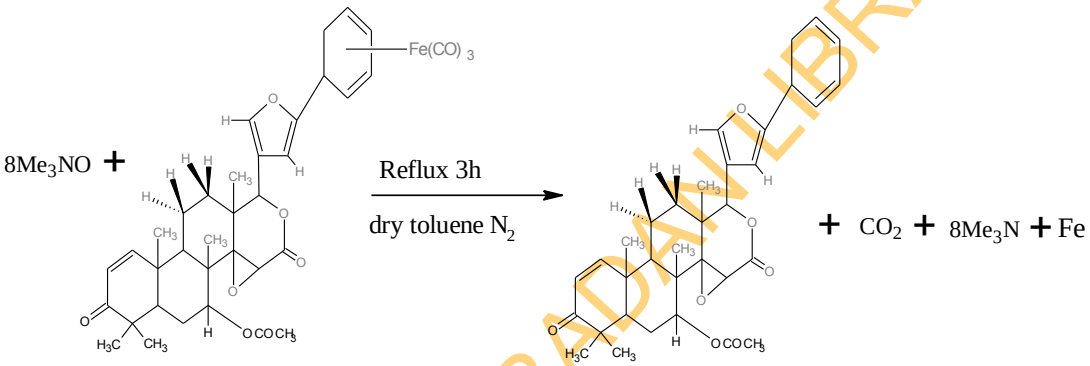

(26)

Procedure:

5-exo-(gedunino) cyclohexa-1,3-diene (26**):**

The adduct (0.1472 g, 0.2339 mmoles) was weighed into a three-necked round-bottom flask (50 mL) and an eight-fold molar excess of Me_3NO (0.1406 g, 1.8721 mmoles) was added under nitrogen in 25 mL dry toluene. The solution was refluxed and the progress of the demetallation reaction was monitored by IR measurement on hourly basis until the disappearance of √(CO) IR bands at 2045 and 1970 cm^{-1} was observed. Demetallation reaction was completed in 3 h. The solution was allowed to cool down to room temperature and was filtered under nitrogen through a celite column to give a yellow filtrate. This was concentrated on a rotary evaporator at reduced pressure to give yellow oil. The product yield was 45%. The IR spectrum of the oil showed absence of the √ (CO) bands earlier observed at 2045 and 1970 cm^{-1}.

$C_{34}H_{40}O_7$: Yellow oil, **IR** (film) ν_{max} cm^{-1}= 2962 (C-H str of alkanes), 1736 (C=O str ester), 1667 (αβ-unsaturated ketone), 1368 (C-H rock of alkanes), 1258 and 1232(C-O str ester), 874 (furan band). **EMS m/z (relative intensity %): MS(560.7),** 151(70.4)

[M-$C_{24}H_{25}O_6$], 173(100) [M-$C_{23}H_{30}O_5$-H^+], 174(6.3) [M-$C_{23}H_{30}O_5$], 422(0.6) [M-$C_8H_{10}O_2$-H^+], 500(3.1) [M-$C_2H_3O_2$-H^+]. **^{1}Hnmr (**$CDCl_3$, 400 MHz, δ ppm): 7.35(1H, d, H^1), 5.79(1H, s, H^2), 1.77(1H, d, H^{6a}), 2.43(1H, q, H^{6b}), 4.49(1H, m, H^7), 2.12(1H, d, H^9), 1.74(1H, t, H^{11a}), 1.86(1H, t, H^{11b}), 1.89(1H, m, H^{12a}), 1.80(1H, t, H^{12b}), 3.46(1H, s, H^{15}), 5.55(1H, s, H^{17}), 1.56(3H, s, H^{18}), 1.16(3H, s, H^{19}), 7.05(1H, s, H^{21}), 7.02(1H, s, H^{22}), 1.09(3H, s, H^{28}), 1.18(3H, s, H^{29}), 1.01(3H, d, H^{30}), 2.04(3H, s, H^{32}), 5.81(1H, s, $H^{1'}$), 6.27(1H, t, $H^{4'}$), and 3.25(1H, s, $H^{5'}$).

SAMPLE CODE= TUN 004(DM)

3.6.2 Demetallation of Tricarbonyl [1-4-η-5-(khivorino) cyclohexa-1,3-diene] iron. The preparation is given as follows:

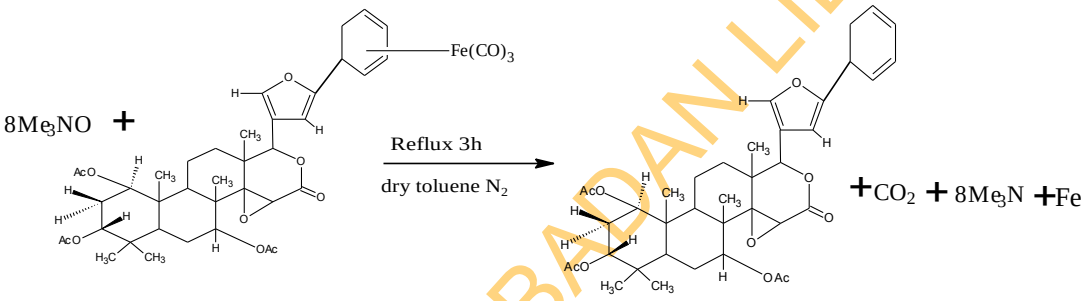

(27)

Procedure:

5-exo-(khivorino) cyclohexa-1,3-diene (27)**:**

The adduct (0.0994 g, 0.1235 mmoles) was weighed into the flask and an eight-fold molar excess of Me_3NO (0.0743 g, 0.9887 mmoles) was added. A similar work-up as for Gedunin above produced a yellow oil. The product yield was 50%. The IR √(CO) bands was observed at 2050 and 1980 cm^{-1}.

$C_{38}H_{48}O_{10}$: Yellow oil, **IR** (film) ν_{max} cm^{-1}= 2962 (C-H str of alkanes), 1728 (C=O str ester), 1257 and 1012(C-O str ester), 863 (furan band), 696 (C-H out of plane aromatics). **EMS m/z (relative intensity %): MS(664.7),** 173(66.7) [M-$C_{27}H_{38}O_8$-H^+], 271(6.8) [M-$C_{22}H_{34}O_6$+H^+], 560(1.6) [M-C_8H_8], 609(100) [M-C_4H_5-$2H^+$]. **^{1}Hnmr** ($CDCl_3$, 400 MHz, δ ppm): 4.55(1H, t, H^1), 1.90(1H, s, H^{2a}), 1.95(1H, s, H^{2b}), 4.45(1H, t, H^3), 1.77(1H, s, H^{6a}), 2.16(1H, d, H^{6b}), 4.64(1H, t, H^7), 1.58(1H, s, H^{11a}), 2.04(1H, d, H^{11b}), 2.00(1H, d, H^{12b}), 3.45(1H, s, H^{15}), 1.17(3H, s, H^{18}), 0.74(3H, s, H^{19}), 5.53(1H, s, H^{22}), 0.85(3H, s, H^{28}), 1.01(3H, s, H^{29}), 0.94(3H, s, H^{30}), 2.29(3H, s,

H^{32}), 2.11(3H, s, H^{33}), 2.08(3H, s, H^{34}), 7.33(1H, m, $H^{1'}$), 6.24(1H, dd, $H^{2'}$) and 7.35(1H, t, $H^{3'}$).

SAMPLE CODE= TUN 005(DM)

3.6.3 Demetallation of Tricarbonyl [1,4-η-5(7-ketokhivorino)cyclohexa-1,3-diene] iron.

The reaction is as shown:

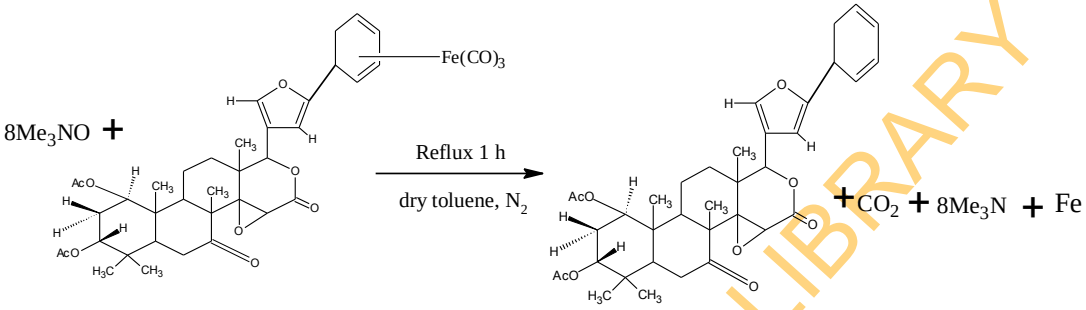

(28)

Procedure:

5-exo-(7-ketokhivorino) cyclohexa-1,3-diene (28)**:**

The adduct (0.1562 g, 0.2017 mmoles) and an eight-fold molar excess of Me_3NO (0.1212 g, 1.61392 mmoles) were weighed followed by the same demetallation method as for Gedunin adduct above. Yellow oil was also obtained. The product yield was 35%. The IR √ (CO) band for the oil was observed at 2050 and 1980 cm^{-1}.

$C_{36}H_{44}O_9$: Yellow oil, **IR** (film) ν_{max} cm^{-1}= 2962 (C-H str of alkanes), 1728 (C=O str of ester), 1257 and 1014 (C-O str of ester), 874 (furan band).

EMS m/z (relative intensity %): MS(620.7), 173(3.4) [M-$C_{25}H_{34}O_7$-H^+], 485(2.8) [M-C_9H_9O-$2H^+$], 516(0.6) [M-C_8H_8], 541(2.8) [M-C_8H_8], 609(100) [M-CH+$2H^+$].

^{1}Hnmr ($CDCl_3$, 400 MHz, δ ppm): 4.64(1H, t, H^1), 1.95(1H, d, H^{2a}), 4.55(1H, t, H^3), 2.13(1H, t, H^5), 1.92(1H, t, H^{6a}), 1.57(1H, d, H^{6b}), 4.45(1H, t, H^9), 1.51(1H, s, H^{11a}), 1.85(1H, t, H^{11b}), 2.16(1H, s, H^{12a}), 1.88(1H, t, H^{12b}), 3.45(1H, s, H^{15}), 5.53(1H, s, H^{17}), 0.94(3H, s, H^{18}), 0.73(3H, s, H^{19}), 7.07(1H, s, H^{21}), 2.08(3H, s, H^{25}), 2.29(3H, s, H^{26}), 1.01(3H, s, H^{28}), 0.84(3H, s, H^{29}), 7.33(1H, m, $H^{1'}$), 7.34(1H, t, $H^{2'}$), 6.24(1H, dd,$H^{3'}$), 7.32(1H, m, $H^{4'}$), 2.79(1H, dd, $H^{5'}$), 1.63(1H, d, $H^{6'a}$) and 2.19(1H, d, $H^{6'b}$).

SAMPLE CODE = TUN007 (DM).

3.6.4 Demetallation of Tricarbonyl [1,4-η-5-(polyavolensinol)cyclohexa-1,3-diene] iron. The reaction is given as follows:

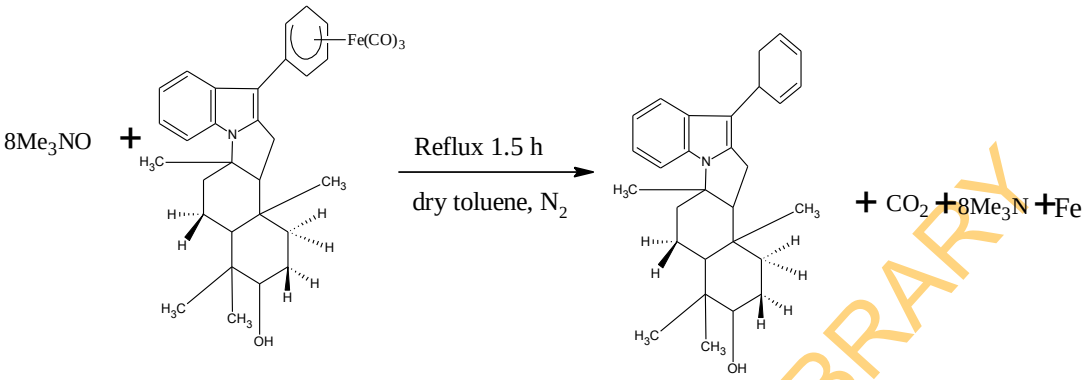

(29)

Procedure:

5-exo-(polyavolensinolino) cyclohexa-1,3-diene (29):

Polyavolensinol adduct (0.1358 g, 0.2446 mmoles) and an eight-fold molar excess of Me_3NO (0.1470 g, 1.9568 mmoles) were weighed followed by the same demetalation method for Gedunin adduct above. Yellow oil which was sensitive to air was obtained. The yield of the product was 35%.

$C_{29}H_{37}NO$: Yellow oil, **IR** (film) ν_{max} Cm-1 = 2961 (C-H str of alkanes), 1604 (C=C str aromatic), 1495 and 1453(C-C str aromatic), 1258 and 1010 (C-O str alcohol), 790 (C-H out of plane).

SAMPLE CODE= TUN 006(DM)

3.6.5 Demetallation of Tricarbonyl [1-4-η-2-methoxy-5-(gedunino) cyclohexa-1,3-diene] iron. The reaction is represented thus:

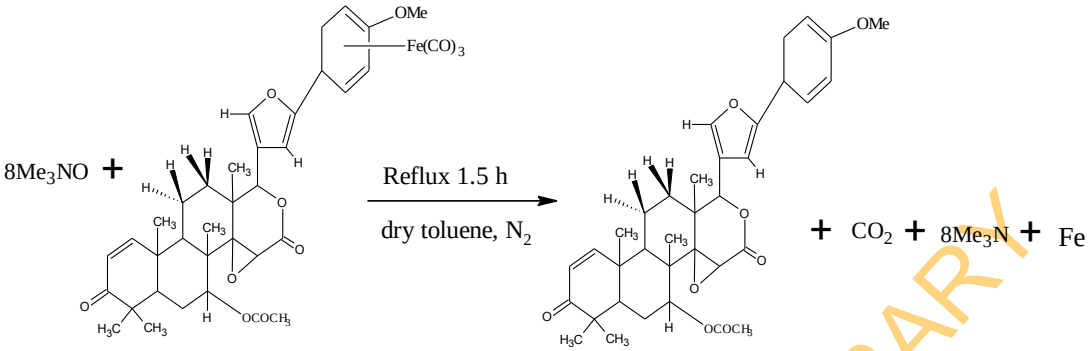

(30)

Procedure:

2-methoxy-5-exo-(gedunino) cyclohexa-1,3-diene (30)**:**

The adduct (0.2197 g, 0.30086 mmoles) and an eight-fold molar excess of Me_3NO (0.1808 g, 2.40688 mmoles) were weighed followed by the same demetallation method for Gedunin adduct above. Colourless oil was obtained. The yield of the product was 58%.

$C_{35}H_{42}O_8$: Colourless oil, **IR** (film) ν_{max} cm^{-1}= 2962 (C-H str of alkanes), 1737 (C=O str esters), 1257 (C-O str esters), 1009 (C-O str ester), 874 (furan band), 789 (C-H vib). **EMS m/z (relative intensity %: MS (590.7),** 151(8.0) [M-($C_{26}H_{32}O_6$)+(H^+)], 173(30.0) [M-($C_{24}H_{31}O_6$)-(2H^+)], 301(9.0) [M-($C_{18}H_{26}O_3$)+(H^+)], 366(25.0) [M-($C_{13}H_{18}O_3$)-(2H^+)], 371(100) [M-($C_{13}H_{14}O_3$)-(H^+)], 372(18.0) [M-($C_{13}H_{14}O_3$)], 387 (5.0) [M-($C_{12}H_{12}O_3$)+(H^+)], 413(10.0) [M-($C_{11}H_{11}O_2$)-(2H^+)], 467(12.0) [M-($C_8H_{12}O$)+(H^+)], 468(4.0) [M-($C_8H_{12}O$) + (2H^+)], 500(29.0) [M-($C_3H_6O_3$)], 505(100) [M-($C_4H_6O_2$) + (H^+)], 506(29.0) [M-($C_4H_6O_2$) +(2H^+)], 521(8.0) [M-(C_4H_5O)], 536(29.0) [M-(C_3H_2O)]. **^{1}Hnmr** ($CDCl_3$, 400 MHz, δ ppm): 7.12(1H, d, H1), 5.80(1H, s, H2), 2.28(1H, s, H6b), 5.55(1H, s, H7), 2.11(1H, s, H12a), 1.7(1H, d, H12b), 3.45(1H, s, H15), 5.78(1H, s, H17), 1.50(3H, s, H18), 1.18(3H, s, H19), 7.32(1H, s, H21), 6.25(1H, s, H22), 1.00(3H, s, H28), 1.20(3H, s, H29), 1.10(3H, s, H30), 2.02(3H, s, H32), 3.24(3H, s, H33(methoxy)), 4.49(1H, m, H1'), 6.80(1H, d, H4'), 2.45(1H, dd,H5').

SAMPLE CODE = TUN009 (DM)

3.6.6 Demetallation of Tricarbonyl [1,4-η-2-methoxy-5-(khivorino)cyclohexa-1,3-diene]iron.

The reaction is given as follows:

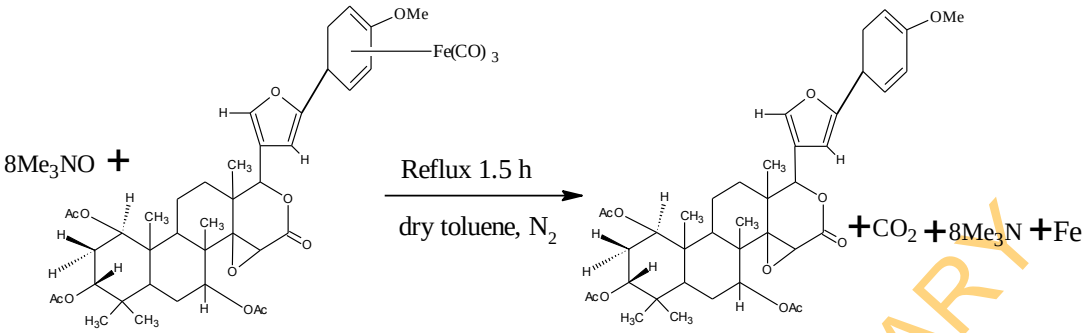

(31)

Procedure:

2-methoxy-5-exo-(khivorino) cyclohexa-1,3-diene (31)**:**

The adduct (0.1878 g, 0.2251 mmoles) and an eight-fold molar excess of Me_3NO (0.1353 g, 1.80096 mmoles) were weighed followed by the same demetallation method for Gedunin adduct above. Yellow oil was obtained. The yield of the product was 40%.

$C_{39}H_{50}O_{11}$: Yellow oil, **IR** (film) ν_{max} cm^{-1}= 2962 (C-H str of alkanes), 1728 (C=O str esters), 1374-1020 (C-O str esters), 874 (furan band), 796 (C-H vib). **EMS m/z (relative intensity %: MS (694.8),** 130(2.0) [M-($C_{32}H_{38}O_9$)+($2H^+$)], 15185.0) [M-($C_{30}H_{40}O_9$)+(H^+)], 173(100) [M-($C_{28}H_{39}O_9$)], 462(6.0) [M($C_{13}H_{14}O_4$)+($2H^+$)], 536(10.0) [M($C_7H_{10}O_4$)], 560(1.0) [M-($C_7H_{10}O_4$)], 609(93.0) [M-($C_4H_6O_2$)+(H^+)]. **^{1}Hnmr** ($CDCl_3$, 400 MHz, δ ppm): 4.55(1H, s, H^1), 1.38(1H, t, H^{2a}), 2.15(1H, t, H^{2b}), 1.57(1H, s, H^{6a}), 4.65(1H, s, H^7), 1.85(1H, m, H^{11a}), 1.89(1H, m, H^{12b}), 3.45(1H, s, H^{15}), 1.17(3H, s, H^{18}), 6.24(1H, s, H^{21}), 5.53(1H, s, H^{22}), 0.85(3H, s, H^{28}), 1.01(3H, s, H^{29}), 0.94(3H, s H^{30}), 2.29(3H, s, H^{31}), 2.08(3H, s, H^{32}), 1.95(3H, s, H^{33}), 3.25(3H, s, $H^{34(methoxy)}$), 4.45(1H, s, $H^{1'}$), 7.34(1H, d, $H^{3'}$), 6.79(1H, d, $H^{4'}$), 2.79(1H, m, $H^{5'}$).

SAMPLE CODE = TUN010 (DM)

3.6.7 Demetallation of Tricarbonyl [1,4-η-2-methoxy-5-(7-ketokhivorino) cyclohexa-1,3-diene] iron.

The reaction is represented thus:

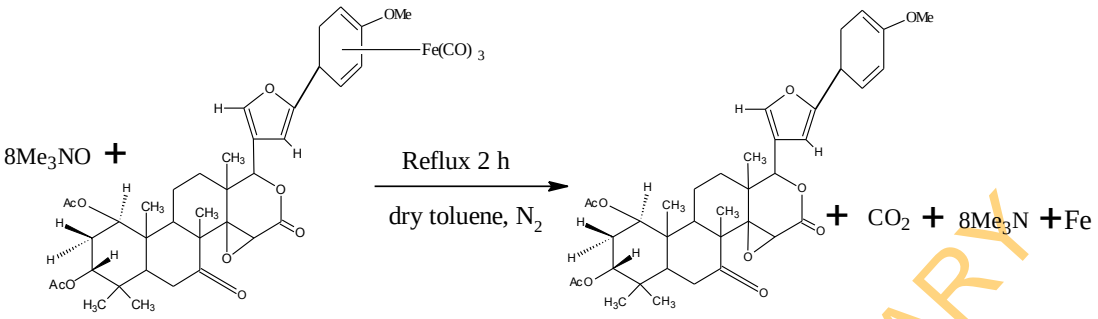

(32)

Procedure:

2-methoxy-5-exo-(7-ketokhivorino) cyclohexa-1,3-diene (32)**:**

The adduct (0.0594 g, 0.07395 mmoles) and an eight-fold molar excess of Me_3NO (0.0444 g, 0.5916 mmoles) were weighed followed by the same demetallation method for Gedunin adduct above. Yellow oil was obtained. The yield of the product was 44%.

$C_{37}H_{46}O_{10}$: Yellow oil, **IR** (film) ν_{max} cm^{-1}= 2962 (C-H str of alkanes), 1258 (C-O str esters), 1008 (C-O str esters), 786 (C-H vib). **EMS m/z (relative intensity %: MS (650.8),** 130(1.0) [M($C_{30}H_{34}O_8$)+(2H+)], 152(100) [M-($C_{28}H_{36}O_8$)+($2H^+$)], 173(15.0) [M-($C_{26}H_{35}O_8$)-($2H^+$)], 200(4.0) [M-($C_{27}H_{30}O_6$)], 242(10.0) [M-($C_{24}H_{26}O_6$)+($2H^+$)], 462(11.0) [M-($C_{12}H_{12}O_2$)], 536(10.0) [M-($C_6H_{10}O_2$)], 565(73.0) [M-($C_4H_6O_2$)+(H^+)], 606(19.0) [M-(CO_2)]. **^{1}Hnmr** ($CDCl_3$, 400 MHz, δ ppm): 1.10(1H, d, H^{2a}), 1.95(1H, s, H^{2b}), 2.72(1H, m, H^{5a}), 1.52(1H, s, H^{11a}), 2.44(1H, d, H^{12a}), 3.71(1H, s, H^{15}), 0.92(3H, s, H^{18}), 7.17(1H, d, H^{21}), 7.07(1H, m, H^{22}), 1.18(3H, s, H^{30}), 2.29(3H, s, H^{31}), 1.89(3H, s, H^{32}), 3.30(3H, s, $H^{33(methoxy)}$), 7.12(1H, m, $H^{4'}$), 2.13(1H, s, $H^{6'b}$).

SAMPLE CODE = TUN011 (DM)

3.7 Antimicrobial Susceptibility Test

Disc diffusion method of Kirby-Bauer was adopted (Bauer *et al*., 1966). The samples were tested against five standard strains of microorganism, *Candida albicans* MTTC 227, *Bacillus substilis* ATTC 33923, *Bacillus cereus* ATTC 14579, *Proteus mirabilis* ATTC 21784 and *Salmonella typhi* ATTC 14028.

3.7.1 Preparation of Agar

Mueller-Hinton agar was prepared according to the manufacturers' instruction. Twenty-eight gram (28 g) of agar was dissolved in 1000 mL of distilled water. The resultant mixture was heated to dissolve and autoclaved at 121^{o}C for 15 mins. This was allowed to cool down in a 45 to 50^{o}C water bath.

The agar was poured into pre-labelled sterilised plastic petri dishes on a level horizontal surface to give a uniform depth of about 4 mm. The agar mediums in the petri dishes were allowed to set.

3.7.2 Preparation of experimental discs

Whatman filter paper No 1 was used to prepare about 6 mm diameter discs. The discs were sterilised in an autoclave and dispensed using forceps.

3.7.3 Preparation of antibiotic stock

The antibiotics used were: gentamycin for the gram-positive and gram-negative bacteria and ketocanazole for the fungus. The antibiotics solutions were prepared following standard method (Bauer *et al.*, 1966).

3.7.4 Preparation of bacteria inoculum

Inoculum was prepared by picking five distinct colonies using inoculating loop from overnight culture and these colonies were suspended in 2 mL sterile saline. The turbidity of the suspension was adjusted to 0.5 MacFarland standards. The turbidity was adjusted until 1x10^{5} cfu/ mL was achieved.

3.7.5 Procedure for disc diffusion test for bacteria

Sterile swabs were dipped into inoculum tubes of the microorganism used. These were used to inoculate the dried surface of the agar plates by streaking the swab three times over the entire agar surface, rotating the plates at 60^{o}C each time to ensure even distribution of the inoculum. The inoculated plates were left at room temperature for 5 mins. Varied concentrations of synthesised compounds which ranged from 2.5 to 405 mg/mL were dissolved in dimethylsulphoxide (DMSO) and were impregnated on the discs. The impregnated discs were placed on the surface of the agar using forceps.

Likewise, discs impregnated with 0.8 mg/mL gentamycin (positive control) dimethylsulphoxide (negative control) were also placed on the surface of the agar separately. The agar plates were inverted and incubated for 24 h at 35^{o}C. The experiments were carried out in triplicate. The zones of inhibition of bacteria growth around the discs were measured in millimeter using ruler.

3.7.6 Preparation of fungi inoculum

Five distincts colonies were picked from a 24 h old culture grown on Dextrose agar. The colonies were suspended in 5 mL sterile saline. The turbidity of the suspension was adjusted to 0.5 MacFarland standard 1x10^{5} cfu/ mL.

3.7.7 Procedure for discs diffusion test of fungi

This is similar to that of the bacteria above but the plates were prepared with Muller-Hinton agar plus 2% glucose and 0.5 µg/mL methylene blue dye. Also the inoculated discs were incubated at 37^{o}C for 72 h. The positive control for procedure is ketocanazole and the negative control is dimethylsulphoxide (DMSO).

3.8 Method for Determining Minimum Inhibitory Concentrations (MIC).

MIC determination is the quantitative susceptibility test procedure (NCCLS, 2002). This was carried out by employing serial two-fold broth dilution method. Inoculum were prepared by picking five distinct colonies of organisms and suspending in 2 mL sterile saline for bacteria and 5mL sterile distilled water for fungi. The turbidity was adjusted to the density of 0.5 MacFarland standards to give a suspension of 1x10^{5}cfu/mL.

From the stock concentrations of synthesised compounds which ranged from 2.5 to 405 mg/mL, were prepared serially diluted concentrations. A total of 12 tubes were used which were filled with 2 mL each of broth solution. To the first tube was introduced 0.4 mL of the solution of the synthesised compounds. 0.2 mL was taken from the first tube to the second tube. Also 0.2 mL was taken from the second tube and transferred to the third tube and so on to the ninth tube form which 0.2 mL was discarded. The tenth tube contained 2 mL broth and 0.2 mL (4 mg/mL) gentamycin the positive control. The eleventh tube also had 2 mL broth and the negative control (DMSO) while the last tube was the blank. All the tubes were convered with cotton wool and were incubated at 37^{o}C for 24 h. The MIC was taken as the lowest concentration that inhibited the growth of the organism after incubation.

3.9 Computational Methods

The quantum chemical calculations were conducted with Spartan'06 software programme. The structures were fully optimised at DFT levelusing Hybrid Beckie-3-Lee Yang Parr (B3LYP) functional density with 6-31G(d) Basis sets in gaseous state. For the adducts, a combination of basis sets of 6-31G(d) and pseudo potential LCVP* were used.

In the optimized structures, no imaginary vibrational modes were obtained. This indicated that a true local minimum of the potential surface energy was obtained. The following molecular parameters were calculated: HOMO energy, LUMO energy, the energy gap and the dipole moments.

CHAPTER FOUR

RESULTS AND DISCUSSION

4.1 SPECTRAL STUDIES OF DIENYLIUM CATIONS

4.1.1 IR studies of $[(1\text{-}5\text{-}\eta\text{-}C_6H_7)Fe(CO)_3][BF_4]$ and $[(1\text{-}5\text{-}\eta\text{-}2\text{-}MeOC_6H_6)Fe(CO)_3][BF_4]$

Tables 4.1 and 4.2 gave the infra red assignment for $[(1\text{-}5\text{-}\eta\text{-}C_6H_7)\ Fe(CO)_3][BF_4]$ and $[(1\text{-}5\text{-}\eta\text{-}2\text{-}MeOC_6H_6)Fe(CO)_3][BF_4]$. The IR spectrum of $[(1\text{-}5\text{-}\eta\text{-}C_6H_7)Fe(CO)_3[BF_4]$ showed the characteristics IR √(CO) bands at 2108 and 2046 cm^{-1} which is comparable to the values reported by Birch (Birch *et al.*, 1968) and Odiaka (Odiaka, 1980) while that of $[(1\text{-}5\text{-}\eta\text{-}2\text{-}MeOC_6H_6)Fe(CO)_3][BF_4]$ was observed at 2049 and 1963 cm^{-1} (Fig 4.2) with an additional band at 1654 cm^{-1} which is peculiar to methoxy dienylium cations (Birch *et al.*, 1968). However, the presence of the methoxy group was further confirmed by C-O str between 1283 and 1236 cm^{-1}. There is a slight variation with the quoted values of Jones (Jones *et al.*, 1962) but important bands observed by them were corroborated in our findings. There is a band of medium intensity at 3078 cm^{-1} assigned to parent arene cation. The solid state spectrum of $[C_6H_7Fe(CO)_3]BF_4$ does not give a band at 2800 cm^{-1} as reported by Jones *et al.*, (1962) . Its absence is attributed to the charge on the complex cation. Signals at 597 cm^{-1} and 598 cm^{-1} were assigned as metal-carbon bond that is Fe-C bond (Brisdon, 1998).

TABLE 4.1: IR assignment of $[(1\text{-}5\text{-}\eta\text{-}C_6H_7)Fe(CO)_3][BF_4]$ (2)

IR bands (cm^{-1})	Intensity	Assignment
3078	m	Parent arene cation
2108& 2046	v.s	metal-carbonyl band for dienyl (Fe-CO)
1457-1286	m	characteristics absorption of C_6H_7Fe-CO
954-816	m	C-H bending vibration of the alkenes
581-598	v.s	Fe-C bond

Keys: s = sharp, vs = very sharp, m = moderate, b = broad

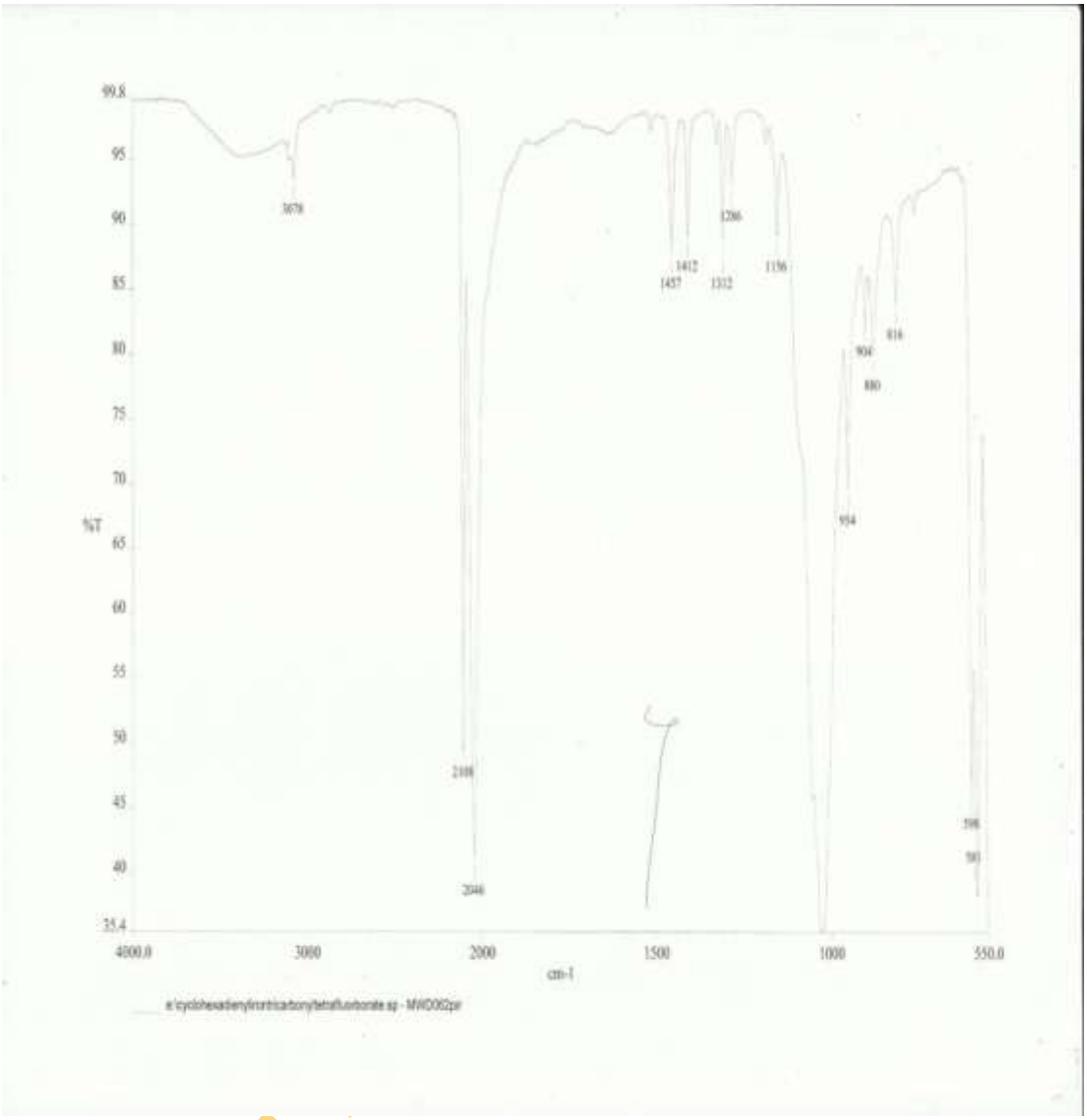

Figure 4.1: IR spectrum of tricarbonyl (cyclohexadienyl) iron tetrafluoroborate (2)

TABLE 4.2: IR assignment for [(1-5-η-2-MeOC$_6$H$_6$)Fe(CO)$_3$][BF$_4$] (3)

IR bands (cm^{-1})	Assignment	Intensity
2049 & 1963	s	√CO band for dienyl
1654	vs	C=C str xteristic of methoxy cyclohexadienyl
1438	m	C=C str aromatic
1415	s	C-C str aromatic
1283 & 1236	s	C-O str methoxide
980-769	s	C-H bending vibration
613	vs	Fe-C band
597	vs	Fe-C band

Keys: s = sharp, vs = very sharp, m = moderate, b = broad

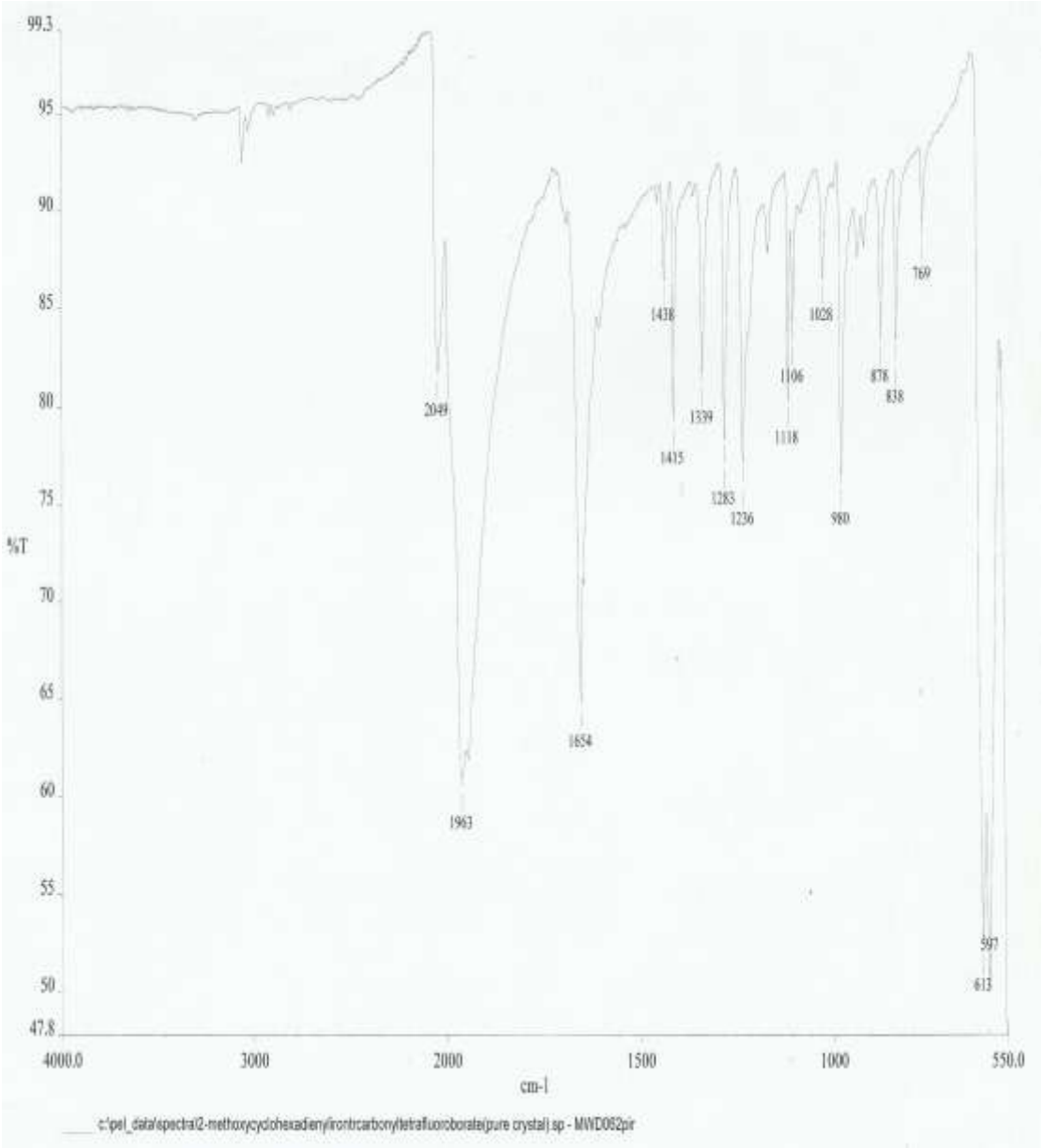

Figure 4.2: IR spectrum of tricarbonyl (2-methoxycyclohexadienyl) irontetra fluoroborate (3)

4.1.2 ^{1}Hnmr studies of [(1-5-η-C_6H_7)Fe(CO)$_3$][BF_4] and [(1-5-η-2-MeOC_6H_6) Fe(CO)$_3$][BF_4]

The ^{1}Hnmr assignments are presented in Tables 4.3 and 4.4 and their structures are shown below

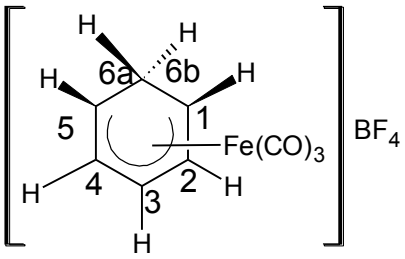

[(1-5-η-C_6H_7)Fe(CO)$_3$][BF_4]

(2)

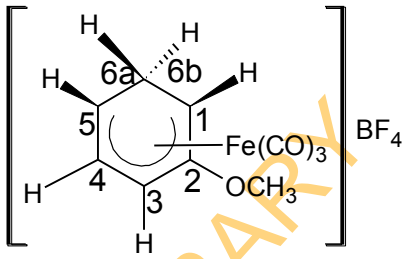

[(1-5-η-2-MeOC_6H_6)Fe(CO)$_3$][BF_4]

(3)

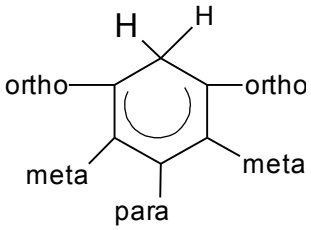

The ^{1}Hnmr spectrum was run using CD_3CN. The proton peaks are shown in the spectrum (Fig 4.3 & 4.4). The subsequent spectra were obtained on expansion of the ^{1}Hnmr spectrum for clarity of the multiplicities of the various peaks. The proton assignments were done using ACD Lab elucidator. There is close similarity in the ^{1}Hnmr spectral values for tricarbonyl (cyclohexadienyl) iron cations and that of its methoxy derivative. The values are similar to the values obtained by Birch *et al* (1968). In [(1-5-η-C_6H_7)Fe(CO)$_3$][BF_4] the para proton (position 3) was the most deshielded as been indicated by its chemical shift value of 7.15 ppm in the aromatic region.

Protons 2 and 4 are chemically equivalent with a chemical shift of 5.83 ppm, the characteristics signal of unsaturated aromatic alkenes. Protons 1 and 5 are also chemicaliy equivalent having the same chemical shift of 4.24 ppm and coupling constant.

TABLE 4.3: **^{1}Hnmr assignment of [(1-5-η-C_6H_7)Fe $(CO)_3$][BF_4]** (2)

Position	**Protons**	**Chemical Shifts(δ) Ppm**	**Jvalues (Hz)**	**Multiplicity**
Methylene	H6a	2.91 & 2.95 (1H)	6	Double triplet (t)
Methylene	H6b	2.17 (1H)	6	Singlet (s)
Ortho	H5	4.24 (2H)	8	Triplet (t)
Meta	H4	5.83	6	Triplet (t)
Para	H3	7.15(1H)	4	Triplet
Meta	H2	5.83	6	Triplet
Ortho	H1	4.24	8	Triplet

δ = (1.95 ppm, multiplet) = Residual solvent signal

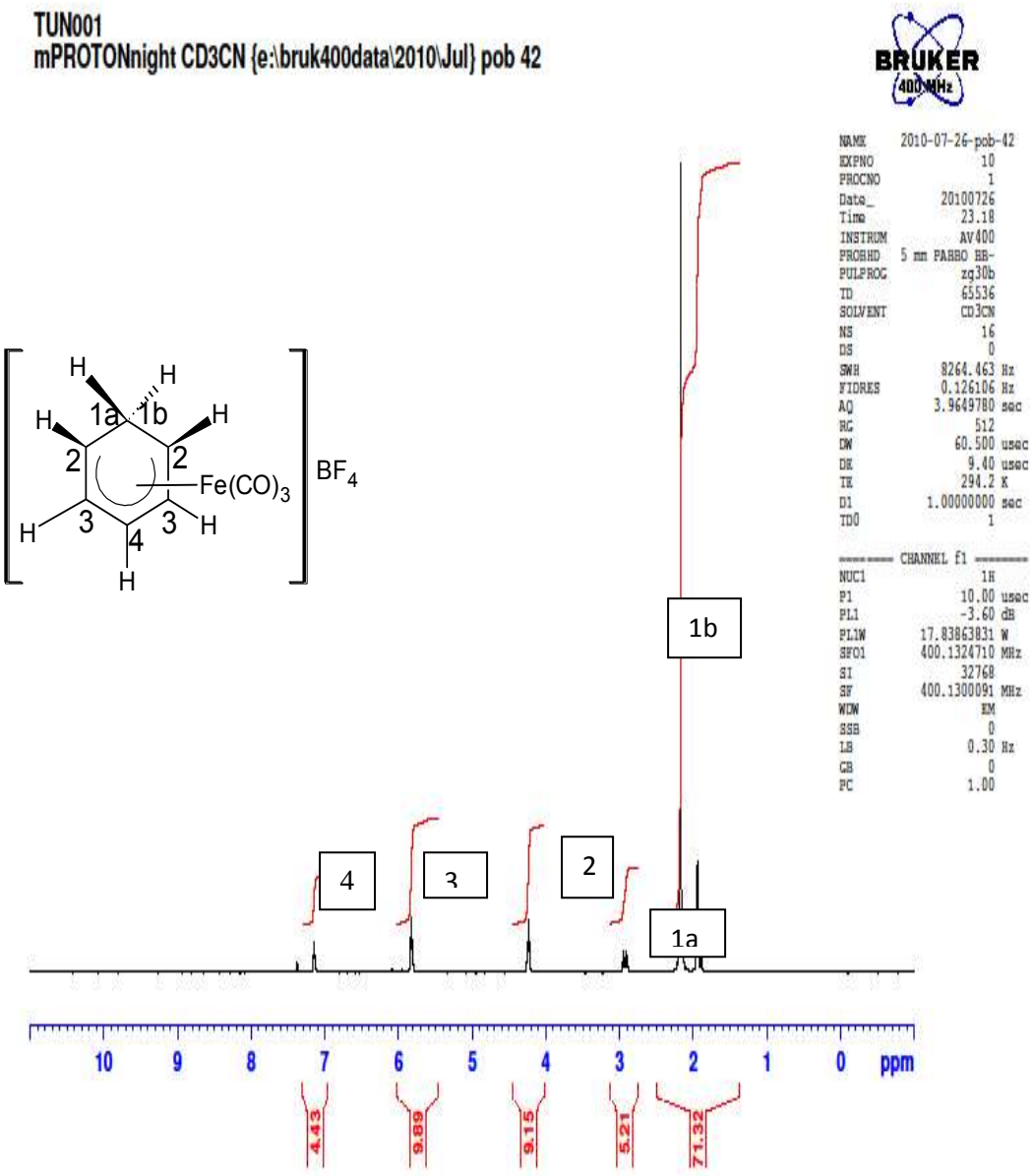

Figure 4.3: ^{1}Hnmr spectrum of tricarbonyl (cyclohexadienyl) iron tetra fluoroborate (2)

TABLE 4.4: ^{1}Hnmr Assignment of [(1-5-η-2-MeOC$_6$H$_6$)Fe(CO)$_3$][BF$_4$] (3)

Position	**Protons**	**Chemical Shifts δ Ppm**	**Multiplicity**
Methylene	H6a	2.31 (1H)	Doublet (d)
Methylene	H6b	2.27 (1H)	Doublet (d)
Ortho	H5	3.34 (1H)	Multiplet (m)
Meta	H4	5.78 (1H)	Multiplet (m)
Para	H3	6.00(1H)	Triplet (t)
Meta(methoxy proton)	H2	2.05 (3H)	Singlet (s)
Ortho	H1	3.10 (1H)	Doublet(d)

δ = (1.87 ppm, multiplet) = Residual solvent signal

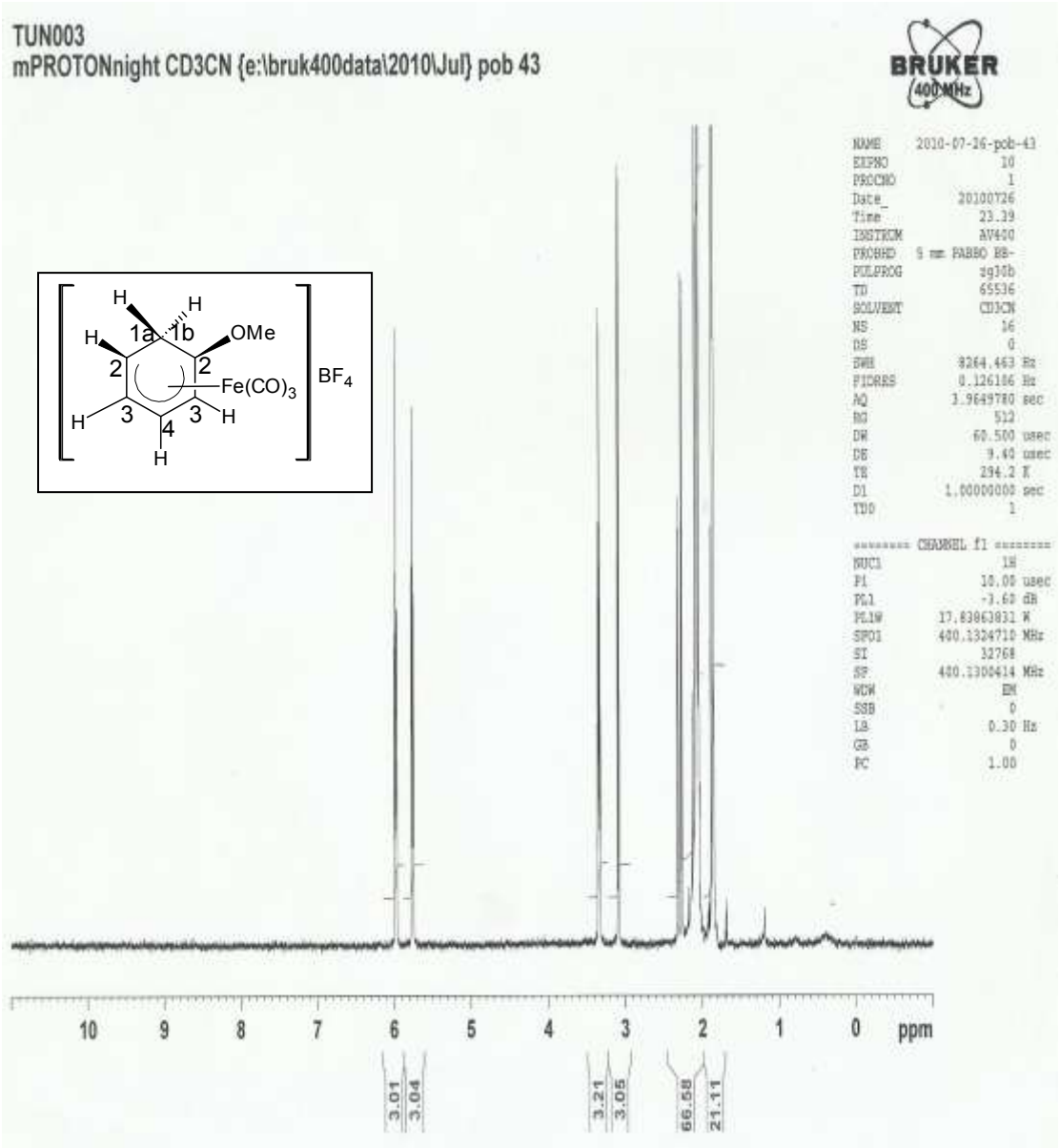

Fig 4.4: ^{1}Hnmr spectrum of tricarbonyl 2-methoxy (cyclohexadienyl)iron tetrafluoroborate (3)

The methylene protons, 6a and 6b, appear as an AB quartet; they are diastotopic in nature and one of the protons gives a double triplet at 2.95 and 2.91 ppm and the other a singlet at 2.17 ppm and 1.89 ppm.

This pattern of splitting was interpreted by Jones (Jones *et al*., 1962) in terms of the non-equivalence of these methylene protons as both coupled in different ways to H^1 and H^2 and also because of the non-planarity of the cyclohexadienyl ring as the methylene carbon is bent out of the other carbons.

4.1.3 ^{13}Cnmr studies of [(1-5-η-C_6H_7)Fe(CO)$_3$][BF_4] and [(1-5-η-2-MeOC_6H_6) Fe(CO)$_3$][BF_4]

The ^{13}Cnmr (CD_3CN) are shown in Fig 4.5 & 4.6. Assignments of NMR peaks were done using ACD lab elucidator as presented in Tables 4.5 & 4.6 respectively.

The values obtained are in agreement with those obtained by Birch *et al.,* (1979) and Brown *et al.,* (1984) though with slight difference. Carbonyl peak was not observed in the spectrum due to the low concentration of the sample but its presence was confirmed by the infra red peak √(CO) band observed at 2108 cm^{-1} and 2048 cm^{-1} which is characteristics of √(CO) band of the dienylium organometallics (Odiaka, 1980).

The methylene carbon was the most shielded with the peak at 22.7 ppm in [(1-5-η-C_6H_7)Fe(CO)$_3$][BF_4] and 54.01 ppm in [(1-5-η-2-MeOC_6H_6)Fe(CO)$_3$][BF_4]**.** The meta carbons (C^1 & C^4) in (2) are the most deshielded at 101.21ppm. In (3**)** C^{1-4} resonate at the same chemical shift values of 117.21 showing their equivalence.

4.1.4 Mass spectral studies of [(1-5-η-C_6H_7)Fe(CO)$_3$][BF_4] and [(1-5-η-2-MeOC_6H_6)Fe(CO)$_3$][BF_4]

The mass spectral data for the dienylium cations (2**)** and (3**)** are presented in Tables 4.7 and 4.8. The assignment of the peaks was done using Mass Spec Professional Calculator by ACD Lab. The expected molecular ions were not observed but fragments of important peaks were observed. For (2**),** the base peak was observed at 191, Fig 4.7 and at 219 in (3**)** Fig 4.8.

TABLE 4.5: ^{13}Cnmr Assignment of [(1-5-η-C_6H_7)Fe $(CO)_3$][BF_4] (2)

Position	Carbon	Chemical shifts (δ) ppm
Ortho	C1	64.10
Meta	C2	101.21
Para	C3	88.74
Meta	C4	101.21
Ortho	C5	64.10
Methylene	C6	22.7

Solvent peak = 117.02ppm

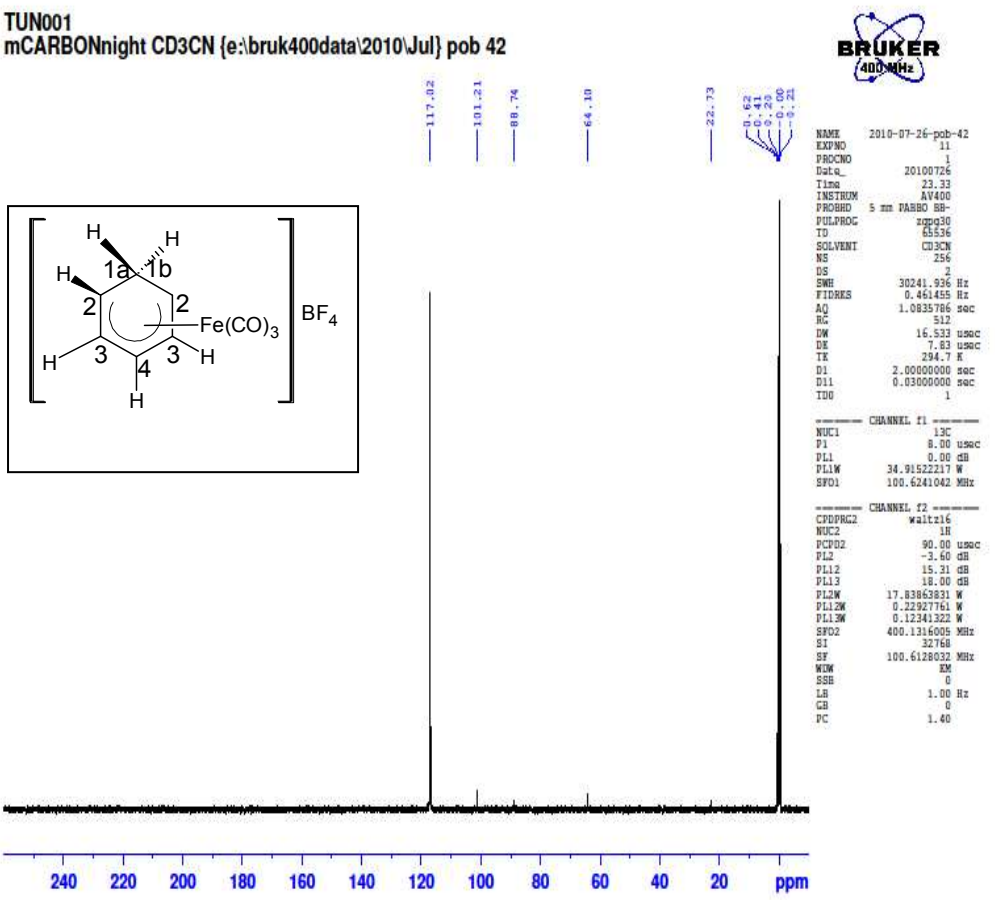

Fig 4.5: ^{13}Cnmr spectrum of tricarbonyl (cyclohexadienyl) iron tetrafluoro borate (2)

TABLE 4.6: ^{13}Cnmr assignment of [(1-5-η-2-MeOC$_6$H$_6$)Fe(CO)$_3$][BF$_4$] (3)

Position	Carbon	Chemical shifts (δ) ppm
Ortho	C1	117.02
Meta	C2	117.02
Para	C3	117.02
Meta	C4	117.02
Ortho	C5	86.91
Methylene	C6	54.01

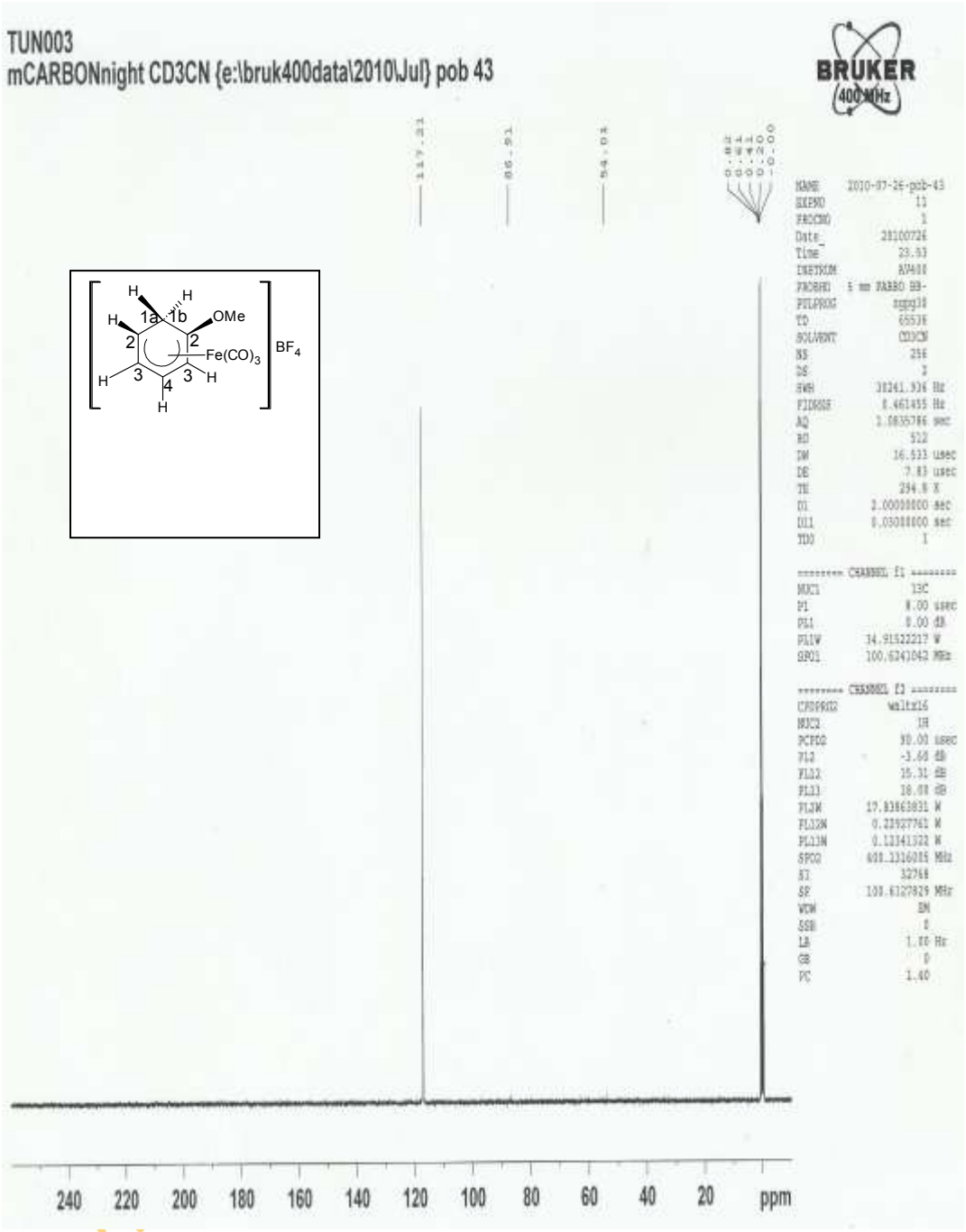

Figure 4.6: ^{13}Cnmr spectrum of tricarbonyl (2-methoxy cyclohexadienyl) iron tetrafluoroborate (3)

TABLE 4.7: Mass spectral assignment of [(1-5-η-C_6H_7)Fe$(CO)_3$][BF_4] (2)

Mass	Fragment	Intensity (m/z)
135	M – 3(CO) – (BF4)	8.0
163	M – 2(CO) – (BF4)	19.0
191	M – (CO) – (BF4)	100
219	M – (BF4)	95.0
249	M – 3(F^-)	3.0

M= 306 (Molecular mass)

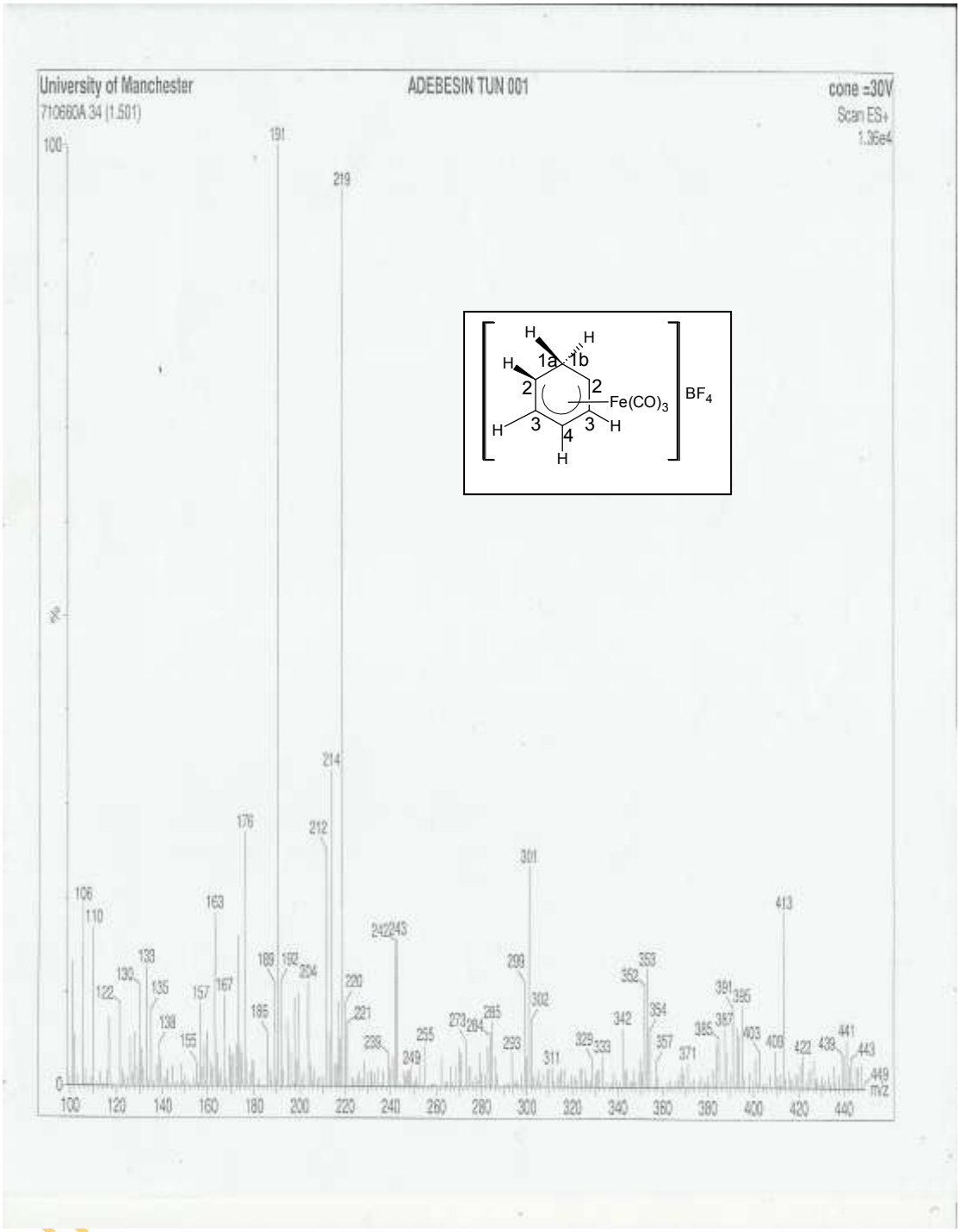

Figure 4.7: Mass spectrum of tricarbonyl (cyclohexadienyl) iron tetrafluoro borate (2)

TABLE 4.8: Mass spectra assignment of [(1-5-η-2-MeOC$_6$H$_6$)Fe(CO)$_3$] [BF$_4$] (3)

Mass	Fragment	Intensity (m/z)
163	M – 2(CO) – (BF_4) – (OCH_3)	2.50
191	M – (CO) – (BF_4) – (OCH_3)	35.0
207	M – (CO) – (BF_4) – (CH_2)	70.0
219	M – (OCH_3) – (BF_4)	100
235	M – (CH_2) – (BF_4)	75.0
242	M – 2(CO) - 2(F^-)	4.0
257	M – (CO) – (CH_2) – 2(F^-)	68.0
270	M – (CO) – 2(F^-)	15.0
298	M – 2(F^-)	27.0

M= 336 (Molecular mass)

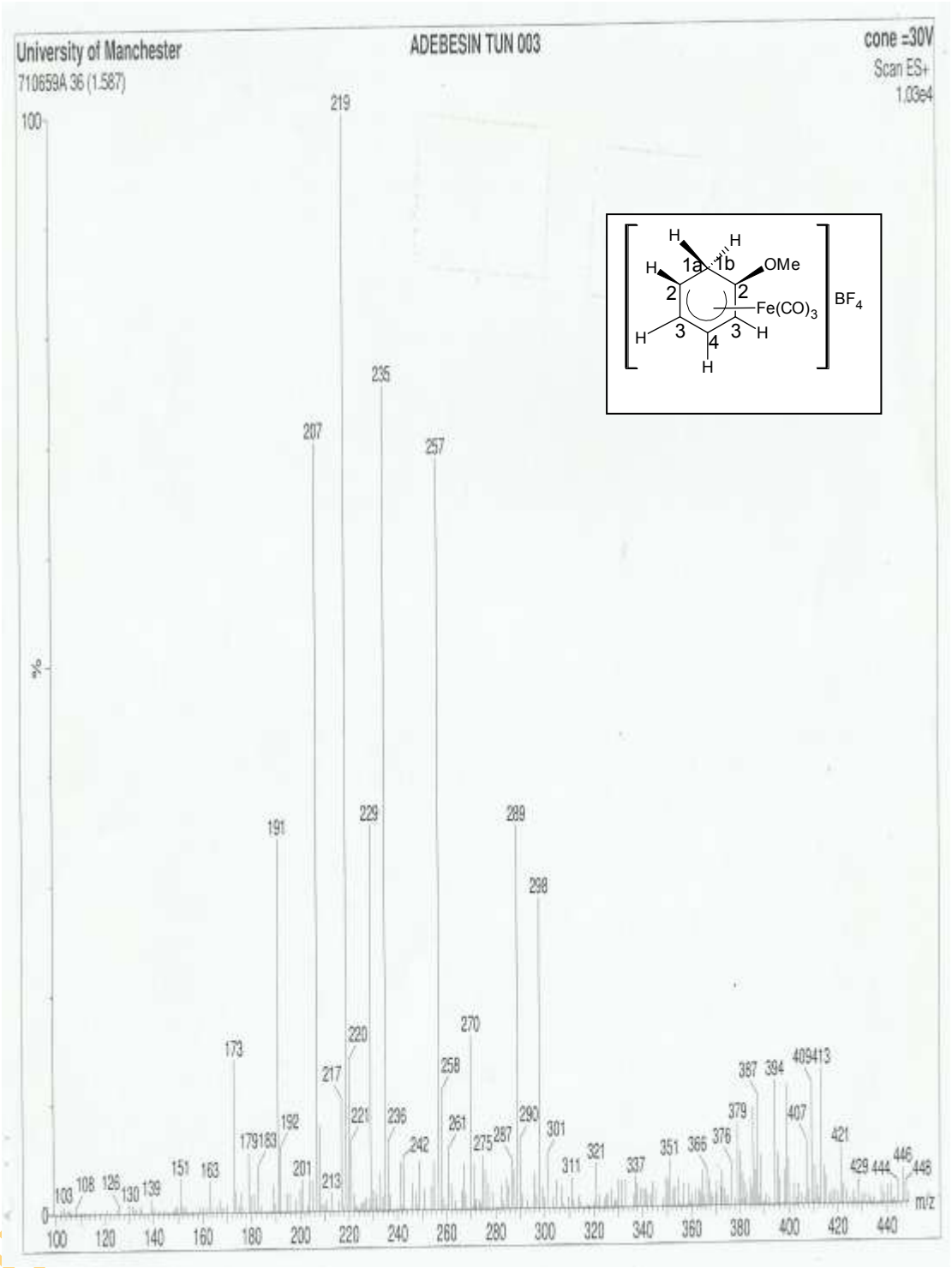

Figure 4.8: Mass spectrum of tricarbonyl (2-methoxy cyclohexadienyl) iron tetrafluoroborate (3)

4.2 SPECTRAL STUDIES OF THE ADDUCTS

4.2.1 IR studies of adducts

The reaction of $[(1\text{-}5\text{-}\eta\text{-}C_6H_7)Fe(CO)_3][BF_4]$ and $[(1\text{-}5\text{-}\eta\text{-}2\text{-}MeOC_6H_6)\ Fe(CO)_3][BF_4]$ with gedunin, khivorin, 7-ketokhivorin and polyavolensinol in refluxing dry toluene affords the corresponding 1,3-diene substituted derivatives. These compounds are air sensitive yellow oils except for products (21), (22), (24) and (25) (Fig. 5.1**)** which are respectively lilac and yellow solids. The IR data are presented in Tables 4.9 to 4.15. The adducts exhibited strong and intense IR √(CO) bands at *ca* 2050 and 1975cm^{-1} (Fig 4.9 to 4.12), characteristic of neutral tricarbonyl (1,3- diene-substituted) iron derivatives (Odiaka and Kane-Maguire, 1979, 1981, 1985; Gower *et al*., 1979; John *et al*., 1983; Kane-Maguire *et al*., 1984). However, these were observed at slightly higher frequency of 2060 and 1990 cm^{-1} for the methoxy derivatives (Fig. 4.13 to 4.15), which are characteristics of cationic tricarbonyl (1,3-diene-substituted)iron derivatives (Odiaka and Kane-Maguire, 1981 ; John and Kane-maguire, 1979a, 1979b) similar to pyridinium adducts.

The addition of the natural products to complexes (2) and (3) involves direct addition to the dienyl ring of the complexes as in the case with the aromatic amines (Birch *et al*., 1982). It has already been demonstrated by kinetic studies that $[(1\text{-}5\text{-}\eta\text{-}2\text{-}MeOC_6H_6\ )\ Fe(CO)_3][BF_4]$ (3) is less reactive towards nucleophiles than the parent complex (2) (Kane- Maguire, 1971; John and Kane-Maguire, 1979a). Thus, reaction of complex (3) involves the use of large excess of nucleophiles. Ten equivalents molar excess of the natural products was used before reaction occurred compared to the use of two molar excess of natural products in the reaction with complex (2). This slower reactivity of (3) with the natural products is attributed to the mesomeric influence of the methoxide group which has been demonstrated from INDO molecular orbital calculations to decrease the positive charge on the dienyl C^5 atom, the site of nucleophilic addition (Clack *et al*., 1976a, 1976b; Odiaka, 1986).

Table 4.9: IR assignment of tricarbonyl [1-4-η-5-(gedunino) cyclohexa-1,3-diene]iron (19)

IR band (cm^{-1})	Intensity	Assignment
2962	m	C-H str for alkanes
2041 and 1964	vs	√-CO band for coordinated diene
1738	vs	C=O str for esters
1667	vs	αβ-unsaturated ketone grp
1495	m	C-C band characteristics of C_6H_7
1368 to 1163	s	C-O str for esters
874	s	Furan
563	vs	M-C band (Fe-C)

Keys: s = sharp, vs = very sharp, m = moderate, b = broad

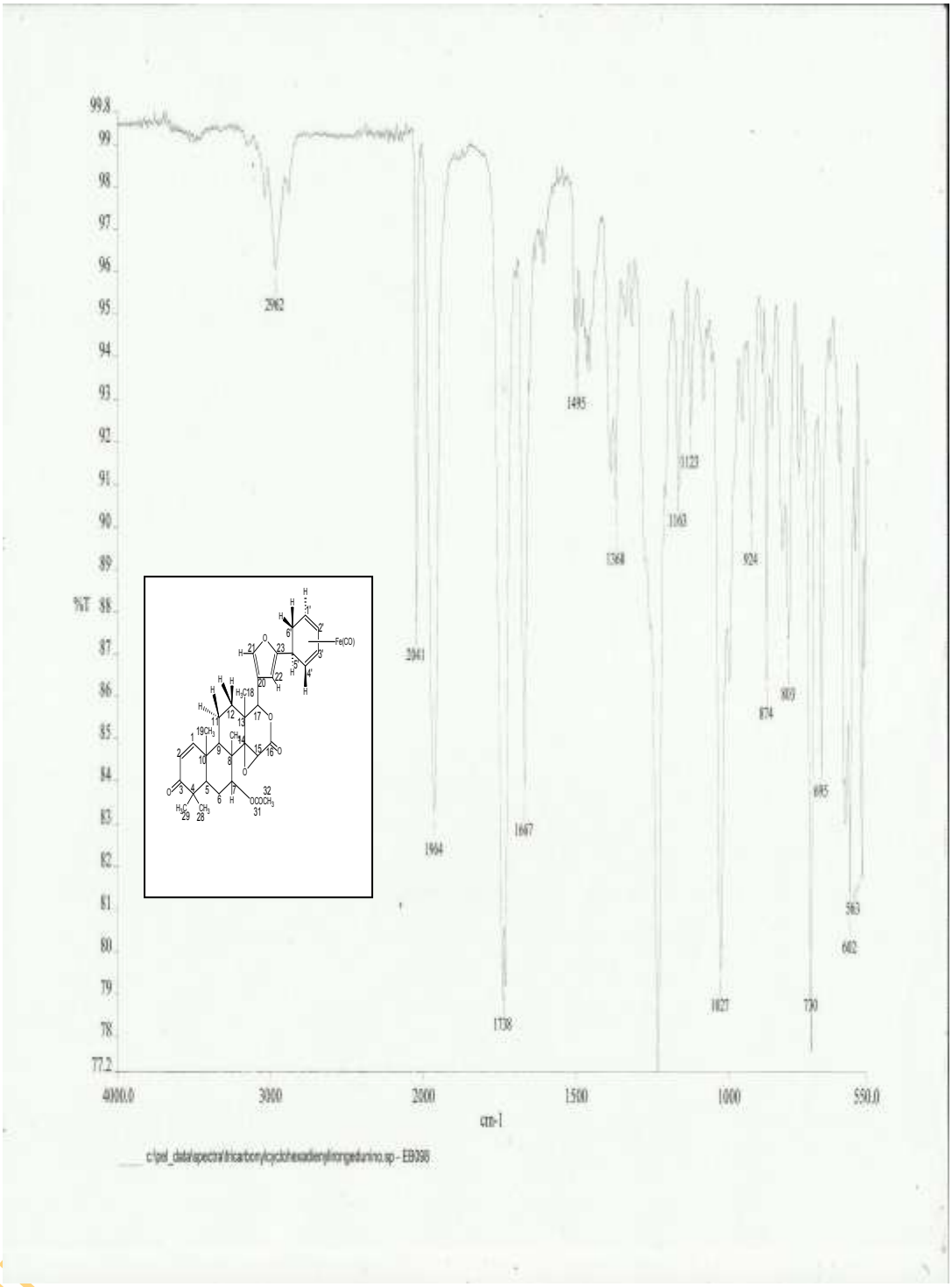

Figure 4.9: IR spectrum of tricarbonyl [1-4-η-5-(gedunino)cyclohexa-1,3-diene]iron adduct (19)

Table 4.10: IR assignment of tricarbonyl[1-4-η-5-(khivorino)cyclohexa-1,3-diene]iron (20)

IR band (cm^{-1})	Intensity	Assignment
2962	s	C-H str of alkanes
2050 and 1980	s	√-CO band for coordinated diene
1730	s	C=O str esters
1374	s	CH_2 and CH_3
1256 to 1013	vs	C-O str ester
873	m	furan
563	m	M-C (Fe-C) band

Key: m = moderate, vs. = very sharp, s = sharp

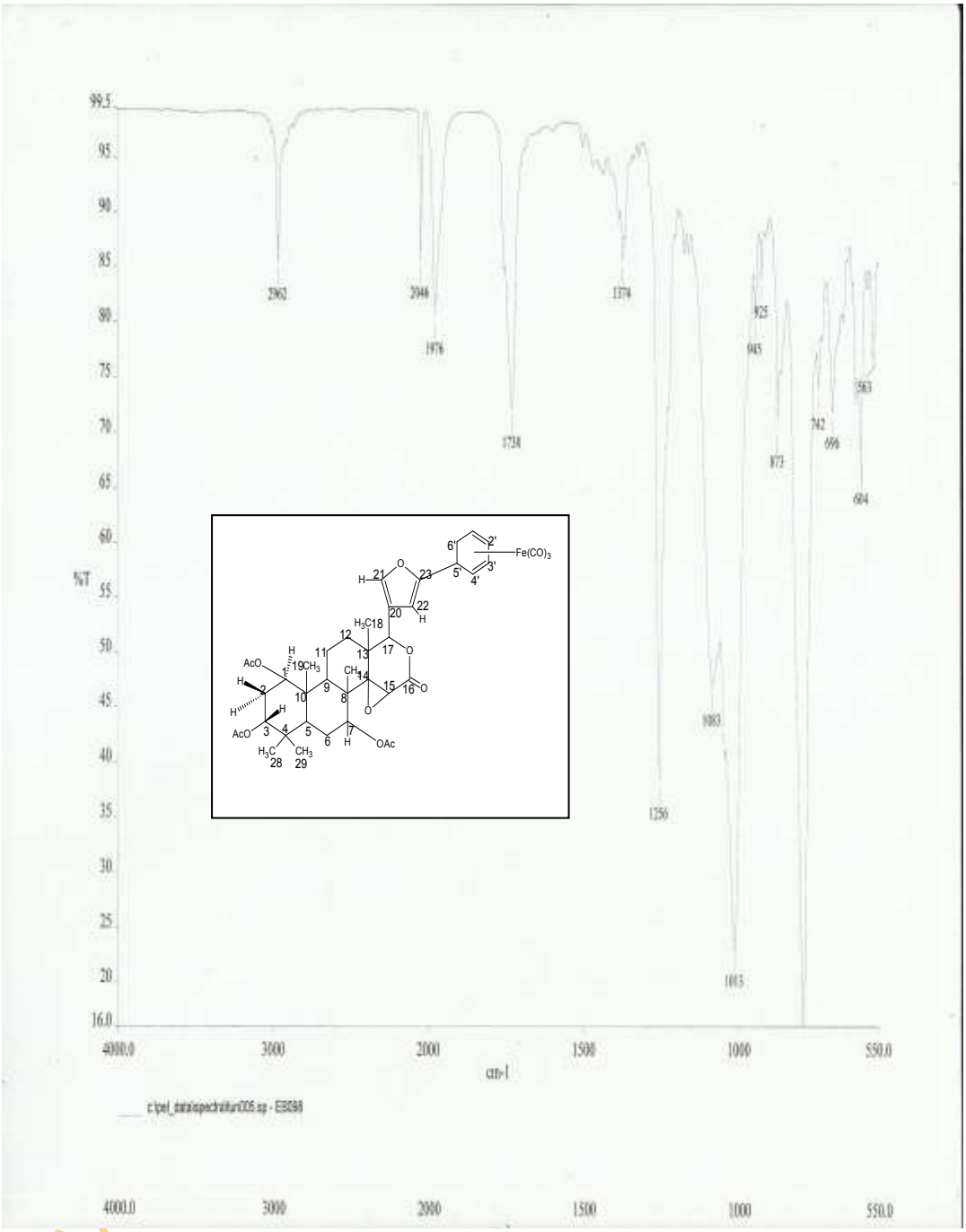

Figure 4.10: IR spectrum of tricarbonyl [1-4-η-5-(khivorino)cyclohexa-1,3-diene]iron (20)

Table 4.11: IR assignment of tricarbonyl [1-4-η-5-(polyavolensinolino) cyclohexa-1,3-diene] iron (22)

IR bands (cm^{-1})	Intensity	Assignment
2962	s	C-H str alkanes
2042 and 1963	s	√ (CO) of coordinated diene
1453	s	C-C str aromatic
1258	vs	CH_3 of alkanes
1011	vs	C-O alcohol
853	m	C-H out of plane
580 to 561	m	M-C bond (Fe-C)

Key: s= sharp, m = moderate, vs = very sharp

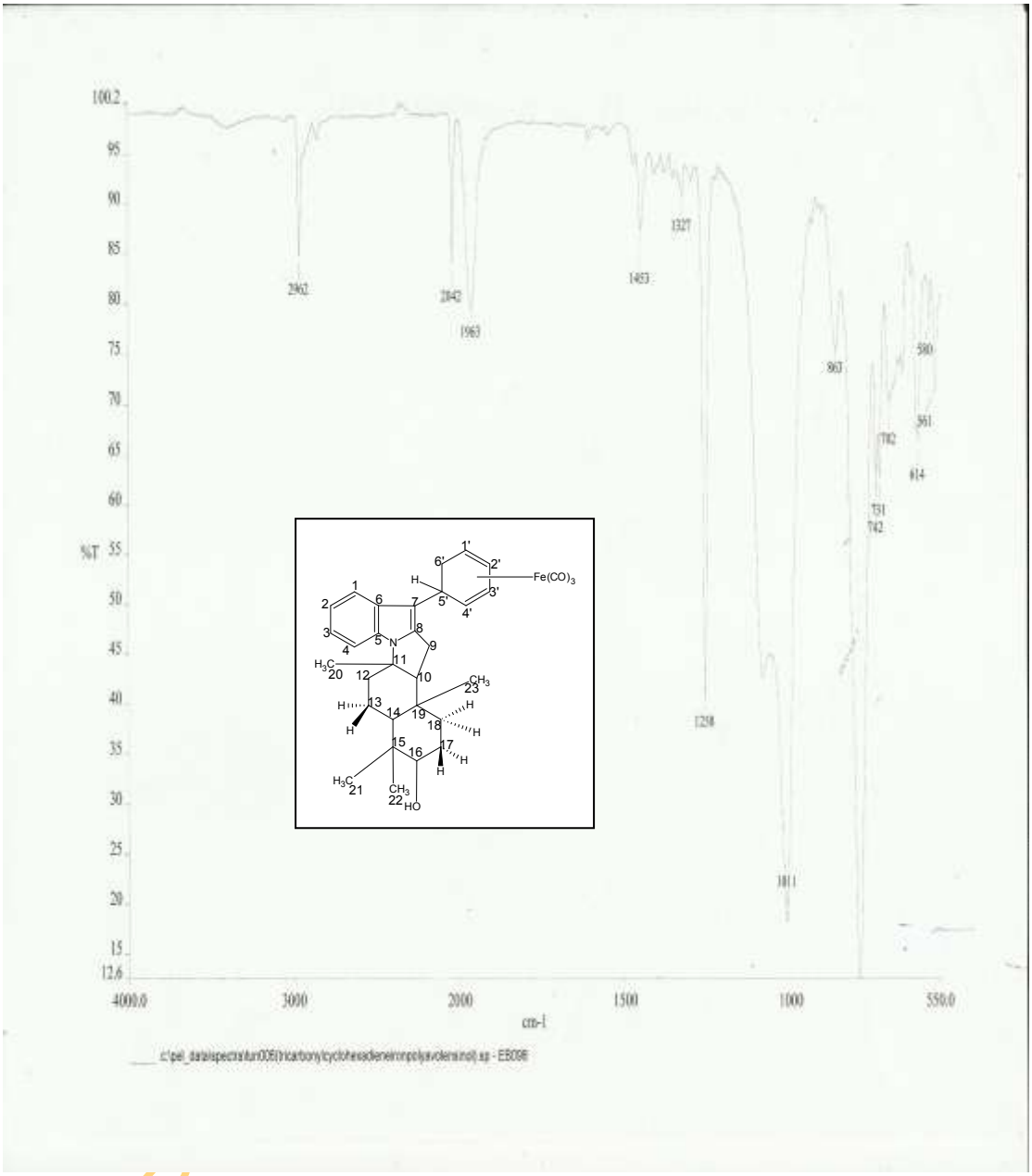

Figure 4.11: IR spectrum of Tricarbonyl [1-4-η-5-(polyavolensinolino)cyclohexa-1,3-diene] iron (22)

Table 4.12: IR assignment of tricarbonyl [1-4-η-5-(7-keto-khivorino) cyclohexa-1, 3-diene] iron (21)

IR bands (cm^{-1})	Intensity	Assignment
2962	s	C-H str alkanes
2050 and 1980	s	√(CO)band of coordinated diene
1728	s	C=O str ester
1374	s	CH_2 and CH_3 alkanes
1256 to 1012	vs	C-O str esters
873	s	furan
565	s	Fe-C

Key: s = sharp, vs = very sharp, m = moderate, b = broad

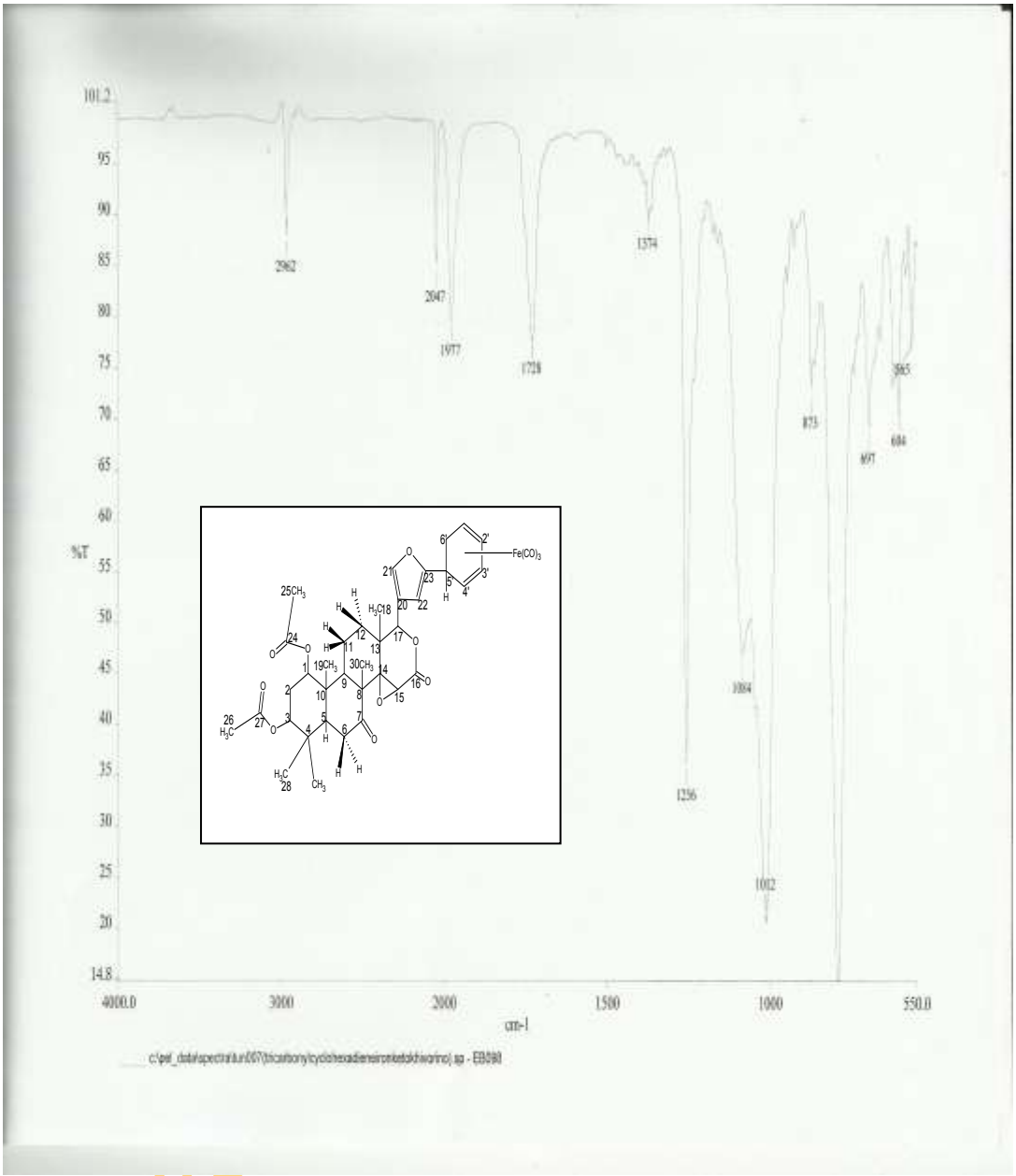

Figure 4.12: IR spectrum of Tricarbonyl [1-4-η-5-(7-ketokhivorino) cyclohexa-1,3-diene] iron (21)

Table 4.13: IR assignment of tricarbonyl [1-4-η-2-methoxy-5-(gedunino) cyclohexa-1,3-diene]iron (23)

IR band (cm^{-1})	Intensity	Assignment
2962	m	C-H str alkanes
2059 and 1989	s	√CO str for coordinated diene
1733	vs	C=O str esters
1667	vs	αβ-unsaturated ketone grp
1368 to 1163	vs	C-O str esters
874	s	furan
693	s	Fe-C band

Key: m= moderate, s= sharp, vs= very sharp, b= broad

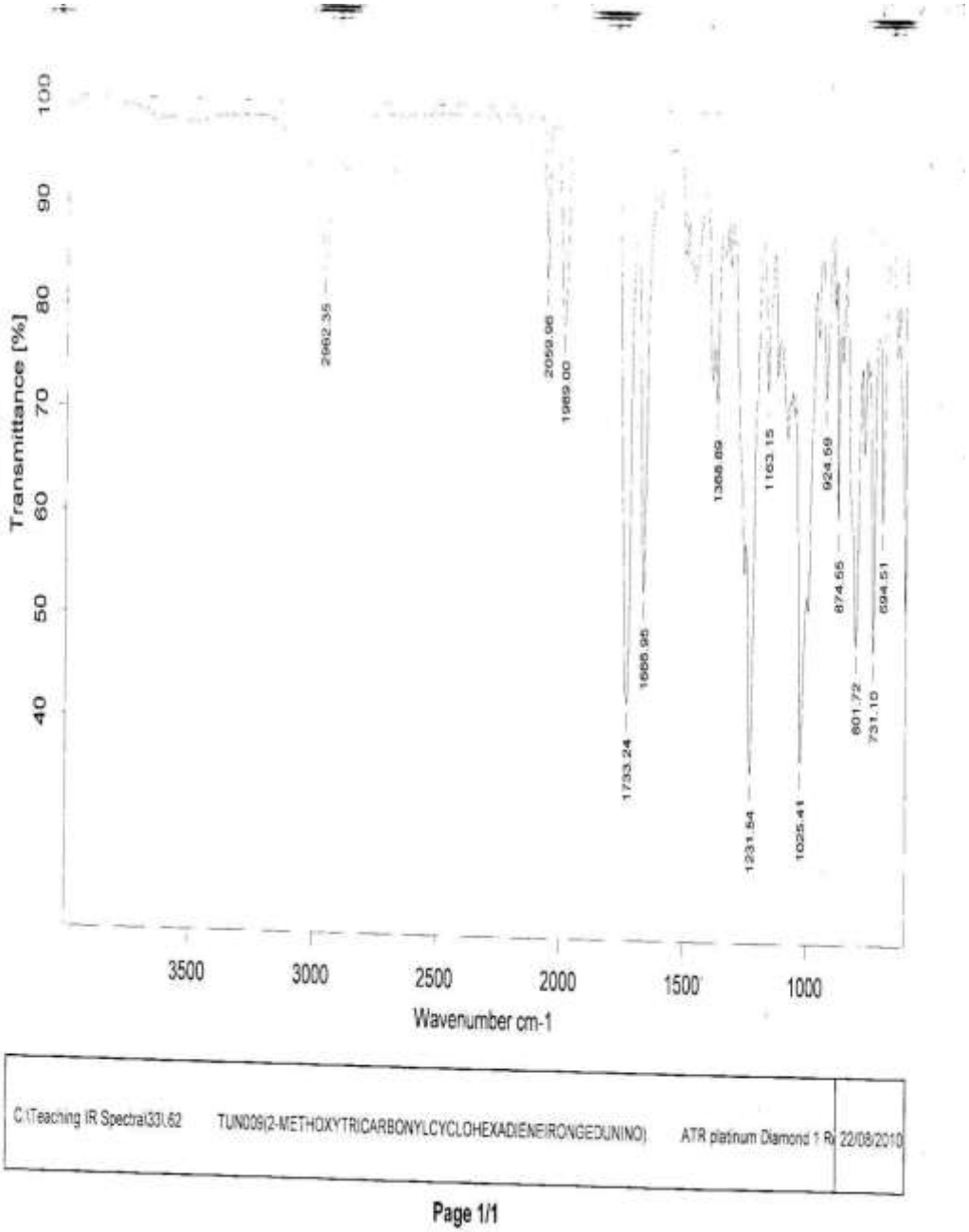

Figure 4.13: IR spectrum of Tricarbonyl [1-4-η-2-methoxy-5-(gedunino) cyclohexa-1,3-diene] iron (23)

Table 4.14: IR assignment of tricarbonyl [1-4-η-2-methoxy-5-(khivorino) cyclohexa-1,3- diene] iron (24)

IR bands (cm^{-1})	Intensity	Assignment
2962	m	C-H str alkanes
2061 and 1986	s	√CO str for coordinated diene
1728	vs	C=O str esters
1374 to 1020	vs	C-O str ester
874	m	furan band
795	vs	C-H vibration
696	s	Fe-C band

Key: m= moderate, s= sharp, vs= very sharp, b= broad

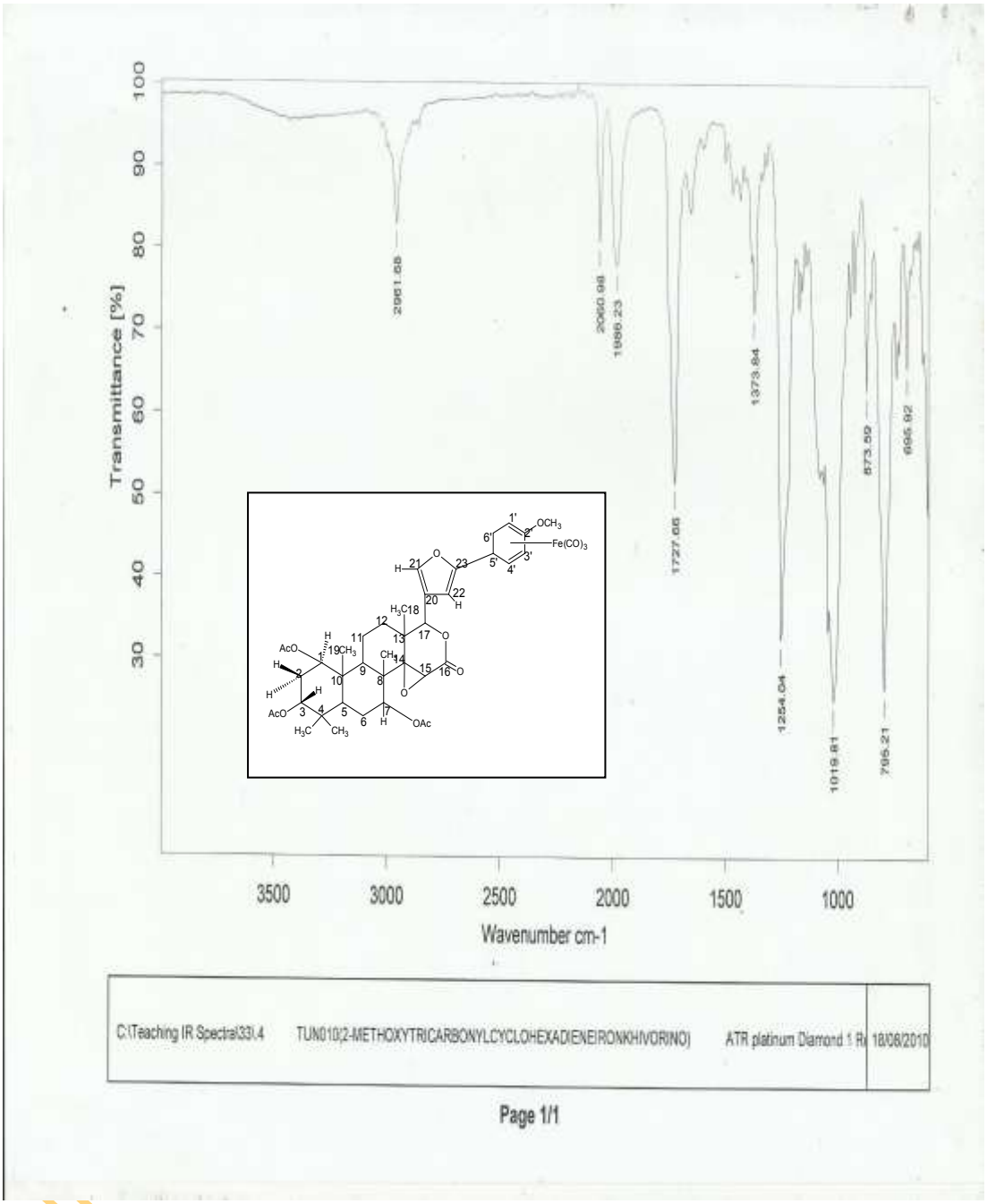

Figure 4.14: IR spectrum of Tricarbonyl [1-4-η-2-methoxy-5-(khivorino) cyclohexa-1,3-diene] iron (24)

Table 4.15: IR assignment of tricarbonyl [1,4-η-2-methoxy-5-(7-ketokhivorino) cyclohexa-1,3-diene]iron (25)

IR bands (cm^{-1})	Intensity	Assignment
2962	m	C-H str alkanes
2061 and 1989	s	√CO str for coordinated diene
1727	vs	C=O str ester
1376 to 1042	s	C-O str ester
801	s	furan band
731	s	C-H vibration
696	s	Fe-C band

Key: m= moderate, s= sharp, vs= very sharp, b= broad

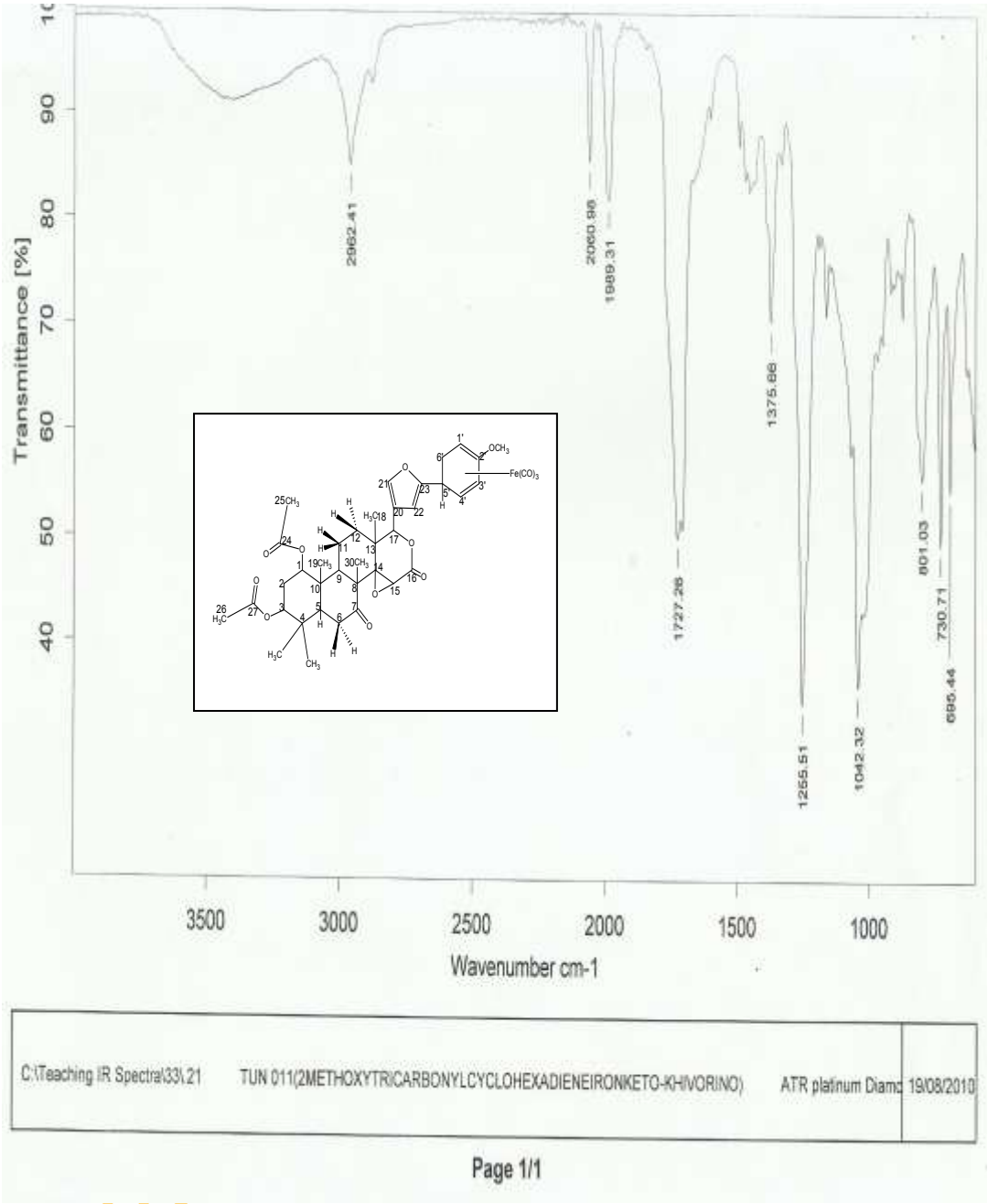

Figure 4.15: IR spectrum of Tricarbonyl [1-4-η-2-methoxy-5-(7-ketokhivorino) cyclohexa-1,3-diene] iron (25)

4.3 ^{1}Hnmr studies of adducts

The adducts are soluble in most organic solvents. The ^{1}Hnmr spectra assignment of Tricarbonyl (5-exo-substituted) cyclohexa-1,3-diene products and their methoxy derivatives for gedunin, khivorin, polavolensinol and 7-ketokhivorin are presented in Tables 4.16 to 4.22. The results clearly demonstrated coordination of the dienylium cations, $[(1\text{-}5\text{-}\eta\text{-}C_6H_7)Fe(CO)_3]^+$ and $[(1\text{-}5\text{-}\eta\text{-}2\text{-}MeOC_6H_6)Fe(CO)_3]^+$ to the natural products to form the isolated 1,3-diene derivatives. INDO molecular orbital calculations (Clack *et al*., 1976 a,b) on complex (2) show accumulation of positive charge on C^5 of the dienylium fragment and all the natural products attacked (2) at this point via the α-carbon of the furan ring for products (19), (20), and (21) and via the β-carbon of the indole fragment for product (22). Similar reaction was observed in the formation of tricarbonyl methoxy (cyclohexa-1,3-diene) derivatives.

The ^{1}Hnmr spectra Fig 4.16 to 4.22 of the four Tricarbonyl (5-exo-substituted) cyclohexa-1,3-diene products showed overlapping resonances characteristic of the outer ($H^{1,4}$) and inner ($H^{2,3}$) 1,3-diene protons at *ca* 7.33 and 5.14 ppm respectively while the $H^{5'}$ proton (bearing the C atom attached to the natural products) appeared at ca 2.79 ppm. For tricarbonyl (2-methoxy-5-exo-substituted) cyclohexa-1,3-diene products, the inner diene protons were observed at a more deshielded value of 7.12 ppm while the outer diene protons resonated at similar values given above. There is the appearance of an additional band at 3.48 ppm assigned to the methoxy protons.

The H^6 (exo) and $H^{6'}$(endo) methylene protons of the coordinated diene resonate at *ca* 1.60 and 2.19 ppm while the methylene protons for the methoxy derivatives resonate at the slightly deshielded values of 2.44 and 2.41 ppm respectively. These strong 1, 3-diene resonances (Odiaka, 1986, 1985, 1989, 1980; Gower *et al*., 1979; Odiaka and Okogun, 1985), clearly confirmed that electrophilic attack by the dienylium cations has occurred on the natural products to form the corresponding 1,3- diene- substituted products Fig 5.1. In products (19), (20), (21), (23), (24) and (25) {see section 1.3.}, results confirmed the attachement of complexes (2) and (3) to the α-carbon or C^{23} of the furan ring. For example, in (19) and (23), the doublet at 7.39 ppm which integrated for two protons (H^{21} and H^{23}) of the starting natural product, collapsed into singlet and integrated for only one proton (H^{21}) in the product (19**)** at a more shielded value of 7.30 ppm and in product (23**)** and the methoxy derivative at 7.32 ppm [Tables 4.16 & 4.20 (Figures 4.16 & 4.20)].

Table 4.16: ^{1}Hnmr assignment of Tricarbonyl [1-4-η-5-(gedunino) cyclohexa-1,3-diene]iron (19)

Protons	Simulated Spectra	Real Spectra
H1	6.433	7.35(d)
H1'	5.735	5.82(s)
H11a	1.344	1.71(d)
H11b	1.98	1.77(t)
H12a	2.122	1.86(t)
H12b	2.022	2.04(s)
H15	3.545	3.46(s)
H17	5.078	5.55(s)
H18	1.111	1.18(s)
H19	1.097	1.16(s)
H2	5.699	5.79(s)
H2'	pt of metallation	pt of metallation
H21	7.437	7.30(s)
H22	6.23	7.02(s)
H28	1.09	1.09(s)
H29	1.19	1.50(s)
H3'	6.291	7.05(s)
H30	1.041	1.01(d)
H32	2.042	2.29(s)
H4'	5.83	6.27(t)
H5	2.116	1.74(t)
H5'	3.041	not observed
H6a	1.637	1.66(d)
H6'a	2.269	not observed
H6b	2.397	2.45(q)
H6'b	2.316	not observed
H7	5.043	4.48(m)
H9	3.115	2.12(m)

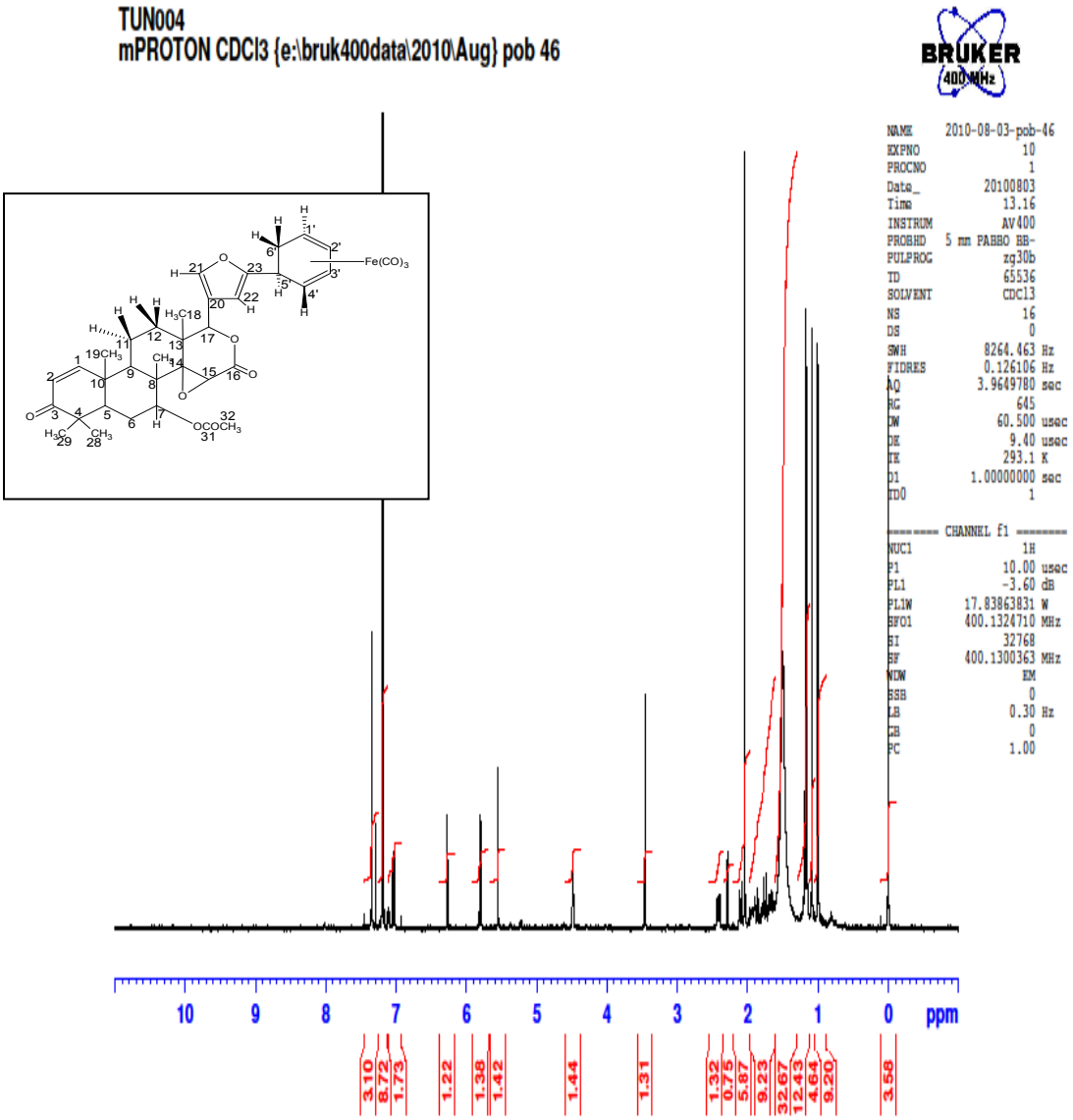

Figure 4.16: ^{1}Hnmr spectrum of Tricarbonyl [1-4-η-5-(gedunino) cyclohexa-1,3-diene]iron (19)

Table 4.17: ^{1}Hnmr assignment of tricarbonyl[1-4-η-5(khivorino)cyclohexa-1,3-diene]iron (20)

Protons	Simulated Spectra	Real Spectra
H1	4.711	4.55(m)
H1'	5.735	not observed
H11	1.407	1.38(m)
H11b	2.043	1.85(m)
H12a	2.107	1.88(m)
H12b	2.007	1.57(m)
H15	3.545	3.45(s)
H17	5.078	not observed
H18	1.111	1.17(s)
H19	0.87	0.74(s)
H2'	pt of metallation	pt of metallation
H21	7.437	6.24(s)
H22	6.23	5.54(s)
H28	0.982	0.85(s)
H29	1.082	1.01(s)
H2a	1.8	1.41(d,d)
H2b	1.95	1.41(d,d)
H3	4.605	4.45(m)
H3'	6.291	7.33(d)
H30	1.022	0.94(s)
H32	2.042	2.08(s)
H33	2.042	1.95(s)
H34	2.04	1.49(s)
H4'	5.83	not observed
H5	2.209	2.12(m)
H5'	3.041	2.79((m)
H6a	1.418	not observed
H6'a	2.269	1.60(m)
H6b	2.178	2.16(m)
H6'b	2.316	2.19(m)
H7	4.951	4.64(m)
H9	3.13	not observed

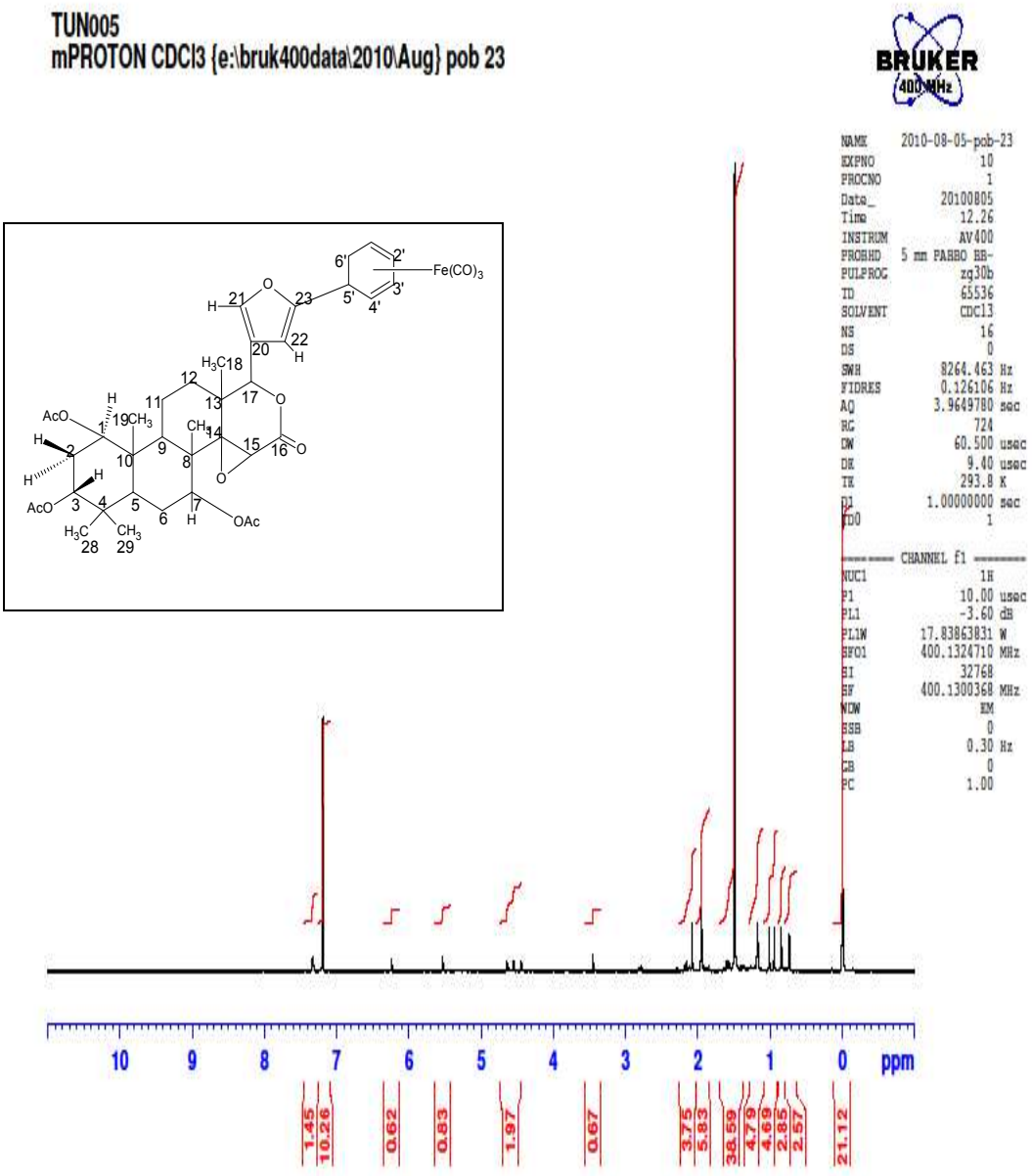

Fig 4.17: [1]Hnmr spectrum of Tricarbonyl [1-4-η-5-(khivorino)cyclohexa-1,3-diene]iron (20)

Table 4.18: ^{1}Hnmr assignment of tricarbonyl [1-4-η-5-(polyavolensinolino) cyclohexa-1, 3-diene] iron (22)

Protons	Simulated Spectra	Real Spectra
H1	7.009	7.24(d)
H2	7.168	7.46(t)
H3	7.167	7.26(t)
H4	7.461	7.47(d)
H9a	3.445	3.25(d)
H9b	3.345	3.23(d)
H10	3.484	3.19(t)
H12a	2.072	2.63(d)
H12b	1.972	1.98(t)
H13a	1.637	1.54(t)
H13b	2.273	2.29(s)
H14	2.017	2.56(t)
H16	3.225	3.22(t)
H17a	2.053	2.60(d)
H17b	1.953	1.49(s)
H18a	1.476	1.31(t)
H18b	1.376	1.37(d)
H20	1.648	1.49(s)
H21	0.975	0.98(d)
H22	1.075	1.14(s)
H23	0.903	0.80(s)
OH proton	4.794	6.10(s)
H1'	5.735	6.97(d)
H2'	pt of met	pt of met
H3'	6.291	7.00(d)
H4'	6.253	6.93(t)
H5'	3.441	2.73(q)
H6'a	2.384	not observed
H6'b	2.431	2.15(d,d)

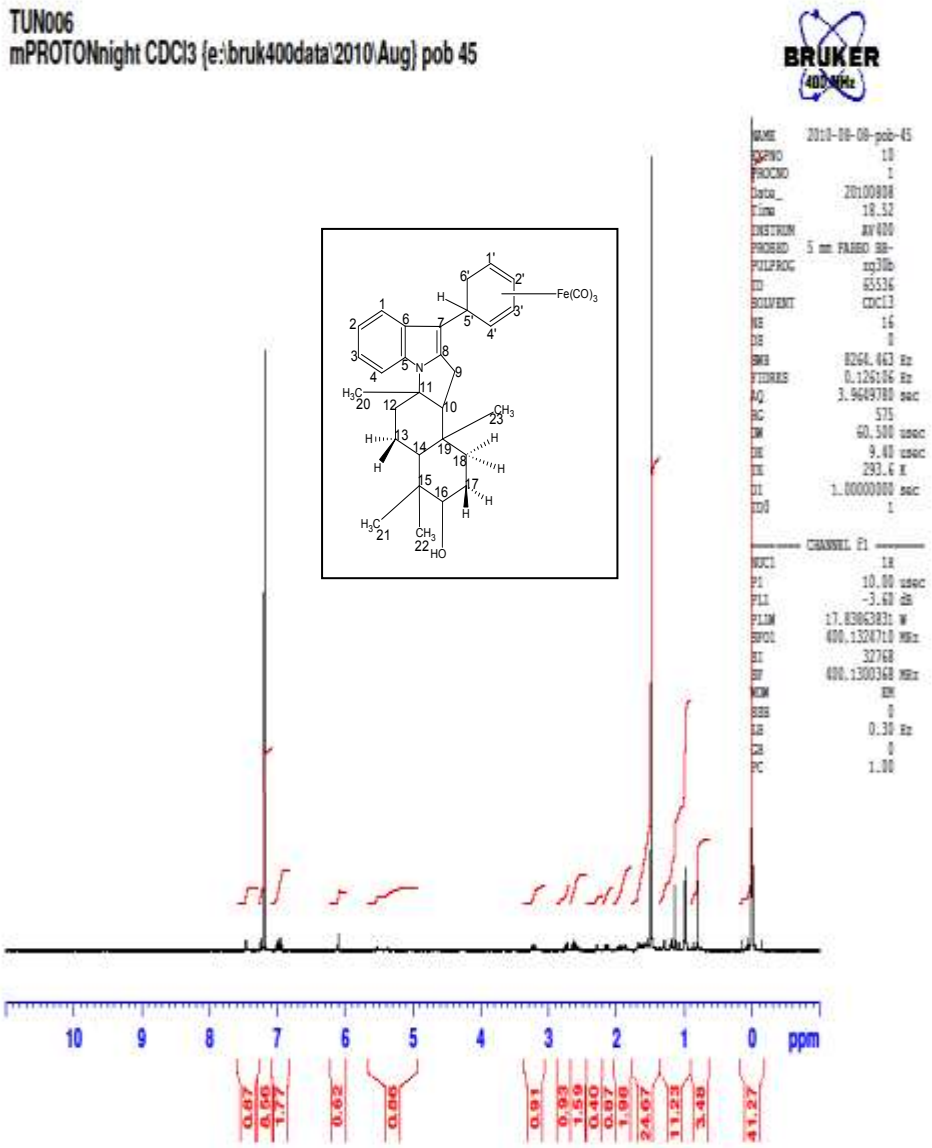

Figure 4.18: ^{1}Hnmr spectrum of Tricarbonyl [1-4-η-5-(polyavolensinolino) cyclohexa-1,3-diene]iron (22)

Table 4.19: ^{1}Hnmr assignment of Tricarbonyl [1-4-η-5-(7-keto-khivorino) cyclohexa-1, 3-diene] iron (21)

Protons	Simulated Spectra	Real Spectra
H1	4.788	4.65(t)
H2a	1.8	1.64(d)
H2b	1.95	1.95(d)
H3	4.682	4.55(t)
H5	2.612	2.12(t)
H6a	2.168	1.92(t)
H6b	2.156	1.55(s)
H9	3.119	4.45(t)
H11a	1.537	1.50(s)
H11b	2.173	1.88(t)
H12a	2.281	2.16(d)
H12b	2.181	1.57(t)
H15	4.021	3.45(s)
H17	5.252	5.53(s)
H18	1.141	0.94(s)
H19	0.966	0.74(s)
H21	7.308	7.17(s)
H22	6.101	7.12(s)
H24	2.04	2.08(s)
H26	2.042	2.29(s)
H28	1.178	1.01(s)
H29	1.079	0.85(s)
H1'	5.676	7.33(m)
H2'	6.098	7.34(t)
H3'	6.323	6.24(d,d)
H4'	pt of met	pt of met
H5'	3.041	2.79(d,d)
H6'a	2.269	1.60(d)
H6'b	2.316	2.19(d)

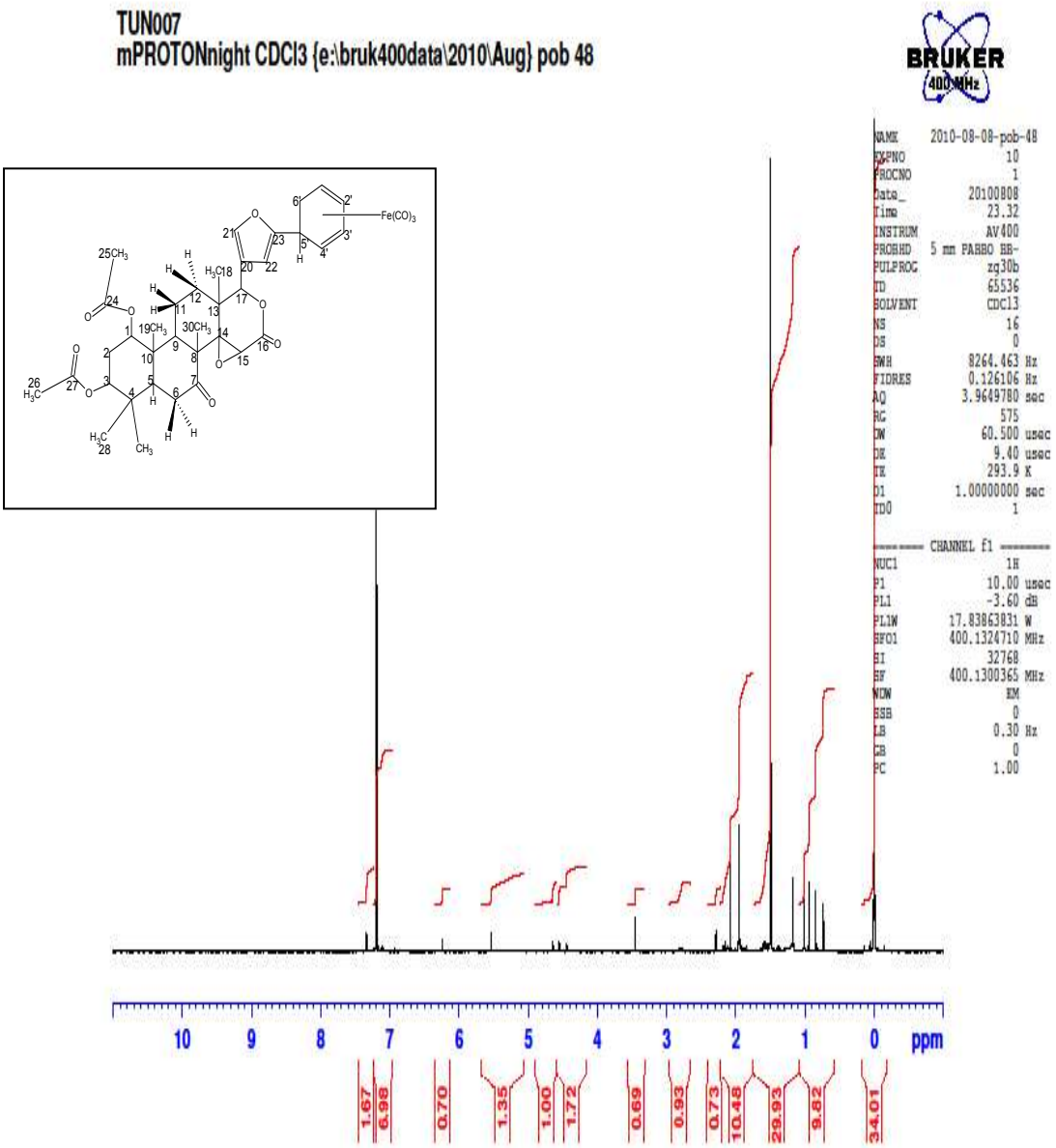

Figure 4.19: ^{1}Hnmr spectrum of Tricarbonyl [1-4-η-5-(7-ketokhivorino) cyclohexa-1,3-diene]iron (21)

Table 4.20: ^{1}Hnmr assignment of Tricarbonyl [1-4-η-2-methoxy-5-(gedunino) cyclohexa-1,3-diene]iron (23)

Protons	Simulated Spectra	Real Spectra
H1	6.433	7.12(d)
H2	5.699	5.82(s)
H5	2.116	not observed
H6a	1.637	not observed
H6b	2.397	not observed
H7	5.043	5.55(s)
H9	3.115	not observed
H11a	1.344	not observed
H11b	1.98	1.85(d)
H12a	2.122	not observed
H12b	2.022	1.75(m)
H15	3.545	3.5(s)
H17	5.078	5.75(s)
H18	1.111	1.50(s)
H19	1.097	1.25(s)
H21	7.437	7.38(s)
H22	6.199	6.30(s)
H28	1.09	1.00(s)
H29	1.19	1.30(s)
H30	1.041	1.18(s)
H32	2.042	2.03(s)
H33(methoxy)	3.514	3.40(q)
H1'	pt of metallation	pt of metallation
H3'	6.046	not observed
H4'	5.925	not observed
H5'	3.059	2.49(d,d)
H6'a	2.523	2.32(s)
H6'b	2.414	2.15(d)

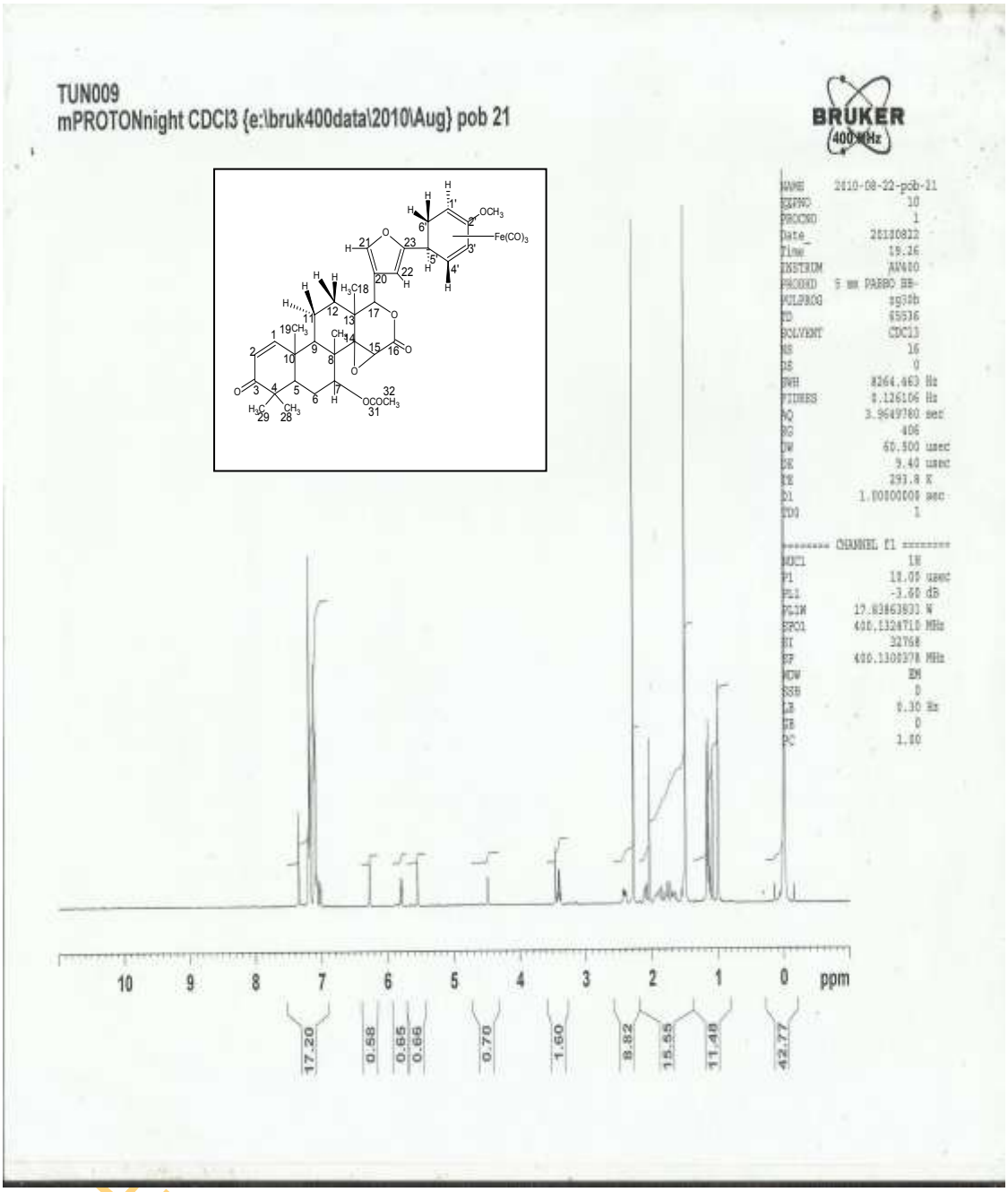

Figure 4.20: ^{1}Hnmr spectrum of tricarbonyl [1-4-η-2-methoxy-5-(gedunino) cyclohexa-1,3-diene]iron (23)

Table 4.21: ^{1}Hnmr assignment of Tricarbonyl [1-4-η-2-methoxy-5-(khivorino) cyclohexa-1,3-diene]iron (24)

Protons	Simulated spectra	Real Spectra
H1	4.711	4.55(t)
H2a	1.8	1.60(s)
H2b	1.95	1.64(d)
H5	2.209	2.11(t)
H6a	1.418	1.50(s)
H6b	2.178	1.92(t)
H7	4.951	4.65(t)
H9	3.13	not observed
H11a	1.407	1.57(t)
H11b	2.043	1.88(t)
H12a	2.107	1.95(d)
H12b	2.007	1.85(t)
H13	4.605	4.45(t)
H15	3.545	3.45(s)
H17	5.078	not observed
H18	1.111	1.17(s)
H19	0.87	0.74(s)
H21	7.437	7.33(s)
H22	6.199	5.53(s)
H28	0.982	0.85(s)
H29	1.082	1.01(s)
H30	1.022	0.94(s)
H31	2.042	2.29(s)
H32	2.042	2.08(s)
H33	2.04	2.01(s)
H34	3.514	3.42(s)methoxy
H1'	pt of metallation	pt of metallation
H3'	6.046	7.34(m)
H4'	5.925	6.24(d,d)
H5'	3.059	2.79(m)
H6'a	2.523	2.19(d)
H6'b	2.414	2.16(d)

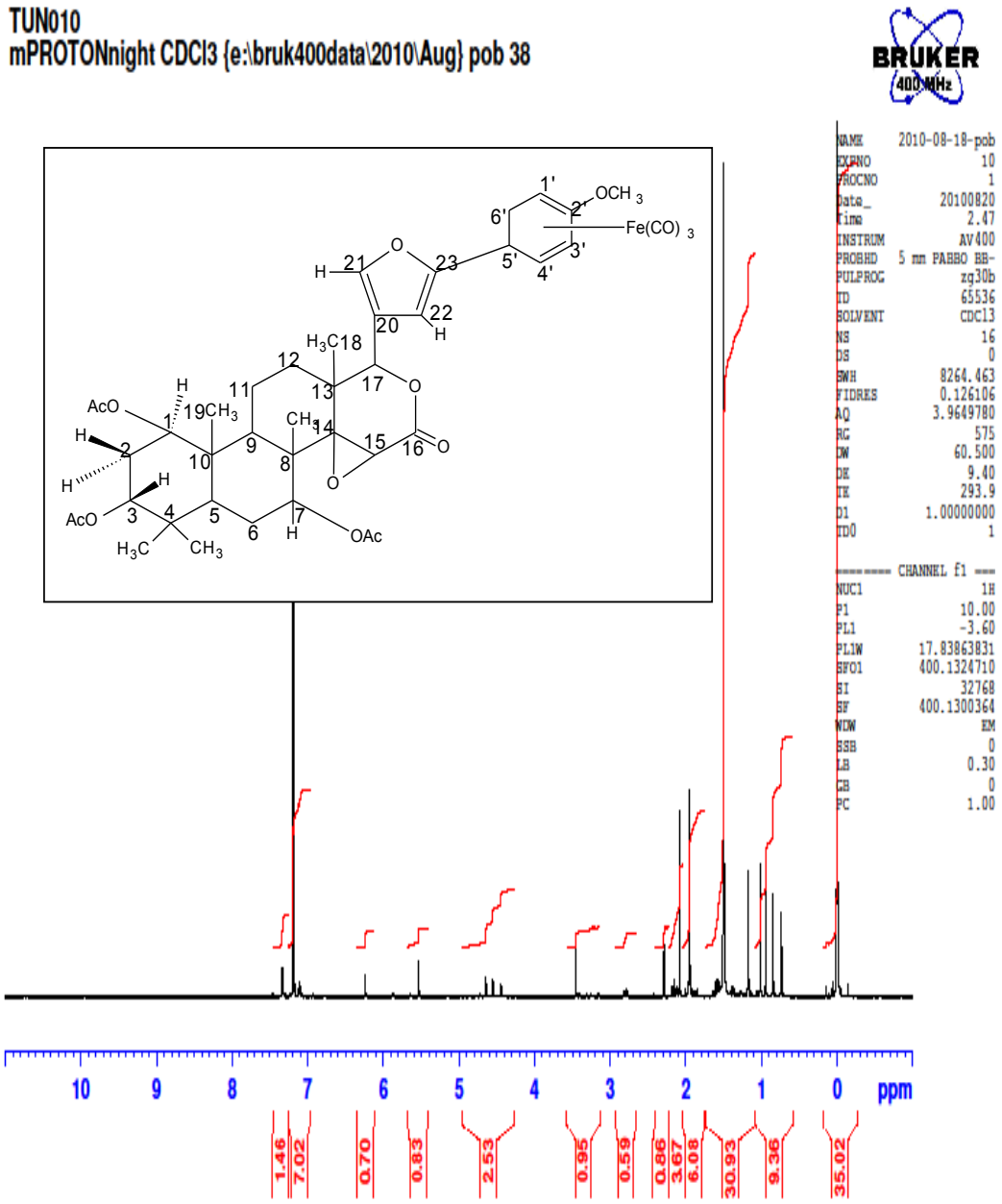

Figure 4.21: ^{1}Hnmr spectrum of tricarbonyl [1-4-η-2-methoxy-5-(khivorino) cyclohexa-1,3-diene]iron (24)

Table 4.22: ^{1}Hnmr assignment of tricarbonyl[1,4-η-2-methoxy-5-(7-keto khivorino) cyclohexa-1,3-diene] iron (25)

Protons	Simulated spectra	Real spectra
H1	4.788	5.38(m)
H2a	1.8	1.18(d)
H2b	1.95	1.98(d)
H3	4.682	5.28(m)
H5	2.612	2.44(d)
H6a	2.169	not observed
H6b	2.156	not observed
H9	3.119	3.72(m)
H11a	1.537	1.52(s)
H11b	2.173	not observed
H12a	2.281	2.45(m)
H12b	2.181	2.18(m)
H15	4.021	not observed
H17	5.252	not observed
H18	1.141	0.83(s)
H19	0.966	1.07(d)
H21	7.308	7.17(s)
H22	6.07	6.26(m)
H30	1.214	not observed
H31	2.042	2.29(s)
H32	2.04	1.89(s)
H33	3.514(methoxy)	3.63(s)
H3'	6.046	7.12(d)
H4'	5.925	7.33(m)
H5'	3.059	3.40(d)
H6'a	2.523	2.69(m)
H6'b	2.414	2.65(m)

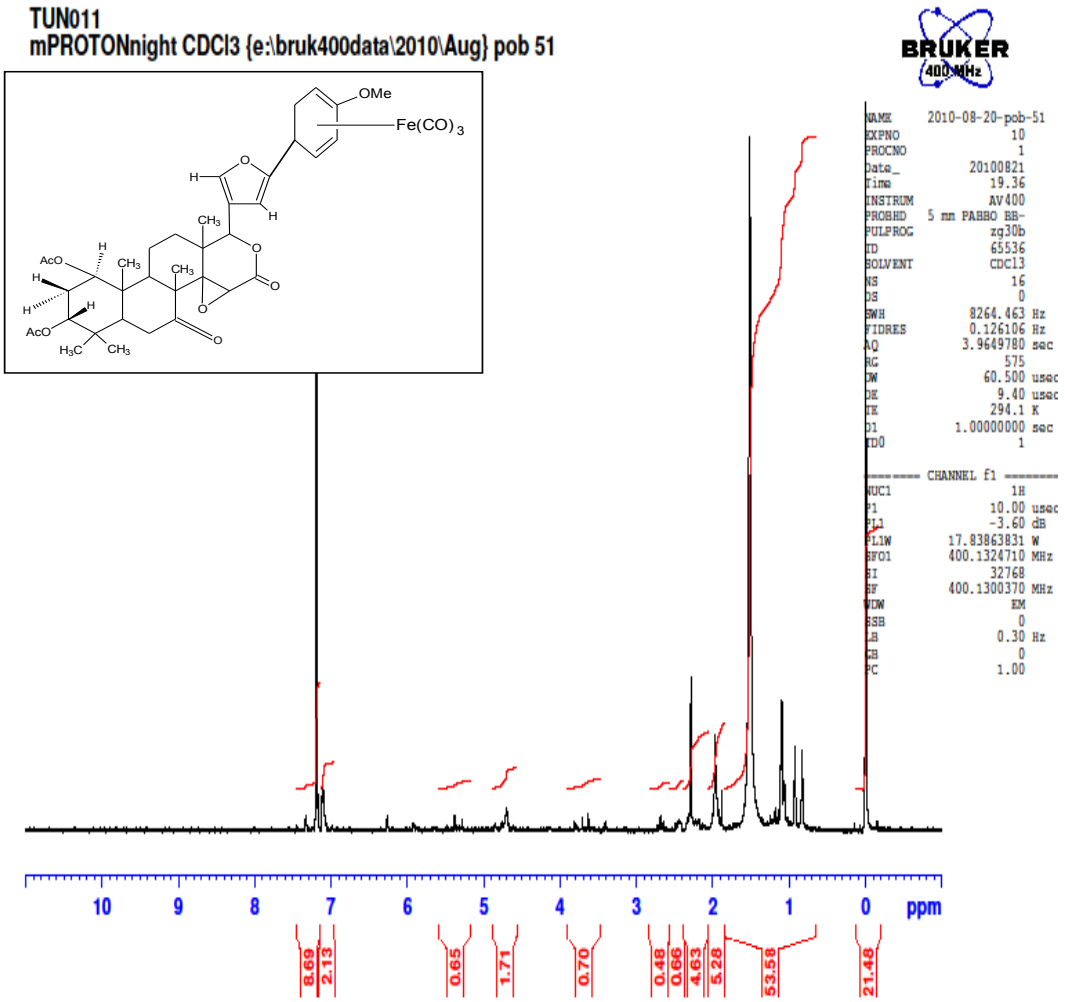

Figure 4.22: ^{1}Hnmr spectrum of tricarbonyl [1-4-η-2-methoxy-5-(7-keto khivorino) cyclohexa-1,3-diene]iron (25)

In addition, the complete disappearance of the proton resonance due to H^{23} in product (19) and (23) (Tables 4.16 & 4.20) supported the addition of the organometallic complex (2) at C^{23} (or α- carbon of Gedunin). The ^{1}Hnmr of the Khivorin and 7-ketokhivorin derivatives showed identical features to the Gedunin products. Our results are in agreement with the acetylation reactions of these natural products where electrophilic addition occurred at C^{23} of the furan ring (Ohochuku and Taylor, 1970). However, in the gedunin reaction, a mixture of acetylation products due to addition at C^{21} and C^{23} was observed (Ohochuku and Taylor, 1970). Our observation of the addition of complex (2) and (3) on C^{23} of the furan ring in products (19), (20), (21), (23), (24) and (25) must be attributed to steric hindrance due to approach of complex (2) and (3) at C^{21}. The ^{1}Hnmr spectrum of Tricarbonyl (1-4-η-5-exo-(polyavolensinolino) cyclohexa1,3-diene) iron (22) is given in figure 4.18 while the proton assignments are collected in Table 4.18. In addition to the characteristics 1,3-diene proton resonances discussed earlier, one immediate observation is the complete disappearance of the proton resonance due to H^{7}, at the β-carbon of the indole fragment in the starting polyavolensinol located at 6.15 ppm. It is therefore obvious that complex (2) attacked the natural product at the β-carbon of the indole fragment to give product (22) as a stable lilac solid.

The ^{13}Cnmr spectra were difficult to obtain due to the problem of low sample concentration

4.4 Mass spectral studies of adducts

The mass spectral data for the compounds are presented in the Tables 4.23 to 4.29. All the products do not show the parent, $[P]^+$ ion expected. We observed the loss of α-β unsaturated ketone fragment in the gedunin adduct during the mass spectral measurement. The loss showed strong peaks at 151 ($C_{10}H_{15}O$) (Figure 4.23), thus explaining why our parent peaks, expected at 700.7 was not observed for gedunin adduct. We also observed the loss of (M-173) in all the compounds indicating weakness of the C (diene)-C (natural product) bond. Loss of the fragments from the adducts (19), (20), (21), (23), (24) and (25) in the mass spectral are not unusual as similar observations have been made (John and Kane-Maguire, 1979a; Games *et al*., 1975; Odiaka, 1980) in the mass spectral studies of a wide range of tricarbonyl (1-4-η-5-exo-1,3-diene-substituted) iron complexes. We suggest that the adducts undergo thermal decomposition in the mass spectrometer, apparently due to the weakness of the C (diene)-C(natural products) bond.

Table 4.23: Mass spectral assignment of tricarbonyl [1-4-η-5-(gedunino) cyclohexa-1,3-diene]iron (19)

Mass	Fragments	Intensity(m/z)
109	M-(2CO)-($C_{32}H_{39}O_7$)	8.13
150	M-(2CO)-($C_{25}H_{26}O_7Fe$)	1.83
201	M-(2CO)-($C_{25}H_{31}O_7$)	1.83
257	M-(2CO)-($C_{23}H_{29}O_5$)-($2H^+$)	6.25
401	M-(2CO)-($C_{12}H_{10}O_2Fe$)-(H^+)	6.25
500	M-(2CO)-($C_3H_3O_3Fe$)-(H^+)	16.25
505	M-(2CO)-(C_5H_5OFe)-($2H^+$)	100.0
547	M-(2CO)-(C_2HOFe)	8.13
546	M-(2CO)-(HOFe)-(H^+)	35.00
604	M-(2CO)-(C_2HO)+(H^+)	3.13

M= 700.7 (molecular mass of adduct)

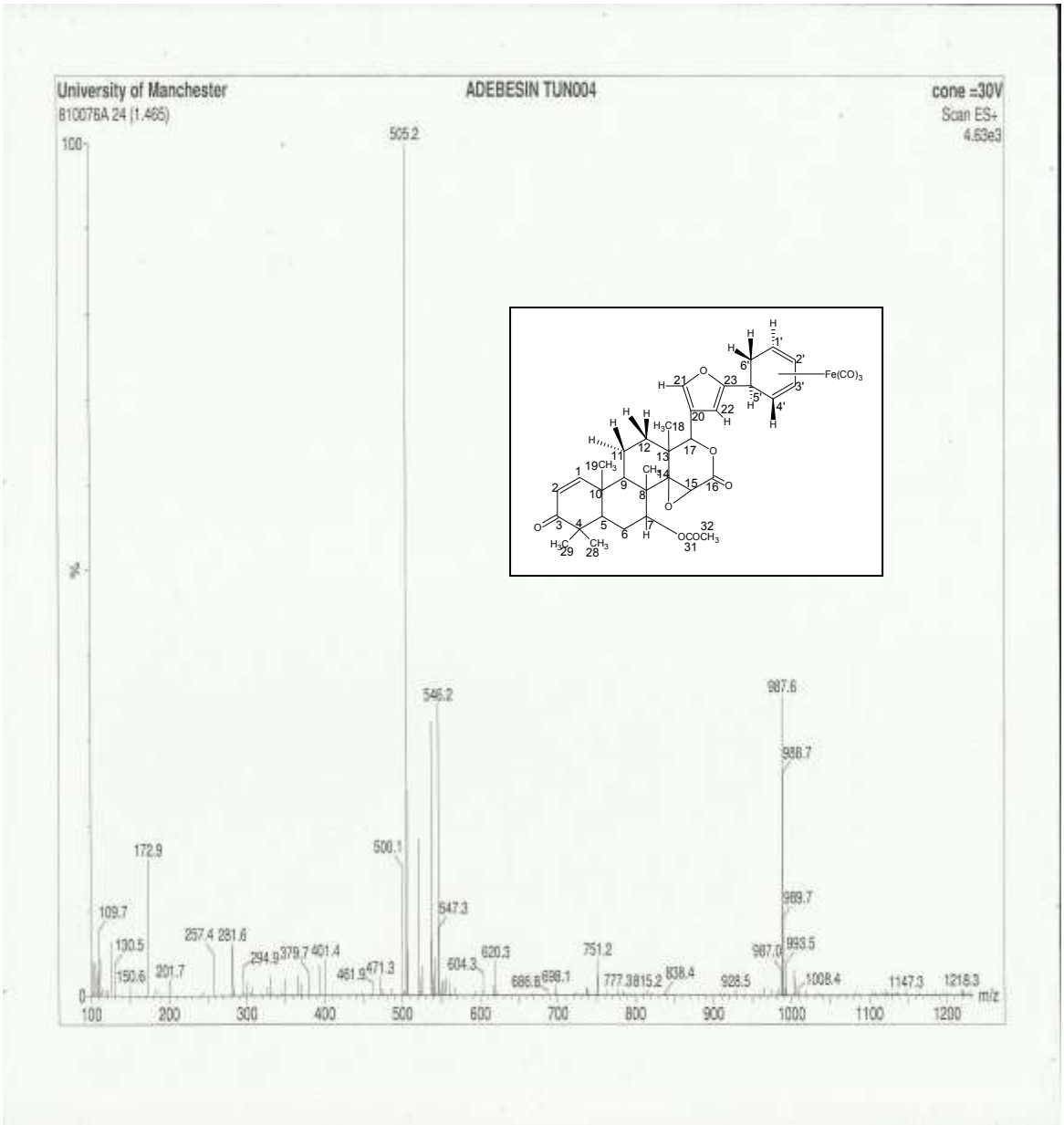

Figure 4.23: Mass spectrum of tricarbonyl [1-4-η-5-(gedunino) cyclohexa-1,3-diene]iron (19)

Table 4.24: Mass spectral assignment of tricarbonyl [1-4-η-5-(khivorino) cyclohexa-1,3-diene]iron (20)

Mass	Fragments	Intensity (m/z)
173	M-(2CO)-($C_{31}H_{41}O_{10}$) - ($2H^+$)	2.27
355	M-(2CO)-($C_{22}H_{34}O_6$) + (H^+)	1.14
541	M-(2CO)-($C_9H_{10}O_2Fe$)-(H^+)	5.00
609	M-(2CO)-(C_5H_5OFe)-($2H^+$)	100.0
625	M-(2CO)-(C_4H_3OFe)	2.27
687	M-(2CO)-($C_2H_3O_2$)-($2H^+$)	1.14

M= 804.8 (Molecular mass of adduct)

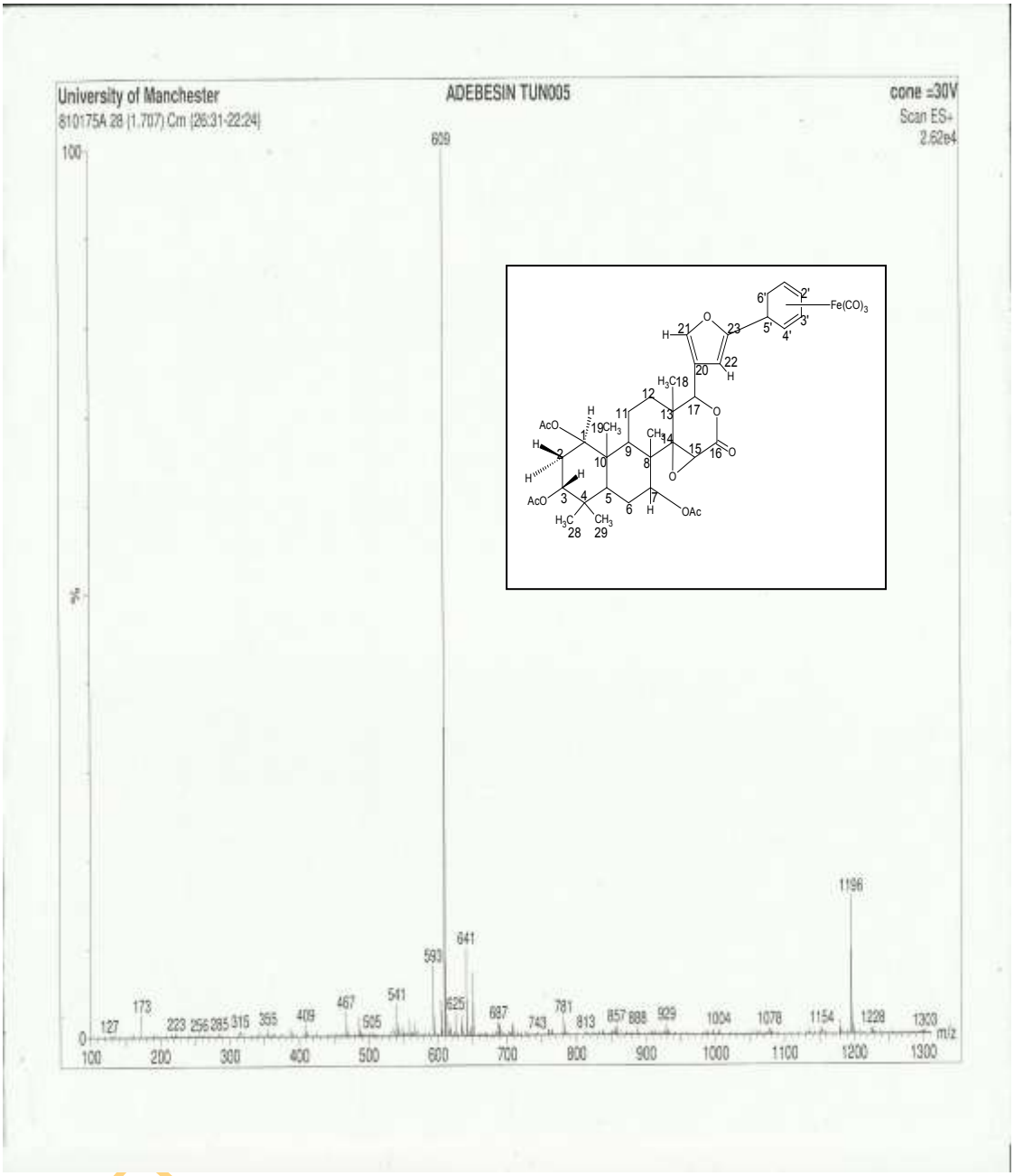

Figure 4.24: Mass spectrum of tricarbonyl [1-4-η-5-(khivorino)cyclohexa-1,3-diene]iron (20)

Table 4.25: Mass spectral assignmentof tricarbonyl [1-4-η-5-(polyavolensinolino cyclohexa-1, 3-diene] iron (22).

Mass	Fragment	Intensity (m/z)
207 base	M-(2CO)-($C_{16}H_{13}ONFe$)-(H^+)	100.0
248	M-(2CO)-($C_{14}H_{11}OFe$)	29.38
279	M-(2CO)-($C_{15}H_{26}O$) + ($2H^+$)	8.75
338	M-(2CO)-(C_7H_7OFe) + ($2H^+$)	7.5
390	M-(2CO)-(C_3H_2OFe) + (H^+)	8.75
467	M-(2CO)-(CH_3OH)	12.5
485	M-(2CO)-(CH_2)	8.75

M = 555.6 (molecular weight of adduct)

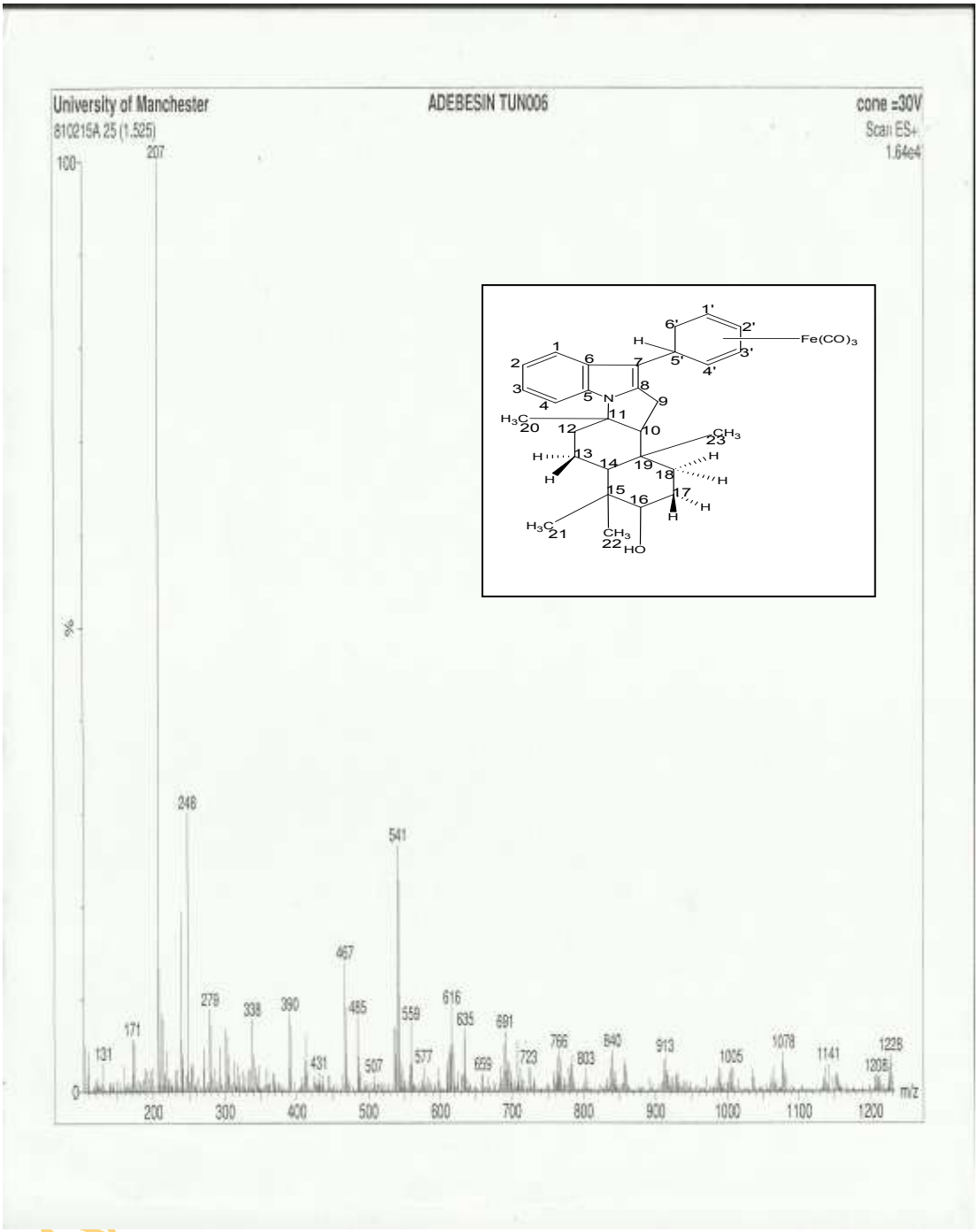

Figure 4.25: Mass spectrum of tricarbonyl [1-4-η-5-(polyavolensinolino) cyclohexa-1,3-diene]iron (22)

Table 4.26: Mass spectral assignment of Tricarbonyl [1-4-η-5-(7-keto-khivorino) cyclohexa-1, 3-diene] iron (21)

Mass	Fragment	Intensity (m/z)
191	M-(2CO)-($C_{29}H_{37}O_8$)	1.70
219	M-(2CO)-($C_{27}H_{35}$-O_8) + ($2H^+$)	2.84
541	M-(2CO)-(C_7H_7OFe)	3.98
560	M-(2CO)-($C_3H_3O_3Fe$)	1.70
593	M-(2CO)-(C_3H_2OFe)-(H^+)	3.98
609 base peak	M-(2CO)-(C_2HOFe) + ($2H^+$)	100.0

M =760.73 (Molecular weight of adduct)

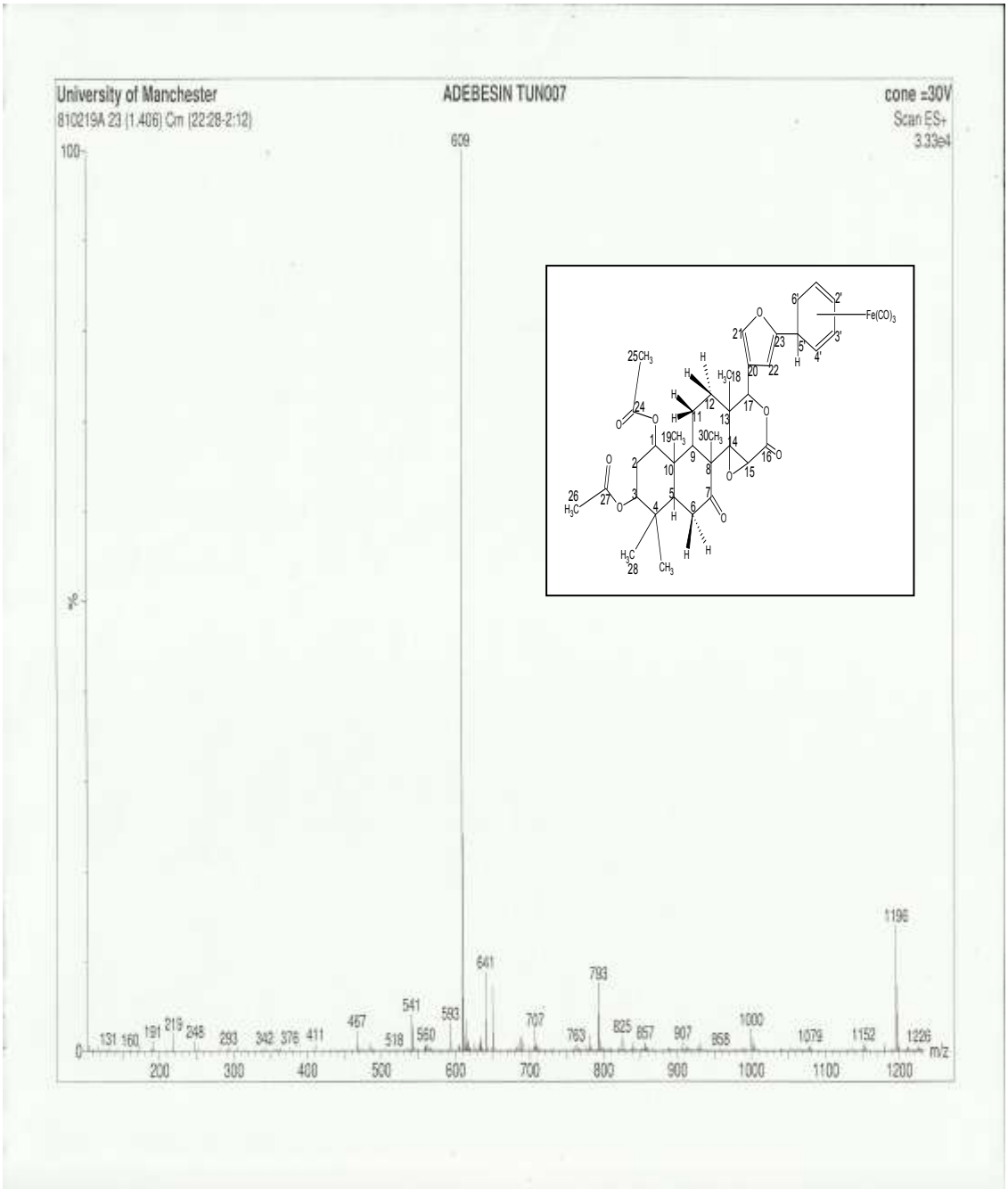

Figure 4.26: Mass spectrum of tricarbonyl [1-4-η-5-(7-ketokhivorino)cyclohexa-1,3-diene]iron (21)

Table 4.27: Mass spectral assignment of Tricarbonyl [1-4-η-2-methoxy-5-(gedunino) cyclohexa-1,3-diene]iron (23)

Mass	Fragments	Intensity (m/z)
107	M-(2CO)-($C_{29}H_{34}O_8Fe$)-(H^+)	1.0
151	M-(2CO)-($C_{26}H_{28}O_8Fe$) + (H^+)	2.0
173	M-(2CO)-($C_{25}H_{28}O_8$ Fe) – (H^+)	13.0
412	M-(2CO)-($C_{16}H_{22}O_3$)	1.0
467	M-(2CO)-($C_9H_{11}O_2Fe$)	3.0
505	M-(2CO)-($C_6H_7O_2Fe$)-($2H^+$)	100
506	M-(2CO)-($C_6H_7O_2Fe$)-(H^+)	20.0
507	M-(2CO)-($C_6H_7O_2Fe$)	7.0
537	M-(2CO)-($C_9H_{12}O$)-(H^+)	16.0
546	M-(2CO)-($C_3H_3O_2Fe$) – (H^+)	15.0
547	M-(2CO)-($C_3H_3O_2Fe$)	4.0
603	M-(2CO)-($C_3H_4O_2$) + (H^+)	3.0

M= 730.7 (molecular mass of adduct)

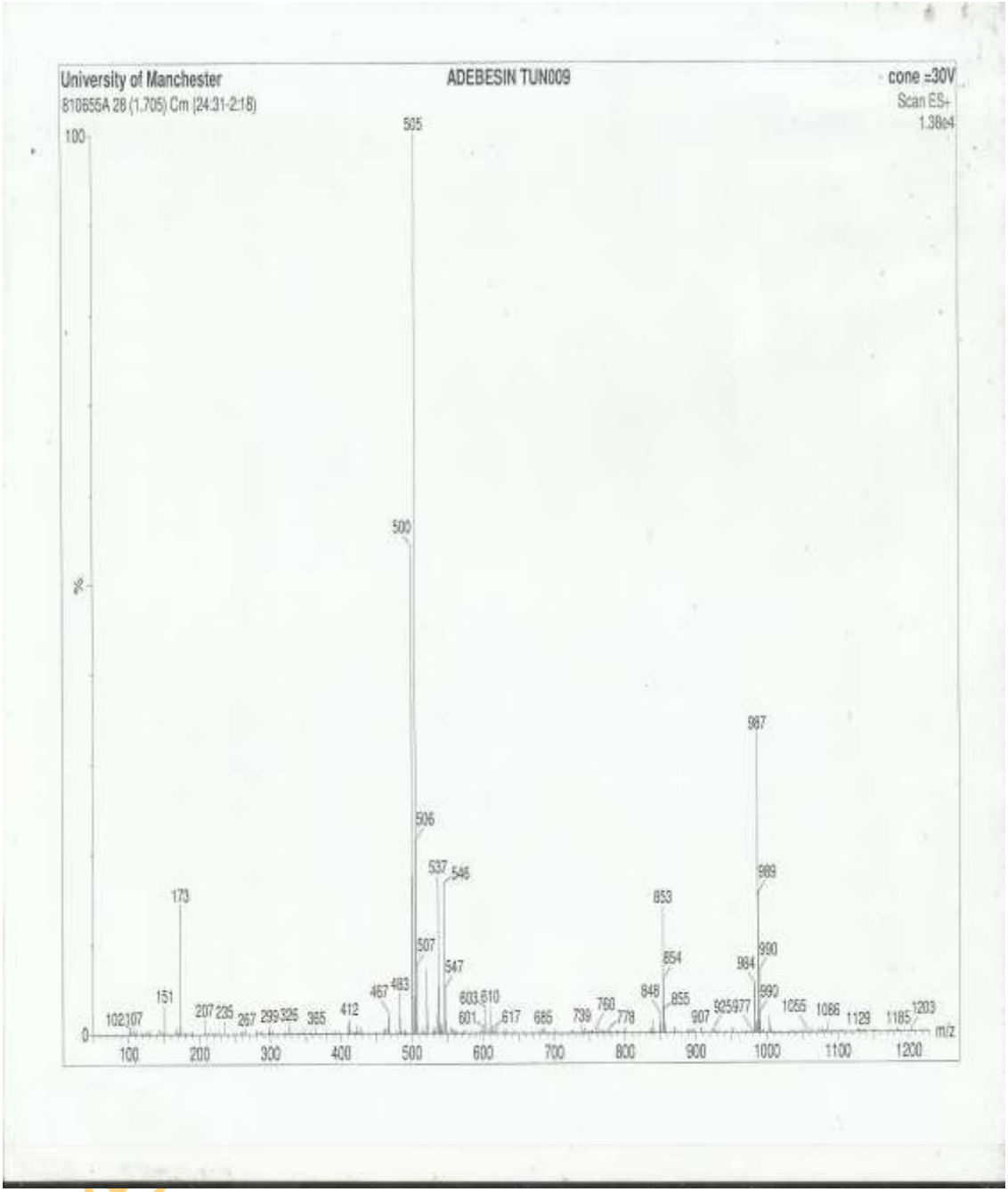

Figure 4.27: Mass spectrum of tricarbonyl [1-4-η-2-methoxy-5-(gedunino) cyclohexa-1,3-diene]iron (23)

Table 4.28: Mass spectral assignment of tricarbonyl[1,4-η-2-methoxy-5-(khivorino) cyclohexa-1,3-diene]iron (24)

Mass	Fragment	Intensity (m/z)
173	M-(2CO)-($C_{29}H_{40}O_{10}Fe$)-H^+	18.0
229	M-(2CO)-($C_{29}H_{42}O_{10}$) + H^+	3.0
257	M-(2CO)-($C_{28}H_{39}O_9$) – ($2H^+$)	9.0
541	M-(2CO)-($C_{10}H_{12}O_3Fe$) - (H^+)	2.0
609	M-(2CO)-($C_6H_7O_2Fe$) – ($2H^+$)	100
707	M-(2CO) - ($C_3H_3O_2$)	2.0

M = 834 (Molecular mass of adduct)

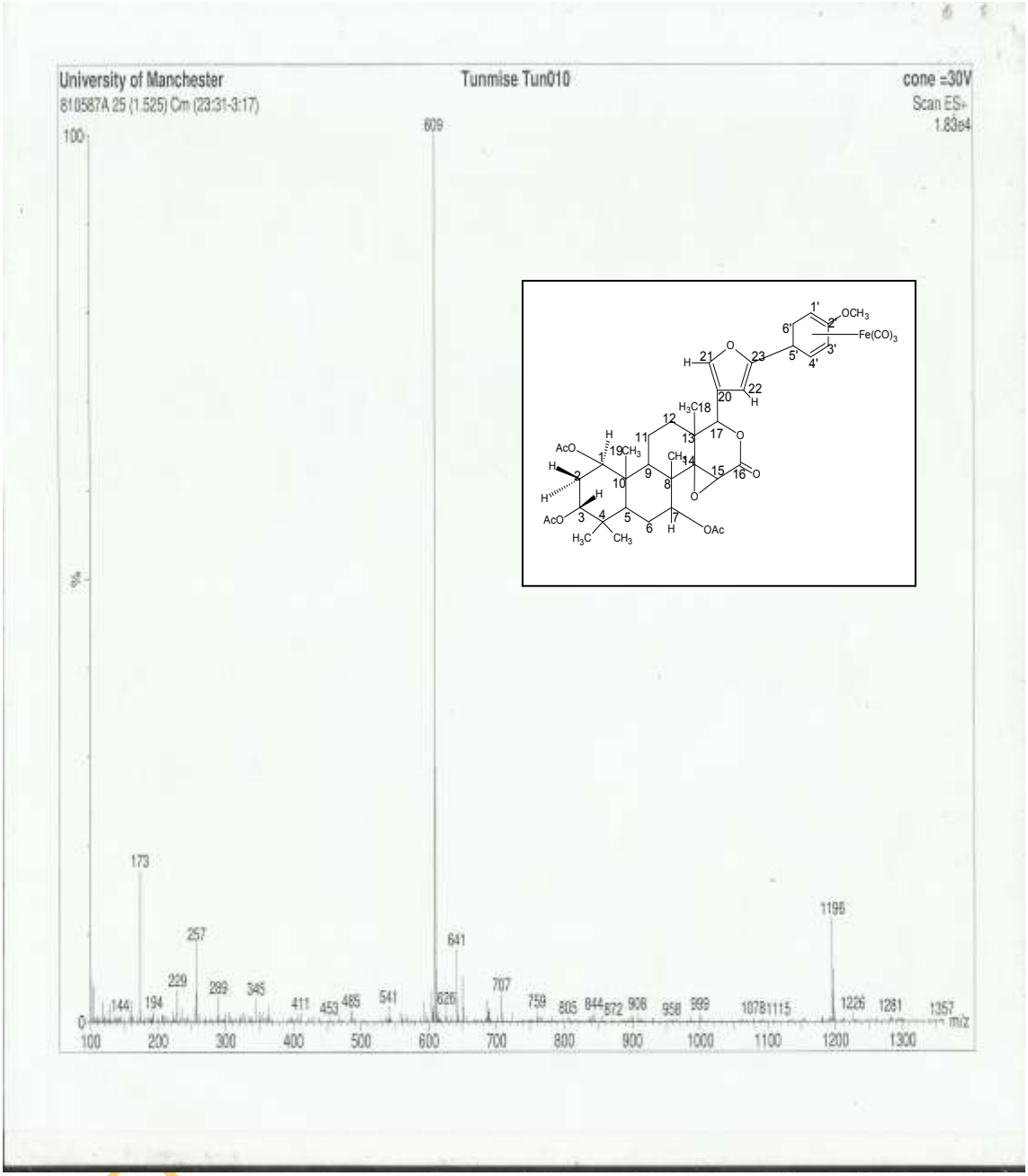

Figure 4.28: Mass spectrum of tricarbonyl [1-4-η-2-methoxy-5-(khivorino) cyclohexa-1,3-diene]iron (24)

Table 4.29: Mass spectra assignment of tricarbonyl [1,4-η-2-methoxy-5-(7-keto-khivorino) cyclohexa-1,3-diene] iron (25)

Mass	Fragment	Intensity (m/z)
152	M-(2CO)-($C_{33}H_{41}O_9$)-(H^+)	5.0
173	M-(2CO)-($C_{27}H_{36}O_9Fe$)-(H^+)	65.0
205	M-(2CO)-($C_{29}H_{37}O_9$)	2.0
254	M-(2CO)-($C_{24}H_{24}O_7Fe$)	3.0
383	M-(2CO)-($C_{20}H_{30}O_5$)-(H^+)	2.0
494	M-(2CO)-($C_{13}H_{20}O_4$)	3.0
541	M-(2CO)-($C_8H_9O_2Fe$)	9.0
565	M-(2CO)-($C_6H_7O_2Fe$)-($2H^+$)	100
581	M-(2CO)-($C_5H_5O_2Fe$)	43.0

M = 790 (Molecular mass of adduct)

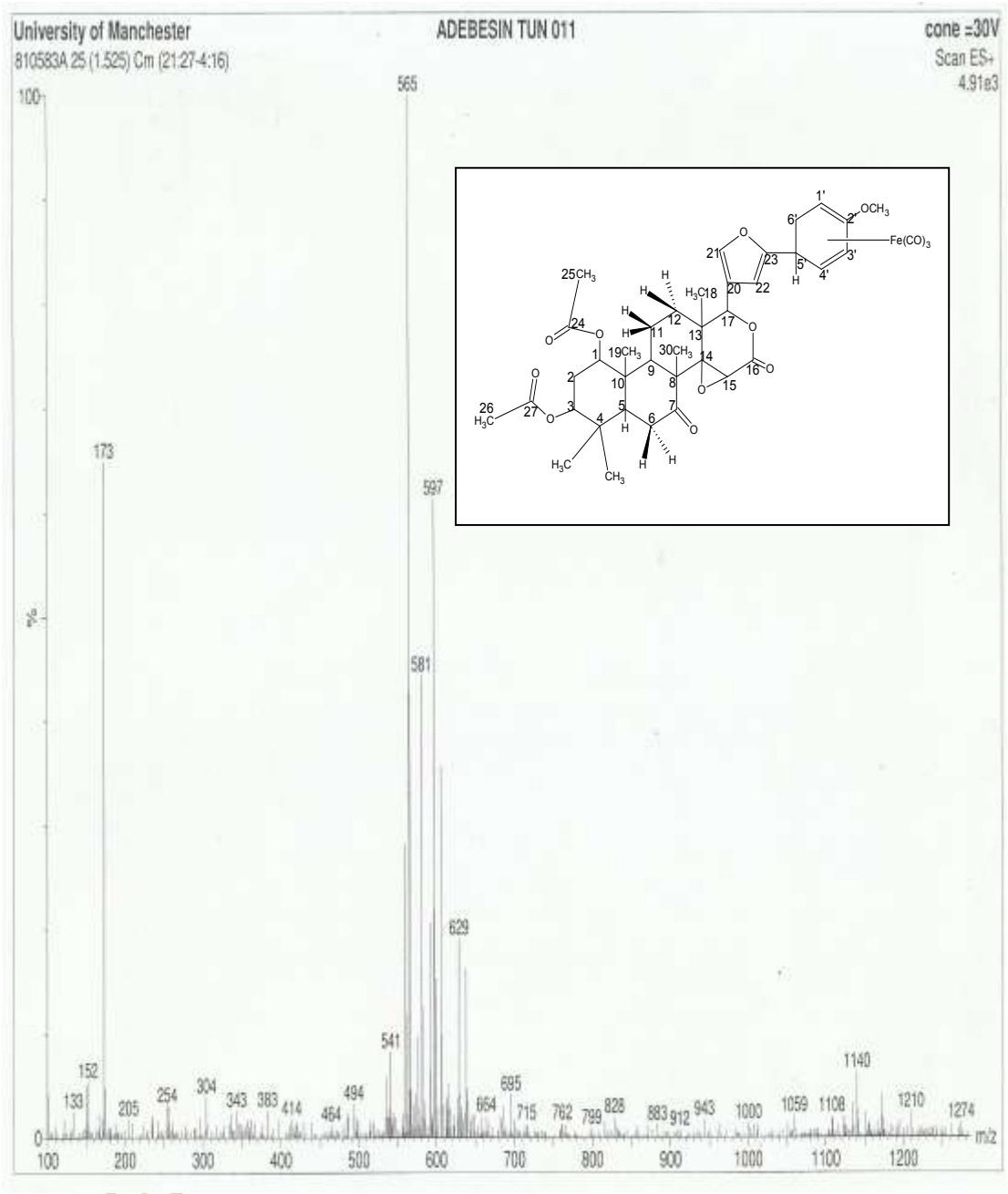

Figure 4.29: Mass spectrum of tricarbonyl [1-4-η-2-methoxy-5-(7-ketokhivorino) cyclohexa-1,3-diene]iron (25)

The loss of a proton from each of the natural products to form the corresponding adducts is not unreasonable if one envisages the formation of cationic intermediate complexes of the type shown below for the furan and indole fragments of the products (Odiaka *et al*., 2007).

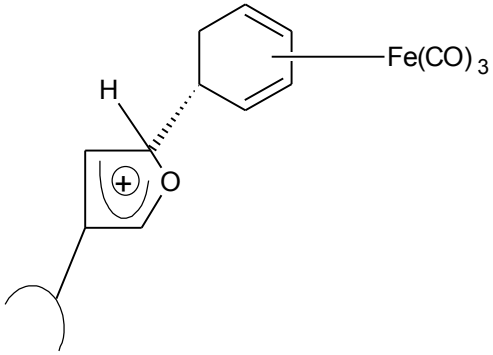

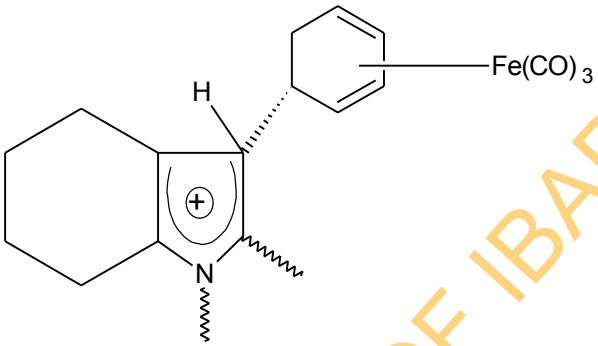

Thus, the well established electron-withdrawing character of the [(diene)$Fe(CO)_3$] moiety (Landsberg and Katz, 1971) allows rapid loss of hydrogen from the furan and indole fragments at the point of coordination to give the isolated adducts as shown above.

4.5 SPECTRAL STUDIES OF DEMETALLATED COMPOUNDS

4.5.1 IR studies of demetallated compounds

The reaction of $[(1\text{-}5\text{-}\eta\text{-}C_6H_7)Fe(CO)_3][BF_4]$ (2) and $[(1\text{-}5\text{-}\eta\text{-}2\text{-}MeOC_6H_6)Fe(CO)_3][BF_4]$ (3) adducts with an oxidizing agent trimethylamine-N-oxide (Me_3NO) brings about the removal of the tricarbonyl iron moiety (Shvo and Hazum, 1974). The demetallated compounds are (26), (27), (28), (29), (30), (31) and (32) Fig 5.1. They are air sensitive yellow oils except for product (30) which is colourless oil.

The IR assignment for these compounds is presented in Tables 4.30 to 4.36 and the spectra are shown in Fig 4.30 to 4.36. The cleavage of the tricarbonyl iron moiety was confirmed by the disappearance of IR √(CO) bands at 2050 and 1975 cm-1 characteristics of neutral tricarbonyl (1,3- diene-substituted) iron derivatives and 2060 and 1990 cm-1 for the cationic tricarbonyl (1,3-diene-substituted)iron derivatives formed from the addition of the natural products to complexes (2) and (3) respectively. In addition, there is also the absence of the M-C bond (Fe-C (organic) observed at 561-580 cm^{-1} and 693-696 cm^{-1} (Brisdon, 1998) which further confirms demetallation.

4.6 ^{1}Hnmr studies of demetallated compounds

The demetallated products are soluble in most organic solvents but 5-exo (polyavolensinol) cyclohexa-1,3-diene product (29**)** is air- sensitive and insoluble in most solvents, thus preventing (^{1}H and ^{13}C) nmr and Mass spectral measurements. The ^{1}Hnmr assignments of the demetallated compounds are collected in Tables 4.37 to 4.42 and the spectra presented in Fig 4.37 to 4.42.

The characteristic inner ($H^{2'}$and $H^{3'}$) and outer ($H^{1'}$ and $H^{4'}$) 1, 3-diene protons were observed in all the demetallated compounds at 6.79 ppm and 7.33 ppm. The furanic protons, H^{21}, H^{22} are observed in (26), (30) at 7.20 ppm. This is a more shielded value than that reported in the Literature at 7.39 and 6.64 ppm (Okorie, 1980, 1981) while the indolic protons H^{7} was not observed in (29).

Table 4.30: IR assignment of 5-exo-(gedunino)-cyclohexa-1,3-diene (26)

IR bands (cm^{-1})	Intensity	Assignment
2962	s	C-H str for alkanes
1736	vs	C=O for esters
1667	s	αβ-unsaturated ketone
1368	m	C-H rock of alkanes
1258	vs	C-O str for ester
1232	vs	C-O str for alkanes
874	s	furan

Key: m = moderate, vs. = very sharp, s = sharp

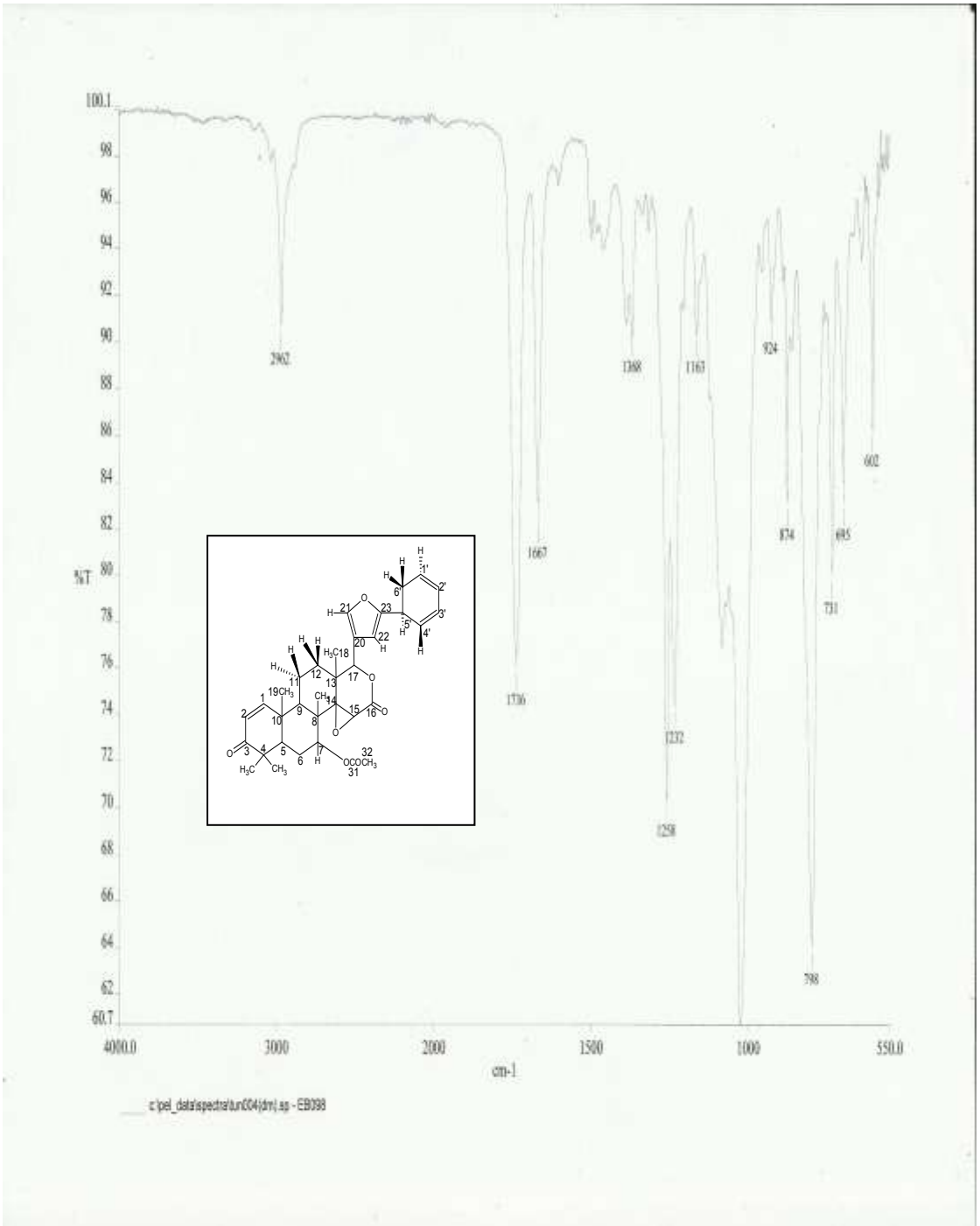

Figure 4.30: IR spectrum of 5-exo-(gedunino) cyclohexa-1,3-diene (26)

Table 4.31: IR assignment of 5-exo-(khivorino) cyclohexa-1,3-diene (27)

IR band (cm^{-1})	Intensity	Assignment
2962	m	C-H str alkanes
1728	m	C=O str esters
1257	s	C-O str esters
1012	s	C-O str esters
863	m	furan
696	m	C-H out of plane aromatics

Key: m = moderate, vs. = very sharp, s = sharp

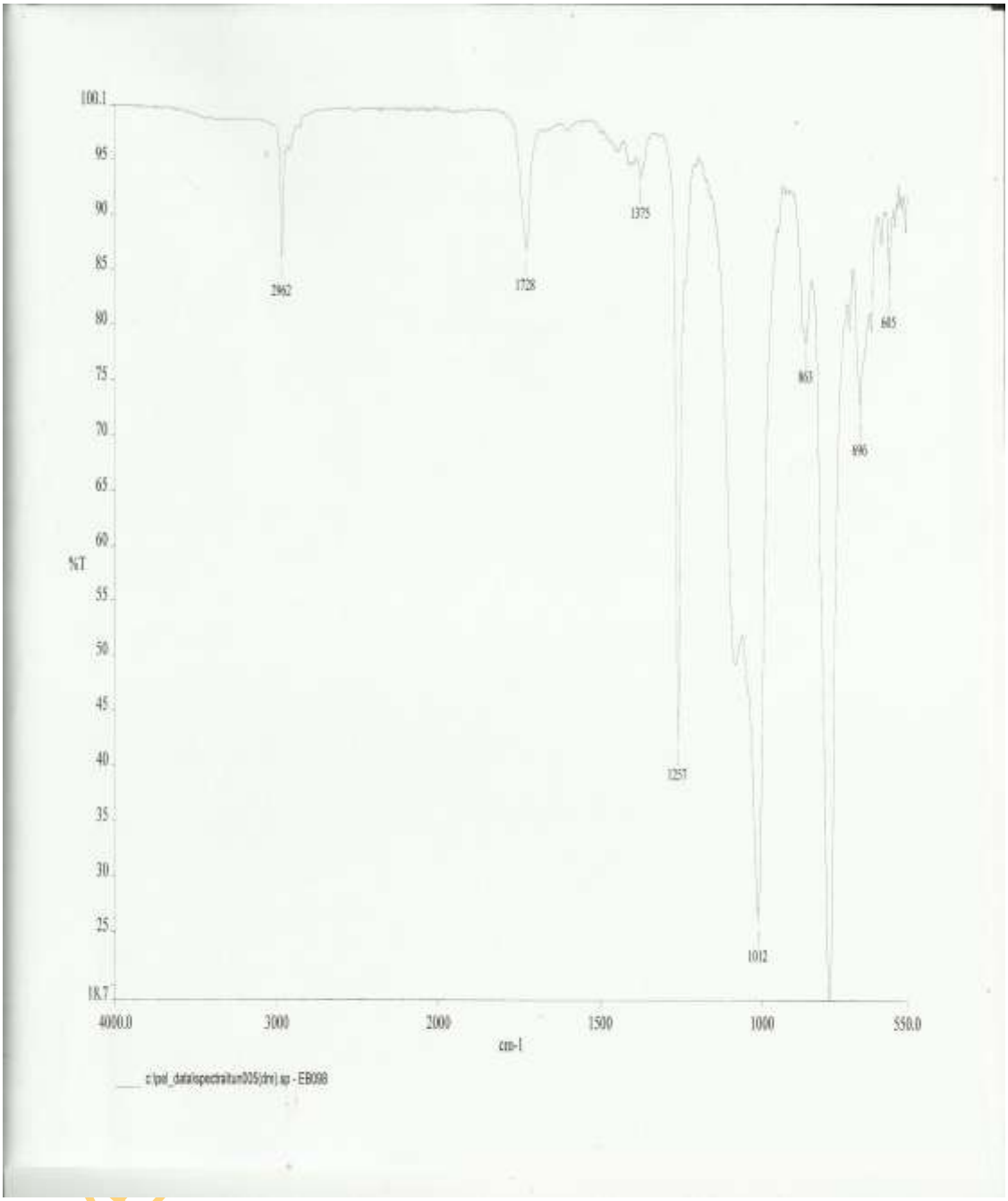

Figure 4.31: IR spectrum of 5-exo-(khivorino) cyclohexa-1,3-diene (27)

Table 4.32: IR assignment of 5-exo-(polyavolensinolino) cyclohexa-1,3-diene (29)

IR bands (cm^{-1})	Intensity	Assignment
2961	s	C-H str alkanes
1604	s	C=C str aromatic
1495	s	C-C str aromatic
1453	s	C-C str aromatic
1258	s	C-O str alcohol
1010	s	C-O str alcohol
790	m	C-H out of plane aromatic

Key: s= sharp, m = moderate, vs = very sharp

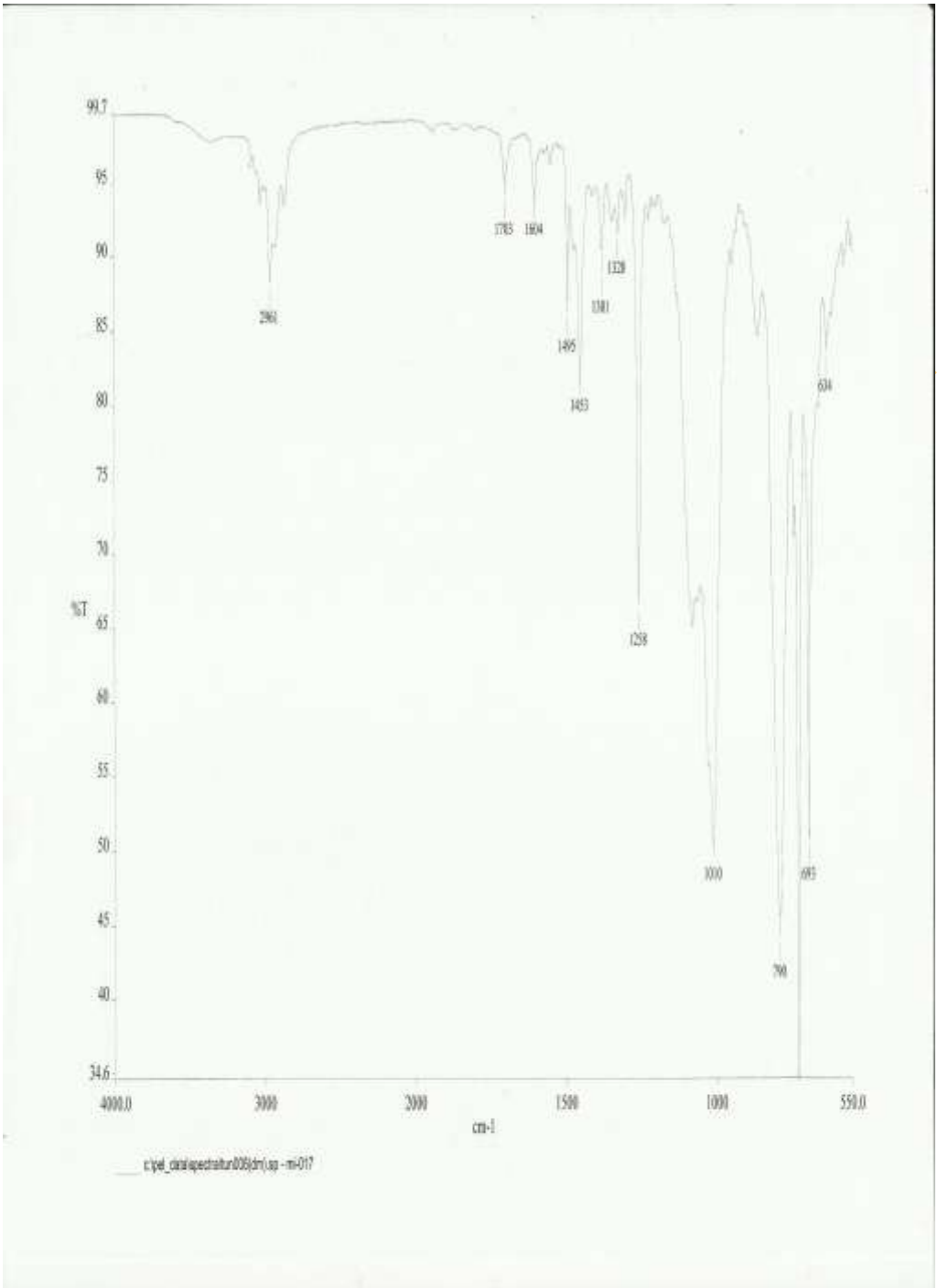

Figure 4.32: IR spectrum of 5-exo-(polyavolensinolino) cyclohexa-1, 3-diene (29)

Table 4.33: IR assignment of 5-exo-(7-ketokhivorino) cyclohexa-1, 3-diene (28)

IR bands (cm^{-1})	Intensity	Assignment
2962	s	C-H str alkanes
1728	vs	C=O str esters
1375	s	CH_2andCH_3
1257	vs	C-O str of esters
1014	vs	C-O str esters
874	s	furan

Key: s = sharp, vs = very sharp, m = moderate, b = broad

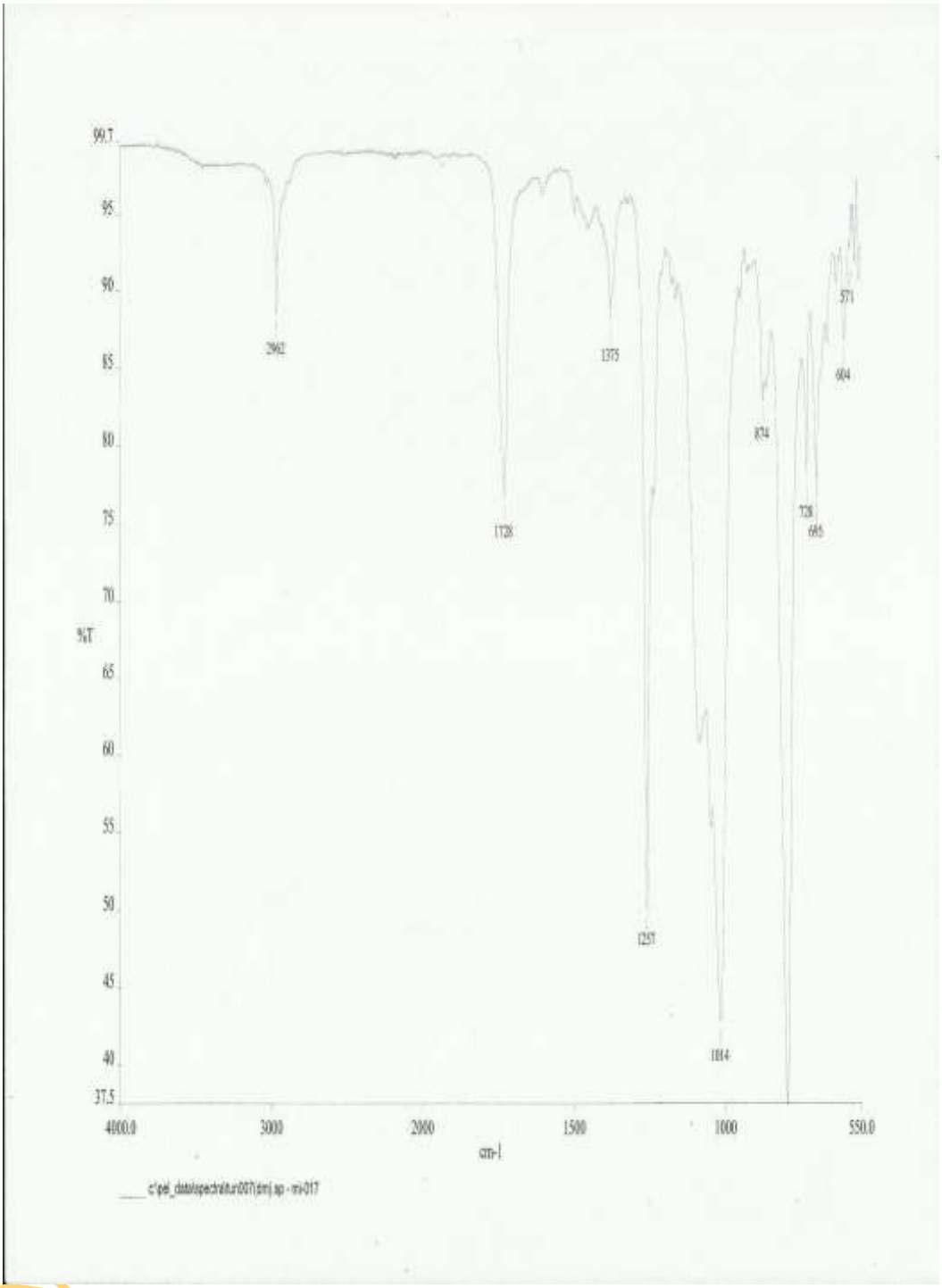

Figure 4.33: IR spectrum of 5-exo-(7-ketokhivorin) cyclohexa-1, 3-diene (28)

Table 4.34: IR assignment of 2-methoxy-5-exo-(gedunino) cyclohexa-1,3-diene (30)

IR band (cm^{-1})	Intensity	Assignment
2962.	m	C-H str alkanes
1737	s	C=O str esters
1257	vs	C-O ester
1009	vs	C-O str ester
789	s	C-H vibration

Key: m= moderate, s= sharp, vs= very sharp, b= broad

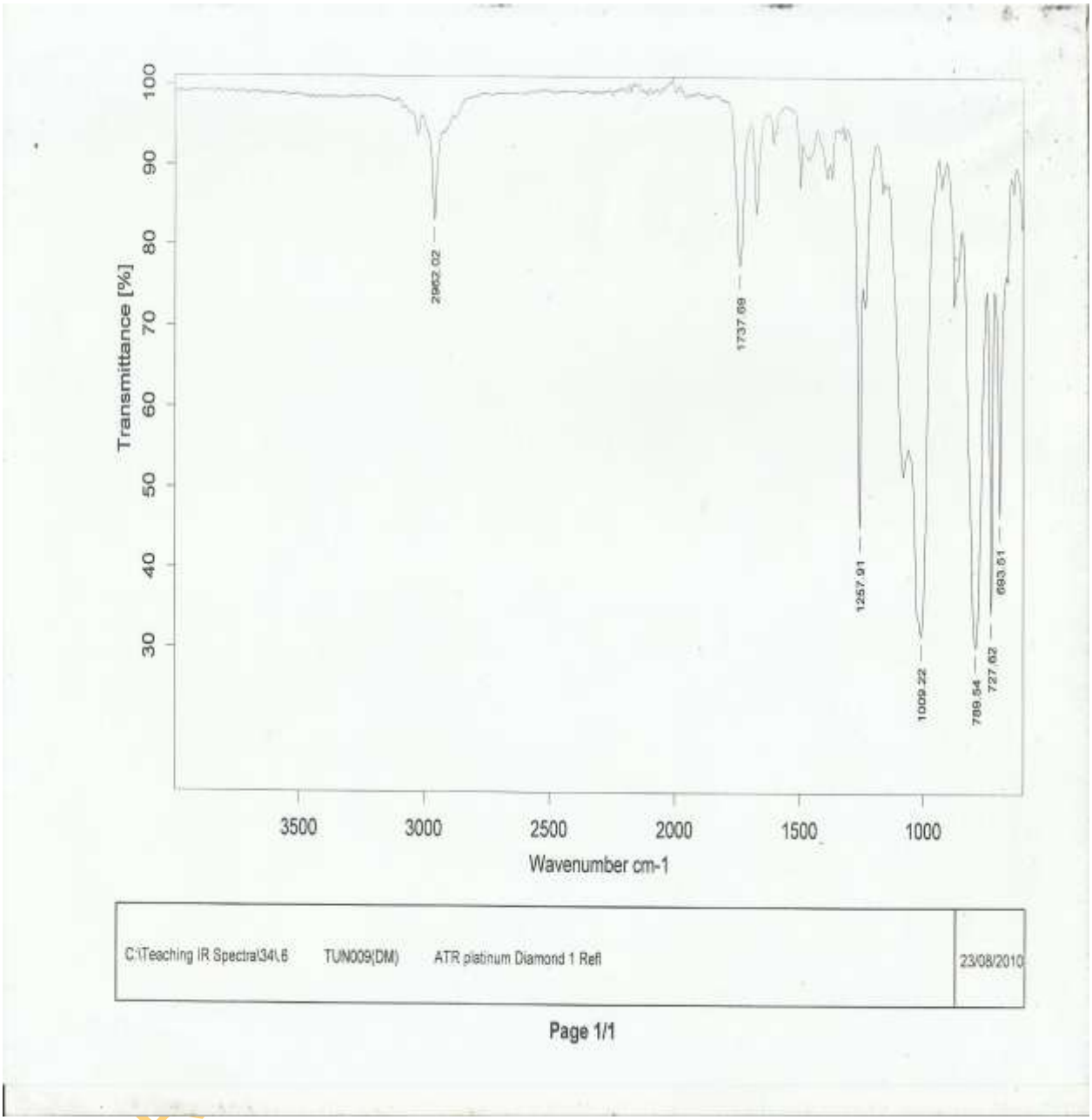

Figure 4.34: IR spectrum of 2-methoxy-5-exo-(gedunino)cyclohexa-1,3-diene (30)

Table 4.35: IR assignment of 2-methoxy-5- exo-(khivorino) cyclohexa-1,3-diene (31)

IR bands (cm^{-1})	Intensity	Assignment
2961	m	C-H str alkanes
1728	vs	C=O str esters
1374-1020	s	C-O str esters
874	m	furan band
796	vs	C-H vibrations

Key: m= moderate, s= sharp, vs= very sharp, b= broad

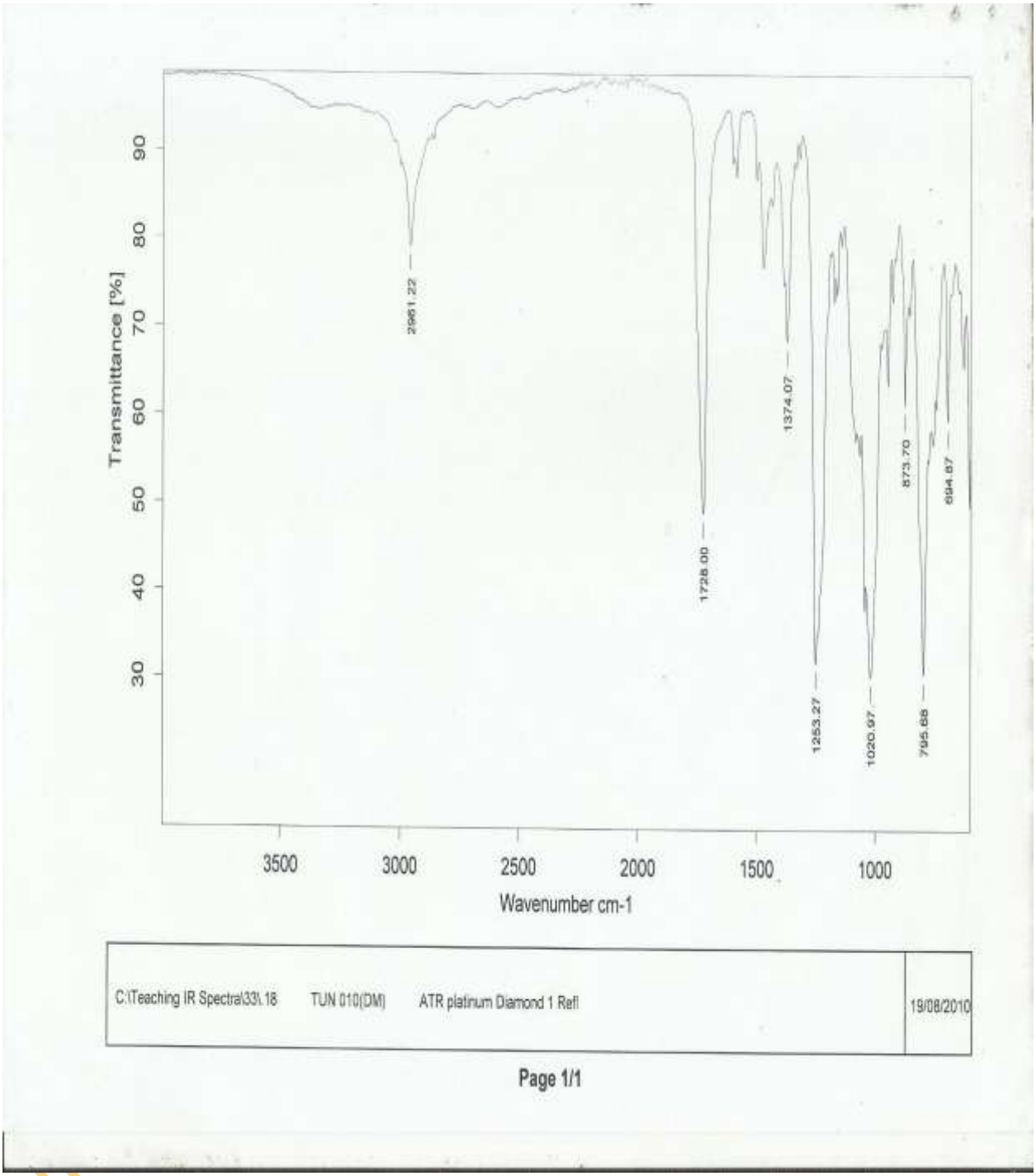

Figure 4.35: IR spectrum of 2-methoxy-5-exo-(khivorino)cyclohexa-1,3-diene (31)

Table 4.36: IR assignment 2-methoxy-5- exo-(7-ketokhivorino) cyclohexa-1,3-diene (32)

IR band (cm^{-1})	Intensity	Assignment
2962	s	C-H str alkanes
1258	vs	C-O str esters
1008	vs	C-O str esters
786	vs	C-H vibrations

Key: m= moderate, s= sharp, vs= very sharp, b= broad

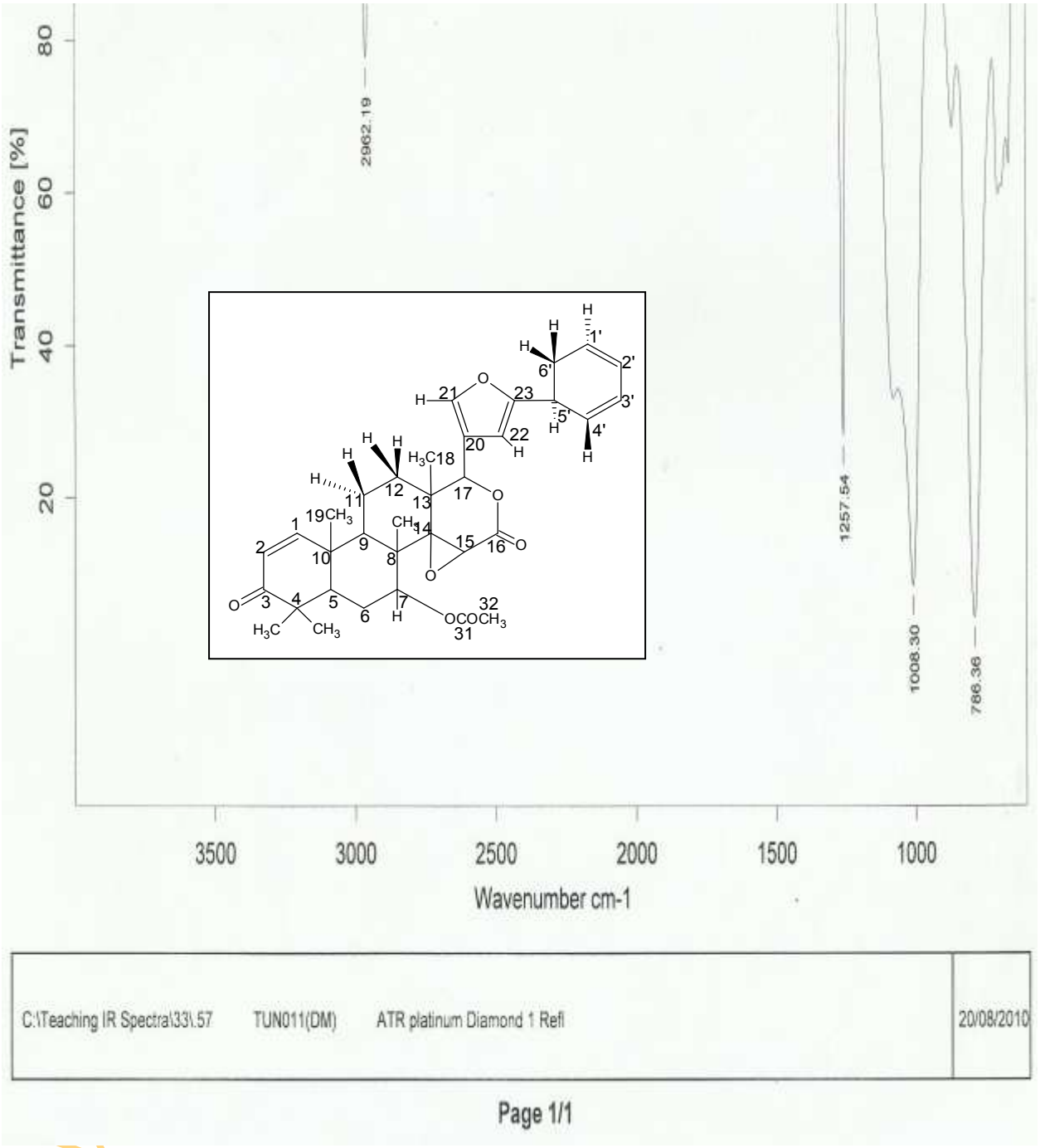

Figure 4.36: IR spectrum of 2-methoxy- 5-exo-(7-ketokhivorino)cyclohexa-1,3-diene (32)

Table 4.37: ^{1}Hnmr assignment of 5-exo-(gedunino)-cyclohexa-1,3-diene (26)

Protons	Simulated Spectra (ppm)	Real Spectra (ppm)
H1	6.433	7.35(d)
H2	5.699	5.79(s)
H5	2.116	not observed
H6a	1.637	1.77(d)
H6b	2.397	2.43(q)
H7	5.043	4.49(m)
H9	3.115	2.12(d)
H11a	1.344	1.74(t)
H11b	1.98	1.86(t)
H12a	2.122	1.89(m)
H12b	2.022	1.80(t)
H15	3.545	3.46(s)
H17	5.078	5.55(s)
H18	1.111	1.56(s)
H19	1.097	1.16(s)
H21	7.437	7.05(s)
H22	6.23	7.02(s)
H28	1.09	1.09(s)
H29	1.19	1.18(S)
H30	1.041	1.01(d)
H32	2.042	2.04(s)
H1'	5.829	5.81(s)
H2'	5.722	not observed
H3'	5.876	not observed
H4'	5.83	6.27(t)
H5'	3.041	3.25(s)
H6'a	2.269	not observed
H6'b	2.316	not observed

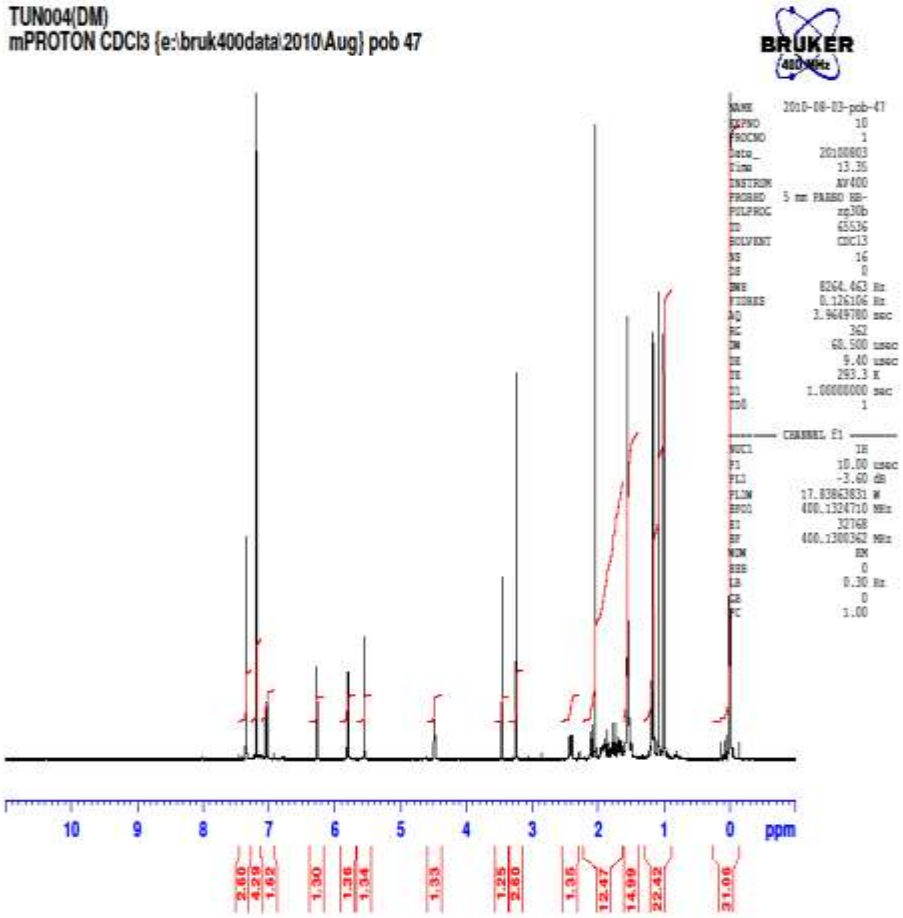

Figure 4.37: ^{1}Hnmr spectrum of 5-exo-(gedunino) cyclohexa-1,3-diene (26)

Table 4.38: ^{1}Hnmr assignment of 5-exo-(khivorino) cyclohexa-1,3-diene (27)

Protons	Simulated Spectra (ppm)	Real Spectra (ppm)
H1	4.71	4.55(t)
H2a	1.8	1.90(s)
H2b	1.95	1.95(s)
H3	4.605	4.45(t)blurred
H5	2.209	not observed
H6a	1.418	1.77(s)
H6b	2.178	2.16(d)
H7	4.951	4.64(t)
H9	3.13	not observed
H11a	1.407	1.58(s)
H11b	2.043	2.04(d)
H12a	2.107	not observed
H12b	2.007	2.00(d)
H15	3.545	3.45(s)
H17	5.078	not observed
H18	1.111	1.17(s)
H19	0.87	0.74(s)
H21	7.437	not observed
H22	6.23	5.53(s)
H28	0.982	0.85(s)
H29	1.082	1.01(s)
H30	1.022	0.94(s)
H32	2.042	2.29(S)
H33	2.042	2.11(s)
H34	2.04	2.08(s)
H1'	5.829	7.33(m)
H2'	5.722	6.24(d,d)
H3'	5.876	7.35(t)
H4'	5.83	not observed
H5'	3.041	not observed
H6'a	2.269	not observed
H6'b	2.316	not observed

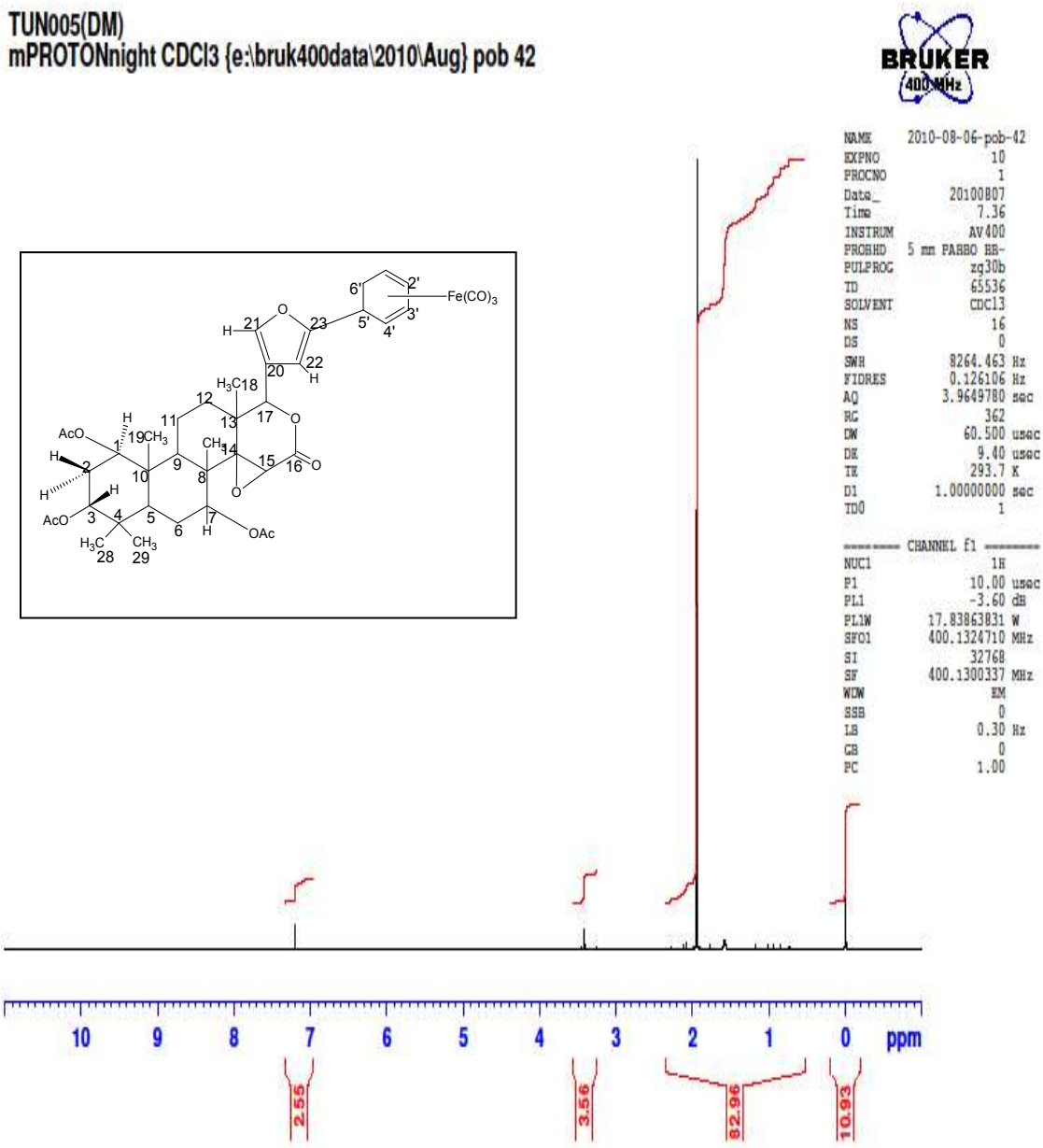

Figure 4.38a: ^{1}Hnmr spectrum of 5-exo-(khivorino) cyclohexa-1,3-diene (27)

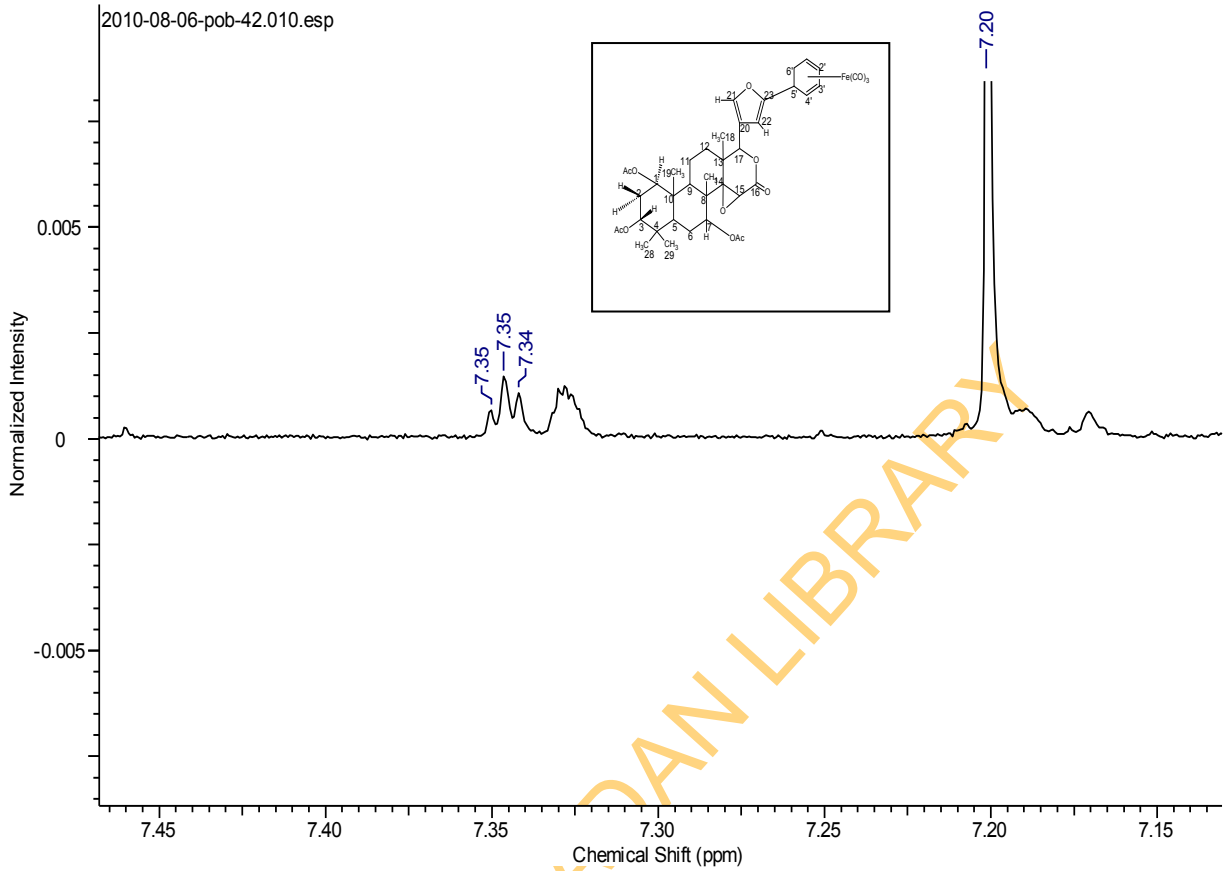

Figure 4.38b: Expanded ^{1}Hnmr spectrum of 5-exo-(khivorino) cyclohexa-1,3-diene (27)

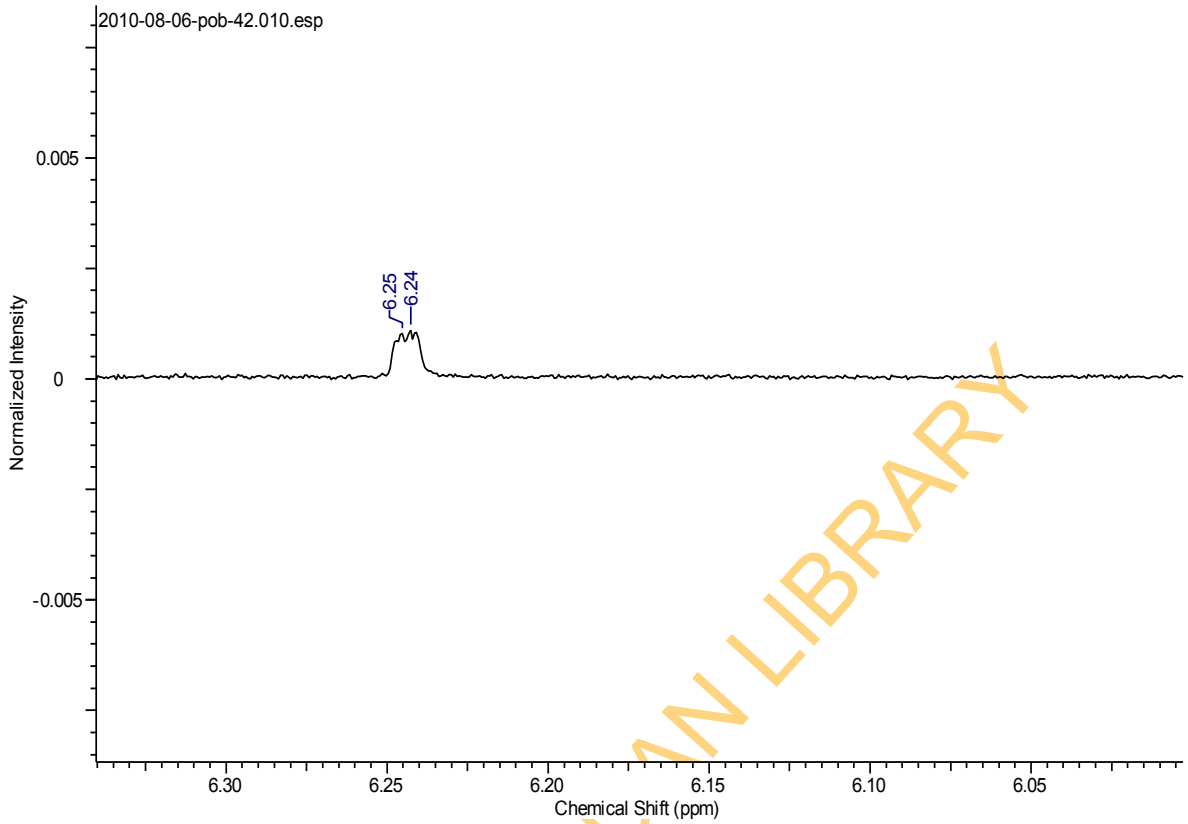

Figure 4.38b: Expanded ^{1}Hnmr spectrum of 5-exo-(khivorino) cyclohexa-1,3-diene (27)

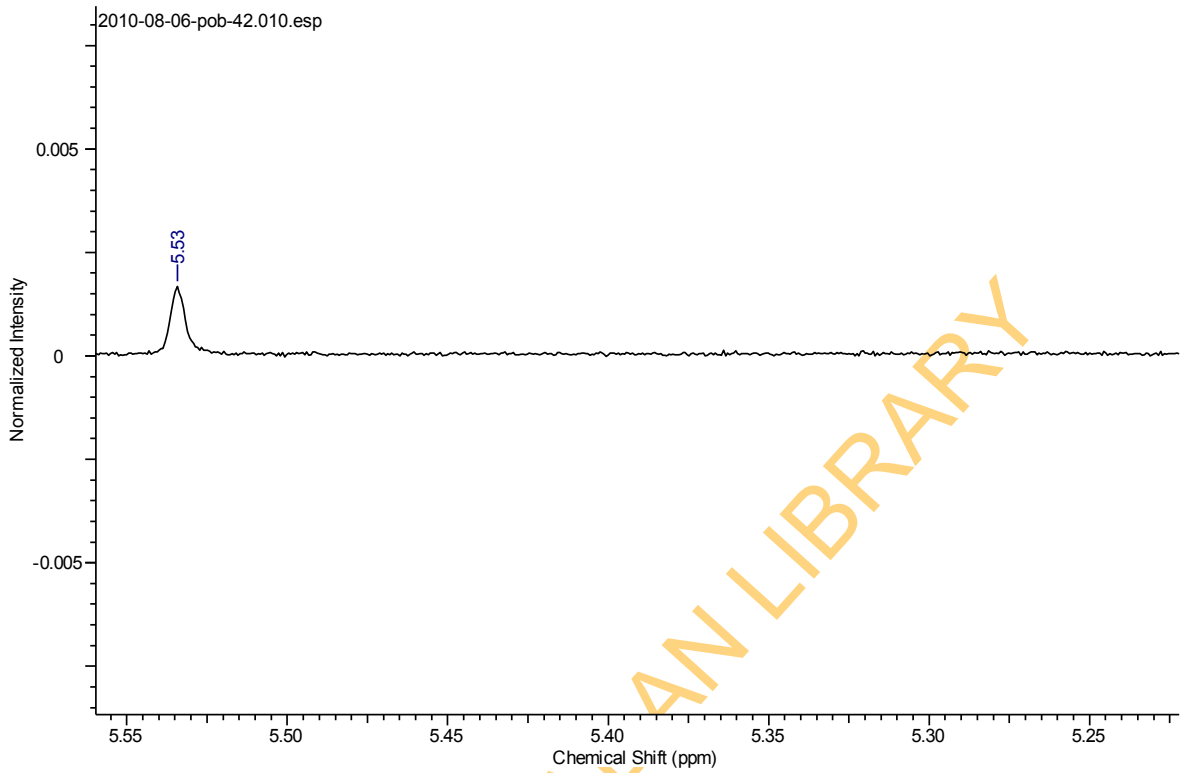

Figure 4.38b: Expanded ^{1}Hnmr spectrum of 5-exo-(khivorino) cyclohexa-1,3-diene (27)

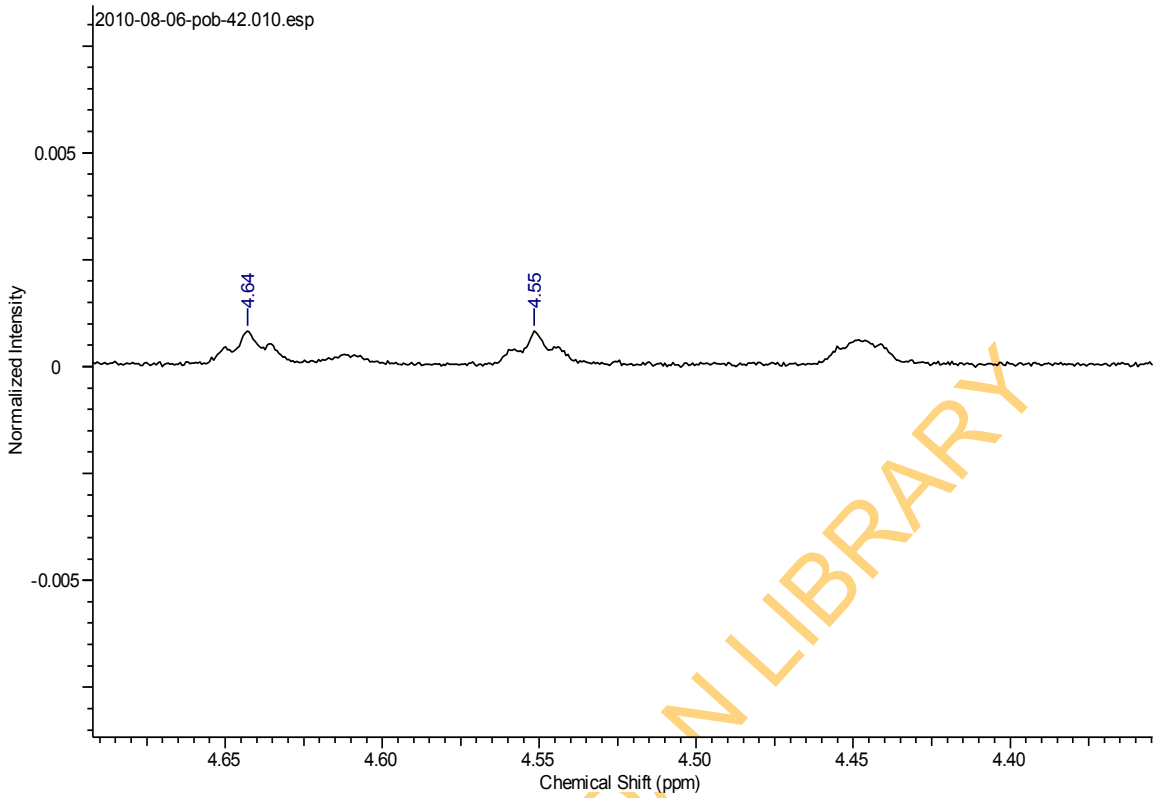

Figure 4.38b: Expanded ^{1}Hnmr spectrum of 5-exo-(khivorino) cyclohexa-1,3-diene (27)

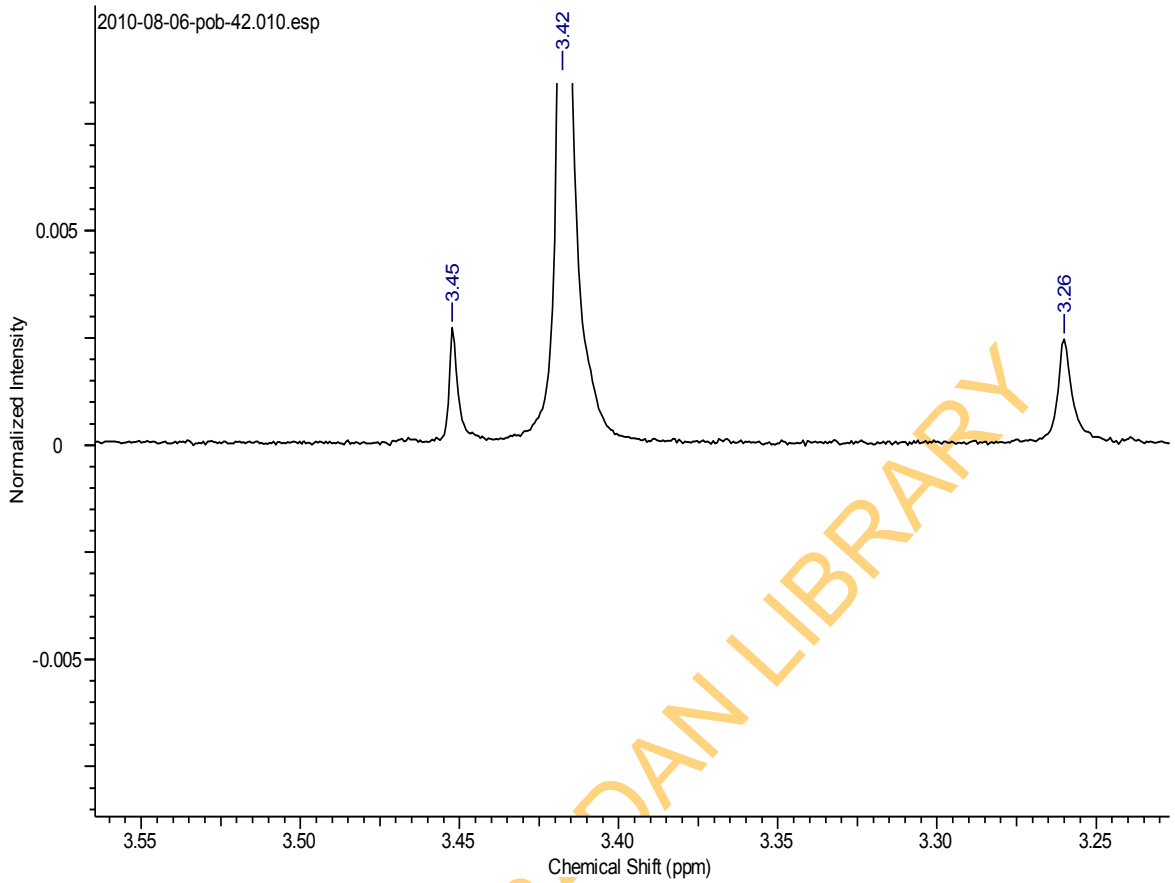

Figure 4.38b: Expanded ^{1}Hnmr spectrum of 5-exo-(khivorino) cyclohexa-1,3-diene (27)

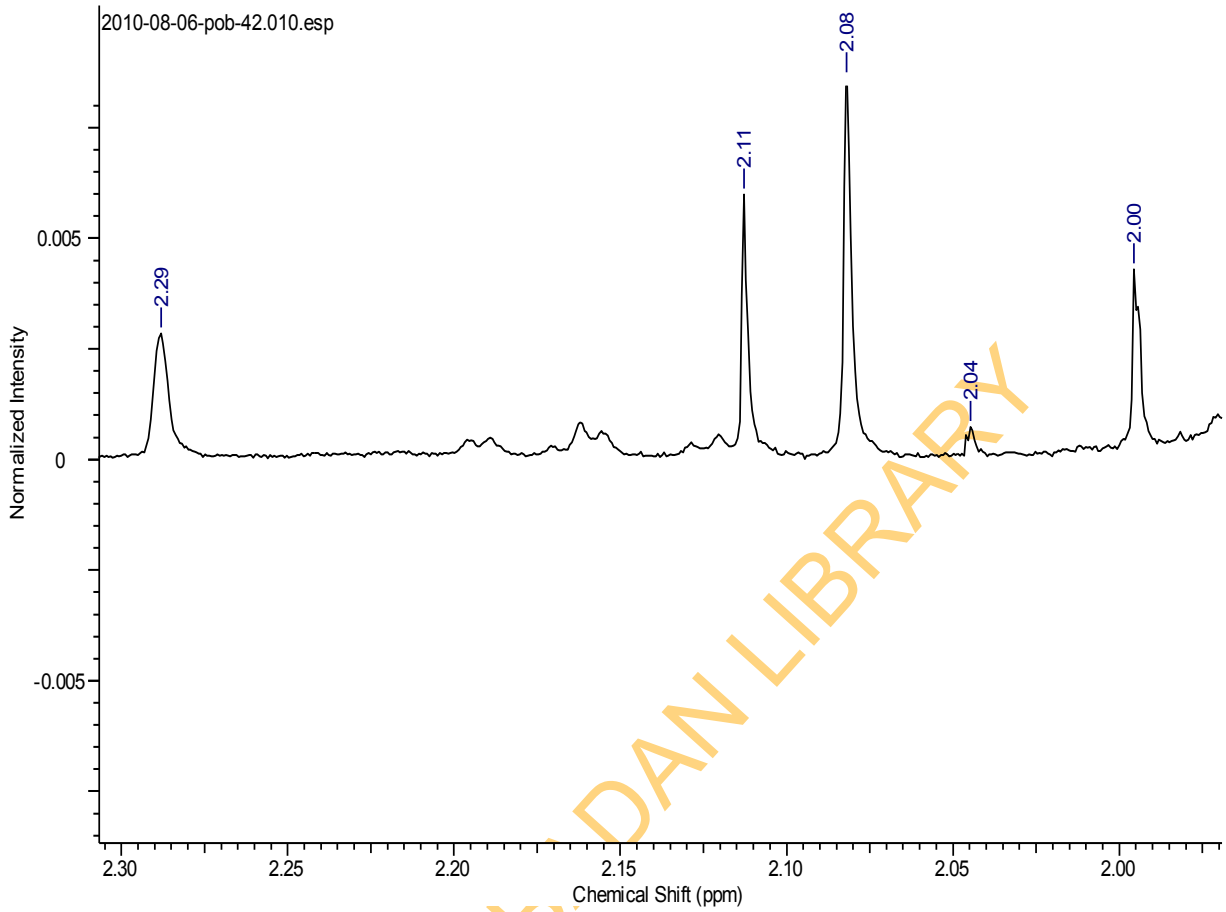

Figure 4.38b: Expanded ^{1}Hnmr spectrum of 5-exo-(khivorino) cyclohexa-1,3-diene (27)

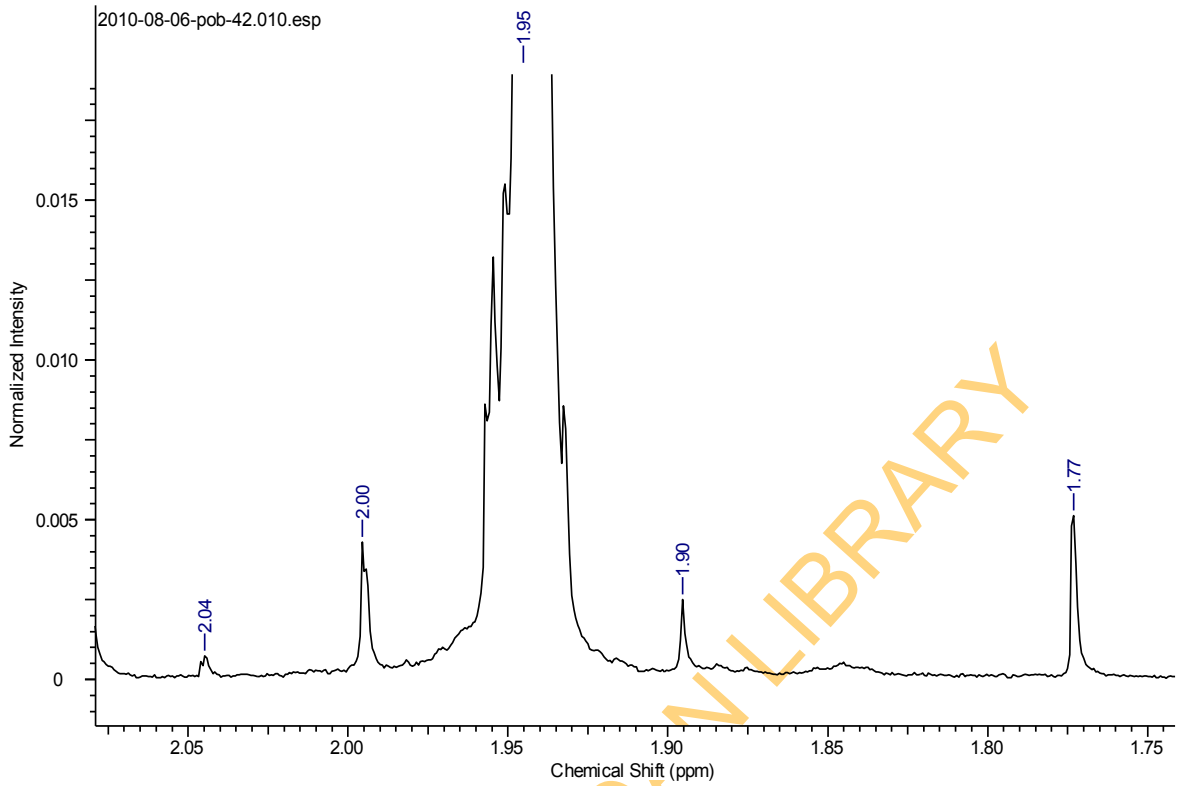

Figure 4.38b: Expanded ^{1}Hnmr spectrum of 5-exo-(khivorino) cyclohexa-1,3-diene (27)

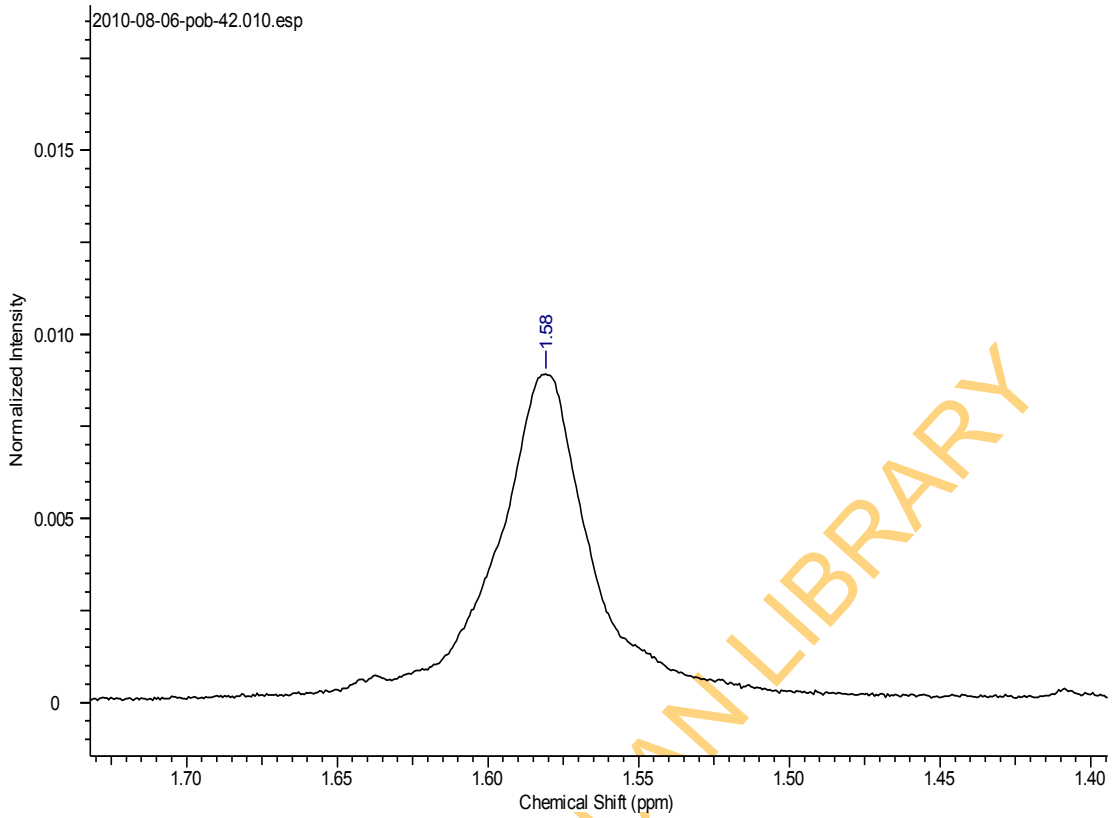

Figure 4.38b: Expanded ^{1}Hnmr spectrum of 5-exo-(khivorino) cyclohexa-1,3-diene (27)

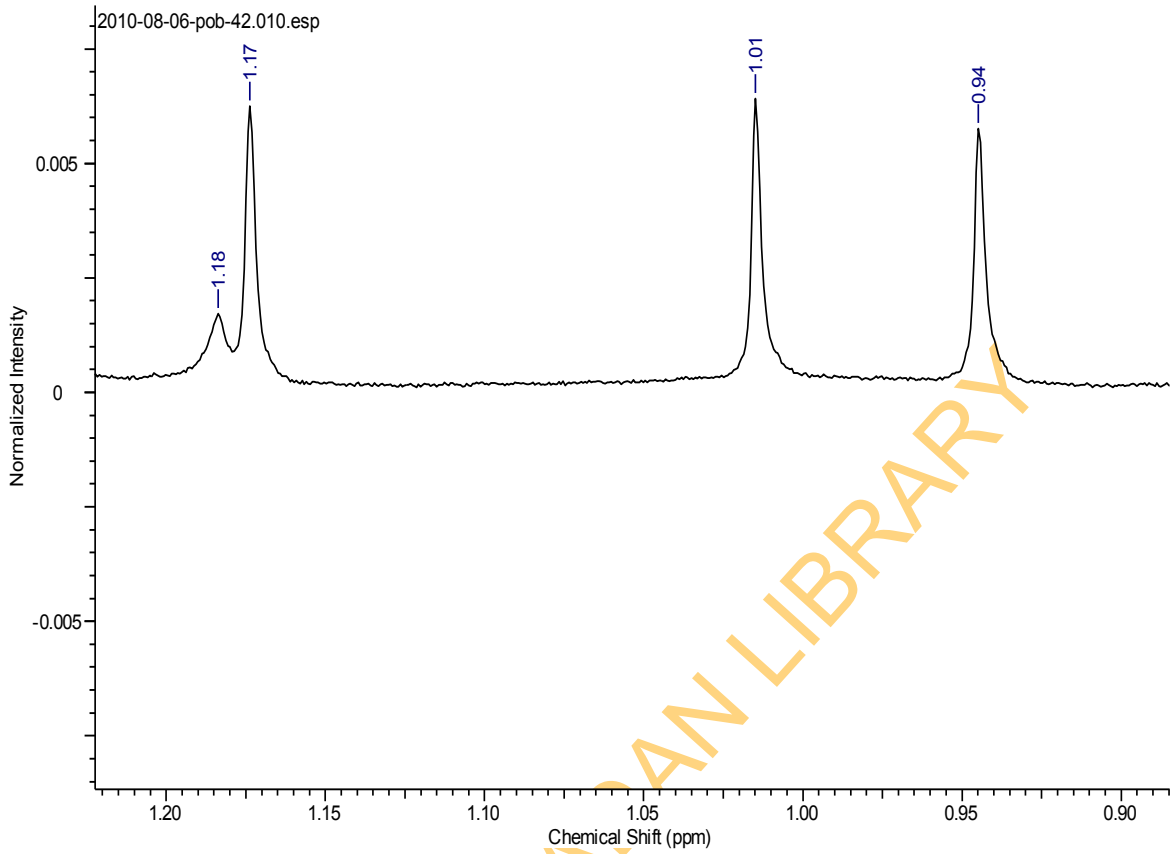

Figure 4.38b: Expanded ^{1}Hnmr spectrum of 5-exo-(khivorino) cyclohexa-1,3-diene (27)

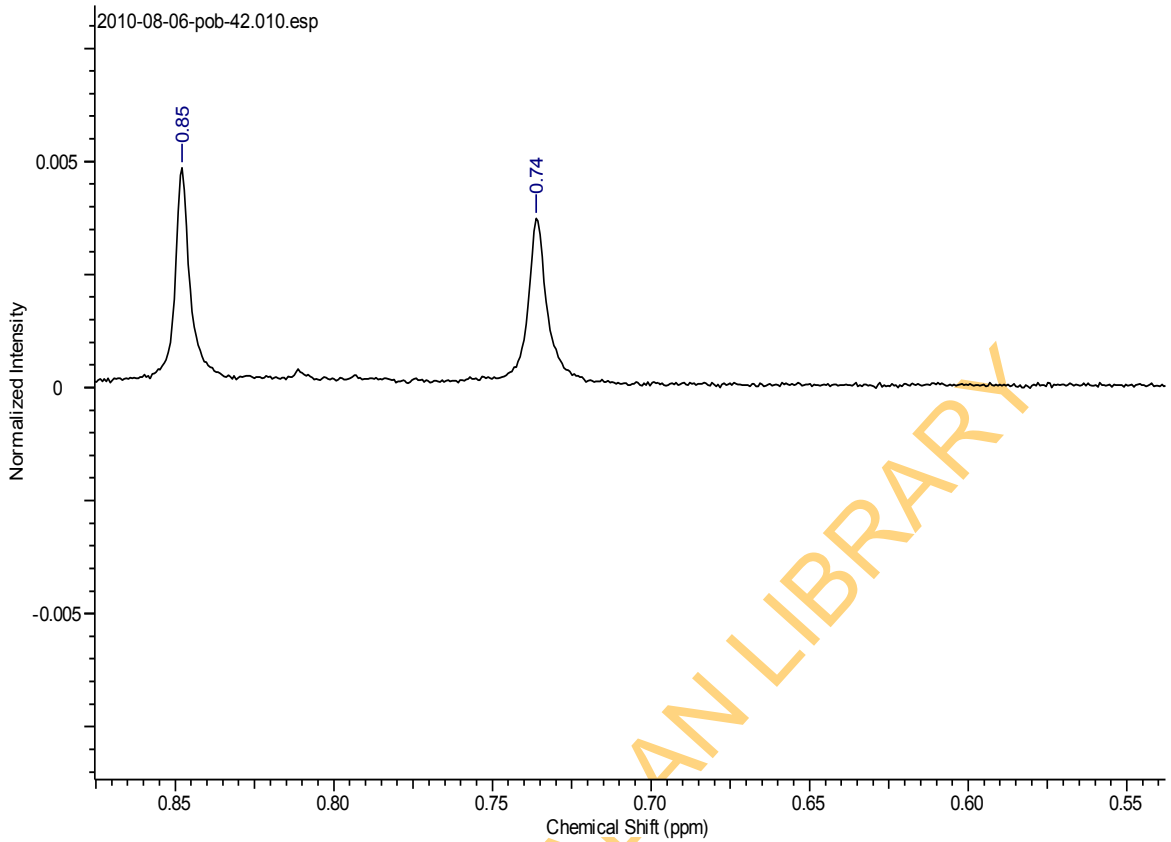

Figure 4.38b: Expanded ^{1}Hnmr spectrum of 5-exo-(khivorino) cyclohexa-1,3-diene (27)

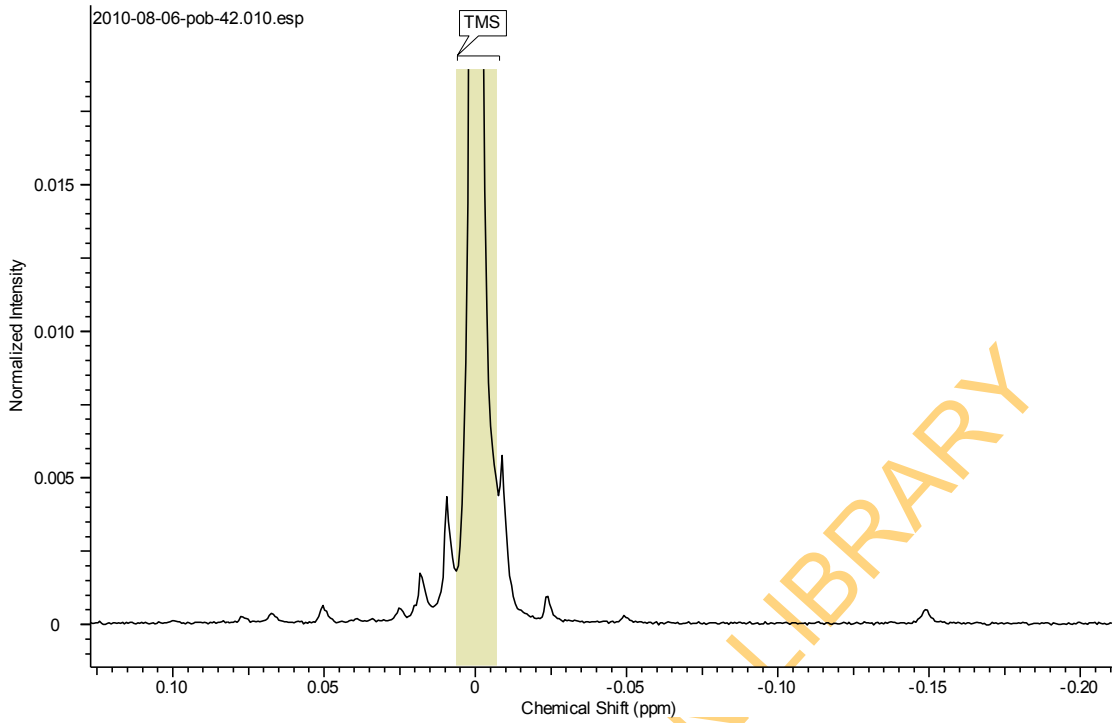

Figure 4.38b: Expanded ^{1}Hnmr spectrum of 5-exo-(khivorino) cyclohexa-1,3-diene (27)

Table 4.39: ^{1}Hnmr assignment of 5-exo-(7-ketokhivorin) cyclohexa-1,3-diene (28)

Protons	Simulated spectra	Real spectra
H1	4.788	4.64(t)
H2a	1.95	1.95(d)
H2b	1.8	not observed
H3	4.682	4.55(t)
H5	2.612	2.13(t)
H6a	2.169	1.92(t)
H6b	2.156	1.57(d)
H9	3.119	4.45(t)
H11a	1.537	1.51(s)
H11b	2.173	1.85(t)
H12a	2.281	2.16(s)
H12b	2.181	1.88(t)
H15	4.021	3.45(s)
H17	5.252	5.53(s)
H18	1.141	0.94(s)
H19	0.966	0.73(s)
H21	7.308	7.07(s)
H22	6.101	not observed
H24	2.04	2.08(s)
H26	2.042	2.29(s)
H28	1.178	1.01(s)
H29	1.079	0.84(s)
H1'	5.829	7.33(m)
H2'	5.722	7.34(t)
H3'	5.867	6.24(d,d)
H4'	5.83	7.32(m)
H5'	3.041	2.79(d,d)
H6'a	2.269	1.63(d)
H6'b	2.316	2.19(d)

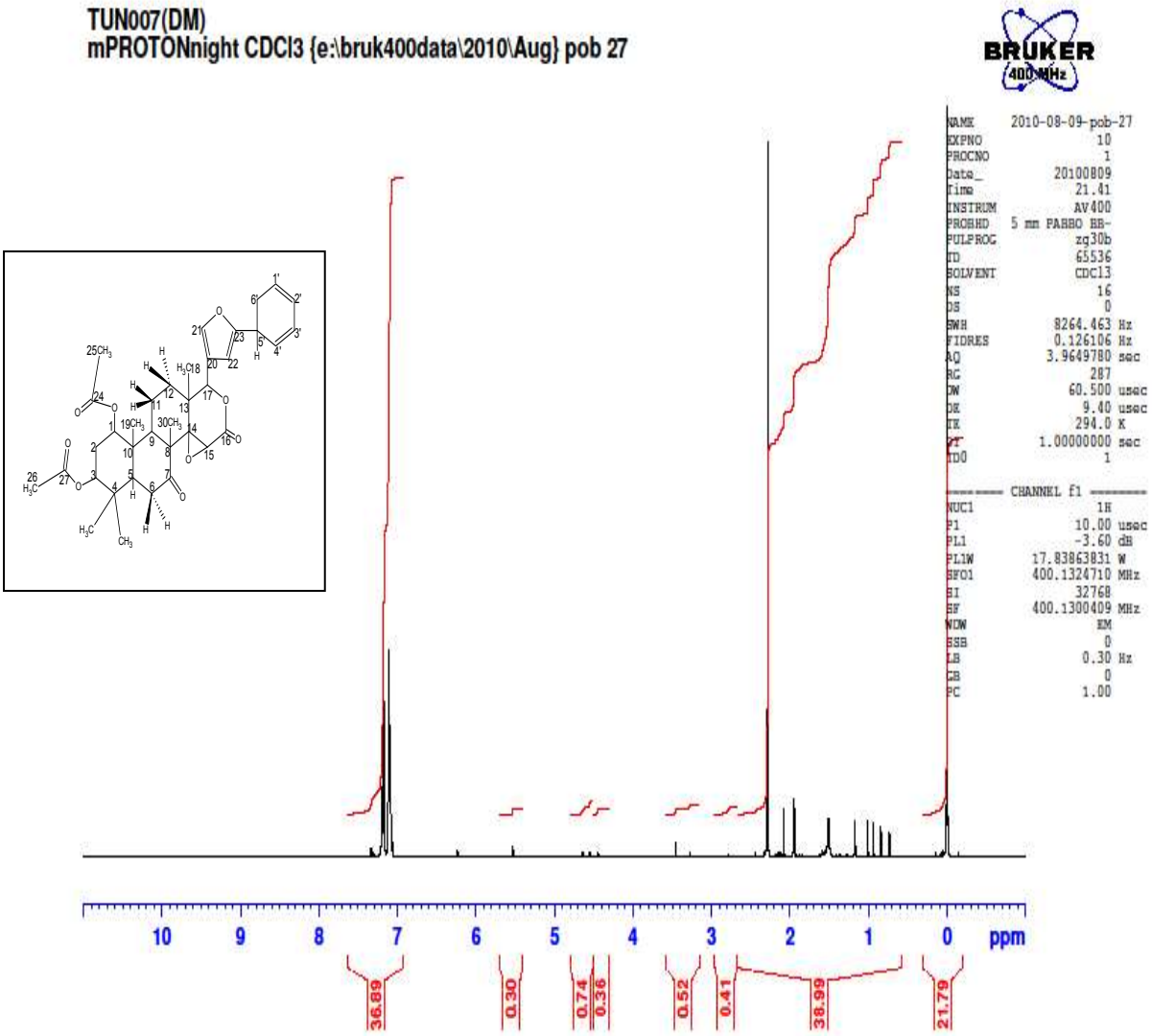

Figure 4.39: ^{1}Hnmr spectrum of 5-exo-(7-ketokhivorin) cyclohexa-1,3-diene (28)

Table 4.40: ^{1}Hnmr assignment of 2-methoxy-5-exo-(gedunino)cyclohexa-1,3-diene (30)

Protons	Simulated Spectra	Real Spectra
H1	6.433	7.12(d)
H2	5.699	5.80(s)
H5	2.116	not observed
H6a	1.637	not observed
H6b	2.397	2.28(s)
H7	5.043	5.55(s)
H9	3.115	not observed
H11a	1.344	not observed
H11b	1.98	not observed
H12a	2.122	2.11(s)
H12b	2.022	1.7(d)
H15	3.545	3.45(s)
H17	5.078	5.78(s)
H18	1.111	1.50(s)
H19	1.097	1.18(s)
H21	7.437	7.32(s)
H22	6.199	6.25(s)
H28	1.09	1.00(s)
H29	1.19	1.20(s)
H30	1.041	1.10(s)
H32	2.042	2.02(s)
H33(methoxy)	3.424	3.24(s)
H1'	4.704	4.49
H3'	6.046	not observed
H4'	5.925	6.80(d)
H5'	2.952	2.45(d,d)
H6'a	2.537	not observed
H6'b	2.584	not observed

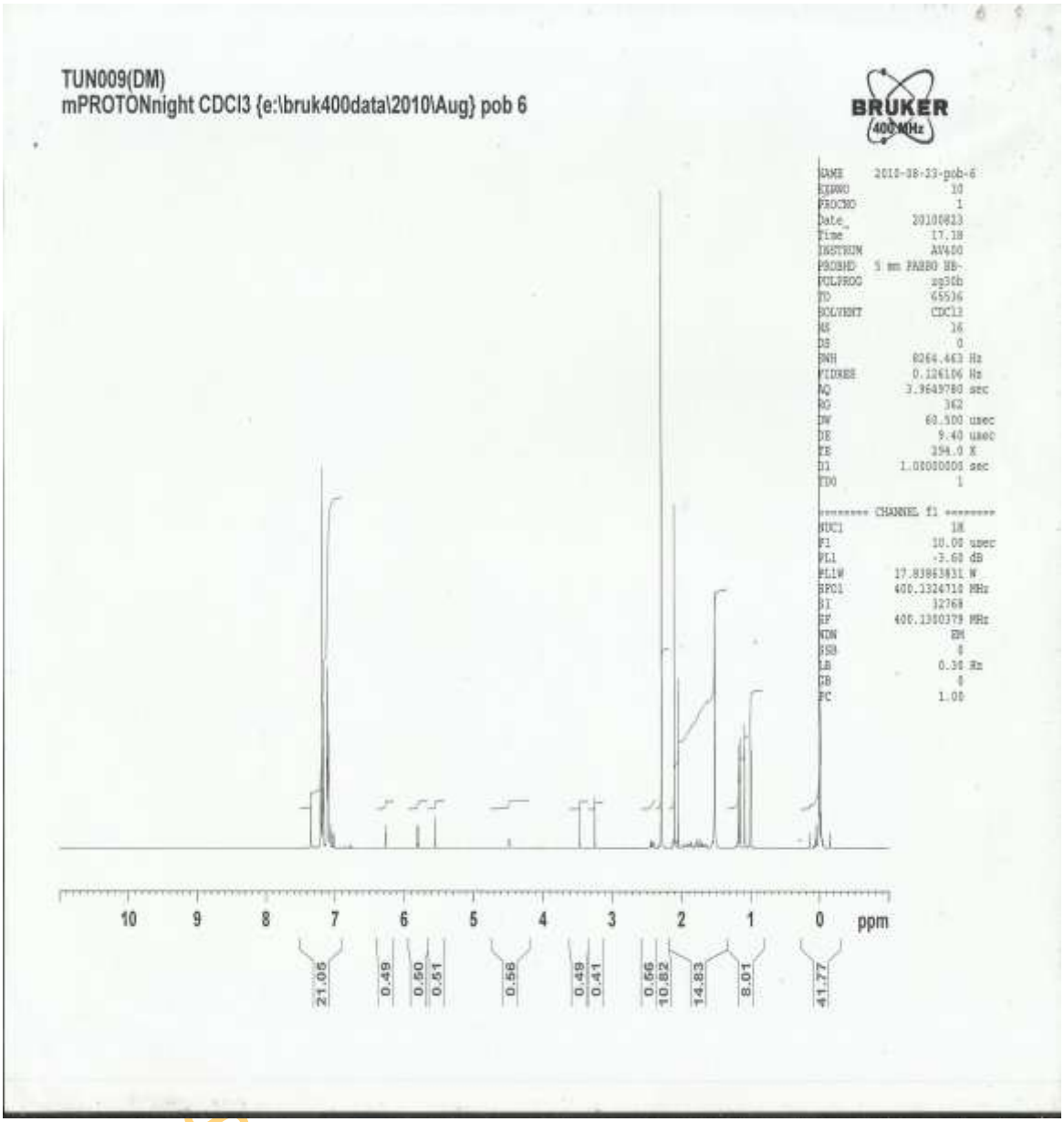

Figure 4.40: ^{1}Hnmr spectrum of 2-methoxy-5-exo-(gedunino) cyclohexa-1,3-diene (30)

Table 4.41: ^{1}Hnmr assignment of 2-methoxy-5- exo-(khivorino)cyclohexa-1,3-diene (31)

Protons	Simulated spectra	Real Spectra
H1	4.711	4.55(s)
H2a	1.8	1.38(t)
H2b	1.95	2.15(t)
H3	4.605	not observed
H5	2.209	not observed
H6a	1.418	1.57(S)
H6b	2.178	not observed
H7	4.951	4.65(s)
H9	3.13	not observed
H11a	1.407	1.85(m)
H11b	2.043	not observed
H12a	2.107	not observed
H12b	2.007	1.89(m)
H15	3.545	3.45(s)
H17	5.078	not observed
H18	1.111	1.17(s)
H21	7.437	6.24(s)
H22	6.199	5.53(s)
H29	1.082	1.01(s)
H28	0.982	0.85(s)
H30	1.022	0.94(s)
H31	2.042	2.29(s)
H32	2.042	2.08(s)
H33	2.04	1.95(s)
H34 (methoxy proton)	3.424	3.25(s)methoxy
H1'	4.704	4.45(s)
H3'	6.046	7.34(d)
H4'	5.925	6.79(d)
H5'	2.952	2.79(m)
H6'a	2.537	not observed
H6'b	2.584	not observed

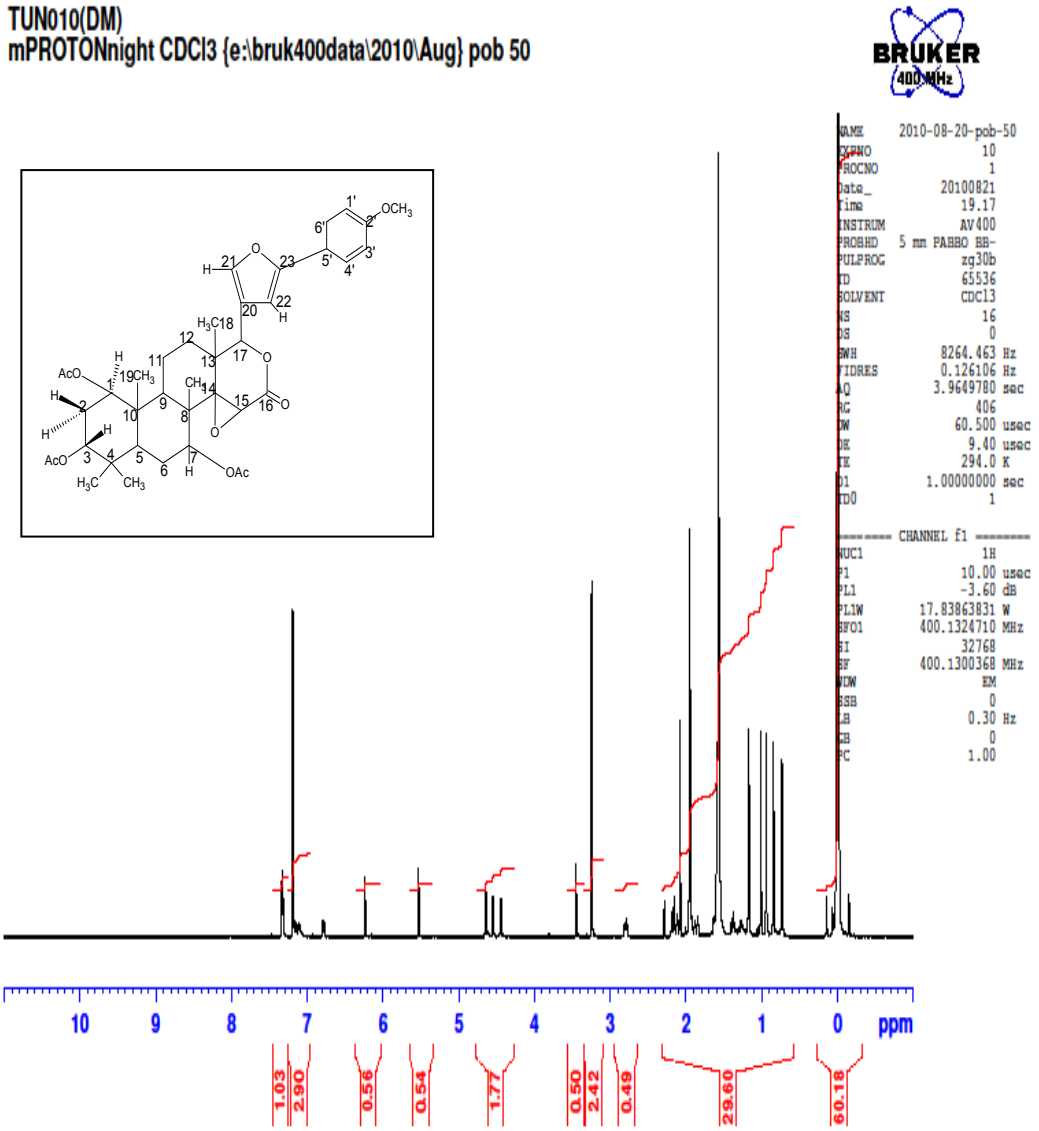

Figure 4.41: ^{1}Hnmr spectrum of 2-methoxy-5-exo-(khivorino)cyclohexa-1,3-diene (31)

Table 4.42: ^{1}Hnmr assignment of 2-methoxy-5-exo-(7-ketokhivorino) cyclohexa-1,3-diene (32)

Protons	Simulated spectra	Real Spectra
H1	4.788	not observed
H2a	1.8	1.10(d)
H2b	1.95	1.95(s)
H3	4.682	not observed
H5	2.612	2.72(m)
H6a	2.169	not observed
H6b	2.156	not observed
H9	3.119	not observed
H11a	1.537	1.52(s)
H11b	2.173	not observed
H12a	2.281	2.44(d)
H12b	2.181	not observed
H15	4.021	3.71(s)
H17	5.252	not observed
H18	1.141	0.92(s)
H19	0.966	not observed
H21	7.308	7.17(d)
H22	6.07	7.07(m)
H30	1.214	1.18(s)
H31	2.042	2.29(s)
H32	2.04	1.89(s)
H33 (methoxy proton)	3.424	3.30(s)
H1'	4.704	not observed
H3'	6.046	not observed
H4'	5.925	7.12(m)
H5'	2.952	not observed
H6'a	2.537	not observed
H6'b	2.584	2.13(s)

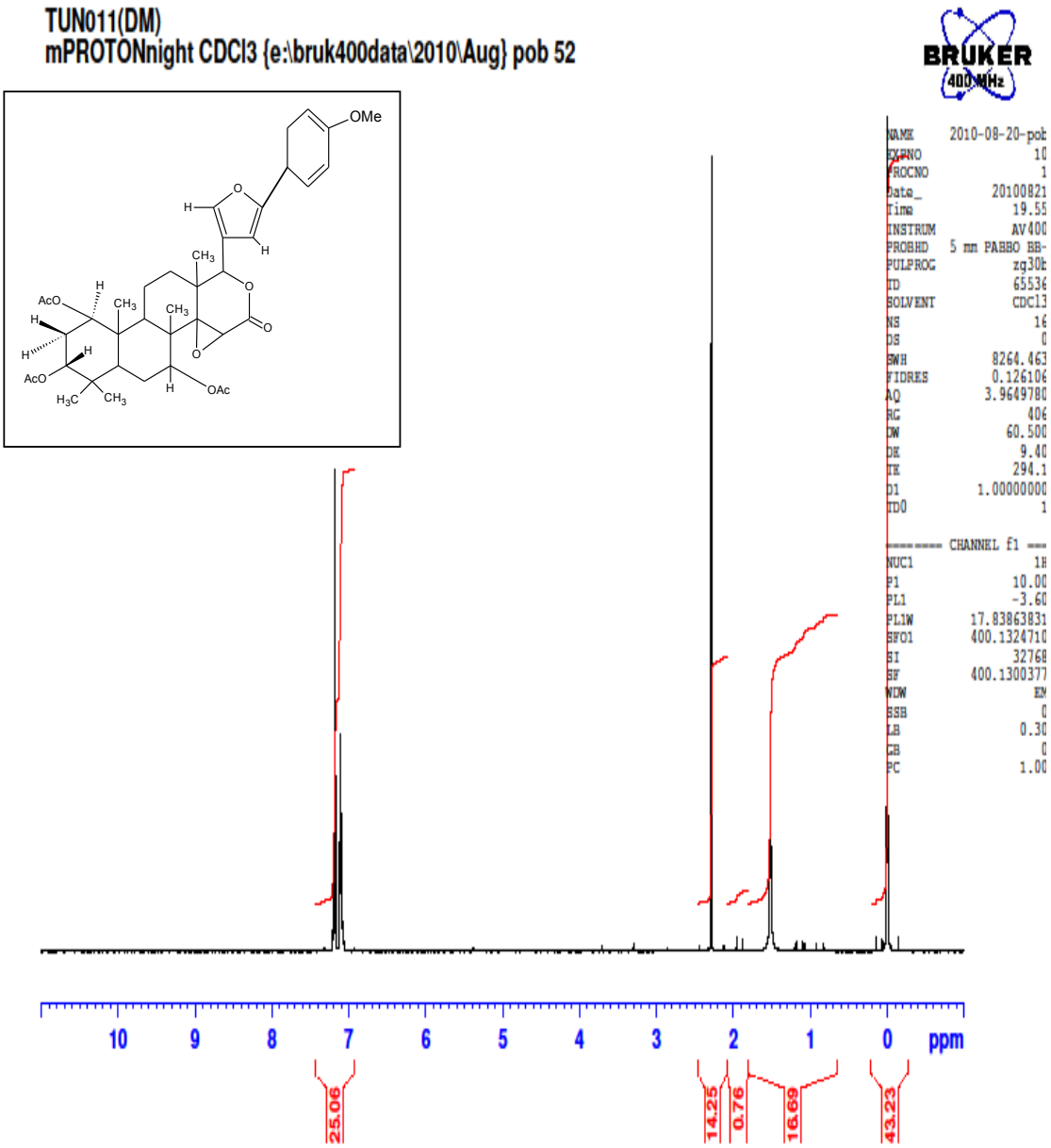

Figure 4.42: ^{1}Hnmr spectrum of 2-methoxy- 5-exo-(7-ketokhivorino) cyclohexa-1,3-diene (32)

4.7 Mass spectral studies of demetallated compounds

The mass spectra assignments for the demetallated compounds are presented in Tables 4.43 to 4.48 and the spectra are collected in Fig 4.43 to 448. The expected molecular ion $[P]^+$ ions are not observed in all the compounds but the characteristic loss of αβ-unsaturated ketone fragment is observed for all the compounds at 151 corresponding to $C_{10}H_{15}O$ fragment Fig 5.2.

4.8 Antimicrobial bioassay results

The antibacterial activity of the demetallated compounds (26), (27), (28), (29), (30) and (31) Fig 5.1 derived from the two dienylium cations are presented in Table 4.49 with zones of inhibition that ranged from 8.5 mm to 17.5 mm. These values are lower in comparison to the values obtained for the positive control (gentamycin) for all the bacteria used which ranged from 26 mm to 31 mm.

The synthesised adducts exhibited no antibacterial activity except for (22) and (24) as shown in Table 4.50. The antibacterial activities of the ligands are presented in Table 4.51. All the ligands were active with zones of inhibition ranging from 8.0 mm to 12.5 mm.

Antifungal activities of the demetallated compounds, the adducts and the ligands are shown in Tables 4.52 to 4.54. Compound (32**)** Table (4.52) was the only demetallated compound that exhibited antifungal activity against *Candida albican* with zone of inhibition of 22.5 mm which is comparable to value of the positive control ketocanazole with a zone of inhibition of 26 mm. Khivorin is also the only active ligand against *Candida albican* with 12 mm zone of inhibition, although khivorin adducts, (20) and (24), showed no antifungal activities as well as (27) and (24) demetallated compounds from khivorin.

Values of Minimum Inhibition Concentration for demetallated compounds are shown in Table 4.55 and ranged from 0.012mg/mL to 29.17mg/mL while that of ligands are presented in Tables 4.57 and 4.58 which also ranged from 0.23mg/mL to 9.24mg/mL.

From Table 4.51, gedunin ligand showed antibacterial activities against *Proteus mirabilis* a gram negative bacterium which causes urinary tract infection (UTI) in individuals resulting in kidney stones (Johnson *et al*., 1993; Mobley and Warren, 1987; Mobley, 1996; Burall *et al*., 2004) with zone of inhibition of 12.5mm at 1.25 mg/mL MIC value. There was a report of gedunin as antimalaria agent (Bray *et al*., 1990), as well inhibiting the proliferation of ovarian cancer (Kamath *et al*., 2009).

Table 4.43: Mass spectral assignment of 5-exo-(gedunino)-cyclohexa-1,3-diene (26)

Mass	Fragments	Intensity (m/z)
151	M-$C_{24}H_{25}O_6$	70.38
173	M-$C_{23}H_{30}O_5$-H^+	100.0
174	M-$C_{23}H_{30}O_5$	6.25
422	M-$C_8H_{10}O_2$-H^+	0.63
500	M-$C_2H_3O_2$-H^+	3.13

M = 560.7 (Molecular mass of adduct)

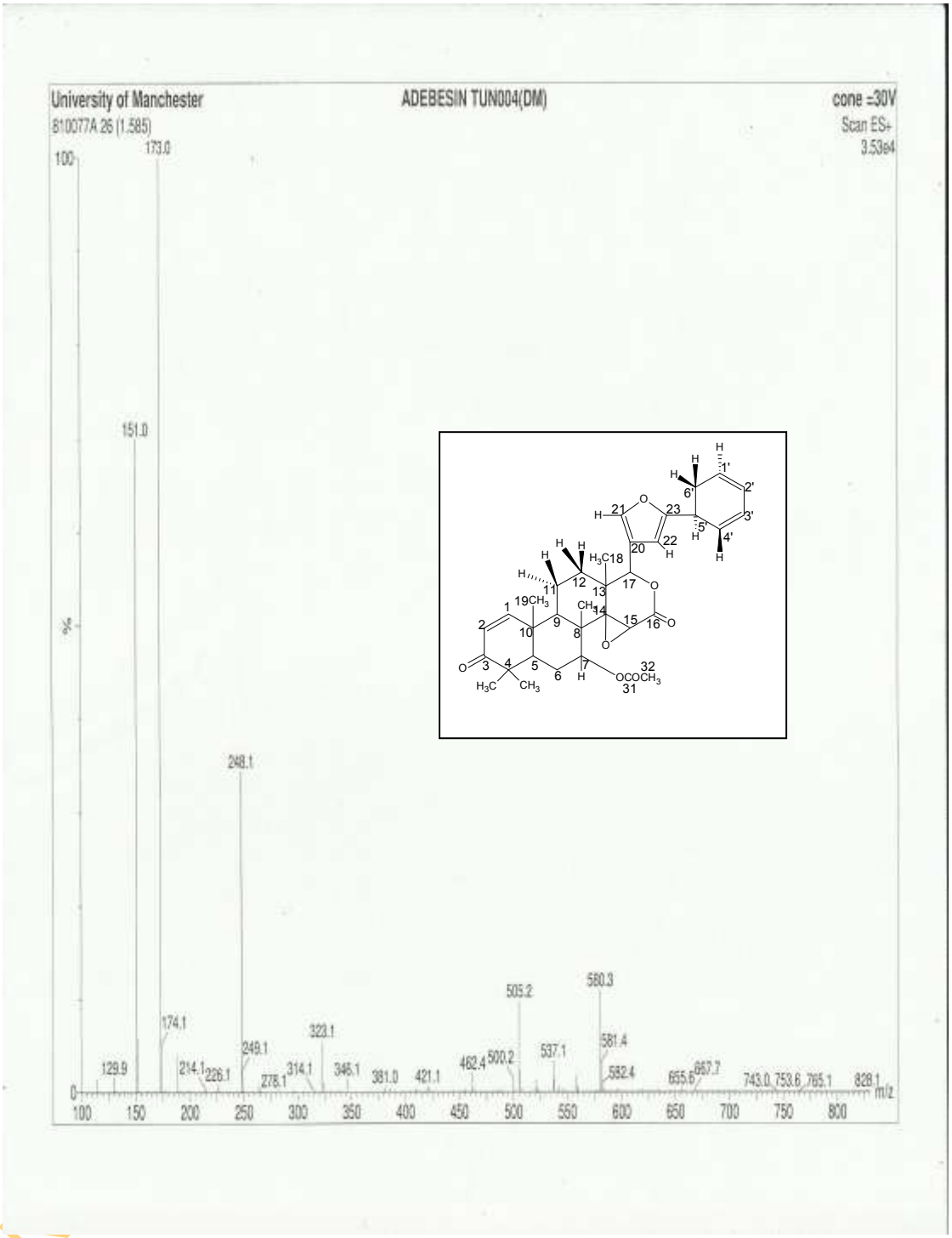

Figure 4.43: Mass spectrum of 5-exo-(gedunino) cyclohexa-1,3-diene]iron (26)

Table 4.44: Mass spectral assignment of 5-exo-(khivorino) cyclohexa-1,3-diene (27)

Mass	Fragments	Intensity (m/z)
127	M- ($C_{31}H_{36}O_8$) – (H^+)	1.0
173	M-($C_{27}H_{38}O_8$) - (H^+)	66.67
271	M-($C_{22}H_{34}O_6$) +(H^+)	6.77
560	M-(C_8H_8)	1.56
609 base peak	M-(C_4H_5) -2(H^+)	100.00

M = 664.8 (Molecular mass)

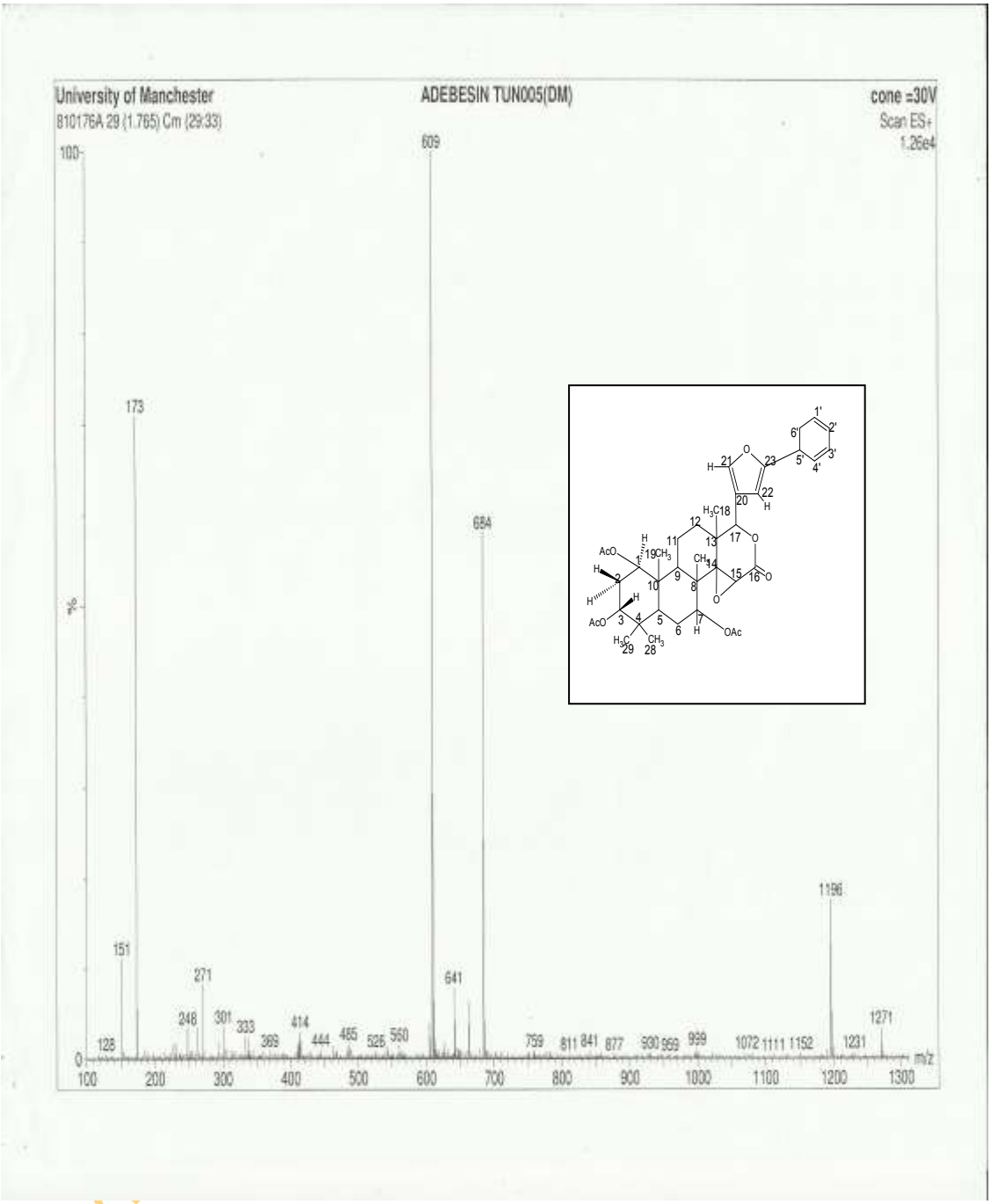

Figure 4.44: Mass spectrum of 5-exo (khivorino) cyclohexa-1,3-diene (27)

Table 4.45: Mass spectra assignment of 5-exo-(7-ketokhivorino) cyclohexa-1,3-diene (28)

Mass	Fragments	Intensity (m/z)
173	M-$C_{25}H_{34}O_7$-H^+	3.41
485	M-C_9H_9O-$2H^+$	2.84
516	M-C_8H_8	0.59
541	M-C_6H_7	2.84
609 base peak	M-(CH)+($2H^+$)	100.0

M = 620.7 (Molecular mass)

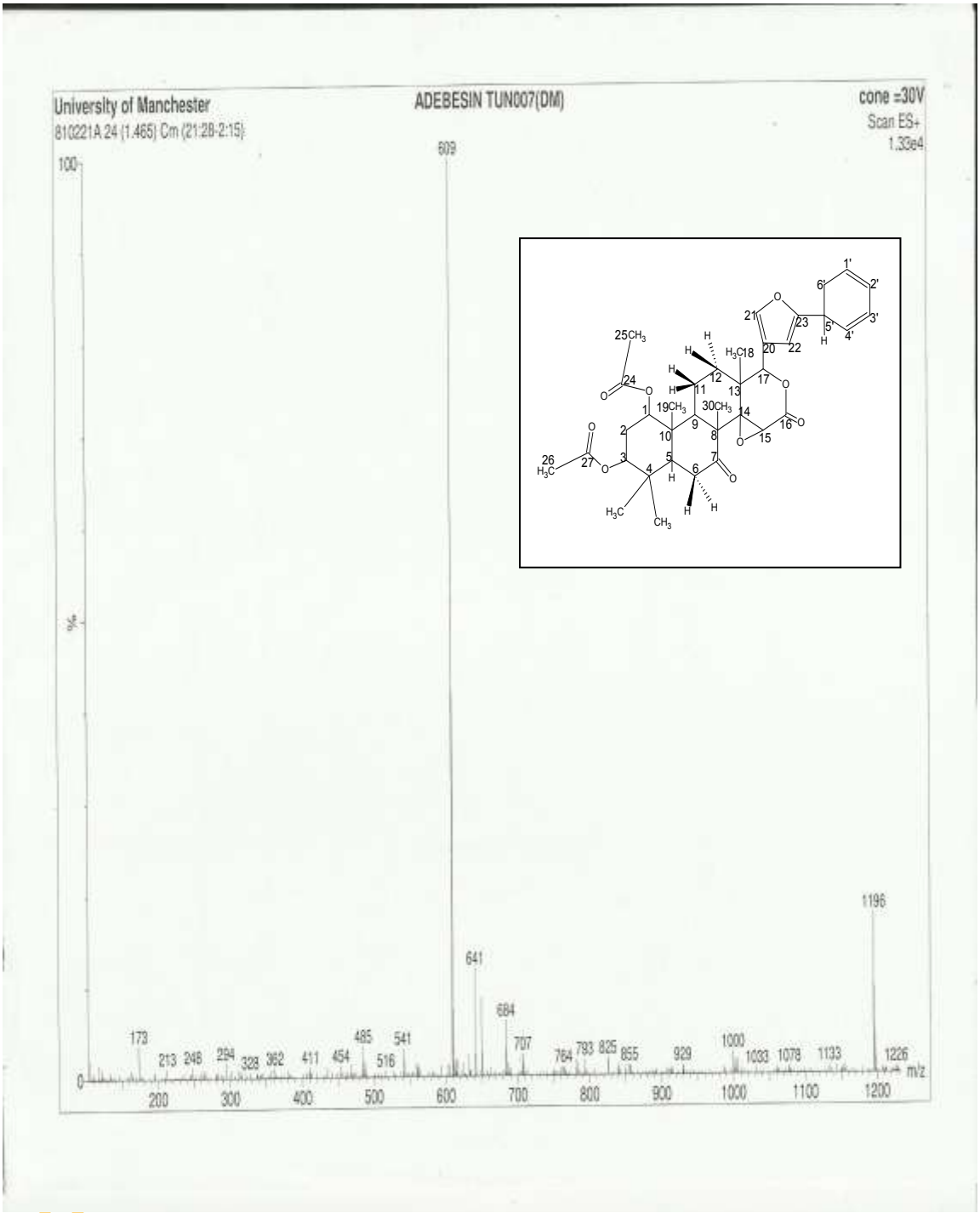

Figure 4.45: Mass spectrum of 5-exo-(7-ketokhivorin) cyclohexa-1, 3-diene (28)

Table 4.46: Mass spectra assignment of 2-methoxy-5-exo-(gedunino) cyclohexa-1,3-diene (30)

Mass	Fragments	Intensity (m/z)
151	M-($C_{26}H_{32}O_6$) + (H^+)	8.0
173	M-($C_{24}H_{31}O_6$) - ($2H^+$)	30.0
301	M-($C_{18}H_{26}O_3$) + (H^+)	9.0
366	M-($C_{13}H_{18}O_3$) – ($2H^+$)	25.0
371	M-($C_{13}H_{14}O_3$) - (H^+)	100
372	M-($C_{13}H_{14}O_3$)	18.0
387	M-($C_{12}H_{12}O_3$) + H^+	5.0
413	M-($C_{11}H_{11}O_2$) – $2H^+$	10.0
467	M-($C_8H_{12}O$) + H^+	12.0
468	M-($C_8H_{12}O$) + $2H^+$	4.0
500	M-($C_3H_6O_3$)	29.0
505	M-($C_4H_6O_2$) + H^+	100
506	M-($C_4H_6O_2$) + $2H^+$	29.0
521	M-(C_4H_5O)	8.0
536	M-(C_3H_2O)	29.0

M = 590.7 (Molecular mass of adduct)

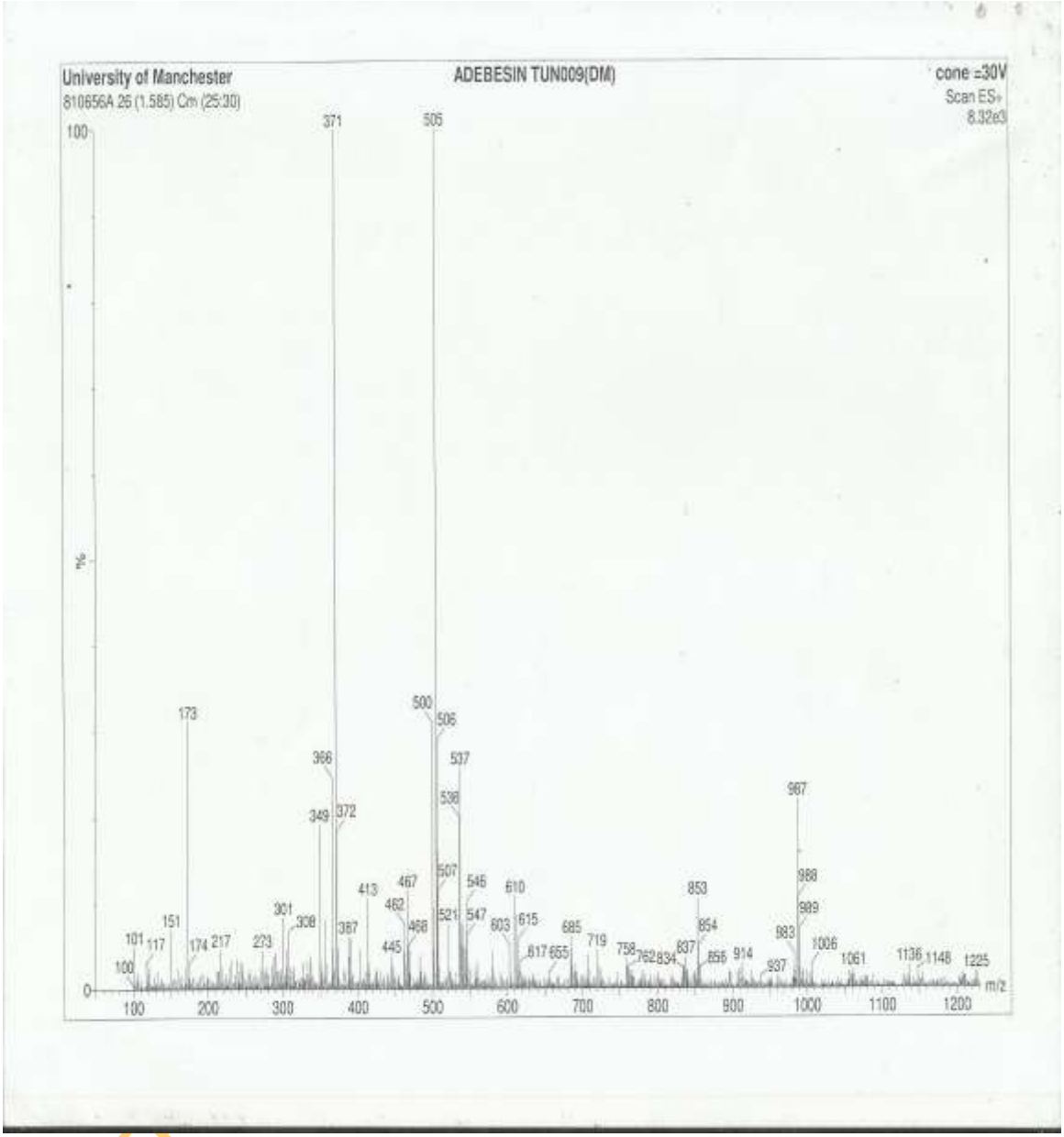

Figure 4.46: Mass spectrum of 2-methoxy-5-exo-(gedunino) cyclohexa-1,3-diene (30)

Table 4.47: Mass spectra assignment of 2-methoxy-5- exo-(khivorino)cyclohexa-1,3-diene (31)

Mass	Fragment	Intensity (m/z)
130	M-($C_{32}H_{38}O_9$) + ($2H^+$)	2.0
151	M-($C_{30}H_{40}O_9$) + (H^+)	85.0
173	M-($C_{28}H_{39}O_9$) – ($2H^+$)	100
462	M-($C_{13}H_{14}O_4$) + ($2H^+$)	6.0
536	M-($C_7H_{10}O_4$)	10.0
560	M-($C_7H_{10}O_4$)	1.0
609	M-($C_4H_6O_2$) + (H^+)	93.0

M = 694.81(Molecular mass)

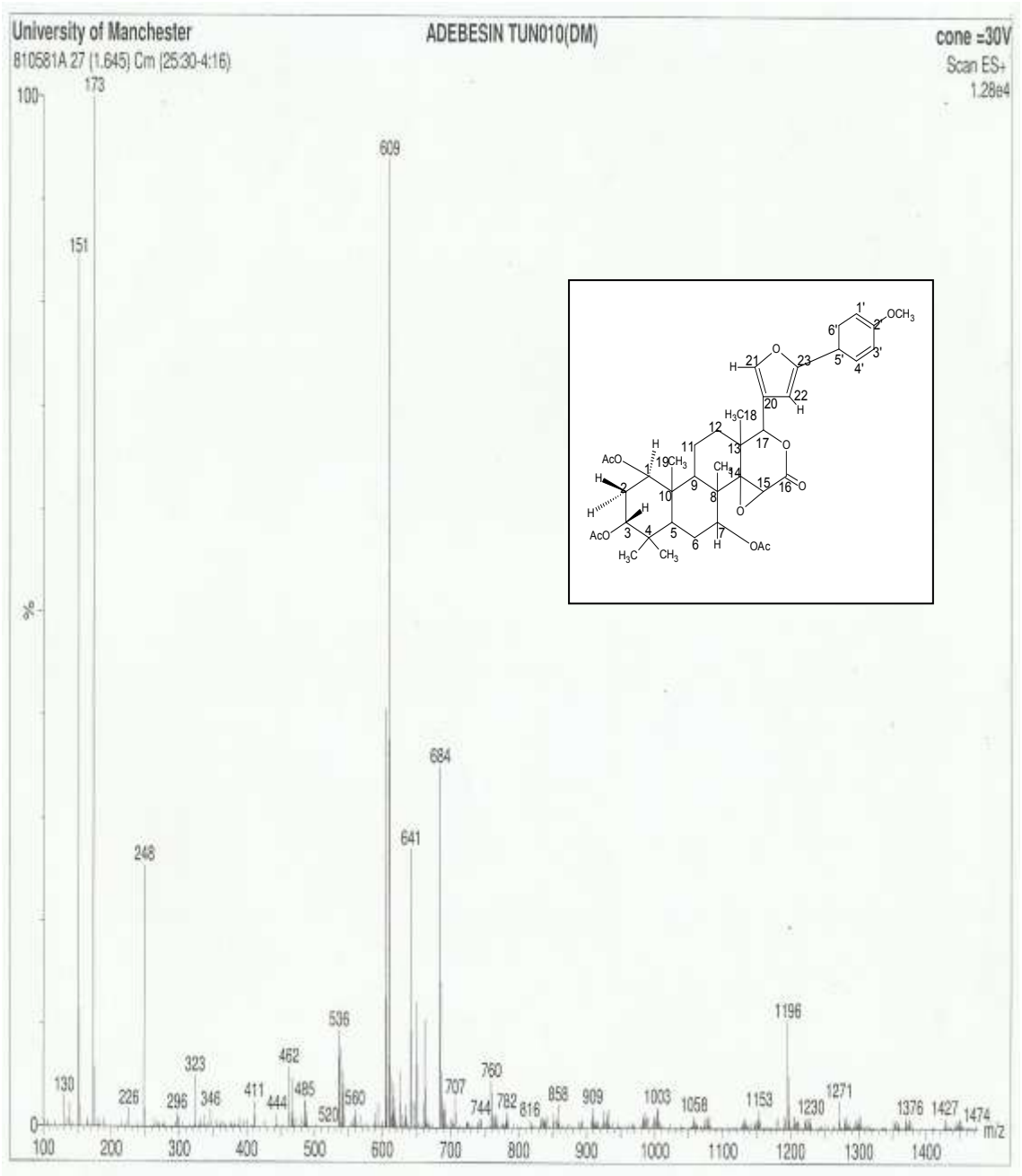

Figure 4.47: Mass spectrum of 2-methoxy- 5-exo-(khivorino) cyclohexa-1,3-diene (31)

Table 4.48: Mass spectra assignment of 2-methoxy-5- exo-(7-ketokhivorino) cyclohexa-1,3-diene (32)

Mass	Fragment	Intensity (m/z)
130	M – ($C_{30}H_{34}O_8$) + ($2H^+$)	1.0
152	M – ($C_{28}H_{36}O_8$) + ($2H^+$)	100
173	M – ($C_{26}H_{35}O_8$) – ($2H^+$)	15.0
200	M – ($C_{27}H_{30}O_6$)	4.0
242	M – ($C_{24}H_{26}O_6$) + ($2H^+$)	10.0
462	M – ($C_{12}H_{12}O_2$)	11.0
536	M – ($C_6H_{10}O_2$)	10.0
565	M – ($C_4H_6O_2$) + (H^+)	73.0
606	M – (CO_2)	19.0

M = 650.8 (Molecular mass)

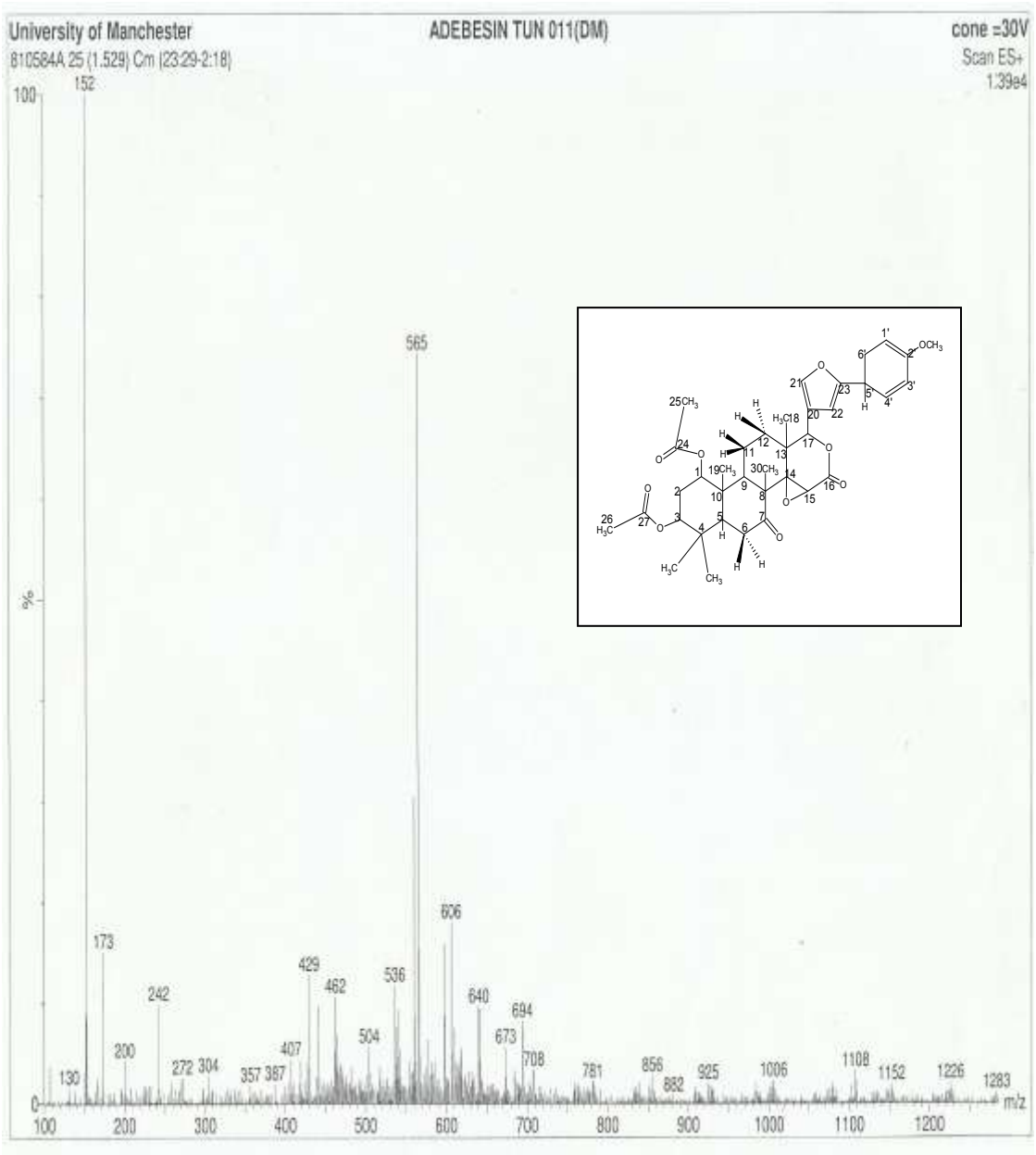

Figure 4.48: Mass spectrum of 2-methoxy- 5-exo-(7-ketokhivorino) cyclohexa-1,3-diene (32)

(26), a demetallated compound derived from gedunin exhibited selective action as it showed activity against *Salmonella typhi* a gram-negative bacterium which is a causative agent of tyhoid fever in human and *Bacillus cereus* with zones of inhibitions 8 mm and 17.5 mm respectively but was not active against *Proteus mirabilis* which gedunin ligand was active against. The activity of (26**)** against *Salmonella typhi* shows its antimicrobial potential against typhoid fever.

However, (30**)**, a demetallated methoxy derivative of gedunin demonstrated no activity against *Salmonella typhi* but showed increase activity against *Proteus mirabilis* with zone of inhibition 15.5 mm compare to 12.5 mm of the starting gedunin ligand. In addition, (30**)** was also active against *Bacillus cereus* and *Bacillus substilis* with 14.5 mm and 11.5 mm zones of inhibition. The adducts of gedunin synthesised from the two dienylium cations show no activity Table 4.52.

Khivorin ligand as shown in Table 4.51 exhibited antibacterial activity against *Proteus mirabilis* and antifungal activity against *Candida albican* with zones of inhibition 12 mm and 12 mm at MIC values of 2.85 mg/mL and 0.85 mg/mL respectively. The demetallated derivative, (27**)**, of khivorin showed an increase in antibacterial activity against *Proteus mirabilis* with zone of inhibition of 14 mm compare to 12 mm of the starting khivorin ligand at 19.77 mg/mL MIC value. It also demonstrated activity against *Bacillus cereus* at 9.5 mm zone of inhibition while the methoxy demetallated derivative of khivorin, (31**)**, have a reduced antibacterial activity against *Proteus mirabilis* at 9.5 mm zone of inhibition compared to 12 mm of khivorin ligand as earlier stated.

It was reported in the literature that polyavolensinol cured blackwater fever and stomach disorder (Okorie, 1980, 1981). However, this research showed that polyavolensinol ligand exhibited antibacterial activity against *Salmonella typhi* at minimum inhibitory concentration of 9.24 mg/mL and 11.5 mm zone of inhibition. In addition, it is also active against *Proteus mirabilis* and *Bacillus cereus* making it the most active of the ligands used. However, the antibacterial activity of its demetallated form, (29**)**, was increased to include activity against *Bacillus substilis* with zone of inhibition of 14.5 mm (Table 4.49 and 4.51) at a minimum inhibitory concentration of 0.012 mg/mL to 0.42 mg/mL.

The antibacterial activity of 7-ketokhivorin ligand is only against *Bacillus cereus* with a zone of inhibition of 8.0 mm Table 4.51.

Table 4.49: Zones of inhibition for antibacterial activities of demetallated compounds in millimeter (mm)

Sample/Organism	*Salmonella typhi*	*Proteus mirabilis*	*Bacillus cereus*	*Bacillus subtilis*
Gentamycin	28 ± 1.02	31 ± 1.45	28 ± 1.18	29 ± 1.23
DMSO	-	-	-	-
$C_{34}H_{40}O_7$ (26)	8.5 ± 1.00	-	17.5 ± 1.23	-
$C_{38}H_{48}O_{10}$ (27)	-	14 ± 1.41	9.5 ± 2.12	-
$C_{36}H_{44}O_9$ (28)	-	10 ± 1.00	8 ± 1.41	-
$C_{29}H_{37}NO$ (29)	16.5 ± 2.12	16 ± 1.15	14.5 ± 0.58	14.5 ± 2.15
$C_{35}H_{42}O_8$ (30)	-	15.5 ± 2.90	14.5 ± 0.56	11.5 ± 1.12
$C_{39}H_{50}O_{11}$ (31)	-	9.5 ± 2.10	-	7.5 ± 1.41
$C_{37}H_{46}O_{10}$ (32)	-	-	-	-

- = **No activity**

(26) = **5-exo-[(gedunino)cyclohexa-1,3-diene]**

(27) = **5-exo-[(khivorino)cyclohexa-1,3-diene]**

(28) = **5-exo-[(7-ketokhivorino)cyclohexa-1,3-diene]**

(29) = **5-exo-[(polyavolensinolino)cyclohexa-1,3-diene]**

(30) = **2-methoxy-5-exo[(gedunino)cyclohexa-1,3-diene]**

(31) = **2-methoxy-5-exo[(khivorino)cyclohexa-1,3-diene]**

(32) = **2-methoxy-5-exo[(7-ketokhivorino)cyclohexa-1,3-diene]**

Table 4.50: Zones of inhibition for antibacterial activities of adducts in millimeter (mm)

Sample/Organism	*Salmonella typhi*	*Proteus mirabilis*	*Bacillus cereus*	*Bacillus subtilis*
Gentamycin	28 ± 1.02	31 ± 1.45	28 ± 1.18	29 ± 1.23
DMSO	-	-	-	-
$C_{37}H_{40}O_{10}Fe$ (19)	-	-	-	-
$C_{41}H_{48}O_{13}Fe$ (20)	-	-	-	-
$C_{39}H_{44}O_{12}Fe$ (21)	-	-	-	-
$C_{32}H_{37}NO_4Fe$ (22)	16.5 ± 2.12	-	-	-
$C_{38}H_{42}O_{11}Fe$ (23)	-	-	-	-
$C_{42}H_{50}O_{14}Fe$ (24)	-	18 ± 1.41	-	7.5 ± 0.50

- = **No activity**

(19) = **Tricarbonyl[1-4-η-5(gedunino)cyclohexa-1,3-diene] iron**

(20) = **Tricarbonyl[1-4-η-5(khivorino)cyclohexa-1,3-diene] iron**

(21) = **Tricarbonyl[1-4-η-5(7-ketokhivorino)cyclohexa-1,3-diene] iron**

(22) = **Tricarbonyl[1-4-η-5polyavolensinolino)cyclohexa-1,3-diene] iron**

(23) = **Tricarbonyl[1-4-η-2-methoxy-5-(gedunino)cyclohexa-1,3-diene] iron**

(24) = **Tricarbonyl[1-4-η-2-methoxy-5-(khivorino)cyclohexa-1,3-diene] iron**

Table 4.51: Zones of inhibition for antibacterial activities of ligands used in millimeter (mm)

Sample/Organism	*Salmonella typhi*	*Proteus mirabilis*	*Bacillus cereus*	*Bacillus subtilis*
Gentamycin	28 ± 1.02	31 ± 1.45	28 ± 1.18	29 ± 1.23
DMSO	-	-	-	-
Gedunin ligand	-	12.5 ± 1.07	-	-
Khivorin ligand	-	12 ± 1.41	-	-
7-ketokhivorin ligand	-	-	8 ± 2.80	-
Polyavolensinol ligand	11.5 ± 2.12	11 ± 1.41	10 ± 1.41	-

- **= No activity**

Table 4.52: Zones of inhibition for antifungal activities of demetallated compounds in millimeter (mm)

Sample/Organism	*Candida albican*
Ketocanazole	26 ± 1.07
DMSO	-
$C_{34}H_{40}O_7$ (26)	-
$C_{38}H_{48}O_{10}$ (27)	-
$C_{36}H_{44}O_9$ (28)	-
$C_{29}H_{37}NO$ (29)	-
$C_{35}H_{42}O_8$ (30)	-
$C_{39}H_{50}O_{11}$ (31)	-
$C_{37}H_{46}O_{10}$ (32)	22.5 ± 1.41

- **= No activity**

(26) = **5-exo-[(gedunino)cyclohexa-1,3-diene]**

(27) = **5-exo-[(khivorino)cyclohexa-1,3-diene]**

(28) = **5-exo-[(7-ketokhivorino)cyclohexa-1,3-diene]**

(29) = **5-exo-[(polyavolensinolino)cyclohexa-1,3-diene]**

(30) = **2-methoxy-5-exo[(gedunino)cyclohexa-1,3-diene]**

(31) = **2-methoxy-5-exo[(khivorino)cyclohexa-1,3-diene]**

(32) = **2-methoxy-5-exo[(7-ketokhivorino)cyclohexa-1,3-diene]**

Table 4.53: Zones of inhibition for antifungal activities of adducts in millimeters

Sample/Organism	***Candida albican***
Ketocanazole	26 ± 1.07
DMSO	-
$C_{37}H_{40}O_{10}Fe$ (19)	-
$C_{41}H_{48}O_{13}Fe$ (20)	-
$C_{32}H_{37}NO_4Fe$ (22)	-
$C_{39}H_{44}O_{12}Fe$ (21)	-
$C_{38}H_{42}O_{11}Fe$ (23)	-
$C_{42}H_{50}O_{14}Fe$ (24)	-
$C_{40}H_{46}O_{13}Fe$ (25)	-

- = **No activity**

(19) = **Tricarbonyl[1-4-η-5(gedunino)cyclohexa-1,3-diene] iron**

(20) = **Tricarbonyl[1-4-η-5(khivorino)cyclohexa-1,3-diene] iron**

(21) = **Tricarbonyl[1-4-η-5(7-ketokhivorino)cyclohexa-1,3-diene] iron**

(22) = **Tricarbonyl[1-4-η-5polyavolensinolino)cyclohexa-1,3-diene] iron**

(23) = **Tricarbonyl[1-4-η-2-methoxy-5-(gedunino)cyclohexa-1,3-diene] iron**

(24) = **Tricarbonyl[1-4-η-2-methoxy-5-(khivorino)cyclohexa-1,3-diene] iron**

(25) = **Tricarbonyl[1-4-η-2-methoxy-5-(7-ketokhivorino)cyclohexa-1,3-diene] iron**

Table 4.54: Zones of inhibition for antifungal activities of ligands used in millimeter (mm)

Sample/Organism	***Candida albican***
Ketocanazole	26 ± 1.07
DMSO	-
Gedunin ligand	-
Khivorin ligand	12 ± 1.15
7-ketokhivorin ligand	-
Polyavolensinol ligand	-

Table 4.55: MIC values of demetallated compounds in mg/mL

Sample/Organism	*Salmonella typhi*	*Proteus mirabilis*	*Bacillus cereus*	*Bacillus subtilis*
Gentamycin	0.0012 ± .0002	0.0004 ± .0001	0.00016 ± .00002	0.0006 ± .0002
$C_{34}H_{40}O$ (26)	3.24 ± 0.01	-	3.24 ± 0.03	-
$C_{38}H_{48}O10$ (27)	-	19.77 ± 0.02	19.77 ± 0.04	-
$C_{36}H_{44}O_9$ (28)	-	5.23 ± 0.05	5.23 ± 0.02	-
$C_{29}H_{37}NO$ (29)	0.012 ± 0.003	0.012 ± 0.001	0.07 ± 0.02	0.42 ± 0.03
$C_{35}H_{42}O_8$ (30)	-	0.66 ± 0.02	3.95 ± 0.04	0.66 ± 0.06
$C_{39}H_{50}O11$ (31)	-	4.86 ± 0.06	-	29.17 ± 0.03
$C_{37}H_{46}O10$ (32)	-	-	-	-

- = **No activity**

(26) = **5-exo-[(gedunino)cyclohexa-1,3-diene]**

(27) = **5-exo-[(khivorino)cyclohexa-1,3-diene]**

(28) = **5-exo-[(7-ketokhivorino)cyclohexa-1,3-diene]**

(29) = **5-exo-[(polyavolensinolino)cyclohexa-1,3-diene]**

(30) = **2-methoxy-5-exo[(gedunino)cyclohexa-1,3-diene]**

(31) = **2-methoxy-5-exo[(khivorino)cyclohexa-1,3-diene]**

(32) = **2-methoxy-5-exo[(7-ketokhivorino)cyclohexa-1,3-diene]**

Table 4.56: MIC values of adducts in mg/mL

Sample/Organism	*Salmonella typhi*	*Proteus mirabilis*	*Bacillus cereus*	*Bacillus subtilis*
Gentamycin	0.0012 ± .0002	0.0004 ± .0001	0.00016 ± .00002	0.0006 ± .0002
$C_{32}H_{37}NO_4Fe$ (22)	-	-	-	-
$C_{42}H_{50}O_{14}Fe$ (24)	-	4.38 ± 0.02	-	4.38 ± 0.03

- = **No activity**

(19) = **Tricarbonyl[1-4-η-5(gedunino)cyclohexa-1,3-diene] iron**

(20) = **Tricarbonyl[1-4-η-5(khivorino)cyclohexa-1,3-diene] iron**

(21) = **Tricarbonyl[1-4-η-5(7-ketokhivorino)cyclohexa-1,3-diene] iron**

(22) = **Tricarbonyl[1-4-η-5polyavolensinolino)cyclohexa-1,3-diene] iron**

(23) = **Tricarbonyl[1-4-η-2-methoxy-5-(gedunino)cyclohexa-1,3-diene] iron**

(24) = **Tricarbonyl[1-4-η-2-methoxy-5-(khivorino)cyclohexa-1,3-diene] iron**

Table 4.57: MIC values of ligands with antibacterial activities in mg/mL

Sample/Organism	*Salmonella typhi*	*Proteus mirabilis*	*Bacillus cereus*	*Bacillus subtilis*
Gentamycin	0.0012 ± .0002	0.0004 ± .0001	0.00016 ± .00002	0.0006 ± .0002
Gedunin ligand	-	1.25 ± 0.01	-	-
Khivorin ligand	-	2.85 ± 0.06	-	-
Polyavolensinol ligand	9.24 ± 0.05	9.24 ± 0.01	9.24 ± 0.03	-
7-Ketokhivorin ligand	-	-	0.23 ± 0.02	-

- **= No activity**

Table 4.58: MIC values of ligands with antifungal activities in mg/mL

Sample/Organism	***Candida albican***
Ketocanazole	0.02 ± 0.01
Gedunin ligand	-
Khivorin ligand	0.85 ± 0.03
Polyavolensinol ligand	-
7-Ketokhivorin ligand	-

- **= No activity**

The corresponding demetallated derivative, (28), showed activity against two organisms *Proteus mirabilis* and *Bacillus cereus* with similar zones of inhibition of 10 mm and 8.0 mm which implied similar activity to that of the ligand. However, the methoxy demetallated derivative showed no antibacterial activity but exhibited antifungal activity against *Candida albican* at 22.5 mm zone of inhibition.

The newly synthesised demetallated compounds showed increased antibacterial and antifungal activities compared to the starting ligands used, thus they can serve as lead in drug development.

4.9 Results of computational studies

The optimised geometries of the synthesised compounds and ligands are presented in Appendix 14 to 52. Geometry optimisation of compounds was carried out at gradient corrected Density Functional Theory (DFT) level using Becke's three parameters hybrid method (Becke, 1993) and the Lee-Yang-Parr correctional functional (B3LYP) (Lee *et al*., 1988) combined wth 6-31G(d) basis set (Francis *et al*., 1982) using Gaussian 09 program package (Becke, 1992) in gaseous state.

The computed quantum descriptors and QSAR parameter based on DFT calculations are energies of highest occupied molecular orbital (E_{HOMO}), energies of lowest unoccupied molecular orbital (E_{LUMO}), HOMO-LUMO energy band gap (ΔE), total energy, dipole moments and the partition coefficient (LogP). These are important physical parameters to understand chemical and biological activities of molecules (Gopalakrishnan *et al*., 2014).

The frontier orbitals HOMO and LUMO of a chemical species are important in defining its reactivity (Gopalakrishnan *et al*., 2014). The energies of frontier orbitals are important properties in several chemical and pharmacological processes (Fleming, 1976). The value of E_{HOMO} is often associated with the electron donating ability of inhibitor molecules; higher value of E_{HOMO} is an indication of the greater ease of donating electrons to the unoccupied orbital of the receptor. The E_{LUMO}, on the other hand indicates the ability of the molecules to accept electrons. The smaller the E_{LUMO}, the smaller the resistance to accept electrons (Boufas *et al*., 2014). Thus, the binding ability of molecule increases with increasing HOMO and decreasing LUMO energies.

The values of HOMO-LUMO energy gap (ΔE) reflect the chemical reactivity of molecule (Gopalakrishnan *et al*., 2014). The larger the HOMO-LUMO energy gap, the harder, more stable and less reactive the molecule (Chattaraj and Maiti, 2003). However, when the HOMO-LUMO energy gap decreases, the reactivity of the molecule increases leading to a decrease in stability of the molecule (Liu, 2005).

The results of the computed DFT quantum calculations are presented in Tables 4.59 to 4.63. From the result, the general observed trend in the HOMO-LUMO energy gap (ΔE) is in the order ligand > adducts > demetallated. This implied that the demetallated compounds are expected to have better chemical reactivities than the adducts and the ligands due to the lower values of their HOMO-LUMO energy gaps. It is also observed that demetallated compounds (27) and (28) have the same high ΔE values 5.0336 eV Tables (4.60 and 4.62), hence may exhibit similar chemical reactivities and greater stablity. The demetallated methoxy derivative of gedunin (30) has the least ΔE value of 4.1656 eV and is expected to be the most chemically reactive and the least stable. It shows appreciable antimicrobial activity but suprisingly is not the most active towards the tested microorganisms.

The adducts from the values of their HOMO-LUMO energy gap are expected to be chemically more reactive than the ligands. Although, they show no activity towards the tested microorganisms, this is likely due to their bulkiness which might not allow them to key-in properly to the receptor sites of microorganisms.

The dipole moments are another important electronic parameter that results from non-uniform distribution of charges on various atoms in a given molecule. It is frequently used to study the intermolecular interactions involving the non-bonded type dipole-dipole interactions; the higher the dipole moment, the stronger are the intermolecular interactions (Boufas *et al*., 2014). The results of the dipole moments show fairly high values for all the synthesised compounds and this indicates possibility of stronger intermolecular interactions of the synthesised compounds with their surrounding, hence aid their absorption into the system. The demetallated compound (30) with the least ΔE value also has the highest dipole moments of 6.76 debye as shown in Table 4.63. Thus, it is expected to have the strongest intermolecular interaction with its surrounding. The compound (29**)** has the least dipole moment of 3.54 debye and hence

Table 4.59: Electronic parameters for Gedunin, Gedunin adduct and demetallated Gedunin compound of dienylium cation

COMPOUNDS	E_{HOMO}	E_{LUMO}	TOTAL ENERGY (au)	ΔE (Energy band gap) (ev)	DIPOLE debye (μ)
Gedunin ligand	-6.48253372	-1.53295864	-1613.86437	4.94957508	5.91
$C_{37}H_{40}O_{10}Fe$ (19)	-6.28434227	-1.49668318	-2309.59085	4.78765909	7.49
$C_{34}H_{40}O_7$ (26)	-5.96079417	-1.5119761	-1846.10667	4.44881807	6.52

(19) = **Tricarbonyl [1-4-η-5(gedunino)cyclohexa-1,3-diene] iron**

(26) = **5-exo-[(gedunino) cyclohexa-1,3-diene]**

Table 4.60: Electronic parameters for Khivorin, Khivorin adduct and demetallated Khivorin compound of dienylium cation

COMPOUNDS	E_{HOMO}	E_{LUMO}	TOTAL ENERGY (au)	ΔE (Energy band gap) (ev)	DIPOLE debye (μ)
Khivorin ligand	-6.5007859	-0.1339145	-1996.81577	6.3668714	6.77
*$C_{41}H_{48}O_{13}Fe$ (20)	-6.24581597	-0.909125757	-2692.51688	5.336690213	5.70
$C_{38}H_{48}O_{10}$ (27)	-5.85241841	-0.8188198	-2229.0187	5.03359861	6.26

*LACVP

(20) = **Tricarbonyl[1-4-η-5(khivorino)cyclohexa-1,3-diene] iron**

(27) = **5-exo-[(khivorino)cyclohexa-1,3-diene]**

Table 4.61: Electronic parameters of Polyavolensinol, Polyavolensinol adduct and demetallated Polyavolensinol product of dienylium cation

COMPOUNDS	E_{HOMO}	E_{LUMO}	TOTAL ENERGY (au)	ΔE (Energy band gap) (ev)	DIPOLE debye (μ)
Polyavolensinol	-5.06608466	0.108356941	-1025.10080	5.174441607	3.84
$C_{32}H_{37}NO_4Fe$ (22)	-5.06892686-	-0.582005085	-2860.98866	4.486921775	4.91
$C_{29}H_{37}NO$ (29)	-4.9592939	-0.414653688	-1257.31967	4.544640212	3.54

(22) = **Tricarbonyl[1-4-η-5polyavolensinolino)cyclohexa-1,3-diene] iron**

(29) = **5-exo-[(polyavolensinolino)cyclohexa-1,3-diene]**

Table 4.62: Electronic parameters for 7-ketokhivorin, 7-ketokhivorin adduct and demetallated 7-ketokhivorin compound of dienylium cation

COMPOUNDS	E_{HOMO}	E_{LUMO}	TOTAL ENERGY (au)	ΔE(Energy band gap) (ev)	DIPOLE debye (μ)
7-ketokhivorin ligand	-6.46752	-0.6141351	-1842.9646	5.8533849	3.82
$C_{39}H_{44}O_{12}Fe$ (21)	-6.1642077	-0.897617	-2538.670	5.2665907	3.09
$C_{36}H_{44}O_9$ (28)	-5.85132798	-0.82028829	-2075.16949	5.03103969	3.56

(21) = **Tricarbonyl[1-4-η-5(7-ketokhivorino)cyclohexa-1,3-diene] iron**

(28) = **5-exo-[(7-ketokhivorino)cyclohexa-1,3-diene]**

Table 4.63: Electronic parameters for Gedunin, 2-methoxygedunin adduct and demetallated 2-methoxygedunin compound

COMPOUNDS	E_{HOMO}	E_{LUMO}	TOTAL ENERGY (au)	ΔE(Energy band gap) (ev)	DIPOLE debye (μ)
Gedunin ligand	-6.48253372	-1.53295864	-1613.86437	4.94957508	5.91
$C_{38}H_{42}O_{11}Fe$ (23)	-6.15852783	-1.47568592	-2424.11300	4.68284191	8.58
$C_{35}H_{42}O_8$ (30)	-5.65614277	-1.49060298	-1960.61575	4.16553979	6.76

(23) = **Tricarbonyl[1-4-η-2-methoxy-5-(gedunino)cyclohexa-1,3-diene] iron**

(30) = **2-methoxy-5-exo[(gedunino)cyclohexa-1,3-diene]**

expected to have weak intermolecular interaction with it surrounding. Suprisingly, it is the most active towards the tested microorganisms with the highest LogP value and the highest hydrophobic nature.

Quantitative Structure-Activity Relationship (QSAR) parameter LogP calculated is a critical parameter that relates the chemical structure of compounds with biological activity (Hansch *et al*., 1995). LogP (partition coefficient) is a measure of the hydrophobic-hydrophilic character of a compound (Hansch and Leo, 1995). The more hydrophobic a compound, the larger the value of LogP (Hansch *et al*., 1995) and lower logP values indicates hydrophilic nature (Eshwari *et al*., 2014). LogP gives information about how molecules cross the cell membrane and is important in receptor interactions in biological system (Eshwari *et al*., 2014). Cell membranes are composed of phospholipids which have hydrophobic tails that produce a very hydrophobic environment in the middle of the membrane bilayer. In the absence of active membrane transport, more hydrophobic drugs have an easier time getting through a membrane (Hansch and Leo, 1995; Franz, 2001).

The computed LogP values of ligands and the synthesised demetallated compounds are presented in Table 4.64. The correlation between LogP values and antimicrobial activities of ligands and demetallated compounds are given in Table 4.65. From the results it is observed that demetallation process increases hydrophobicity as all demetallated compounds have higher values of LogP than the ligands, hence are more hydrophobic than the starting ligands. This trend is also justified in the antimicrobial susceptibility assay. The demetallated products of the two parents show enhanced diameter of zones of inhibition when compared to the starting ligand, though some selectivities were observed between the demetallated product and the ligands. A typical example is the result of zones of inhibition obtained in (26) and (27) where the organisms inhibited differs from the one the ligand inhibited. It was also observed that the compound (29) with the highest LogP value of 7.40 showed the greatest activity against the tested organism due to its high hydrophobic nature which enables better penetration into the cell membrane of the organisms.

Table 4.64: LogP values of ligands and demetallated compounds

Ligands/Synthesised compounds	LogP
Gedunin ligand	2.72
Khivorin ligand	3.35
Polyavolensinol ligand	5.76
7- Ketokhivorin ligand	3.18
$C_{34}H_{40}O_7$ (26)	4.37
$C_{38}H_{48}O_{10}$ (27)	5.02
$C_{36}H_{44}O_9$ (28)	4.85
$C_{29}H_{37}NO$ (29)	7.4
$C_{35}H_{42}O_8$ (30)	3.67
$C_{39}H_{50}O_{11}$ (31)	4.3
$C_{37}H_{46}O_{10}$ (32)	4.14

(26) = **5-exo-[(gedunino)cyclohexa-1,3-diene]**

(27) = **5-exo-[(khivorino)cyclohexa-1,3-diene]**

(28) = **5-exo-[(7-ketokhivorino)cyclohexa-1,3-diene]**

(29) = **5-exo-[(polyavolensinolino)cyclohexa-1,3-diene]**

(30) = **2-methoxy-5-exo[(gedunino)cyclohexa-1,3-diene]**

(31) = **2-methoxy-5-exo[(khivorino)cyclohexa-1,3-diene]**

(32) = **2-methoxy-5-exo[(7-ketokhivorino)cyclohexa-1,3-diene]**

Table 4.65: Correlation between LogP values and antimicrobial activities of ligands and demetallated compounds

Ligands/Synthesised compounds	LogP	Microorganisms and Zones of inhibition in (mm)
Gedunin ligand	2.72	PM (12.5)
Khivorin ligand	3.35	PM (12) ,CA (12.0)
Polyavolensinol ligand	5.76	ST (11.5), PM (11.0), BC (10.0)
7- Ketokhivorin ligand	3.18	BC (8.0)
$C_{34}H_{40}O_7$ (26)	4.37	ST (8.5), BC (17.5)
$C_{38}H_{48}O_{10}$ (27)	5.02	PM (14), BC (9.5)
$C_{36}H_{44}O_9$ (28)	4.85	PM (10.0), BC (8.0)
$C_{29}H_{37}NO$ (29)	7.4	ST (16.5), PM (16.0), BC (14.5), BS (14.5)
$C_{35}H_{42}O_8$ (30)	3.67	PM (15.5), BC (14.5), BS (11.5)
$C_{39}H_{50}O_{11}$ (31)	4.3	PM (9.5), BS (7.5)
$C_{37}H_{46}O_{10}$ (32)	4.14	CA (22.5)

(26) = **5-exo-[(gedunino)cyclohexa-1,3-diene]**

(27) = **5-exo-[(khivorino)cyclohexa-1,3-diene]**

(28) = **5-exo-[(7-ketokhivorino)cyclohexa-1,3-diene]**

(29) = **5-exo-[(polyavolensinolino)cyclohexa-1,3-diene]**

(30) = **2-methoxy-5-exo[(gedunino)cyclohexa-1,3-diene]**

(31) = **2-methoxy-5-exo[(khivorino)cyclohexa-1,3-diene]**

(32) = **2-methoxy-5-exo[(7-ketokhivorino)cyclohexa-1,3-diene]**

CA = *Candida albican*

ST = *Salmonella typhi*

BC = *Bacillus cereus*

BS = *Bacillus subtilis*

PM = *Proteus mirabilis*

CHAPTER FIVE

CONCLUSION

The reactions of dienylium cations [1-5-η-(dienyl)Fe(CO)$_3$]BF$_4$(dienyl = C_6H_7,2-$MeOC_6H_6$) with selected natural products: gedunin, khivorin, 7-ketokhivorin and polyavolensinol isolated from Nigerian trees have yielded the corresponding 1, 3-diene substituted derivatives. The demetallation of these adducts have provided a convenient method of achieving C-C bond formation which is otherwise difficult to achieve by conventional organic synthetic technique. The synthesized compounds have been characterised using spectroscopic methods: IR (Infrared), NMR (Nuclear Magnetic Resonance) and MS (Mass Spectroscopic) techniques. The antimicrobial and electronic properties were also investigated.

The antimicrobial assay showed that the new compounds were more active than the starting natural products while their adducts indicated little or no activity towards the tested microorganisms. The Minimum Inhibitory Concentration values (MIC) ranged from 0.01 to 29.17 mg mL^{-1}. From this result the newly synthesized natural products could serve as leads in drug development.

The computed quantum descriptors and QSAR parameter based on DFT calculations are energies of highest occupied molecular orbital (E_{HOMO}), energies of lowest unoccupied molecular orbital (E_{LUMO}), HOMO-LUMO energy band gap (ΔE), total energy, dipole moments and the partition coefficient (LogP). These are important physical parameters to understand chemical and biological activities of molecules

It is pertinent to note that the calculated energy band gap (Table 4.59 to 4.63) decreased in the order ligand > adduct > demetallated compounds. Thus, the newly synthesised natural products are chemically more reactive than the starting ligands due to their low ΔE values. The adducts from the values of their HOMO-LUMO energy gap are expected to be chemically reactive than the ligands. Although, they show no activity towards the tested microorganisms, this is likely due to the bulkiness of their nature which might not allow them to key-in properly to the receptor sites of microorganisms.

The results of the dipole moments show fairly high values for all the synthesised compounds and this indicates possibility of stronger intermolecular interactions of the synthesised compounds with their surrounding, hence aid their absorption into the system.

It is observed that demetallation process increases hydrophobicity as all demetallated compounds have higher values of LogP than the ligands, hence are more hydrophobic than the starting ligands. This trend is also justified in their enhanced antimicrobial activities compared to the staring ligands.

Adducts

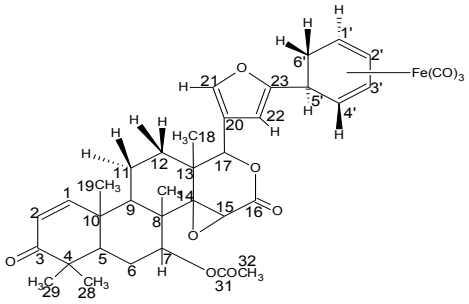

(19)

Molecular Formula: $C_{37}H_{40}O_{10}Fe$

Calculated mass = 700.677

Tricarbonyl [1-4-η-5-(gedunino) cyclohexa-1, 3-diene]iron

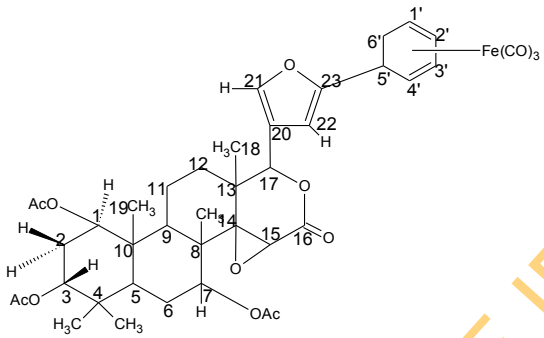

(20)

Molecular formula: $C_{41}H_{48}O_{13}Fe$

Calculated mass = 804.782

Tricarbonyl [1-4-η-5-(khivorino) cyclohexa-1,3-diene]iron

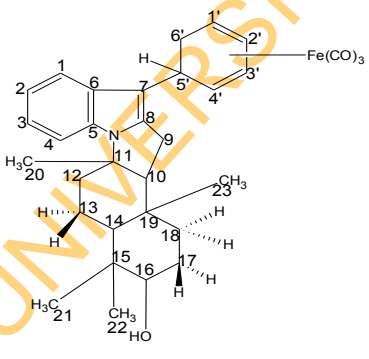

(22)

Molecular formula: $C_{32}H_{37}NO_4Fe$

Calculated mass = 555

Tricarbonyl[1,4-η-5(polyavolensinolino)cyclohexa-1,3-diene]iron

Modified NaturalProduct

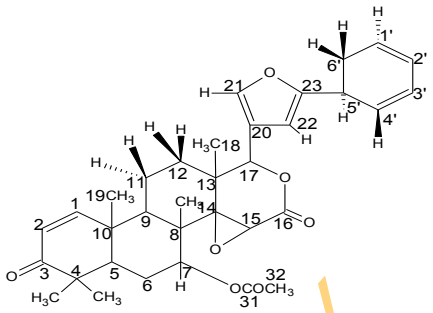

(26)

Molecular formula $C_{34}H_{40}O_7$

Calculated mass = 560.677

5-exo-(gedunino) cyclohexa-1,3-diene

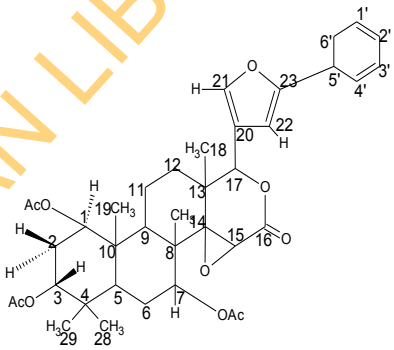

(27)

Molecular formula $C_{38}H_{48}O_{10}$

Calculated mass = 664.782

5-exo-(khivorino)cyclohexa-1,3-diene

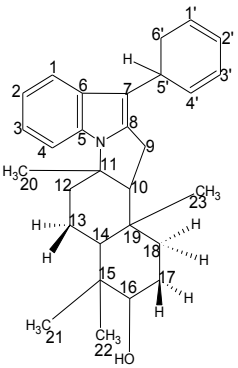

(29)

Molecular formula: $C_{29}H_{37}NO$

Calculated mass = 415.61

5-exo-(polyavolensinolino)cyclohexa-1,3-diene

Figure 5.1: Structures of adducts and the demetallated Products

Adducts **Modified NaturalProduct**

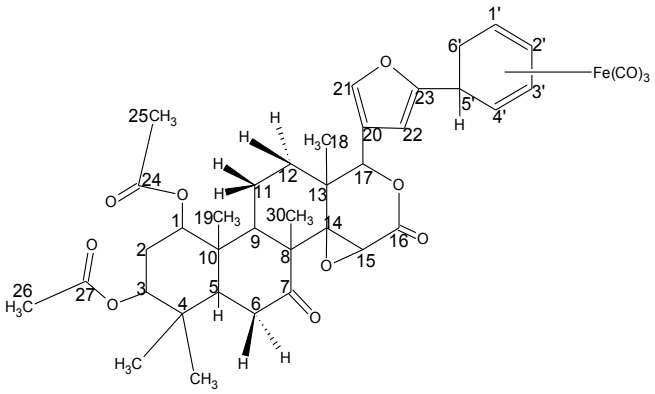

(21)

Molecular formula: $C_{39}H_{44}O_{12}Fe$

Calculated mass = 760.73

Tricarbonyl[1,4-η-5-(7-ketokhivorino) cyclohexa-1,3-diene] iron

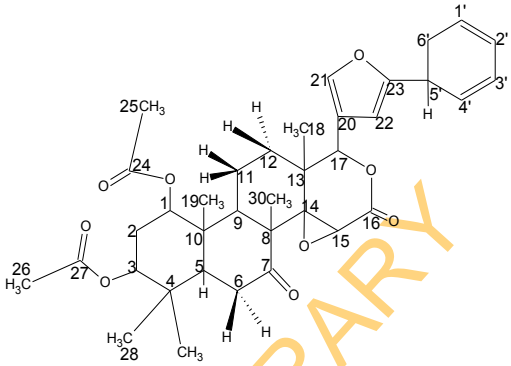

(28)

Molecular formula: $C_{36}H_{44}O_9$

Calculated mass = 620.73

5-exo-(7-ketokhivorino)cyclo hexa-1,3-diene

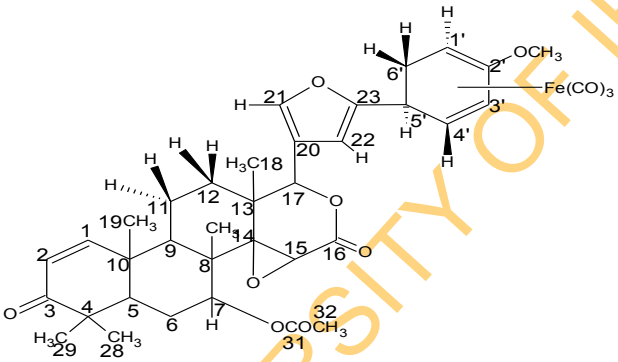

(23)

Molecular formula: $C_{38}H_{42}O_{11}Fe$

Calculated mass = 730.7

Tricarbonyl [1-4-η-2-methoxy-5-(gedunino)cyclo hexa-1,3-diene]iron

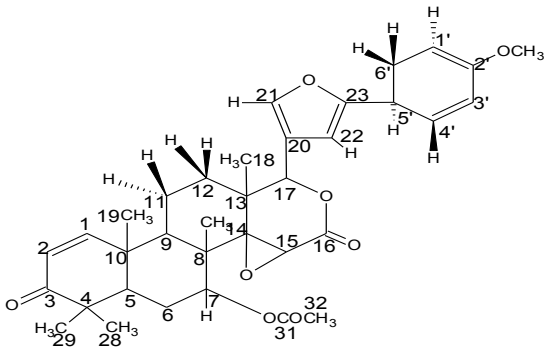

(30)

Molecular formula: $C_{35}H_{42}O_8$

Calculated mass = 590.7

2-methoxy-5-exo-(gedunino) cyclohexa-1,3-diene

Figure 5.1: Structures of adducts and the demetallated Products

Adducts **Modified NaturalProduct**

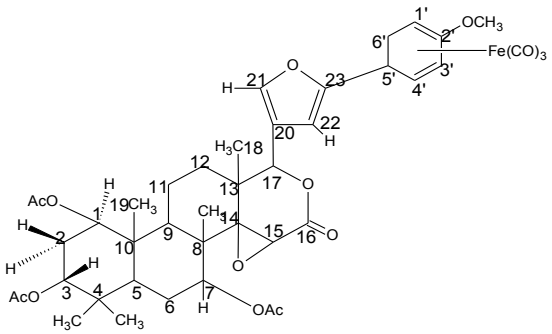

(24)

Molecular formula: $C_{42}H_{50}O_{14}Fe$

Calculated mass = 834.81

Tricarbonyl [1-4-η-2-methoxy-5-(khivorino)cyclohexa-1,3 -diene]iron

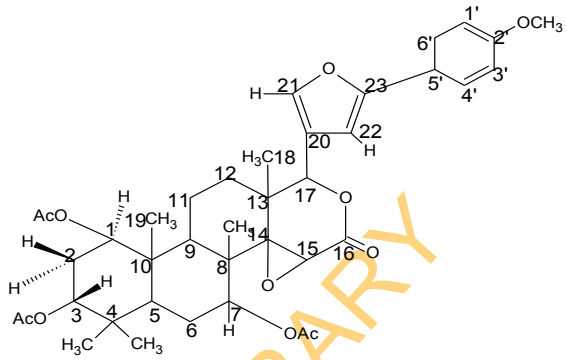

(31)

Molecular formula: $C_{39}H_{50}O_{11}$

Calculated mass = 694.81

2-methoxy-5-exo-(khivorino) cyclohexa1,3-diene

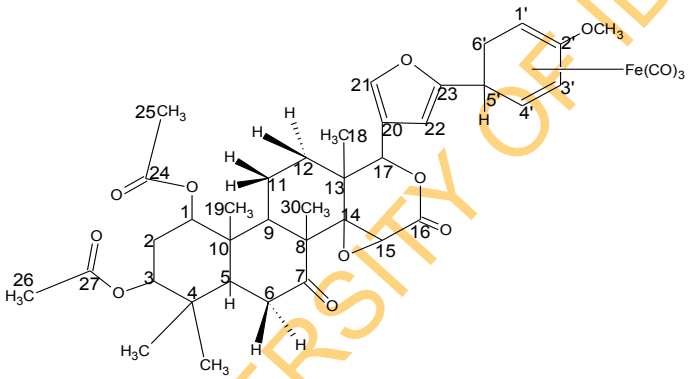

(25)

Molecular formula: $C_{40}H_{46}O_{13}Fe$

Calculated mass = 790.76

Tricarbonyl[1,4-η-5-(7-ketokhivorino)cyclohexa -1,3-diene]iron

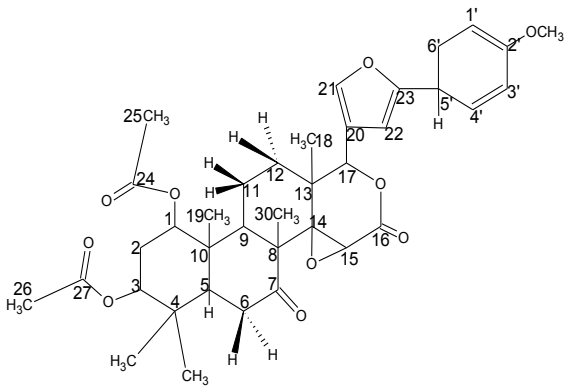

(32)

Molecular formula: $C_{37}H_{46}O_{10}$

Calculated mass = 650.76

2-methoxy-5-exo-(7-ketokhivorino) cyclohexa-1,3-diene

Figure 5.1: Structures of adducts and the demetallated Products

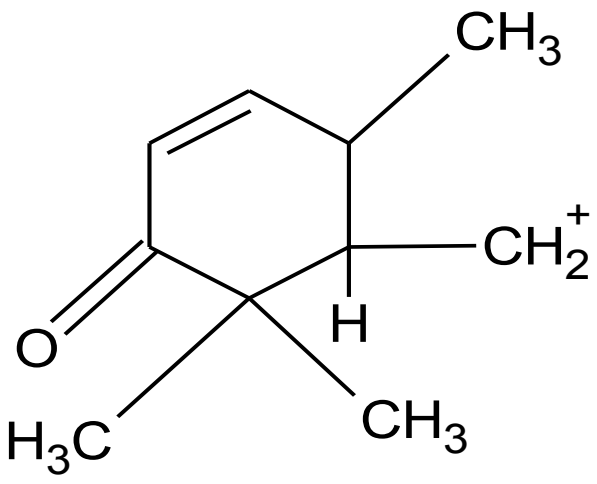

151($C_{10}H_{15}O$)

Figure 5.2: Mass spectral Fragment from adduct

REFERENCES

Adejoro, I. A., Odiaka, T. I and Akinyele, O. F. 2012. Molecular modeling and computational studies of dimethyl pyridino-1,4-η-2-methoxy cyclohexa-1,3-diene iron tricarbonyl complexes. *Asian Journal of Research in Chemistry* 5.1: 146-152.

Adejoro, I. A., Odiaka, T. I and Akinyele, O. F. 2013. Structure and electronic properties of aminopyridino-1,4-η-2methoxycyclohexa-1,3-diene iron tricarbonyl complexes. A Semi-Empirical PM3 approach. *Asian Journal of Research in Chemistry* 6.11: 1034-1039.

Adejoro, I. A., Odiaka, T. I and Akinyele, O. F. 2014. Density functional theory and reactivity parameters of dimethylpyridino-1,4-η-cyclohexa-1,3-dieneiron tricarbonyl complexes. *Journal of Natural Sciences Research* 4.1: 38-45.

Adesogan, E. K., Powell, J. W and Taylor, D. A. H. 1967. Extractives from the seed of *Khaya senegalensis*. *Journal of Chemical Society* C: 554-556. DOI: 10.1039/J39670000554.

Ahmed, I., Bond, A. M., Colton, R., Jurcevic, M and Traeger, J. C. 1993. Mass spectrometric studies of some cationic and anionic Group 6 and Group 7 metal carbonyl complexes. *Journal of Organometallic Chemistry* 447.1: 59-65.

Akinsanya, A., Bevan, C. W. L., Halsall, T. G., Powell, J. W and Taylor, D. A. H. 1961. West African timbers. Part IV. Some reactions of gedunin. *Journal of Chemical Society*. 3705-3708. DOI: 10.1039/JR9610003705.

Atton, J. G and Kane-Maguire, L. A. P. 1983. Mechanisms of nucleophilic attack at coordinated carbonmonoxide ligand in $[(1\text{-}5\text{-}\eta\text{-dienyl})Fe(CO)_3)]^+$ cations (dienyl = C_6H_7, C_7H_9). *Journal of Organometallic Chemistry* 246.1: C23-C26.

Bauer, A. W., Kirby, W. M. M., Sherris, J. C and Turck, M. 1996. Antibiotic susceptibility testing by a standardised single disk method. *American Journal of Clinical Pathology* 36: 493-496.

Becker, Y., Eisenstadt, A and Shvo, Y. 1972. Reactions of transitions metal carbonyl with heterocyclic systems. *Tetrahedron Letters* 13.31: 3183-3186.

Becke, A. D. 1992. Density Functional Thermochemistry. II. The effect of the Perdew-Wang generalized gradient correlation correction. *Journal of Chemical Physics* 97.12: 9173-9177.

Becke, A. D. 1993. Density Functional Thermochemistry. III. The role of exact exchange. *Journal of Chemical Physics* 98: 5648-5652.

Bevan, C. W. L., Halsall, T. G., Nwaji, M. N and Taylor, D. A. H. 1962. West African timbers. Part V. The structure of khivorin, a constituent of *Khaya ivorensis. Journal of Chemical Society* 768-771. DOI: 10.1039/JR9620000768.

Birch, A. J. 1950. Reduction by dissolving metals. Part VII. The reactivity of mesomeric anions in relation to the reduction of benzene rings. *Journal of Chemical Society* 321: 1552-1556.

Birch, A. J., Cross, P. E., Lewis, J., White, D .A and Wild, S. B. 1968. The Chemistry of coordinated ligands Part II: Iron tricarbonyl complexes of some cyclohexadienes. *Journal of Chemical Society* A: 332-340. DOI: 10. 1039/J19680000332.

Birch, A. J., Liepa, A. J and Stephenson, G. R. 1979. Organometallic compounds in organic synthesis- some tricarbonyl (cyclohexadienyl) iron cations and nitrogen containing nucleophiles. *Tetrahedron Letter* 20.37: 3565- 3568.

Birch, A. J., Liepa, A. J and Stephenson, G. R. 1982. Organometallic complexes in synthesis. Part16: Reactions of tricarbonyl(cyclohexadienyl) iron(+1) salts with aromatic amines. *Journal Chemical Society Perkin* 1. 713-717. DOI: 10.1039/P19820000713.

Birney, D. M., Crane, A. M and Sweigart, D. A. 1978. Kinetics of nucleophilic addition of tertiary phosphines to dicarbonylnitrosyl (cyclobutadiene) iron cation and tricarbonyl(cycloheptatriene) manganese cation. *Journal of Organometallic Chemistry* 152.2: 187-192.

.

Boufas, W., Dupont, N., Berredjem, M., Berrezag, K., Becheker, I., Berredjem, H and Aouf, N. E. 2014. Synthesis and antibacterial activity of sulfonamides. SAR and DFT studies. *Journal of Molecular Structure* 1074: 180-185.

Bray, D. H., Warhust, D. C., Conolly, J. D., O'Neill, M. J and Phillipson, J. D. 1990. Plants as sources of antimalaria drugs. Part 7. Activity of some species of *Meliaceae* plants and their constituent limonoids. *Phytotherapy Research* 4.1: 29-35.

Brisdon, A. K. 1998. Resonance spectroscopy. *Inorganic spectroscopic methods* Oxford University Press Chapter 3: 30-56.

Bromfield, K.M., Graden, H., Liungdahl, N and Kann, N. 2009. Synthetic applications of cationic iron and cobalt carbonyl complexes. *Journal of Chemical Society Dalton Transaction* 26: 5051-5061. DOI: 10.1039/b900434n

Brown, D. A., Chawla, S. K., Glass, W. K and Hussein, F. M. 1982. Nucleophilic substitution and addition reactions of the tricarbonyl (.eta.-1,5-cycloheptadienylium) iron cation. *Journal of Inorganic Chemistry* 21.7: 2726-2732.

Brown, D. A., Fitzpatrick, N. J., Glass, W. K and Sayal, P. K. 1984. Nucelophilic substitution and addition reactions of tricarbonyl(.eta.5-cyclopentadienyl)-,tricarbonyl(.eta-1,5-cyclohexadienylium) and tricarbonyl(.eta-1,5-cyclohepta dienylium) iron cations. *Organometallics* 3.8: 1137-1144.

Burall, L. S., Harro, J. M., Xin Li, C., Lockatell, V., Himpsi, S. D., Hebel, J. R., Johnson, D. E and Mobley, H. L. T. 2004. *Proteus mirabilis* genes that contribute to pathogenesis of urinary tract infection. Identification of 25 signature-tagged mutants attenuated at least 100-fold. *Infection and Immunity* 72.5: 2922-2938.

Busetto, L and Angelici, R. J. 1968. Reactions of cyclopentadienyliron carbonyl cations with amines. *Inorganic Chimica Acta* 2: 386-390.

Cattalini, L. 1972. Reaction mechanisms in inorganic Chemistry MTP International *Review of Science. Inorganic Chemistry series* 1. Butterworths London 9 Chapter 7.

Chatt, J. and Duncanson, L. A. 1953. Olefin coordination compounds. Part III. Infra red spectra and structure: attempted preparation of acetylene complexes. *Journal of Chemical Society*. 2939-2947. DOI: 10.1039/JR9530002939.

Chattaraj, P. K and Maiti, B. 2003. HSAB principle applied to the time evolution of chemical recations. *Journal of the American Chemical Society* 125.9: 2705-2710.

Clack, D. W., Monshi, M and Kane-Maguire, L. A. P. 1976a. Correlation of the reactivity of coordinated π-hydrocarbons with electronic parameters. I. Indo calculations on the cation $[(C_6H_7)Fe(CO)_3]^+$. *Journal of Organometallic Chemistry* 107.3: C40-C42.

Clack, W., Monshi, M and Kane-Maguire, L. A. P. 1976b. Correlation of the reactivity of coordinated π-hydrocarbons with electronic parameters II. INDO calculation on the $[(C_7H_6X)\ Cr(CO)_3]^+$ (X= H, OMe, COOMe). *Journal of organometallic Chemistry* 120: C25-C27.

Cooper, J. N and Powell, R. E. 1963. On the purported tetraphenylboric acid. *Journal of American Chemical Society* 85.11: 1590-1592.

Cotton, F. A and Monchamp, R. R. 1960. The heat of sublimation and the metal-metal bond energy in $Mn_2(CO)_{10}$. *Journal of Chemical Society*. 533-536. DOI: 10.1039/JR9600000533.

Cowles, R. J. H., Johnson, B. F. G., Josty, P. L and Lewis, J. 1969. Relative reactivity of coordinated ligands in the dienyltricarbonyl-ruthenium cation $[(dienyl)\ Ru(CO)_3]^+$. *Journal Chemical Society D Chemical Communications* 8: 392a-392a.

Dauben, H and Bertelli, D. 1961. Additions and corrections, iron tricarbonyl complexes of cycloheptatriene, cycloheptadiene and cycloheptadienium ion. *Journal American Chemical Society* 83.24: 5049-5049.

Dewar, M. J. S. 1951. A review of π complex theory. *Bulletin de la Societe Chimique de France* 18: C71-79.

Eisenstein, O., Butler, W. M and Pearson, A. J. 1984. A theoretical study of the formation and reactivity of substituted cyclohexadienyl iron complexes. The structures and reactivities of tricarbonyl(2-methoxycyclohexadienyl) iron cation and tricarbonyl(1-methyl-4-methoxy cyclohexadienyl) iron cation. *Organometallics* 3.8: 1150-1157.

Emeleus, H. J and Sharpe, A. G. 1973. Modern aspects of Inorganic Chemistry. John Wiley and Sons.

Emerson, G. F., Mahler, J. E., Kochnar, R and Pettit, R. 1964. Organo-iron complexes. IV. Reactions of substituted dienes with iron pentacarbonyl. *Journal of Organic Chemistry* 29.12: 3620-3624.

Eshwari, K., Mamtha, P., Ravi, M., Aparna, B., Reddy, P. H and Devi, C. S. 2014. Spectro-analytical, computational and biological studies on 4-pyridine carboxaldehyde-3-hydroxy-5-(hydroxyl methyl)-2-methyl hydrazone hydro chloride and its Cu (II) complexa. *International Journal of Pharmacy and Pharmaceutical Sciences* 6.8: 136-143.

Evans, D. J and Kane-Maguire, L. A. P. 1982. Kinetics of nucleophilic attack on coordinated organic moieties Part 22. Reaction of $[Fe(CO)_3(1\text{-}5\text{-}\eta\text{-dienyl}]^+$ cations with imidazole. *Inorganic Chimica Acta* 62: 109-112.

Evans, D. J., Kane-Maguire, L. A. P and Kanitz, R. 1996. Kinetics of nucleophilic attack on coordinated organic moieties. Part 31. Addition of imidazole to $[Fe(CO)_3(1\text{-}5\text{-}\eta\text{-dienyl}]^+$ cations. *Journal of Coordination Chemistry* 39.1: 71-88.

Evans, J., Howe, D. V., Johnson, B. F. G and Lewis, J. 1973. The addition of triphenylphosphine and pyridine to cyclohexadienyl and cycloheptadienyl iron tricarbonyl cations. *Journal of Organometallic Chemistry* 61: C48-C50.

Falshaw, C. P., King, T. J and Okorie, D. A. 1982. West African timbers Part V. The structure of khivorin, a constituent of *Khaya ivorensis*. *Tetrahedron* 38.15: 2311-2313.

Fischer, E. O and Fischer, R. D. 1960. Ein cyclohexadienyl-eisen-tricarbonyl-kation. *Angewandte Chemie* 72.23: 919-919.

Fleming, I. 1976. Frontier orbitals and organic chemical reactions. Wiley and Sons, New York.

Francis, M. M., Pietro, W. J., Hehre, W. J., Binkley, J. S., Gordon, M. S., Defrees, D. J and Pople, J. A. 1982. Self- consistent molecular orbital methods. XXIII. A polarisation-type basis set for second row elements. *Journal of Chemical Physics* 77.7: 3654-3665.

Franz, R. G. 2001. Comparison of Pka and Log P values of some carboxylic and phosphonic acids, synthesis and measurement. *American Association of Pharmaceutical Scientists Pharmaceutical Science Journal* 3.2: 1-13.

Games, D. E., Jackson, A. H., Kane-Maguire, L. A. P and Taylor, K. 1975. Field desorption mass spectrometry of organometallic complex salts. *Journal of Organometallic Chemistry* 88: 345-349.

Genco, N., Marten, D., Raghu, S and Rosenblum, M. 1976. Metal assisted carbon-carbon bond formation. Synthesis of hydroazulene complexes. *Journal of the American Chemical Society* 98.3: 848-849.

Gopalakrishnan, S. B., Kalaiarasi, T and Subramanian, R. 2014. Comparative DFT study of phytochemical constituents of the fruits of *Cucumis trigonus* Roxb. and *Cucumis sativus* Linn. *Journal of Computational Methods in Physics* 2014:1-6.Retrieved Nov.27,2014, from http://dx.doi.org/10.1155/2014/623235

Govindachari, T. R and Kumari, G. N. K. 1998. Tetranortriterpenoids from *Khaya senegalensis*. *Phytochemistry* 47.7: 1423-1425.

Gower, M., John, G. R., Kane-Maguire, L. A. P., Odiaka, T. I and Salzer, A. 1979. Mechanism of attack by trialkylphosphines on dicarbonyl (dienyl)iodoiron complexes. *Journal of chemical Society Dalton Transaction* 12: 2003-2010.

Hall, H. K. 1957. Correlation of the base strength of amines. *Journal of the American Chemical Society* 79.20: 5441-5444.

Hallam, B. F and Pauson, P. L. 1958. Metal derivatives of conjugated dienes. Part I. Butadiene- and cyclohexadiene- iron carbonyls. *Journal of Chemical Society.* 642-645. DOI: 10.1039/JR9580000642.

Hansch, C., Hoekman, D., Leo, A., Zhang, L and Li, P. 1995. The expanding role of Quantitative Structure-Activity Relationships (QSAR) in toxicology. *Journal of Toxicology Letters* 79.1-3: 45-53.

Hansch, C and Leo, A. 1995. Exploring QSAR, Fundamentals and Applications in Chemistry and Biology. *American Chemical Society*. Washighton DC. Chapter 13.

Hashmi, M. A., Munro, J. D., Pauson, P. L and Williamson, J. M. 1967. Metal derivatives of conjugated dienes. Part III. Some cyclohexa- and cycloheptadienyl iron compounds. *Journal of Chemical Society* A: 240-243. DOI: 10.1039/J19670000240.

Hudson, R. F and Loveday, G. 1962. Nucleophilic reactivity. Part III. The significance of bronsted relation with particular reference to acylation and alkylation. *Journal of Chemical Society*. 1068-1075. DOI: 10.1039/JR9620001068.

Ito, C., Ohta, H., Hugh, T. W and Furukawa, T. H. 1996. Constituents of *Clausena excavata*. Isolation and structural elucidation of seven new carbazoles alkaloids and a new coumarin. *Chemical and Pharmaceutical Bulletin* 44.12: 2231-2235.

John, G. R and Kane-Maguire, L. A. P. 1979a. Kinetics of nucleophilic attack on coordinated organic moieties. Part 7: Mechanisms of addition of tertiary phosphines and phosphites to tricarbonyl(dienyl) iron cations. *Journal Chemical Society Dalton* 5: 873-878.

John, G. R and Kane-Maguire, L. A. P. 1979b. Kinetics of nucleophilic attack on coordinated organic moieties. Part 8. Addition of N,N-dimethylaniline to the tricarbonyldienyl iron, ruthenium and osmium cations and related complexes. *Journal Chemical Society Dalton Transaction* 7: 1196-1199.

John, G. R., Kane-Maguire, L. A. P and Kanitz, R. 1986. Mechanismsof nucleophilic attack at coordinated carbonmonoxide II: Iodide addition to a carbonmonoxide ligand in $[Fe(CO)_3(1\text{-}5\text{-}\eta\text{-dienyl}]^+$ cations (Dienyl = C_6H_7, C_7H_9, 2-$MeOC_6H_6$). *Journal of Organometallic Chemistry, Preliminary Communication* 312.2: C21-C23.

John, G. R., Kane-Maguire, L. A. P., Odiaka, T. I and Earborn, C. 1983. Synthetic and mechanistic studies of electrophilic attack by the cations $[Fe\ (CO)_3(1\text{-}5\text{-}\eta\text{-dienyl})]^+$(dienyl = C_6H_7 or 2-$MeOC_6H_6$) on aryltrimethylsilanes and –stannanes. *Journal of Chemical Society Dalton Transaction* 8: 1721-1727.

John, G. R., Mansfield, O. A and Kane-Maguire, L. A. P. 1977. Kinetics of nucleophilic attack on coordinated organic moieties. Part 5. Mechanisms of addition of heterocyclic aromatic species to tricarbonyl (1-5-cyclohexadienyl) iron and ruthenium cations. *Journal Chemical Society Dalton Transaction* 6: 574-578.

Johnsons, B. F. G., Lewis, J., Odiaka, T. I and Raithby, P. 1981. Reactions of $[Os_3(CO)_{10}(NCMe)_2]$ with amides and aldehydes; X-ray crystal structure of $[Os_3(CO)_{10}(\mu\text{-}H)(COCH_2Ph)]$. *Journal of Organometallic Chemistry* 216.3: C56-C60.

Johnson, D. E., Rusell, R. G., Lockatell, C. V., Zulty, J. C., Warren, J. W and Mobley, H. L. T. 1993. Contribution of *Proteus mirabilis* urease to persistence, urolithiasis and acute pyelonephritis in a mouse model of ascending urinary tract infection. *Infection and Immunity* 61.7: 2748-2754.

Jones, D., Pratt, L and Wilkinson, G. 1962. π-cyclohexadienyl compounds of manganese, rhenium, iron and ruthenium. *Journal of Chemical Society* 4458-4463. DOI: 10.1039/JR9620004458.

Joule, J. A. 1984. Recent advances in the Chemistry of 9H- carbazoles. *Advances in Heterocyclic Chemistry*. Academic Press New York 35: 83-198.

Kamath, S. G., Cheng, N., Xiong, Y., Wenham, R., Apte, S. H. M., Cragun, J and Lancaster, J. M. 2009. Gedunin, a novel natural substance inhibits ovarian cancer cell proliferation. *International Journal of Gynaecological Cancer* 19.9: 1564-1569.

Kaneda, M., Sakano, K., Nakamura, S., Kushi, Y and Litaka, Y. 1981. The structure of carbazomycins B. *Heterocycles* 15.2: 993-998.

Kane-Maguire, L. A. P. 1971. Kinetics of nucleophilic attack on coordinated organic moieties. Part 1. Addition of diketones on cyclic dienyl complexes. *Journal of Chemical Society* A: 1602-1606. DOI: 10.1039/J19710001602.

Kane-Maguire, L. A. P and Mansfield, O. A. 1973. Cationic metal-dienyl complexes as electrophilic reagents on aromatic molecules. *Journal of Chemical Society Chemical Communication* 15: 540-541.

Kane-Maguire, L. A. P and Mansfield, C. A. 1976. Kinetics of nucleophilic attack on coordinated organic moieties. Part 4. Mechanisms of addition of indole and substituted indoles to tricarbonyl(cyclohexadienyl) iron and ruthenium cations. *Journal of Chemical Society Dalton Transaction* 21: 2192-2196.

Kane-Maguire, L. A. P., Honig, E. D and Sweigart, D. A. 1984. Nucleophilic addition to coordinated cycli-π hydrocarbons: Mechanistic and synthetic studies. *Chemical Review* 84: 525-543.

Kane-Maguire, L. A. P., Odiaka, T. I and Williams, P. A. 1981a. Kinetics of nucleophilic attack on coordinated organic moieties. Part 15. Addition of p-toluidine to tricarbonyl (1-5-η-dienyl) iron cations. *Journal of Chemical Society Dalton Transaction* 1: 200-204. DOI: 10.1039/DT9810000200.

Kane-Maguire, L .A. P., Odiaka, T. I., Turgoose, S and Williams, P. 1981b. Kinetics of nucleophilic attack on co-ordinated organic moieties. Part 19. Addition of anilines to tricarbonyl(1-5-η-dienyl) iron cations. *Journal Chemical Society Dalton Transaction* 12: 2489-2495.

Kataeva, O., Krahl, M. P and Knolker, H. J. 2005. First total synthesis of the biologically active 2,7-dioxygenated tricyclic carbazole alkaloids 7-methoxy-o-methylmukonal, Clausine H (Clauszoline-C), Clausine K (Clausine-J) and Clausine O. *Organic and Bimolecular Chemistry* 3.17: 3099-3101.

Khalid, S. A., Duddeck, H and Gonzalez-Sierra, M. 1989. Isolation and characterization of an antimalarial agent of the neem tree *Azadirachta indica*. *Journal of Natural Products* 52.5: 922-926.

Knolker, H. J. 1992. Iron mediated synthesisof heterocyclic ring systems and applications in alkaloid chemistry. *Synlett Letter* 5: 371-387.

Knolker, H. J., Bauermeister, M and Pannek, J. B. 1993. Transition metal-diene complexes in organic synthesis-13. Highlychemo and stereoselective oxidations of tricarbonylironcyclohexadiene complexes: Synthesis of deoxycarbazomycin B. *Tetrahedron Letters* 49.4: 841-862.

Knolker, H. J. 1999. Transition metal complexes in organic organic synthesis. Part 47. Organic synthesis via tricarbonyl (η^4-diene) iron complexes. *Chemical Society Reviews* 28.3: 151-157.

Knolker, H. J. 2004. Transition metal complexes in organic synthesis. Part71: First total synthesis of furoclausine-A. *Synlett Letter* 3: 528-530.

Kruger, C., Sekutowski, C., Hoberg, H and Krause-Going, R. 1977. (Pentaphenyl) aluminacyclopentadiene as a complexing ligand. The molecular structure of (Pentaphenyl)aluminacyclopentadiene and its complex with 1,5-cyclooctadienenickel. *Journal of Organometallic Chemistry* 141.2: 141-148.

Lakshmi, V and Gupta, P. 2008. An overview of the genus xylocarpus. *Natural Product Research* 22.14: 1197-1224.

Landsberg, J. M and Katz, L. 1971. Electronic effect in dienecarbonyl iron derivatives: II on the electron donor capacity. *Journal of Organometallic Chemistry* 33.1:C15-C16.

Lee, C., Yang, W and Parr, R. G. 1988. Development of the Colle-Salvetti correlation energy formula into a functional of the electron density. *Physical Review B* 37.2: 785-789.

Liu, S. 2005. Dynamic behavior of chemical reactivity indices in density functional theory: A Bohn-Oppenheimer quantum molecular dynamics study. *Journal of Chemical Sciences* 117.5: 477-483.

Love, R. A., Koetzle, T. F., Williams, G. J. B., Andrews, L. C and Bau, R. 1975. Neutron diffraction study of the structure of Ziese's salt $KPtCl_3(C_2H_4).H_2O$. *Inorganic Chemistry American Chemical Society* 14.11: 2653-2657.

Maglio, G., Musco, A and Palumbo, R. 1971. Reactivity of π-pentadienyl complexes. Stereochemistry of the addition of amines to the syn-1,5-dimethylpentadienyl iron tricarbonyl cation. *Journal of organometallic Chemistry* 32.1: 127-136.

Maglio, G and Rosario. 1974. Stereochemistry of the reaction between amines and the pentadienyl iron tricarbonyl cation. *Journal of Organometallic Chemistry* 76.3: 367-371.

Mansfield, C. A., Al-Kathumi, K. M and Kane-Maguire, L. A. P. 1974. Cationic metal π-enyl complexes as electrophilic reagents on aromatic molecules. *Journal of Organometallic Chemistry* 71.1: C11-C13.

Mansfield, C. A and Kane-Maguire, L. A. P. 1976. Kinetics of nucleophilic attack on coordinated organic moieties. Part 3. Effect of solvent on addition of pentane-2,4-dione to complexes of cyclic dienyls . *Journal of Chemical Society Dalton Transaction* 21: 2187-2191.

Mathieu.J and Weill-Raynal, J. 1973. Formation of C-C bonds. George Thieme Stuttgart Germany 1: 120-145.

Minclone, E., Pearson, A. J., Bovicelli, P., Chandler, M and Heywood, G. C. 1981. New approach to the synthesis of 6-ketosteroids via organoiron complexes. *Tetrahedron Letters* 22.30: 2929-2932.

Mobley, H. L and Warren, J. W. 1987. Urease-positive bacteriuria and obstruction of long-term urinary catheters. *Journal of Clinical Microbiology* 25.11: 2216-2217.

Mobley, H. L. 1996. Virulence of *Proteus mirabilis* in urinary tract infections: Molecular Pathogenesis and Clinical Management. *American Society for Microbiology* Press. Washington D.C. 245-269.

Mond, L., Langer, C and Quincke, F. 1890. L- Action of carbon monoxide on nickel. *Journal of Chemical Society* 57: 749-753.

Mond, L and Quincke, F. 1891. LV- Note on a volatile compound of iron with carbonic oxide. *Journal of Chemical Society* 59: 604-607.

Moscona, A. 2005. Drug therapy: Neuraminidase inhibitors for influenza. *The New England Journal of Medicine* 353.13: 1363-1373.

Nakamoto, K. 1986. Infrared and Raman spectra of Inorganic and Coordination compounds. 4th edition Wiley-Interscience.

National Committee for Clinical Laboratory Standards. 2002. Reference method for broth dilution antifungal susceptibility testing of yeasts. *Approved Standard M27-A2* .Second Edition. Wayne.

Nunn, K., Mosset, P., Gree, R and Saalfrank, R. W. 1988. Short highly enantioselective synthesis of a key intermediate for the preparation of Leucotriene B4 and its 14, 15-didehydroderivative. *Angewandte Chemie* 27.9: 1188-1189.

Odiaka, T. I and Kane-Maguire, L. A. P. 1979a. Addition of N,N-dimethylaniline to tricarbonyl(cyclohexadienyl) ruthenium cation. *Inorganic Chimica Acta* 37: 85-87.

Odiaka, T. I and Kane-Maguire, L. A. P. 1979b. Kinetics of nucleophilic attack on coordinated organic moieties. Part10. Addition of N,N-dimethylaniline to tricarbonyl(cyclohexadienyl) ruthenium cation. *Inorganic Chimica Acta* 37: 85-87.

Odiaka, T. I. 1980. Synthesis and mechanistic studies of nucleophilic attack on organic molecules coordinated to metal carbonyls. PhD. Thesis. Department of Chemistry. University of Cardiff. Wales. U.K.

Odiaka, T. I and Kane-Maguire, L. A. P. 1981. Kinetics of nucleophilic attack on coordinated organic moieties. Part 17. Addition of pyridines to $[Fe(CO)_3(1\text{-}5\text{-}\eta\text{-dienyl}]^+$ cations (Dienyl = C_6H_7, C_7H_9, 2-$MeOC_6H_6$). *Journal of Chemical Society Dalton Transaction* 5: 1162-1168.

Odiaka, T. I. 1985a. Mechanism of addition of aryltrimethyl-silanes and –stannanes to tricarbonyl (cyclohexadienyl) ruthenium(II) cation. *Journal of Chemical Society Dalton Transaction* 5: 1049-1052.

Odiaka, T. I. 1985b. Mechanism of attack on tricarbonyl (cycloheptatrienyl) tungsten cation by triphenylphosphine. *Inorganic Chimica Acta* 103: 9-13.

Odiaka, T. I and Kane-Maguire, L. A. P. 1985. Mechanisms of addition of primary aromatic amines and cyclohexylamine to tricarbonyl(cycloheptatrienyl) tungsten cation. *Journal of Organometallic Chemistry* 284: 35-46.

Odiaka, T. I and Okogun, J. I. 1985. New tricarbony (amido-substituted -1,3-diene) iron complexes. *Journal of Organometallic Chemistry* 288: C30-C32.

Odiaka, T. I. 1986. Mechanism of addition of 2-ethylpyridine to tricarbonyl [(1-5-η-dienyl iron (II)]$^+$ cations (Dienyl = C_6H_7, C_7H_9, 2-$MeOC_6H_6$). *Journal of Chemical Society Dalton Transaction* 12: 2707-2710.

Odiaka, T. I. 1989. Addition of anilines to the $[Fe\ (CO)_3(1\text{-}5\text{-}\eta\text{-}C_7H_9)]BF_4$ complex and the 'Ordered Transition State Mechanism'. *Journal of Chemical Society Dalton Transaction* 4: 561-565.

Odiaka, T. I. 2004. Modern Organometallic Chemistry, University Press Ibadan. 39-84.

Odiaka, T. I., Okogun, J. I and Okorie, D. A. 2007. New iron Tricarbonyl (cyclohexa-1,3-dienesubstituted) natural products. *Journal of Science Research* 7.1: 1-8.

Odiaka, T. I., Adejoro, I. A and Akinyele, O. F. 2012. Semi-empirical (PM3) studies of novel aminopyridino-1,4-η-cyclohexa-1,3-dieneiron tricarbonyl complexes. *American Journal of Scientific and Industrial Research* 3: 1-13.

Ohochuku, N. S and Taylor, D. A. H. 1970. 6β-Hydroxygedunin. *Journal of Chemical Society* C.3: 421-423.

Okorie, D. A. 1980. A new class of indolesesquiterpene alkaloids from *Polyathia suaveolens*. *Tetrahedron* 36: 2005-2008.

Okorie, D. A. 1981. Polyavolinamide an indolesesquiterpene alkaloid from *Polyathia suaveolen*. *Phytochemistry* 20: 2575-2578.

Pearson, A. J., Mincione, E., Chandler, M and Raithby, P. R. 1980. Organoiron complexes in organic synthesis. Part7. Regio and stereo-chemistry of ring connection reactions relevant to steroid and terpene synthesis. X-ray crystal structure determination of tricarbonyl (methyl1-[2-5-η-4-methoxy-1-methycyclohexa-2,4-dienyl]3-hydroxymethyl-3-methyl-2-oxocyclohexane carboxylate) iron. *Journal of Chemical Society Perkin 1*: 2774-2780. DOI: 10.1039/P19800002774.

Pearson, A. J and Rees, D. C. 1980. New synthetic approaches to aspidosperma alkaloids with functionalized (C20) substituents: Some key intermediates via diene-Fe $(CO)_3$ complexes. *Tetrahedron Letters* 21.40: 3937-3940.

Pearson, A. J and Heywood, G. C. 1981. New methodology for steroid total synthesis via organoiron complexes. *Tetrahedron Letters* 22.17: 1645-1648.

Pearson, A. J and Ong, C. W. 1981. Organoiron complexes in organic synthesis. Part 19. Trichothecene analogs. Total synthesis of 12,13-epoxy-14-methoxy trichothecene via organoiron complexes. *Journal of the American Chemical Society* 103.22: 6686-6690.

Pearson, A. J and Rees, D. C. 1982. Total synthesis of Limaspermine derivatives using organoiron. *Journal of the American Chemical Society* 104.5: 1118-1119.

Pearson, A. J. 1983. Natural products synthesis using organoiron complexes. *Pure and Applied Chemistry* 55.11: 1767-1779.

Pearson, A. J. 1994. Iron compounds in organic synthesis. Academic Press London. 97-101.

Pearson, R. G., Sobel, H. R and Songstad, J. 1968. Nucleophilic reactivity constants toward methyl iodide and transdichloridi(pyridine) platinum (II). *Journal of the American Chemical Society* 90.2: 319-326.

Qu, Y and Bian, X. 2005. Electronic structure and stability of Al_nP_n (n = 2-4) clusters. *Journal of Computational Chemistry* 26.3: 226-234.

Reihlen, H., Gruhl, A., Hebling, V and Pfrengle, O. 1930. Uber carbonyle und nitrosyle. IV. *Justus Liebigs Annal Chemistry* 482.1: 161-182.

Ritchie, C. D., Wright, D. J., Huang, D. S and Kamego, A. A. 1975. Cation-anion combination reaction. XII. Rates equilibriums and activation parameters for reactions of triarylmethylcations in aqueous solution. *Journal of the American Chemical Society* 97.5: 1163-1170.

Sakano, K., Ishimaru, K and Nakamura, S. 1980. New antibiotics , carbazomycins A and B. I. Fermentation, extraction, purification and physic-chemical properties. *Journal of Antibiotics* 33.7: 683-689.

Sakano, K and Nakamura, S. 1980. New antibiotics carbazomycins A and B. II. Structural elucidation. *Journal of Antibiotics* 33.9: 961-966.

Schmidt, A. 2004. Antiviral therapy for influenza. *Drugs* 64.18: 2031-2046.

Shvo, Y and Hazum, E. 1974. A simple method for the disengagement of organic ligands from iron complexes. *Journal of Chemical Society Chemical Communication* 9: 336-337.

Siu, A. F. H., David, D. A., Kane-Maguire, L. A. P., Pyne, S. G and Lambrecht, R. H. 1998. Kinetics of nucleophilic attack on coordinated organic moieties. Part 32.Synthetic and mechanistic studies of the reaction of iodine ion with [(η^5-dienyl) $Fe(CO)_3]^+$ cations (Dienyl = C_6H_7, C_7H_9, 2-$MeOC_6H_6$). *Journal of Coordination Chemistry* 46.2: 125-143.

Stephenson, G. R. 1982. Transition metal mediated asymmetric synthesis. Part 3. Preparation and stereospecific alkylation of unsymmetrically substituted tricarbonyl (cyclohexadienyl) iron (1+) salts. An organometallic approach to the synthesis of carvone, cryptomerion and bilobanone. *Journal of Chemical Society Perkin Transaction 1*. 2449-2456. DOI: 10.1039/P19820002449.

Sundarasivarao, N. B and Madhusudhana, R. J. 1977. Antifungal activity of gedunin. *Current Science* 46.20: 714-716.

Sunthitikawinsakul, A., Kongkathip, N., Kongkathip, B., Phonnakhu, S., Daly, J. W., Spande, T. F., Nimit, Y and Rochanaruangrai, S. 2003. Coumarins and carbazoles from *Clausena excavata* exhibited antimycobacterial and antifungal activities. *Planta Medica Letter* 69.2: 155-157.

Thompson, D. J. 1976. Reactions of tricarbonylcyclohexadiene iron complexes with cupric chloride. *Journal of Organometallic Chemistry* 108.3: 381-383.

Wu, T. S., Huang, S. C and Wu, P. L. 1997. Pyrano and Furocarbazole alkaloids fron the root bark of *Clausena excavata*. *Heterocycles* 45.5: 969-973.

Yamasaki, K., Kaneda, M and Watanabe, K. 1983. New antibiotics, carbazomycins A and B. III. Taxonomy and biosynthesis. *Journal of Antibiotics* 36.5: 552-558.

Yenjai, C., Sripontan, S., Sriprajun, P., Kittakoop, P., Jintasirikul, A., Tanticharoen, M and Thebtaranonth, Y. 2000. Coumarins and carbazoles with antiplasmodial activity from *Clausena harmandiana*. *Planta Medica Letter* 66.3: 277-279.

APPENDICES

Appendix 1: Fragmentation Pattern of tricarbonyl[1-4-η-5-(gedunino) cyclohexa-1,3-diene] iron (19)

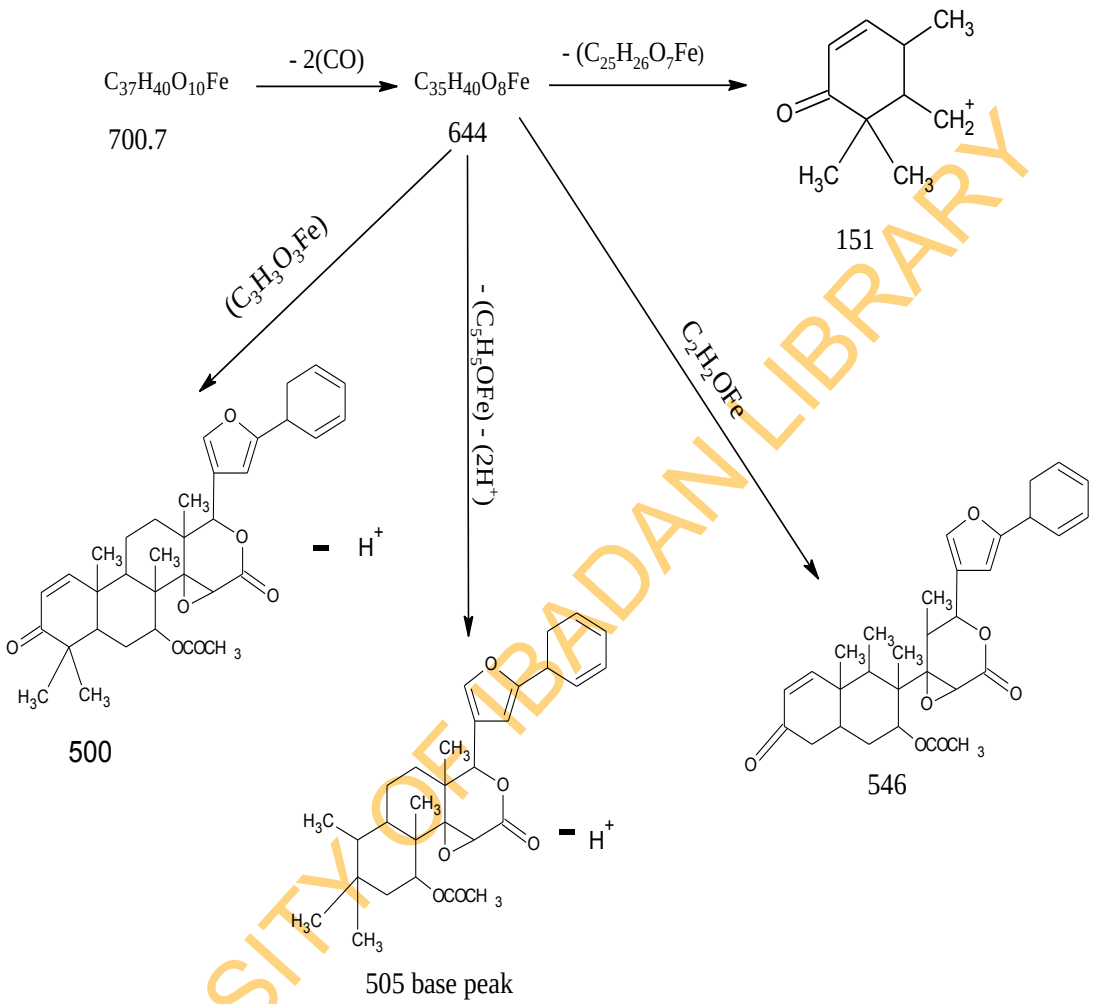

Appendix 2: Fragmentation Pattern of tricarbonyl[1-4-η-5-(khivorino) cyclohexa-1,3-diene] iron (20)

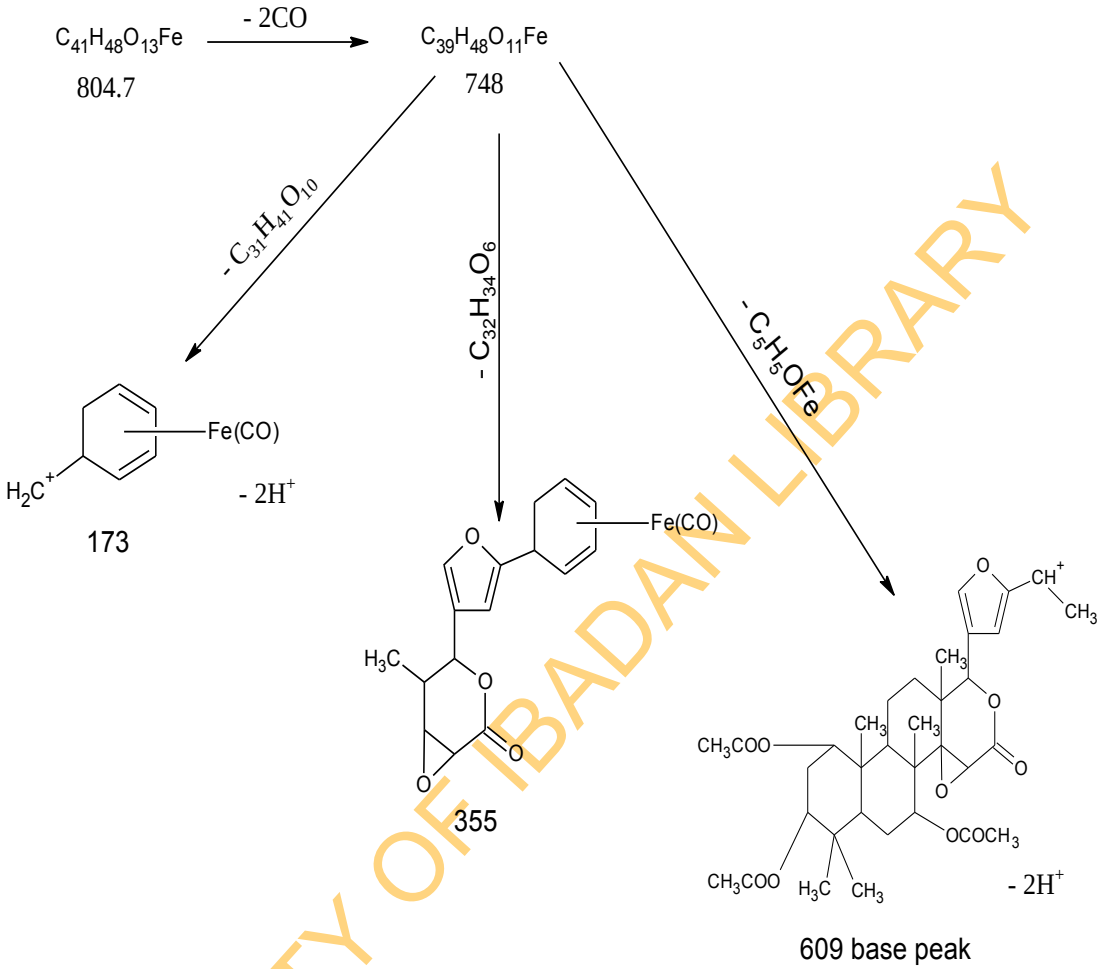

Appendix 3: Fragmentation Pattern of tricarbonyl[1-4-η-5-(polyavolensinolino) cyclohexa-1,3-diene] iron (22)

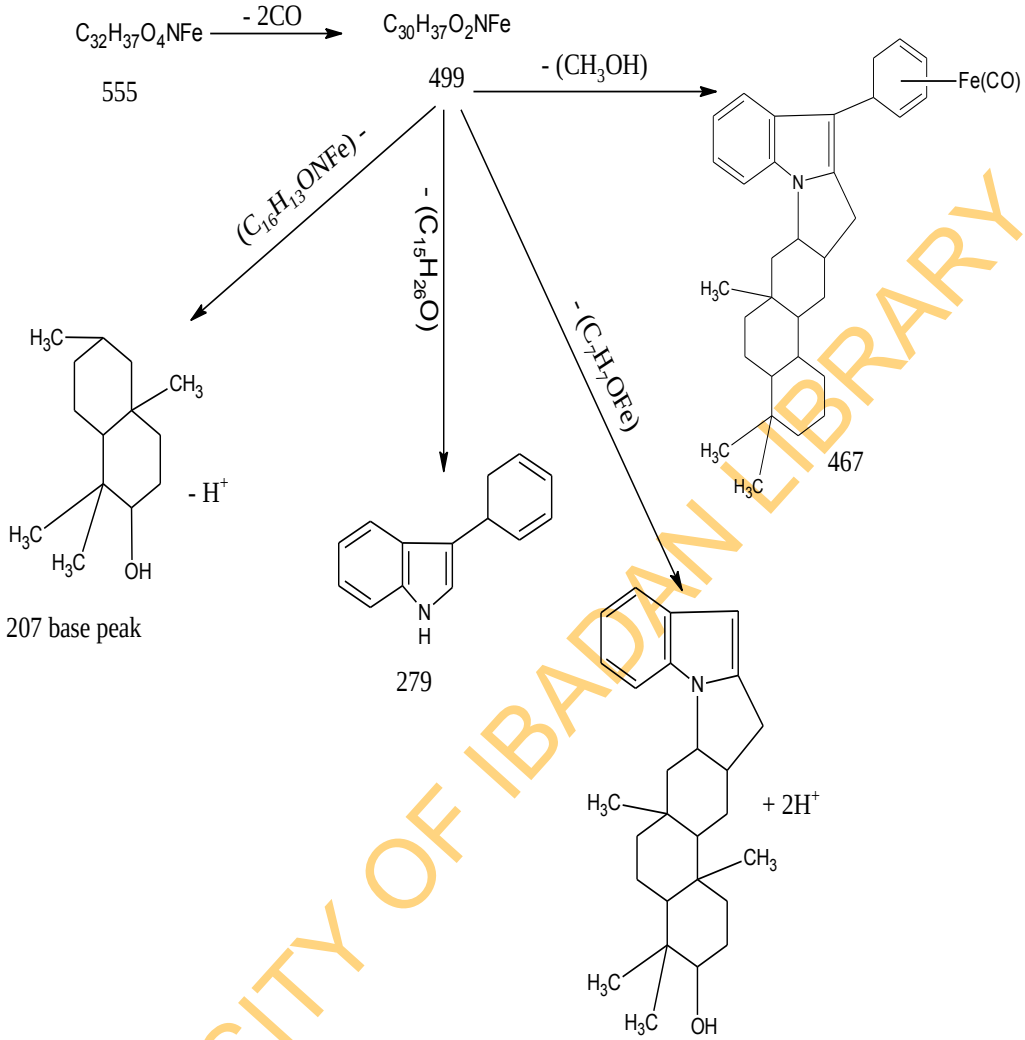

Appendix 4: Fragmentation Pattern of tricarbonyl[1-4-η-5-(7-ketokhivorino) cyclohexa-1,3-diene] iron (21)

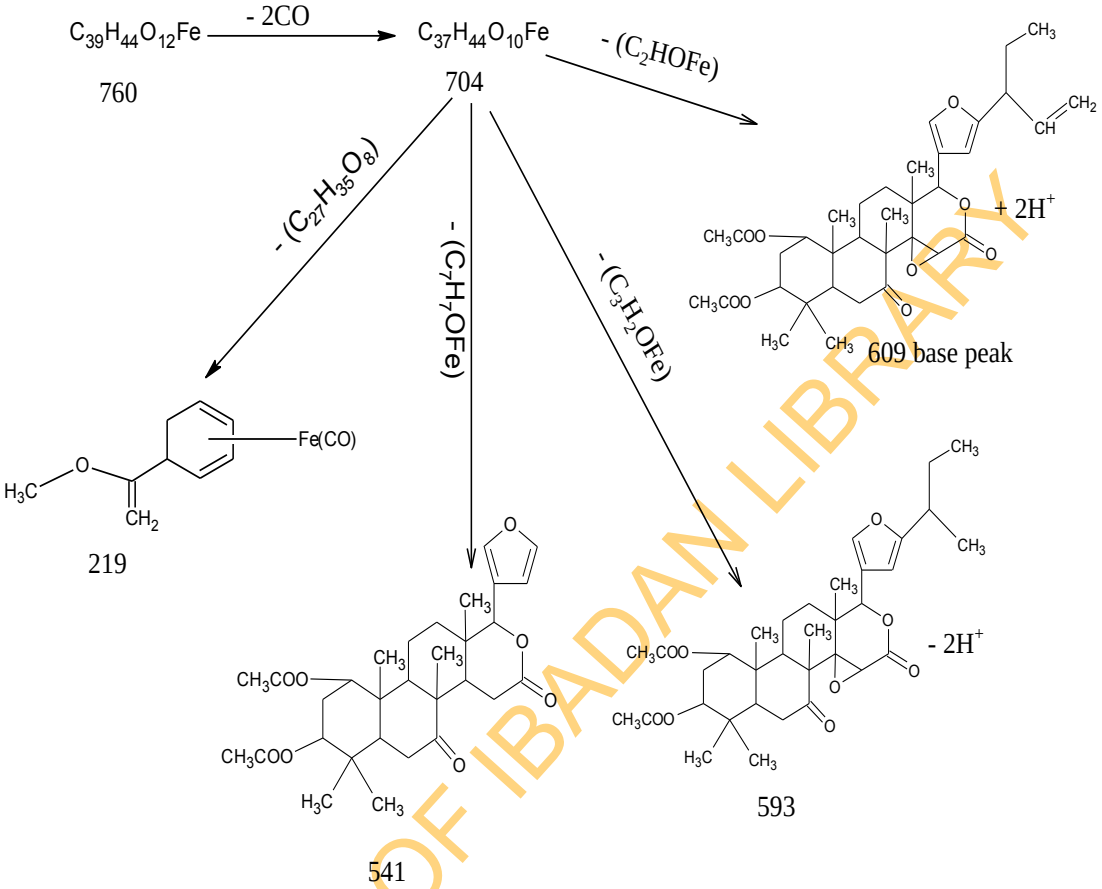

Appendix 5: Fragmentation Pattern of tricarbonyl [1-4-η-2-methoxy-5-(gedunino) cyclohexa-1,3-diene] iron (23)

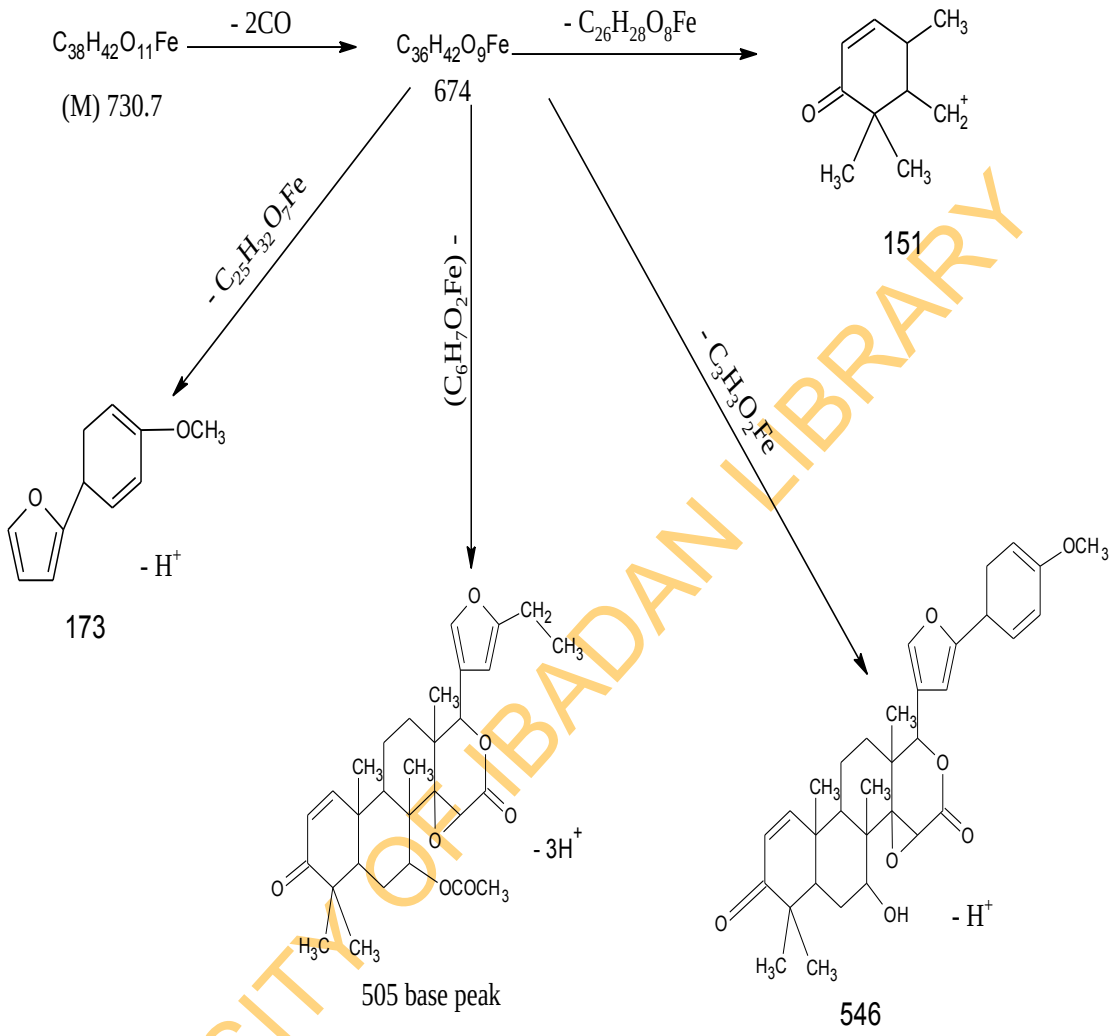

Appendix 6: Fragmentation Pattern of tricarbonyl [1-4-η-2-methoxy-5-(khivorino) cyclohexa-1,3-diene] iron (24)

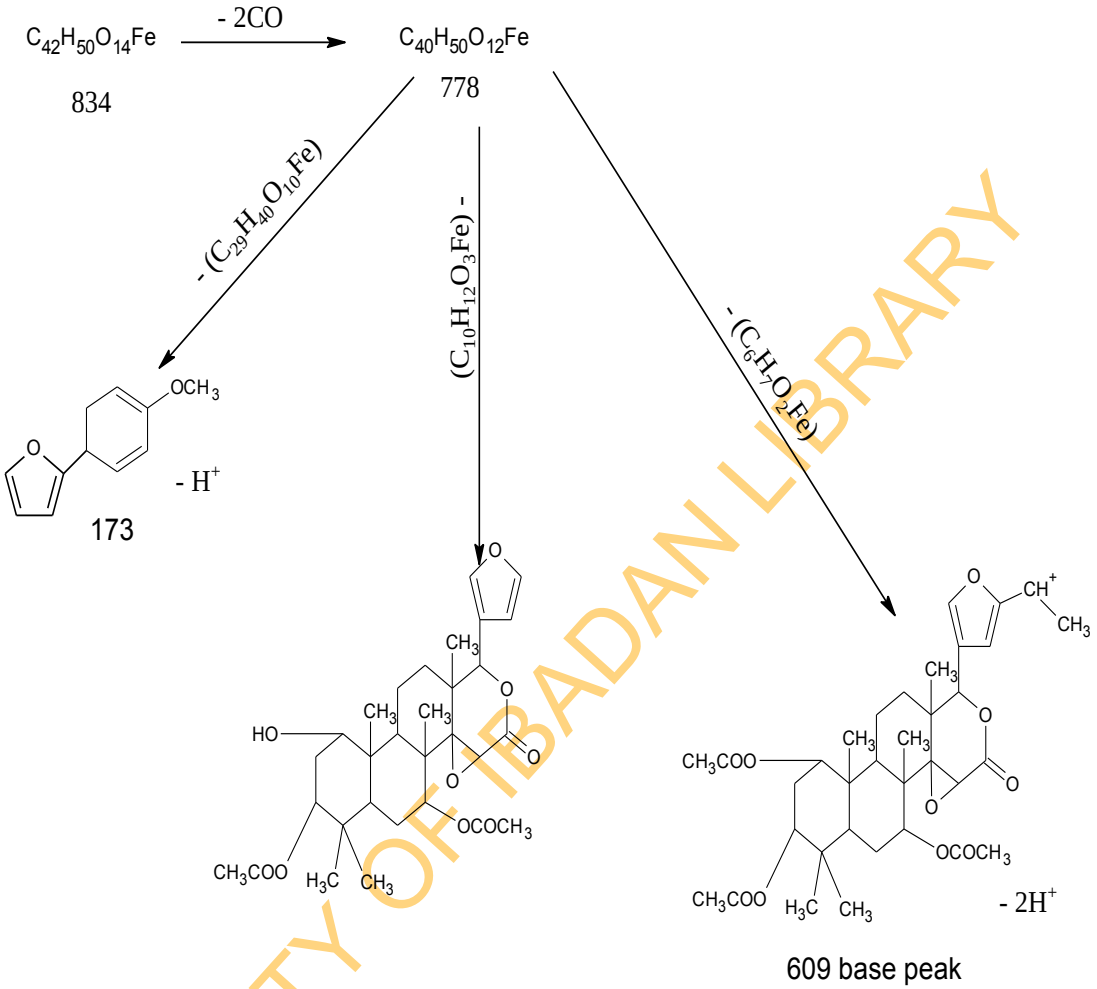

Appendix 7: Fragmentation Pattern of tricarbonyl [1-4-η-2-methoxy-5-(7-ketokhivorino) cyclohexa-1,3-diene] iron (25)

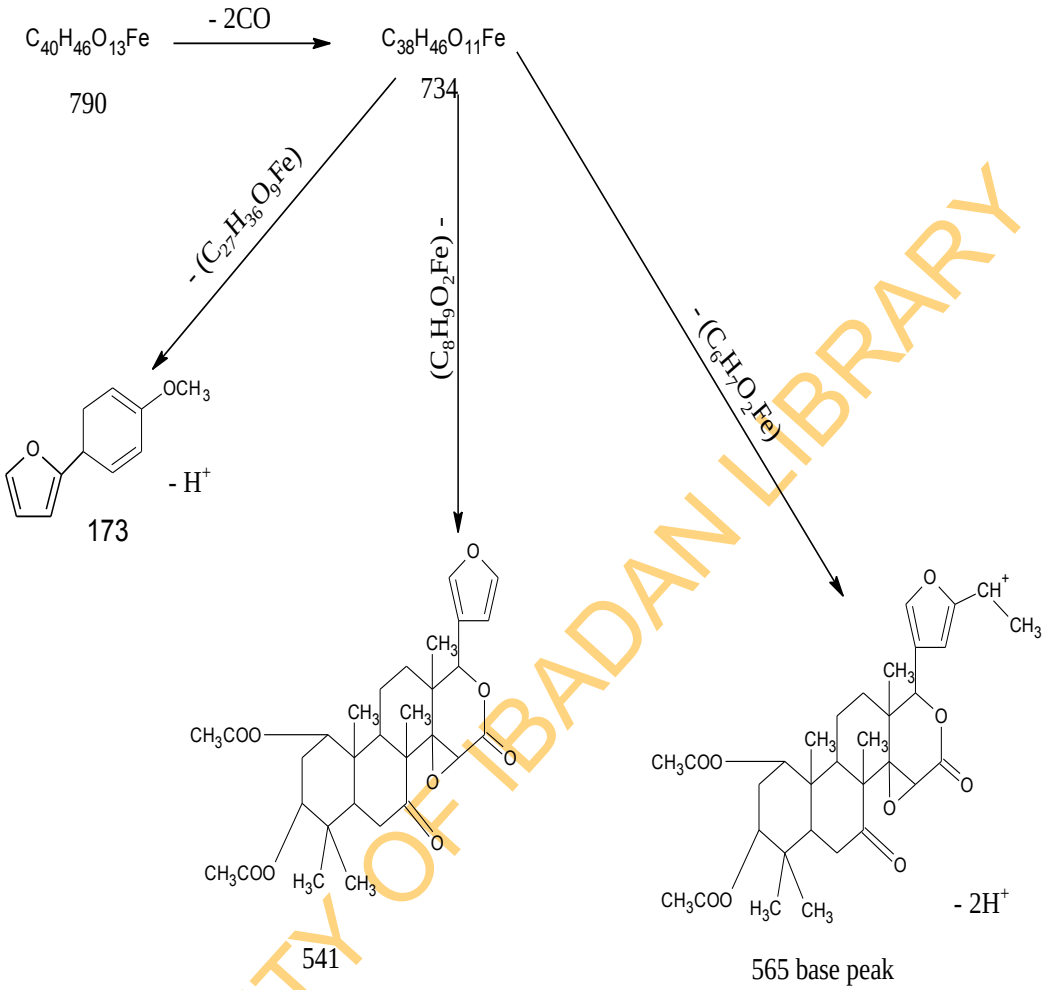

Appendix 8: Fragmentation Pattern of 5-exo-(gedunino) cyclohexa-1,3-diene iron (26)

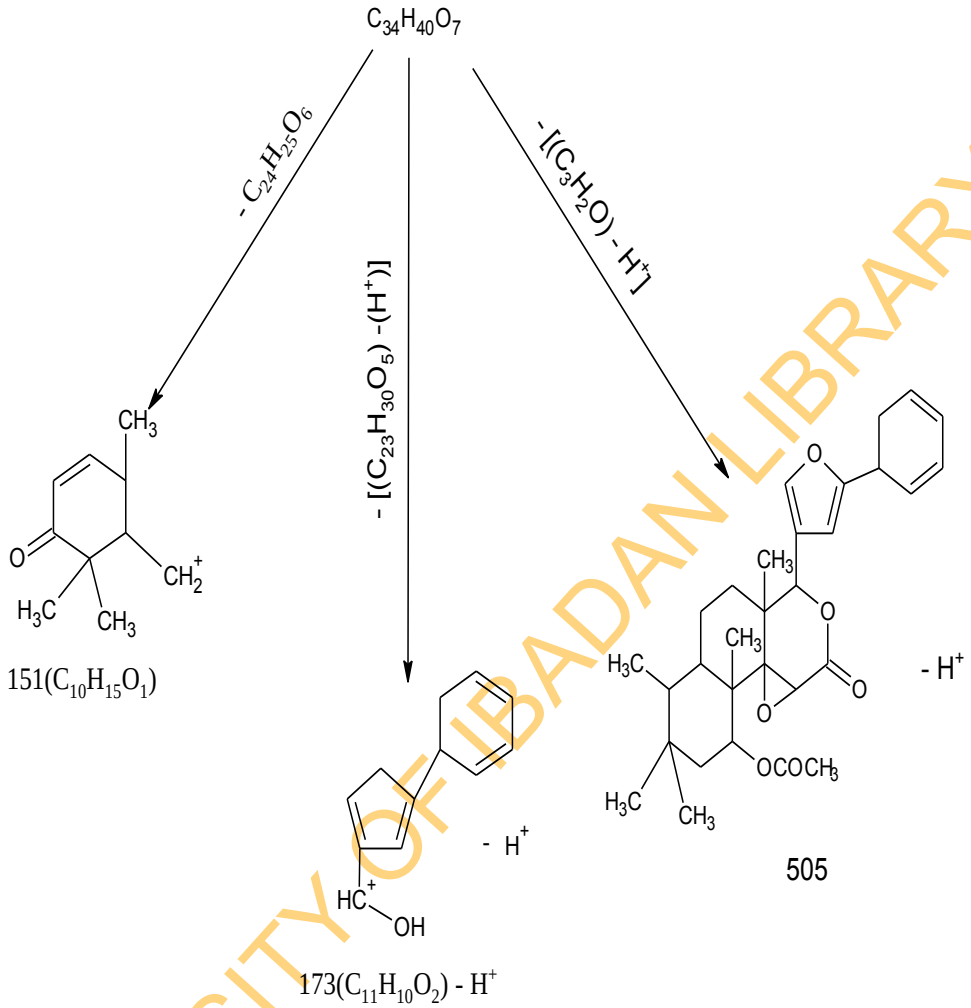

Appendix 9: Fragmentation Pattern of 5-exo-(khivorino) cyclohexa-1,3-diene iron (27)

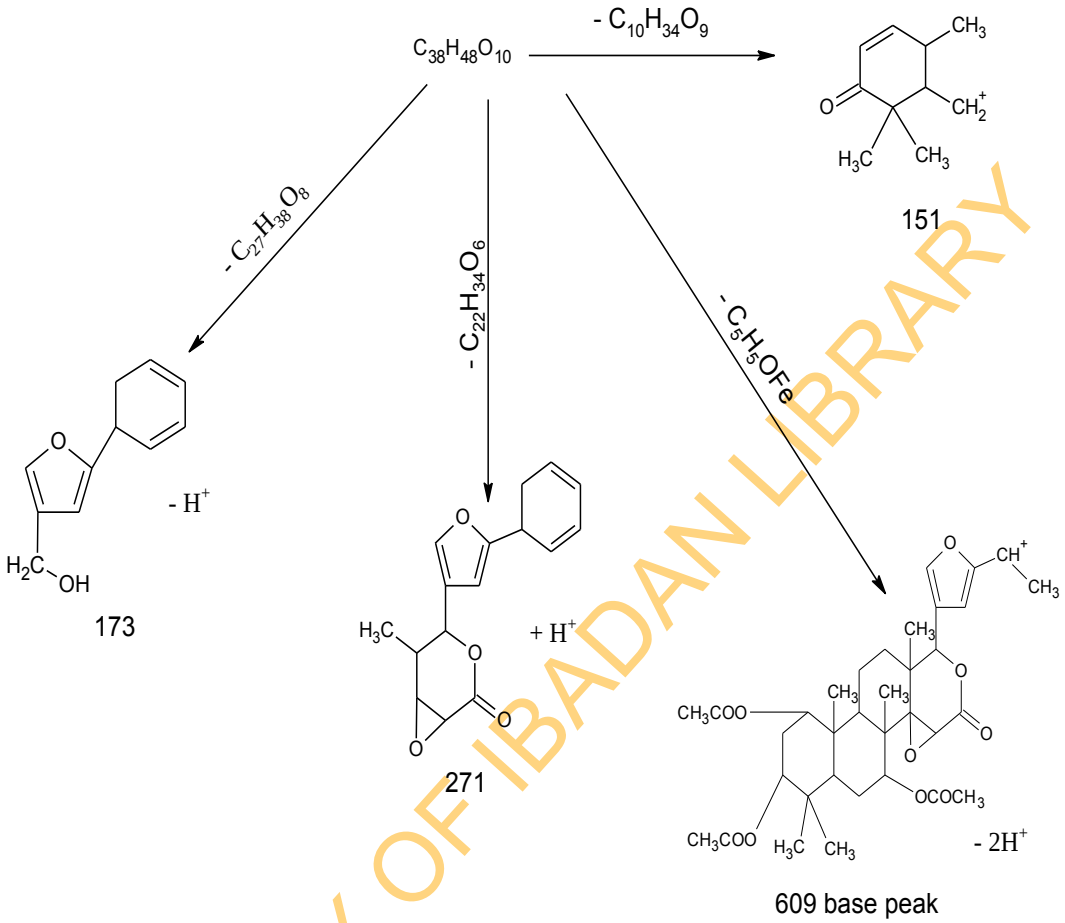

Appendix 10: Fragmentation Pattern of 5-exo-(7-ketokhivorino) cyclohexa-1,3-diene iron (28)

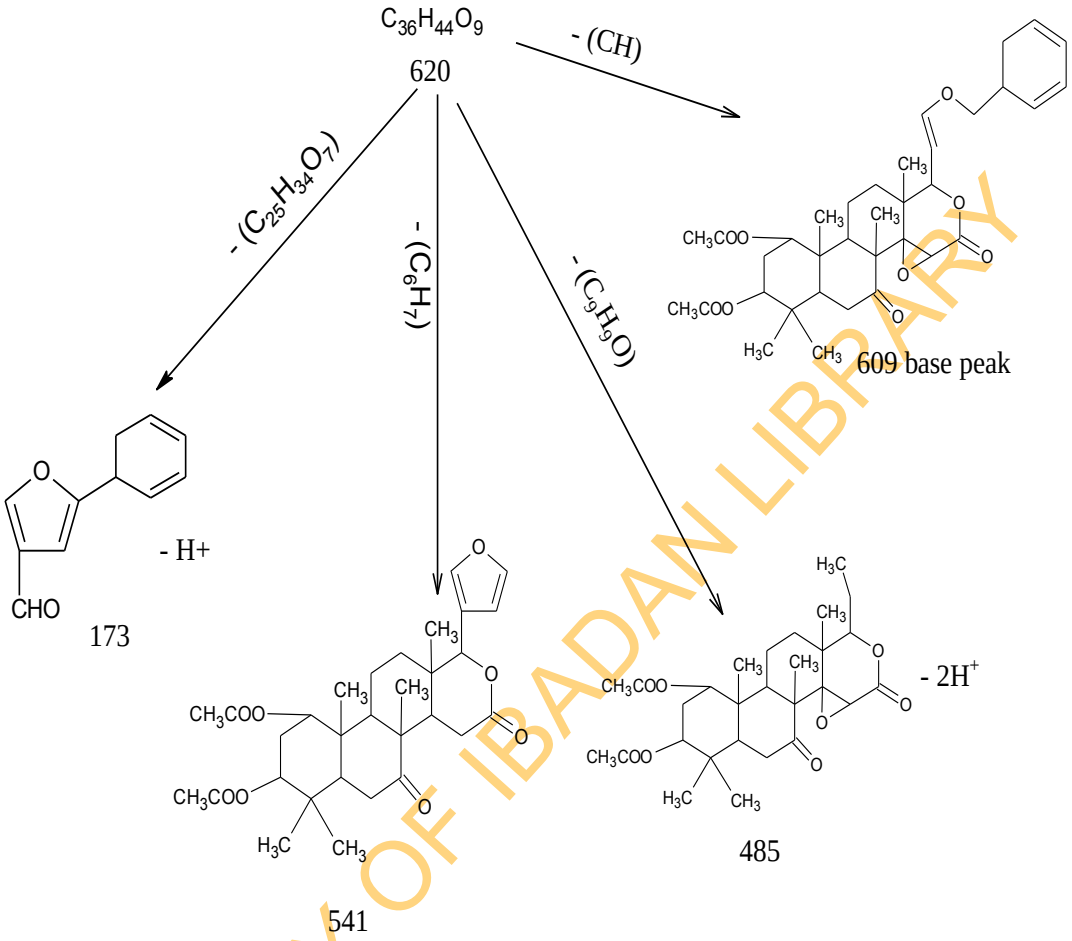

Appendix 11: Fragmentation Pattern of 2-methoxy-5-exo-(gedunino) cyclohexa-1,3-diene (26)

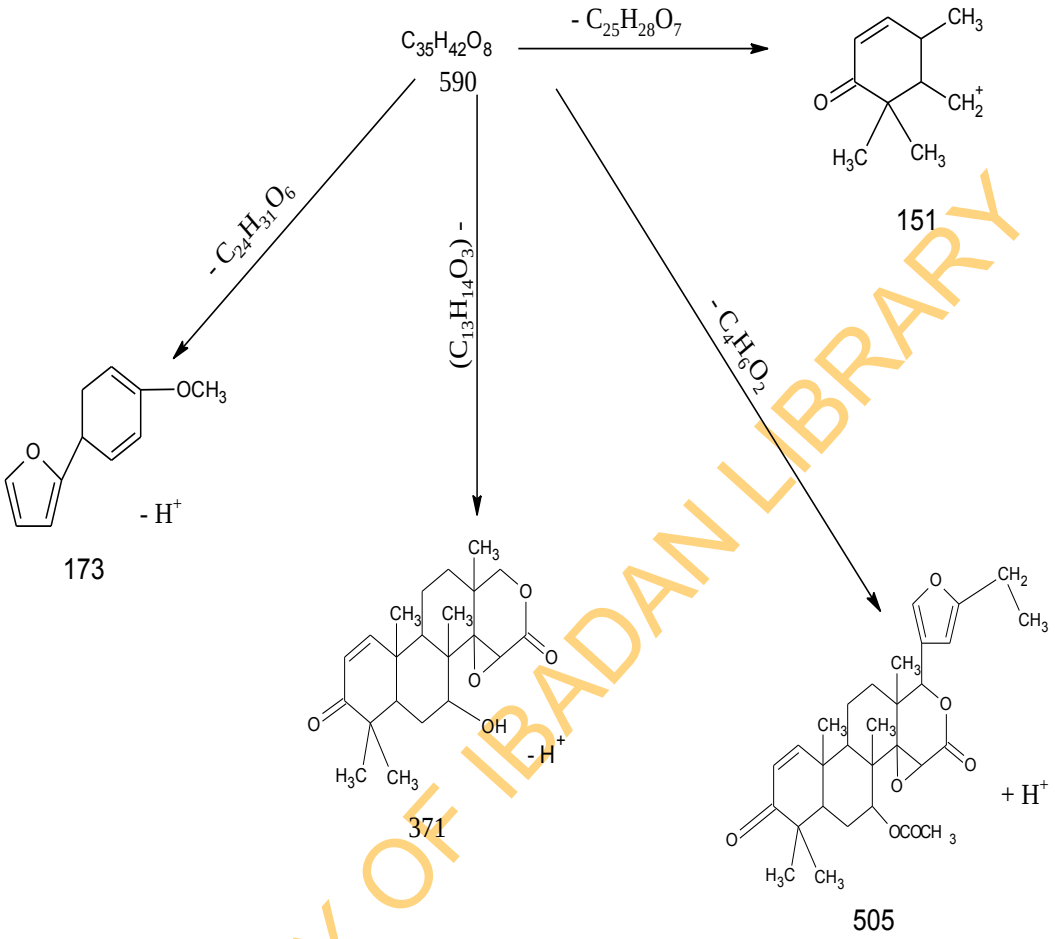

Appendix 12: Fragmentation Pattern of 2-methoxy-5-exo-(khivorino) cyclohexa-1,3-diene (27)

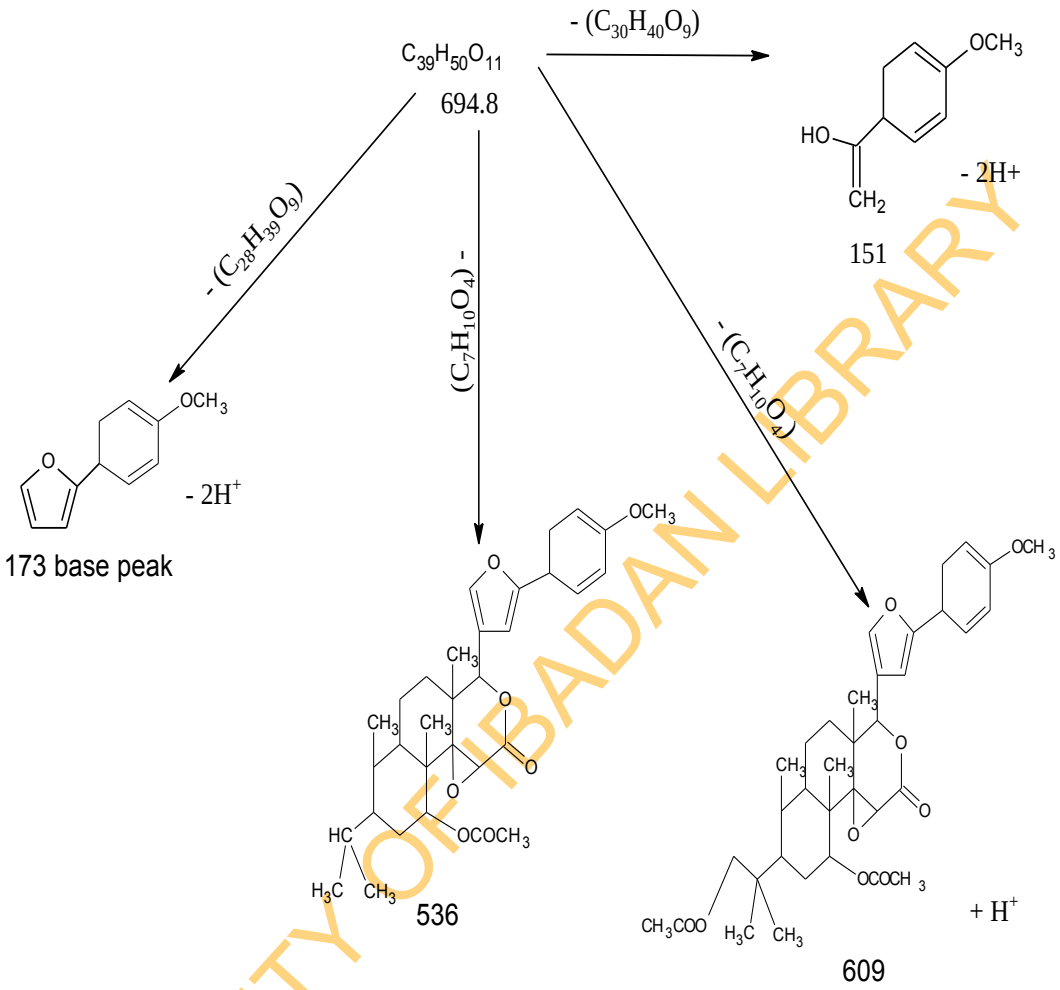

Appendix 13: Fragmentation Pattern of 2-methoxy-5-exo-(7-ketokhivorino) cyclohexa-1,3-diene (28)

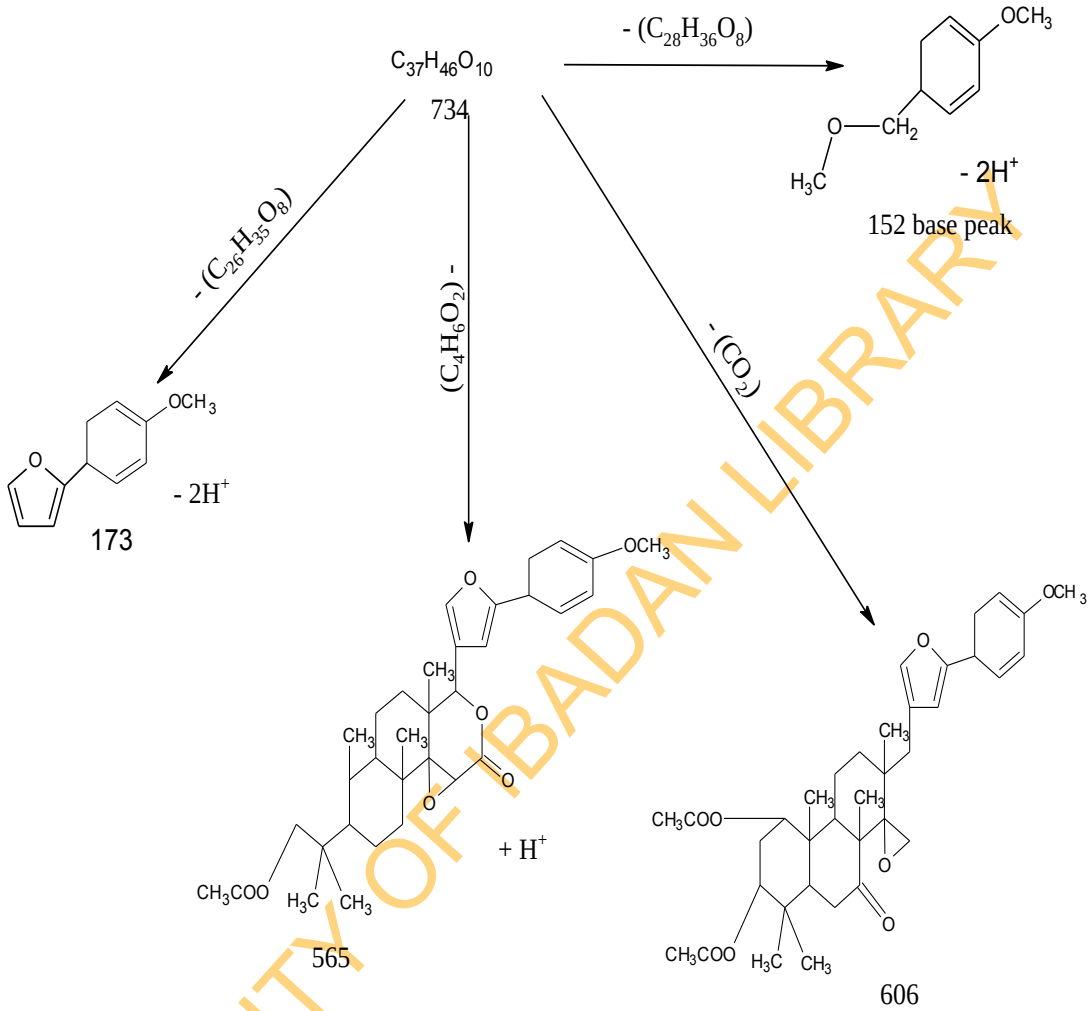

Appendix 14: Computational graphic model of gedunin ligand

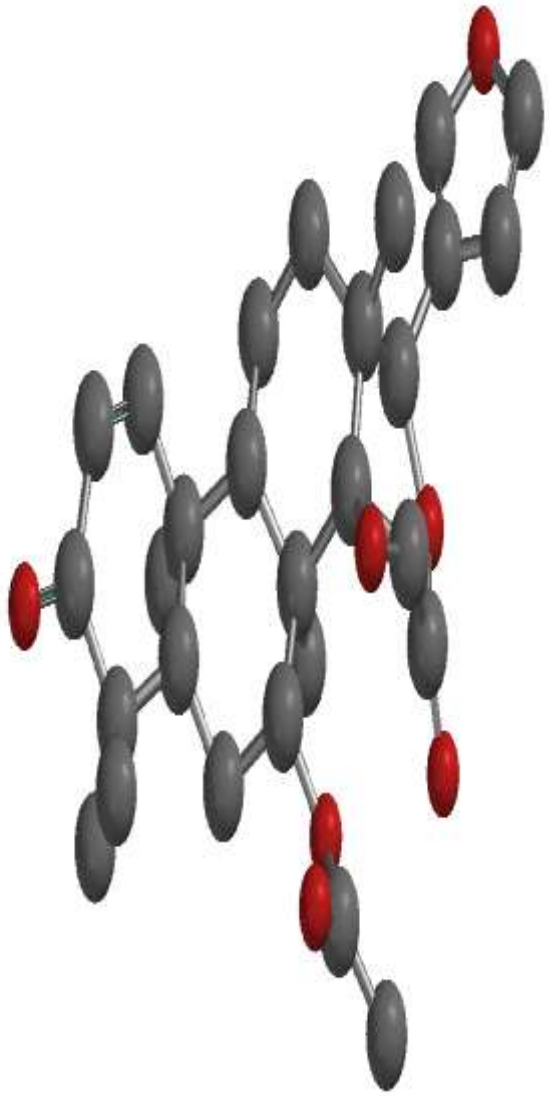

Appendix 15: Computational graphic model of gedunin ligand showing HOMO

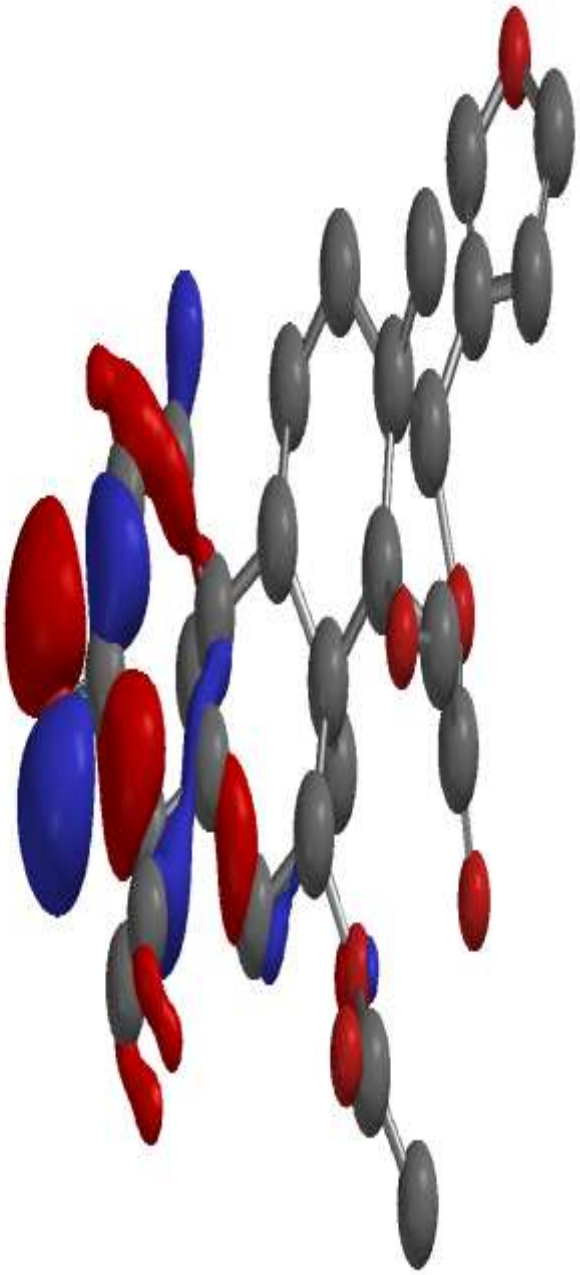

Appendix 16: Computational graphic model of gedunin ligand showing LUMO

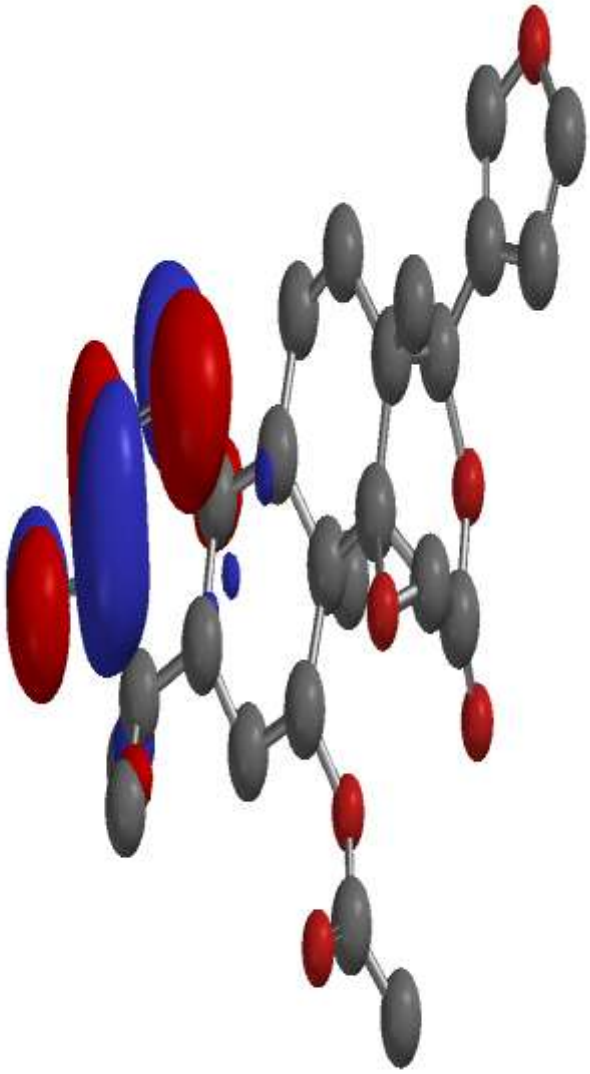

Appendix 17: Computational graphic model of gedunin adduct (tricarbonyl [1-4-η-5-(gedunino) cyclohexa-1,3-diene]iron (19)

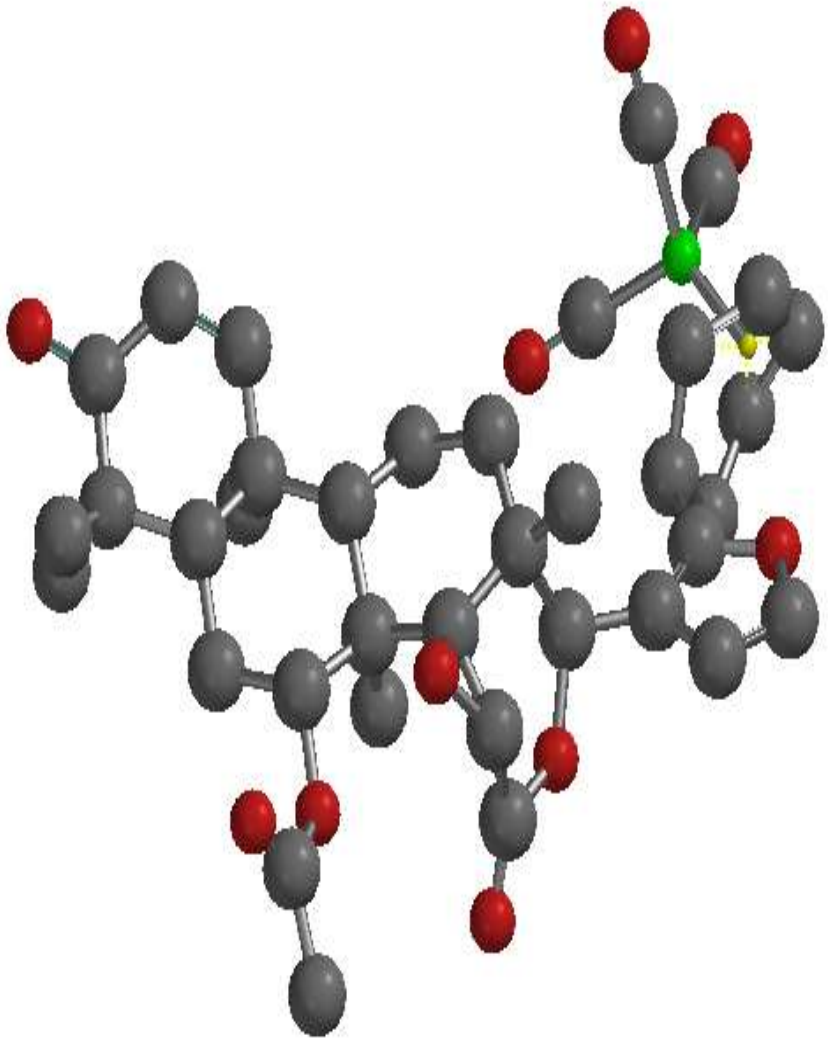

Appendix 18: Computational graphic model of demetallated gedunin (5-exo-(gedunino) cyclohexa-1,3-diene) (26)

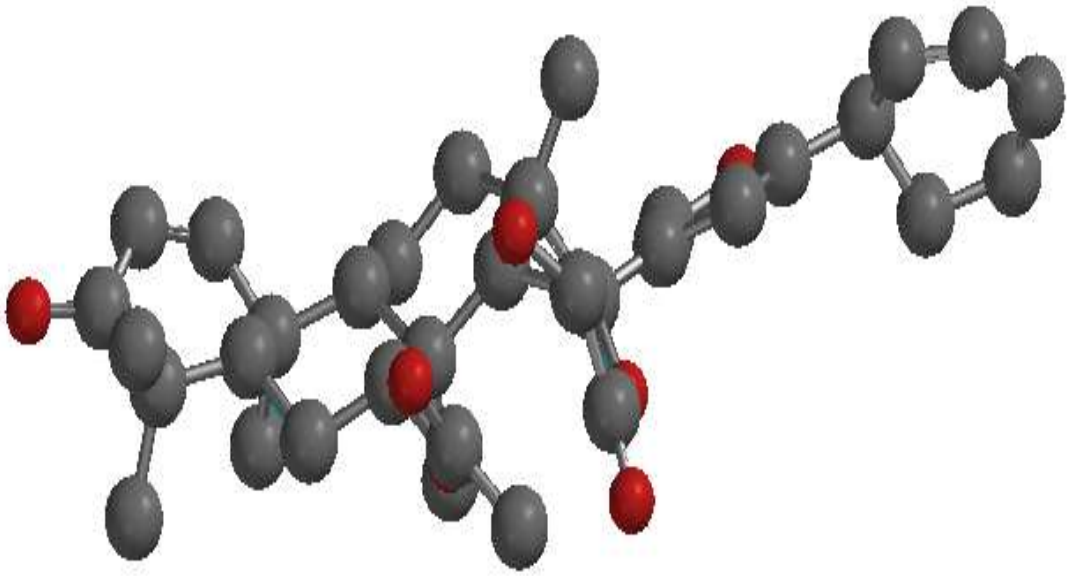

Appendix 19: Computational graphic model of demetallated gedunin (5-exo-(gedunino) cyclohexa-1,3-diene) (26) **showing HOMO**

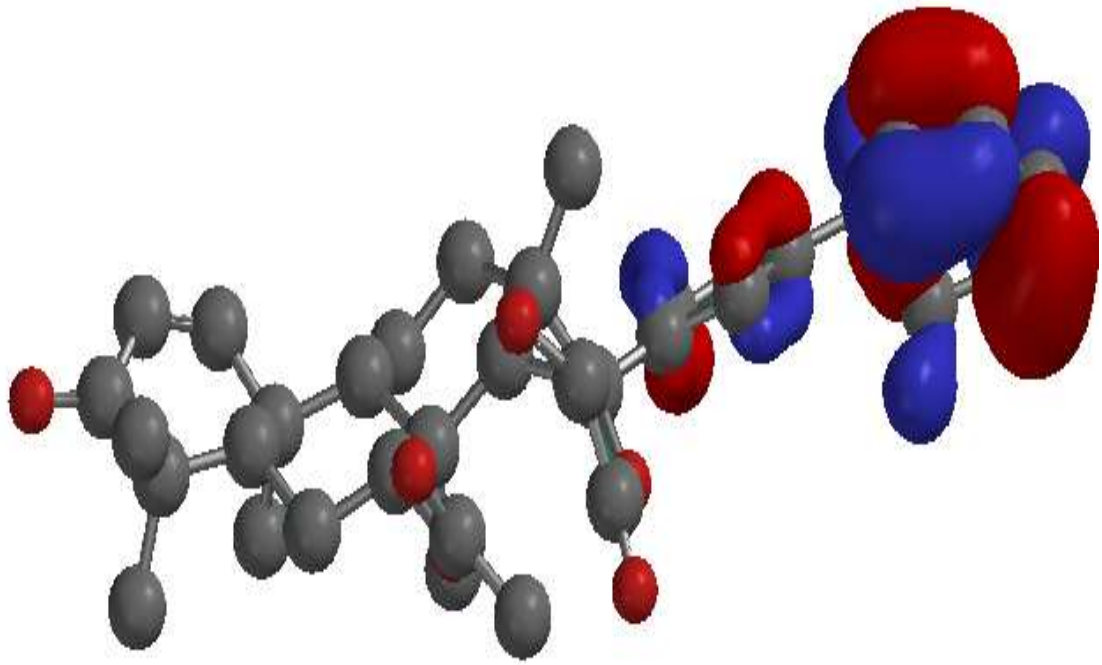

Appendix 20: Computational graphic model of demetallated gedunin (5-exo-(gedunino) cyclohexa-1,3-diene) (26) **showing LUMO**

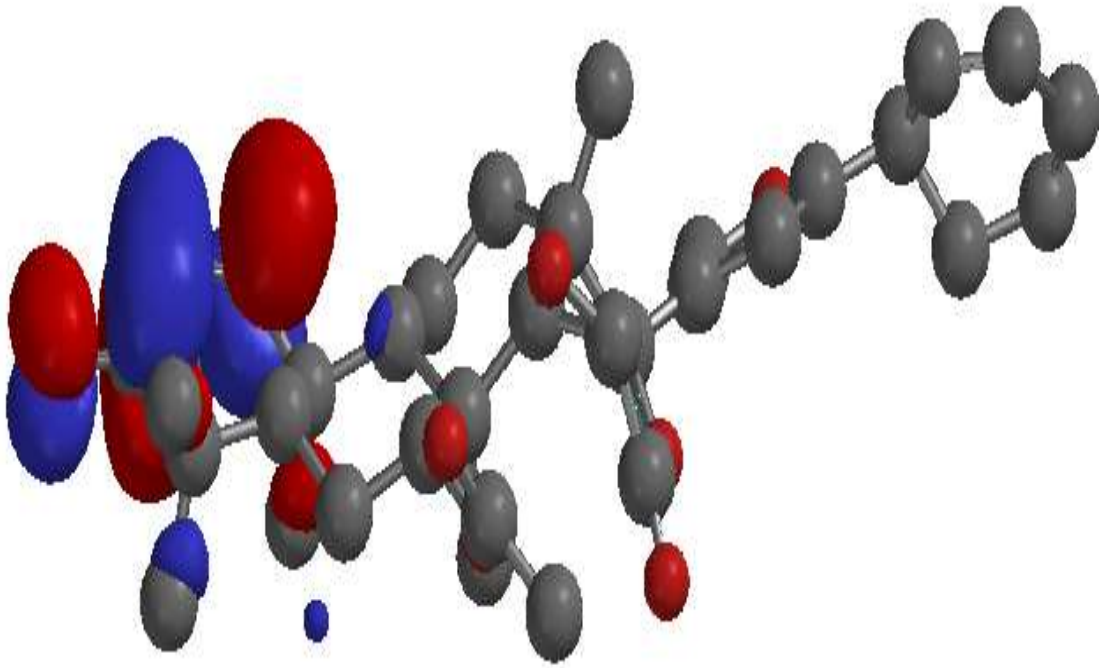

Appendix 21: Computational graphic model of khivorin ligand

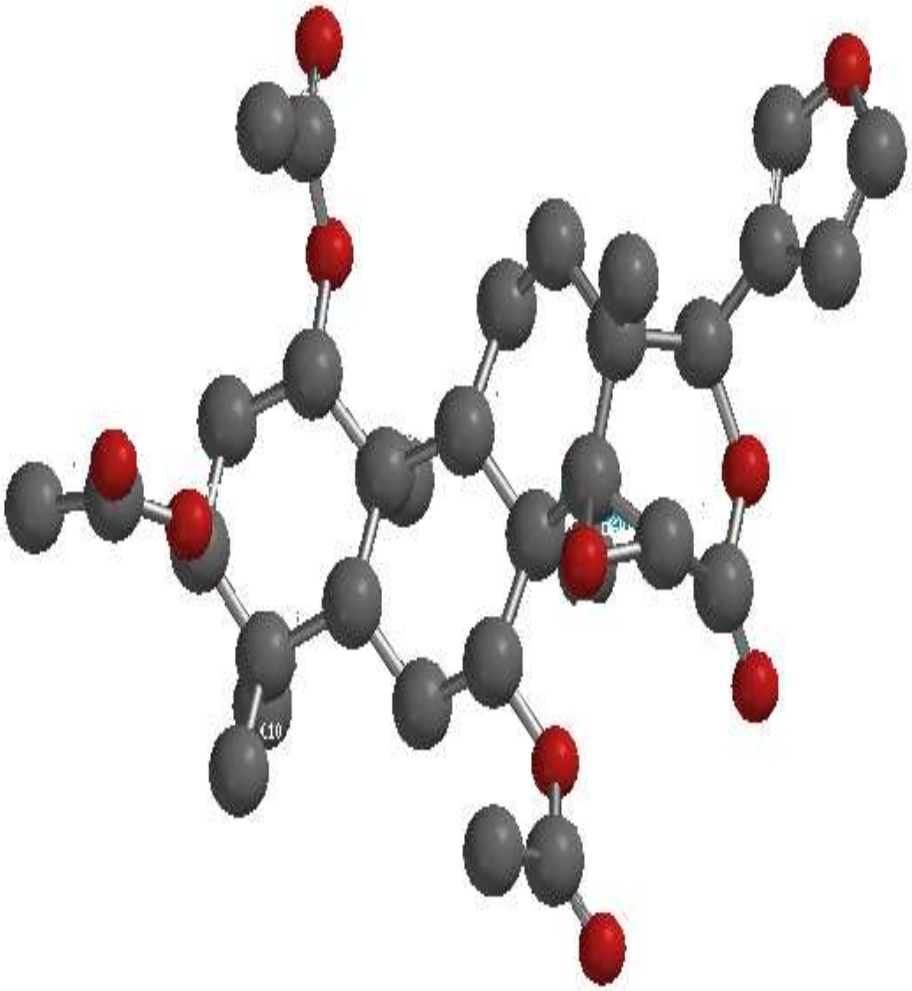

Appendix 22: Computational graphic model of khivorin ligand showing HOMO

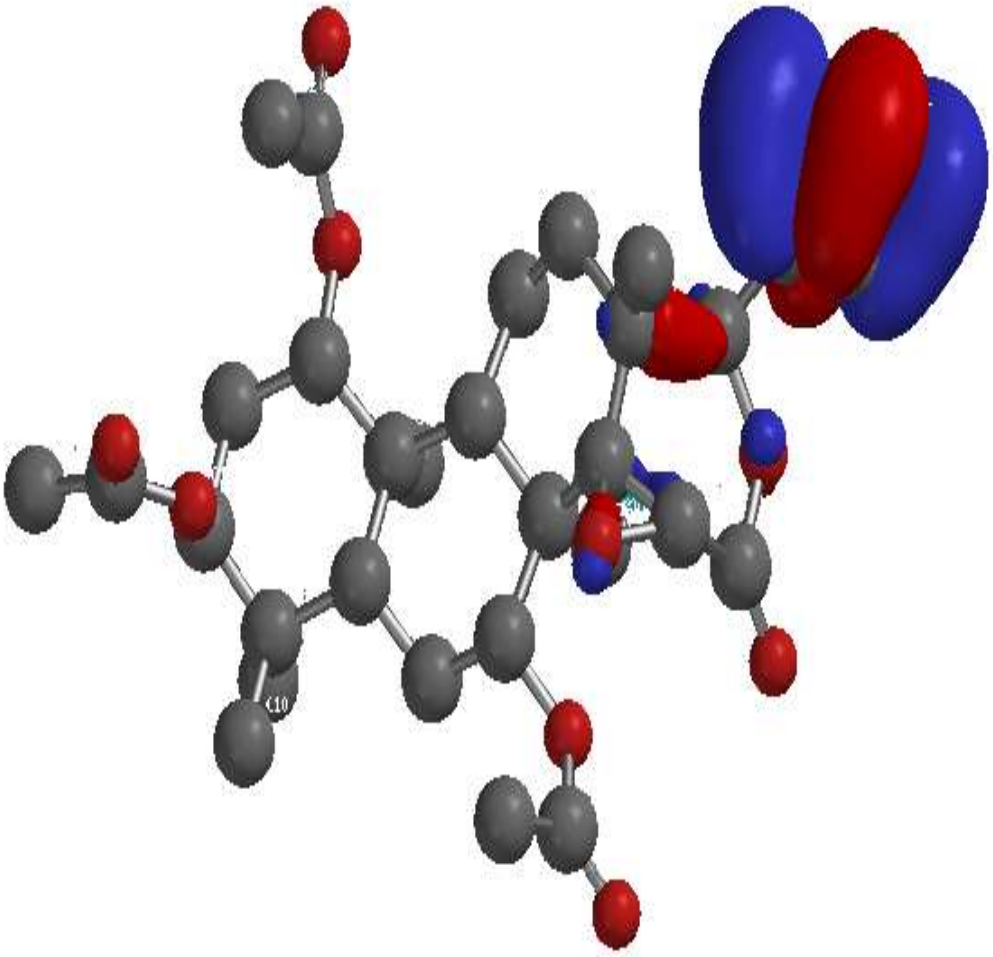

Appendix 23: Computational graphic model of khivorin ligand showing LUMO

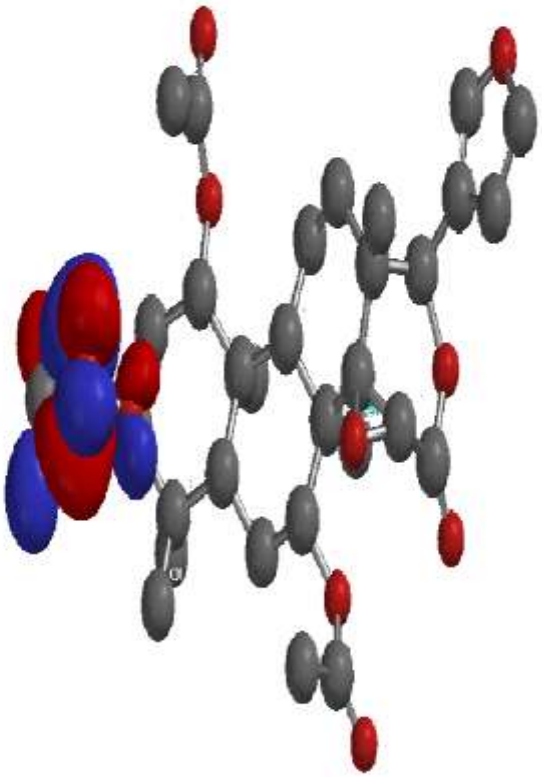

Appendix 24: Computational graphic model of khivorin adduct (tricarbonyl [1-4-η-5-(khivorino)cyclohexa-1,3-diene] iron (20)

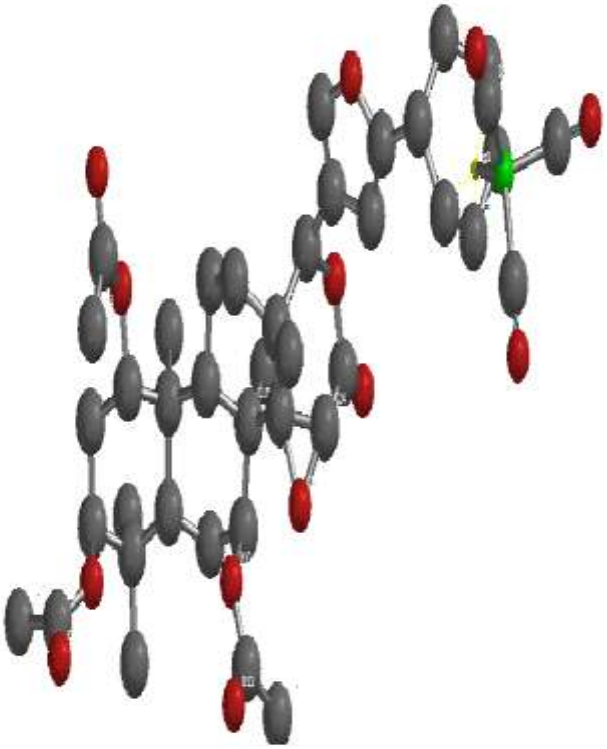

Appendix 25: Computational graphic model of khivorin adduct (tricarbonyl [1-4-η-5-(khivorino)cyclohexa-1,3-diene] iron (20) **showing HOMO**

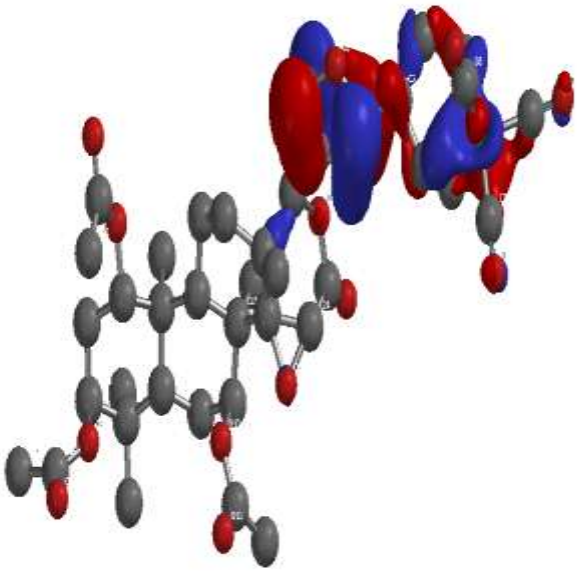

Appendix 26: Computational graphic model of khivorin adduct (tricarbonyl [1-4-η-5-(khivorino)cyclohexa-1,3-diene] iron (20) **showing LUMO**

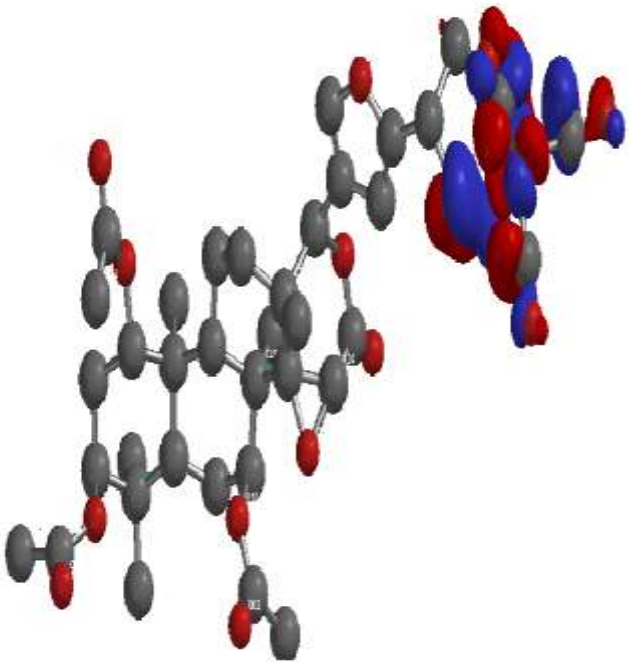

Appendix 27: Computational graphic model of demetallated khivorin (5-exo-(khivorino) cyclohexa-1,3-diene) (27)

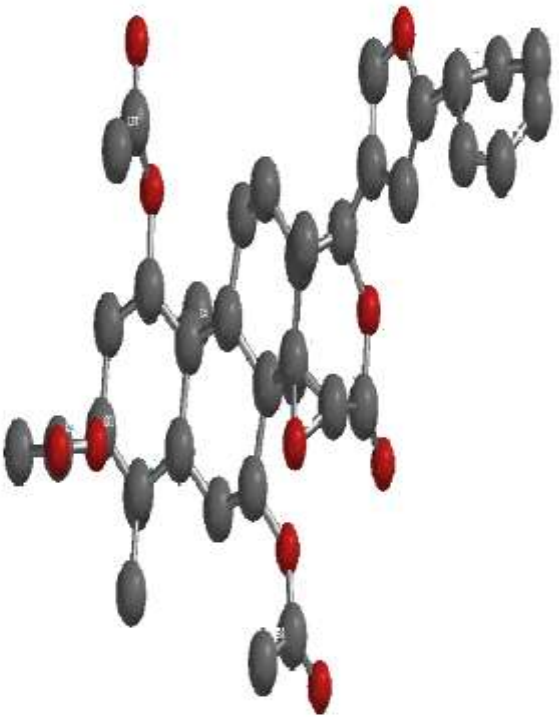

Appendix 28: Computational graphic model of demetallated khivorin (5-exo-(khivorino) cyclohexa-1,3-diene) (27) **showing HOMO**

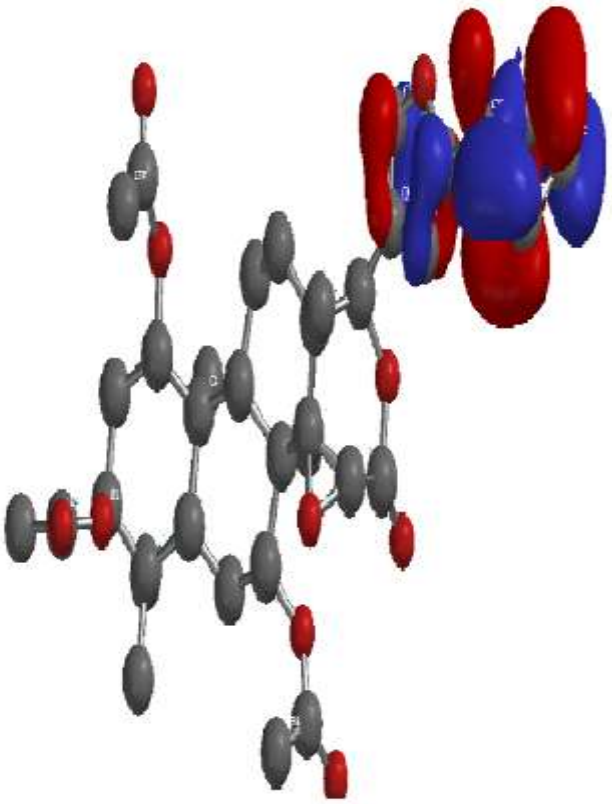

Appendix 29: Computational graphic model of demetallated khivorin (5-exo-(khivorino) cyclohexa-1,3-diene) (27) **showing LUMO**

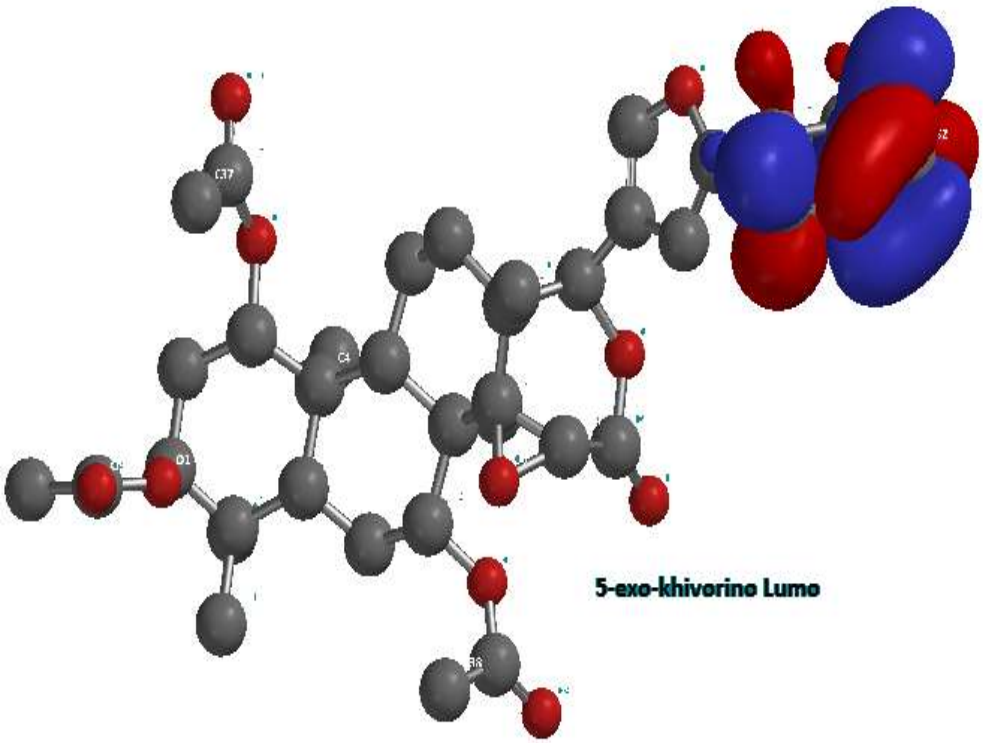

Appendix 30: Computational graphic model of polyavolensinol ligand

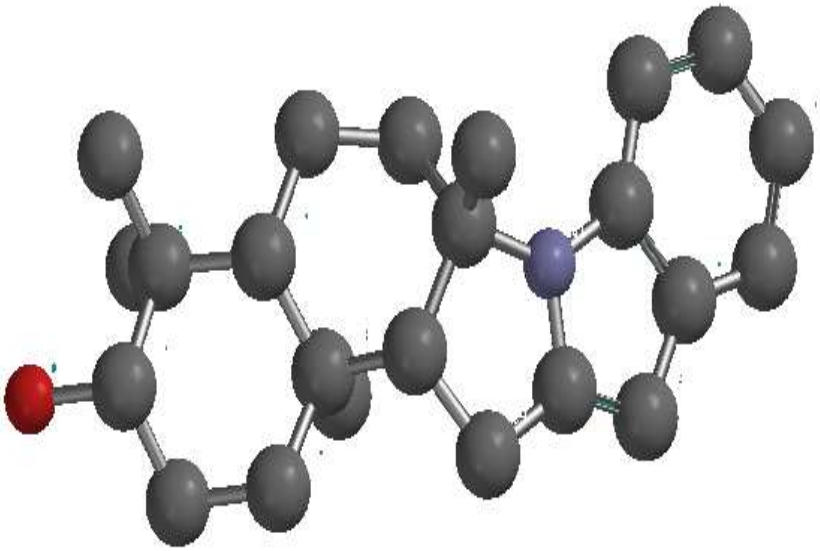

Appendix 31: Computational graphic model of polyavolensinol ligand showing HOMO

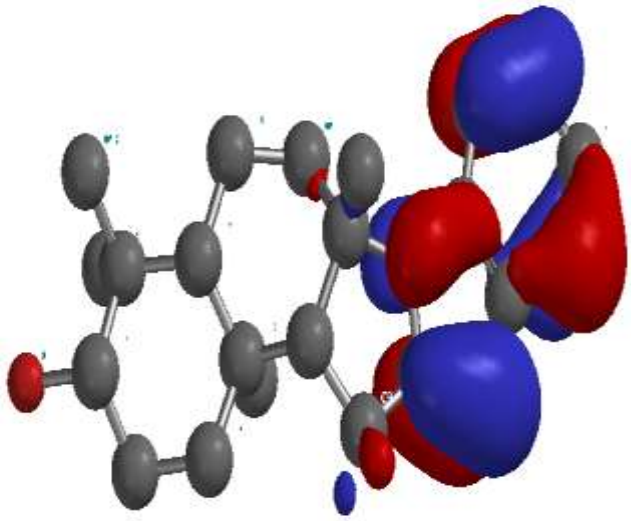

Appendix 32: Computational graphic model of polyavolensinol ligand showing LUMO

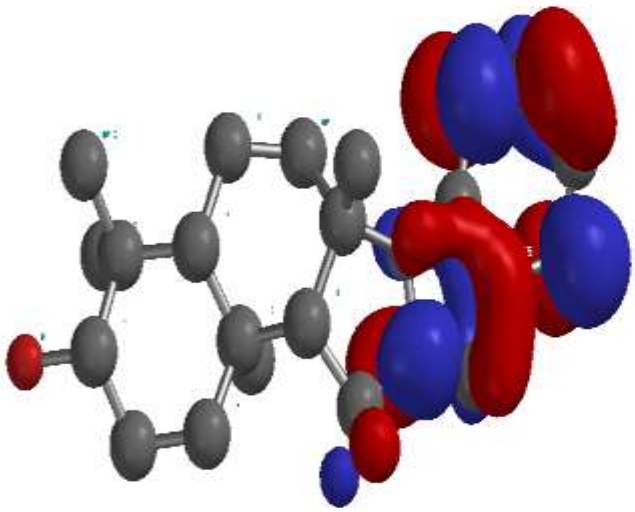

Appendix 33: Computational graphic model of polyavolensinol adduct (tricarbonyl[1,4-η-5-(polyavolensinolino) cyclohexa-1,3-diene] iron (22)

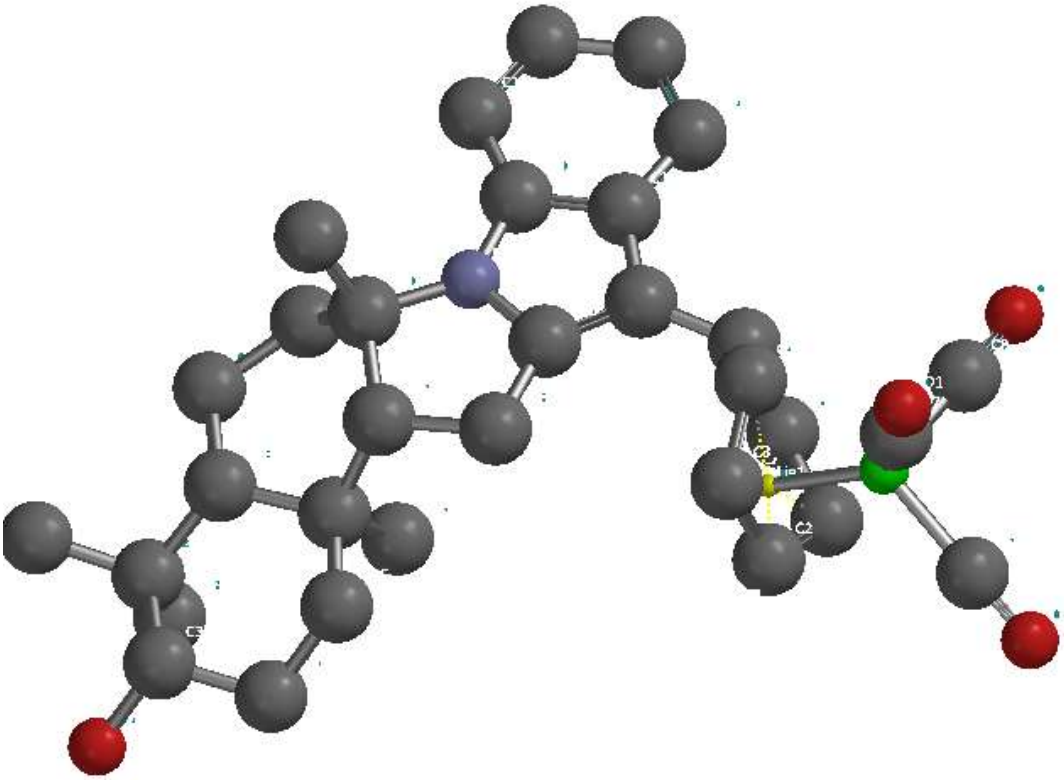

Appendix 34: Computational graphic model of polyavolensinol adduct (tricarbonyl [1,4-η-5-(polyavolensinolino) cyclohexa-1,3-diene] iron (22) **showing HOMO**

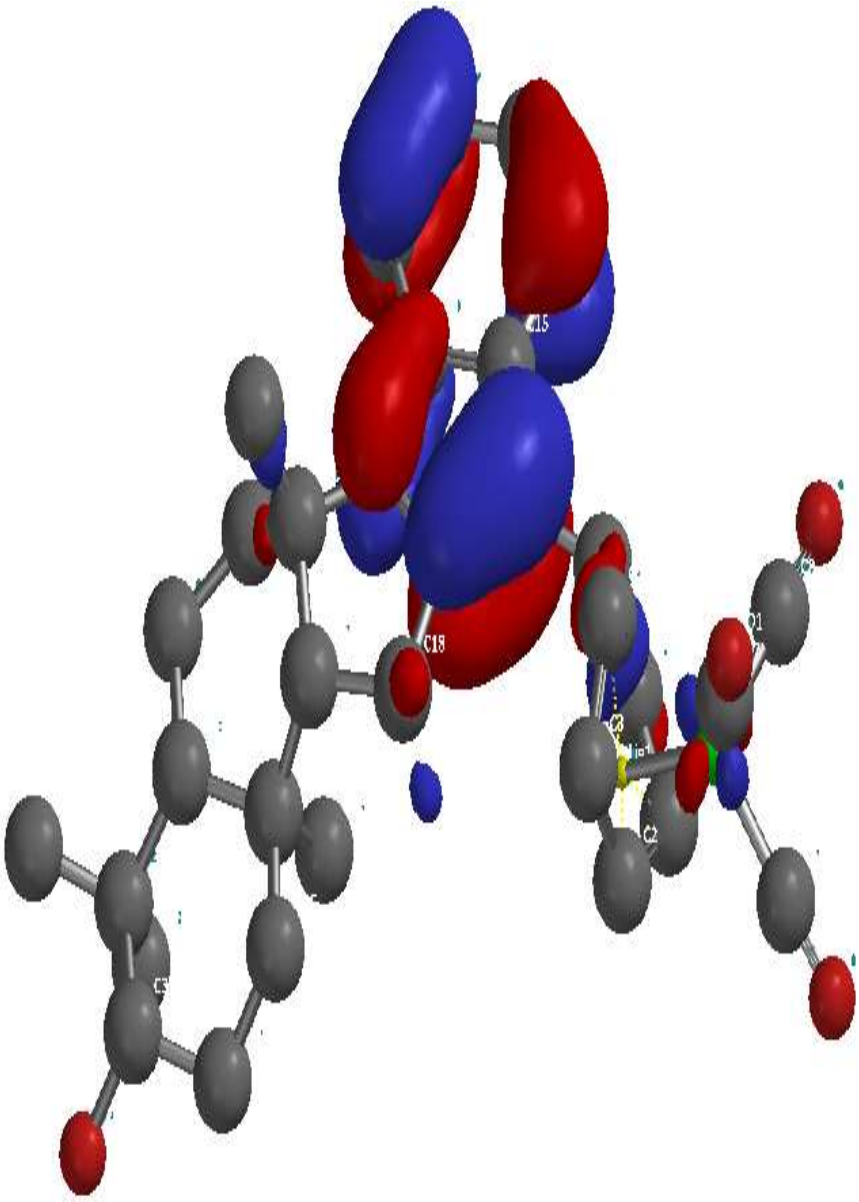

Appendix 35: Computational graphic model of polyavolensinol adduct tricarbonyl [1,4-η-5-(polyavolensinolino) cyclohexa-1,3-diene] iron (22) **showing LUMO**

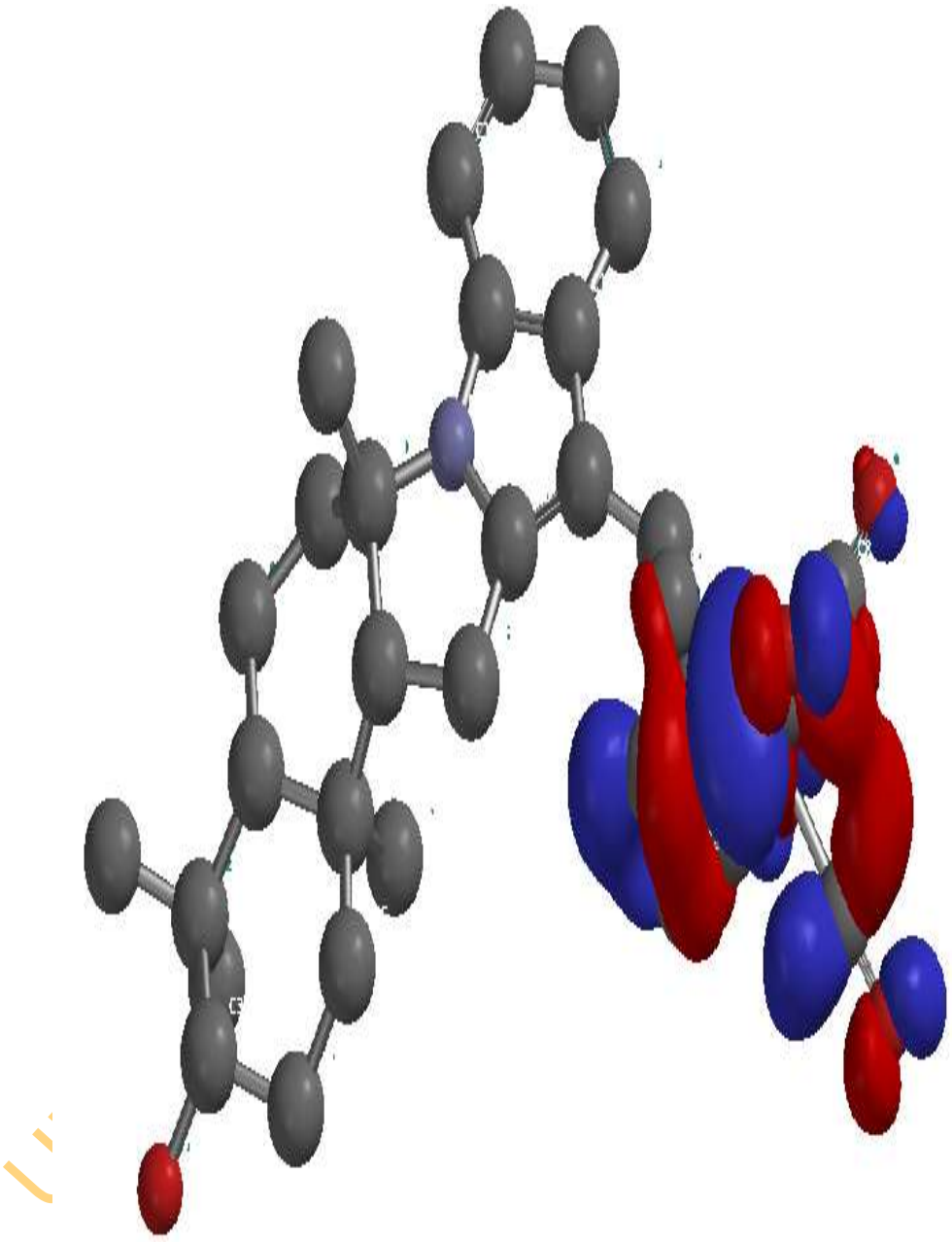

Appendix 36: Computational graphic model of demetallated polyavolensinol (5-exo-(polyavolensinolino) cyclohexa-1,3-diene) (29)

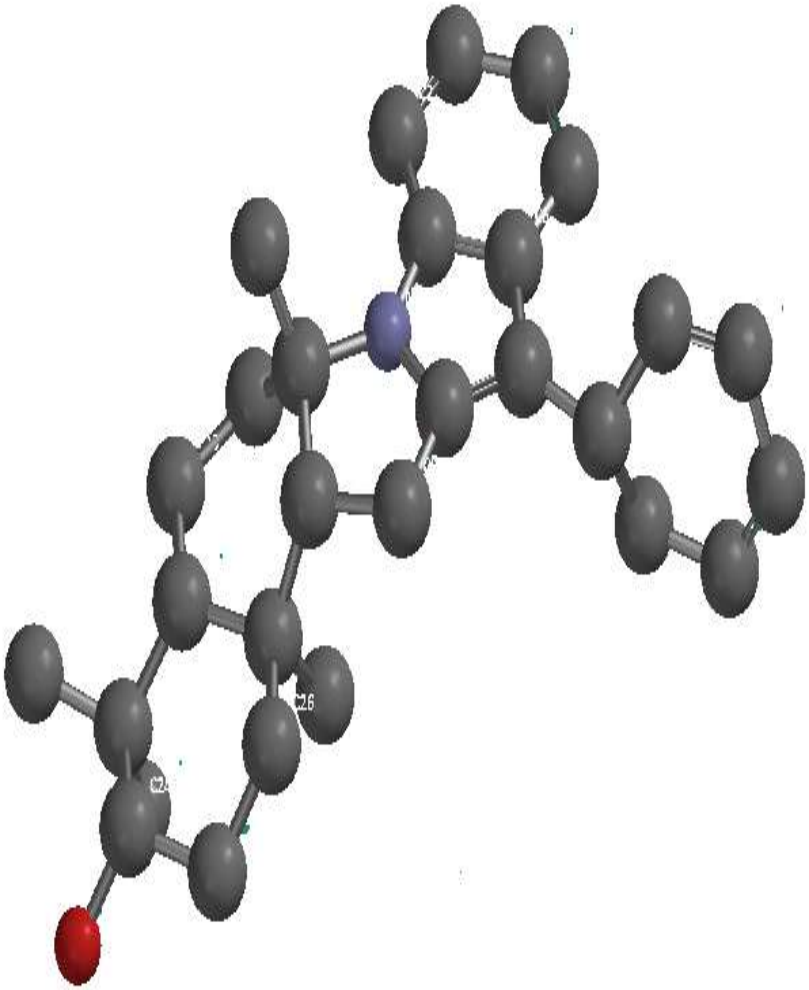

Appendix 37: Computational model of demetallated polyavolensinol (5-exo-(polyavolensinolino) cyclohexa-1,3-diene) (29) **showing HOMO**

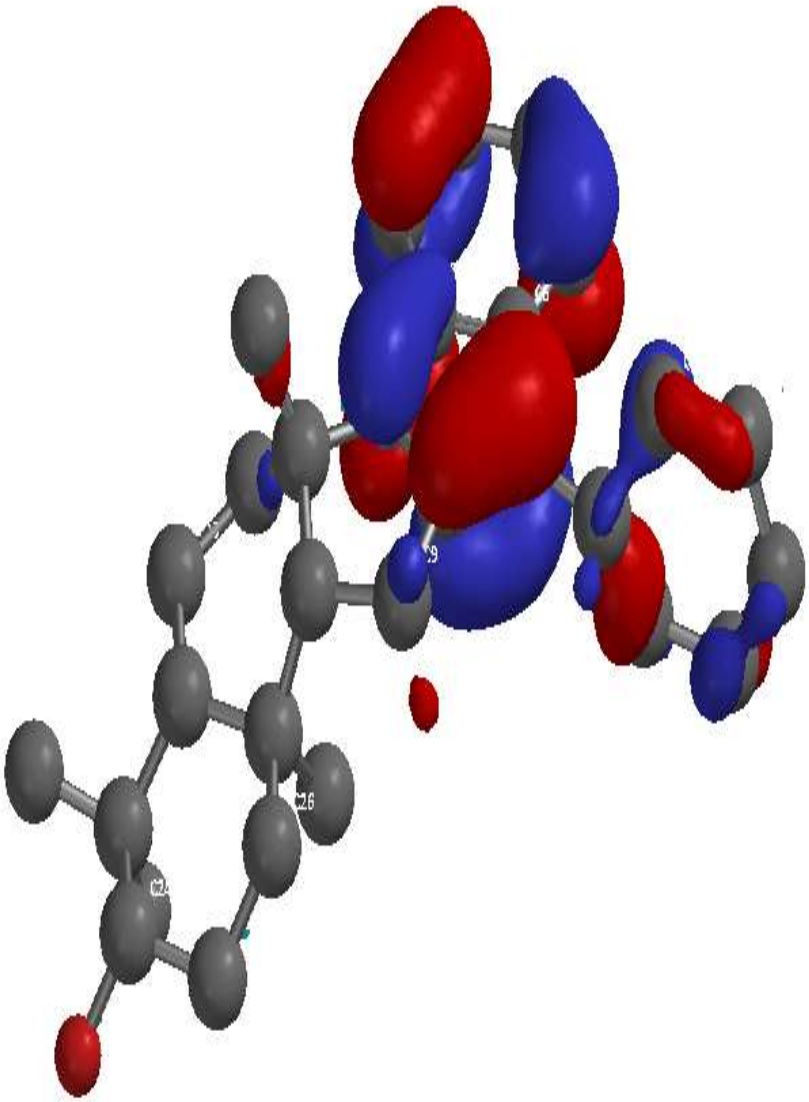

Appendix 38: Computational graphic model of demetallated polyavolensinol (5-exo-(polyavolensinolino) cyclohexa-1,3-diene) (29) **showing LUMO**

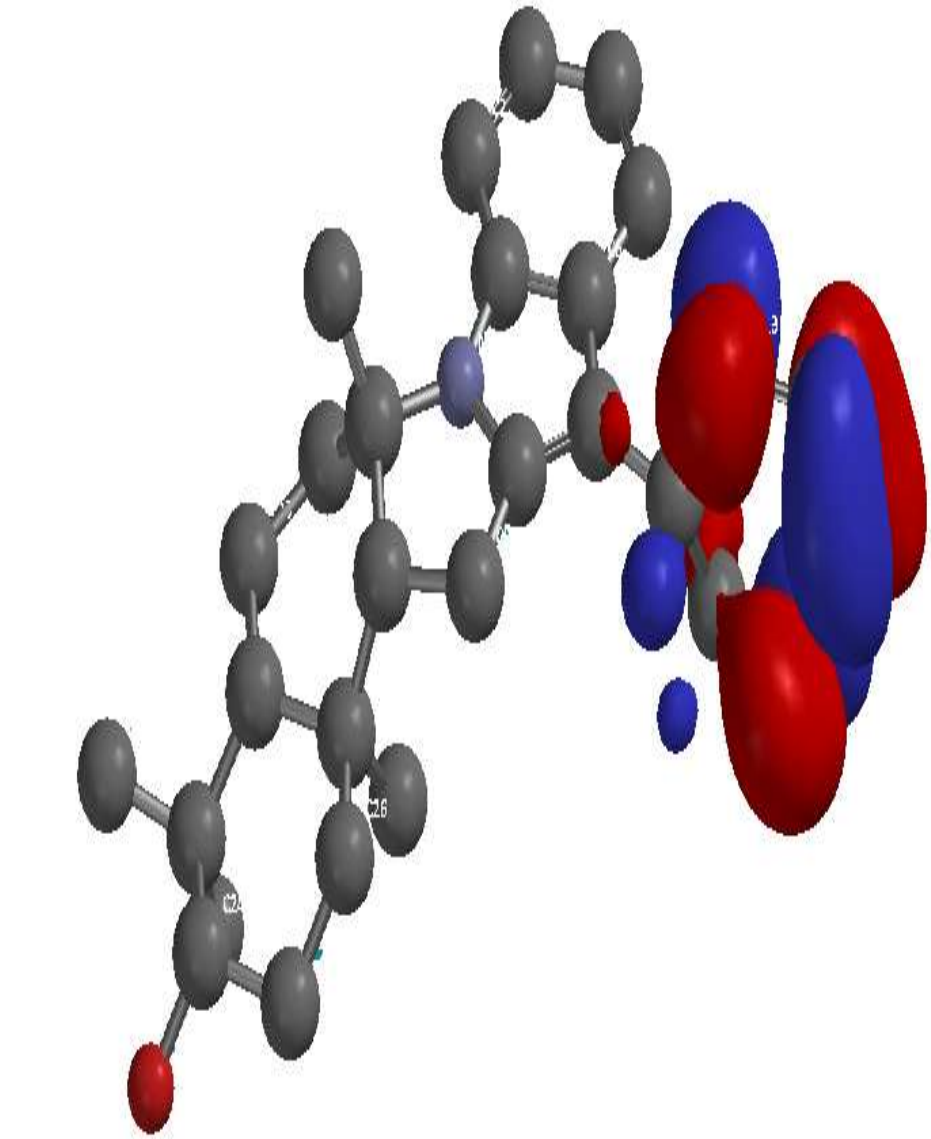

Appendix 39: Computational graphic model of 7-ketokhivorin ligand

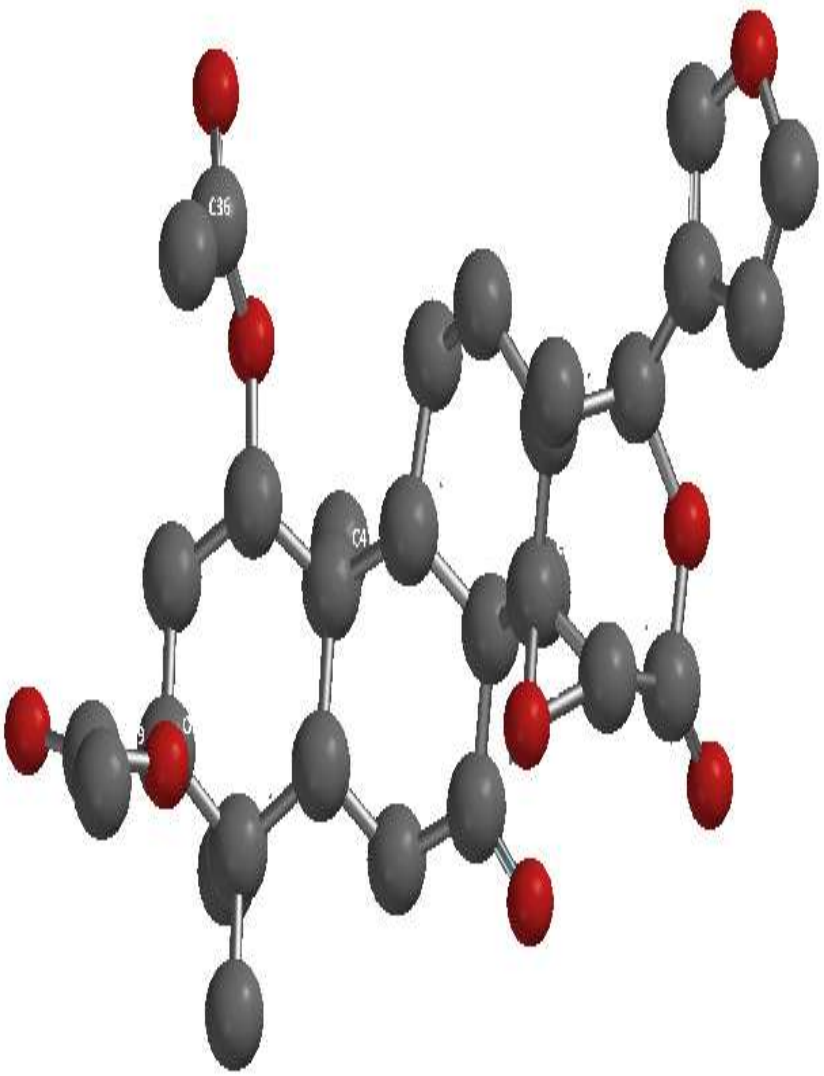

Appendix 40: Computational graphic model of 7-ketokhivorin ligand showing HOMO

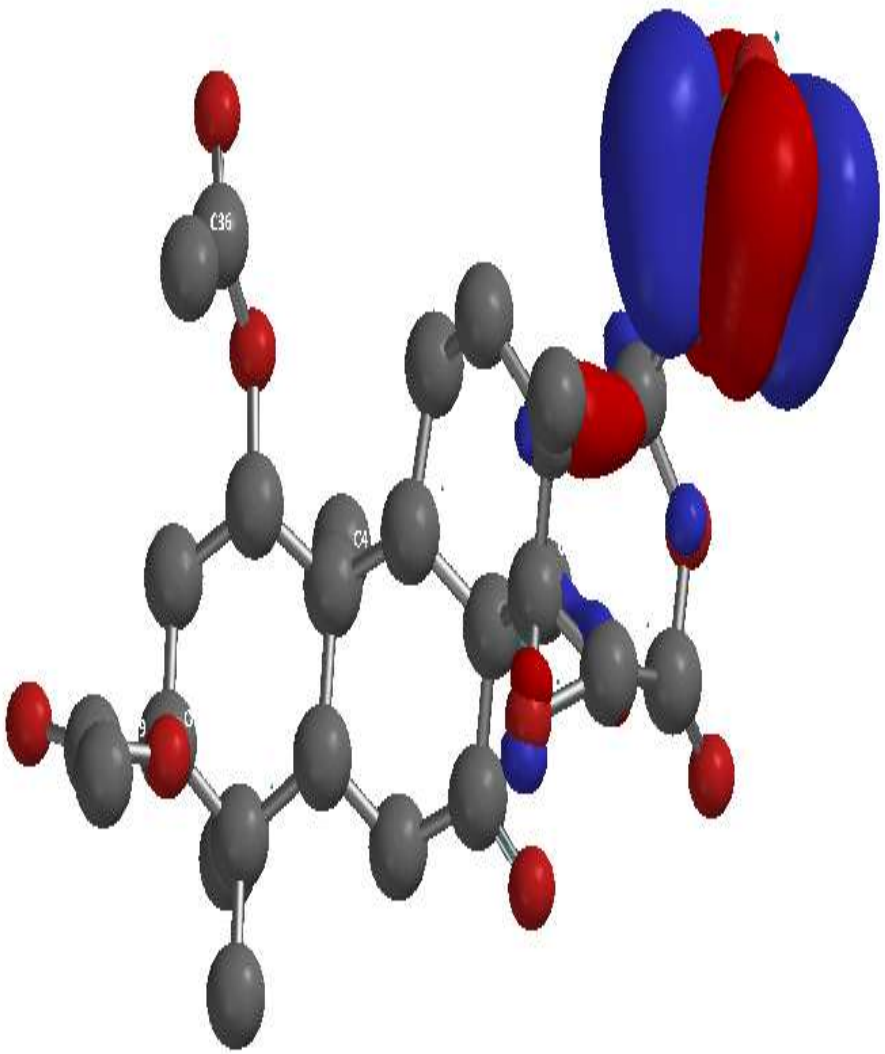

Appendix 41: Computational graphic model of 7-ketokhivorin ligand showing LUMO

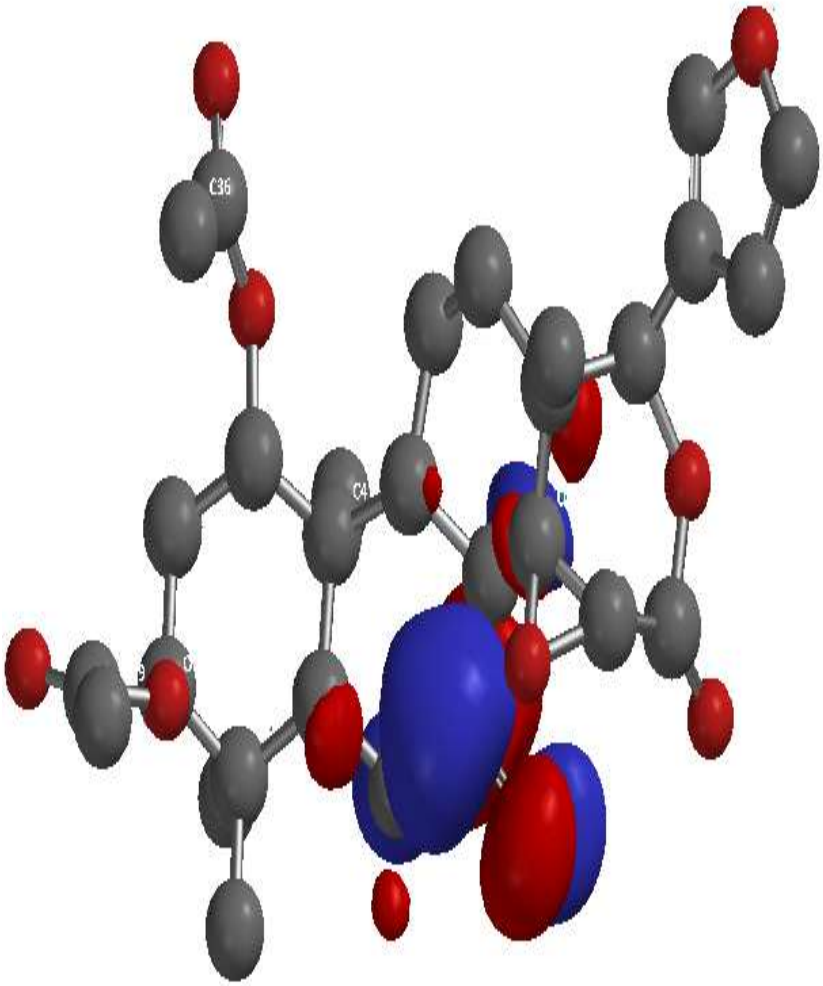

Appendix 42: Computational graphic model showing 7-ketokhivorin adduct (tricarbonyl[1-4-η-5-(7-ketokhivorin) cyclohexa-1,3-diene]) iron (21)

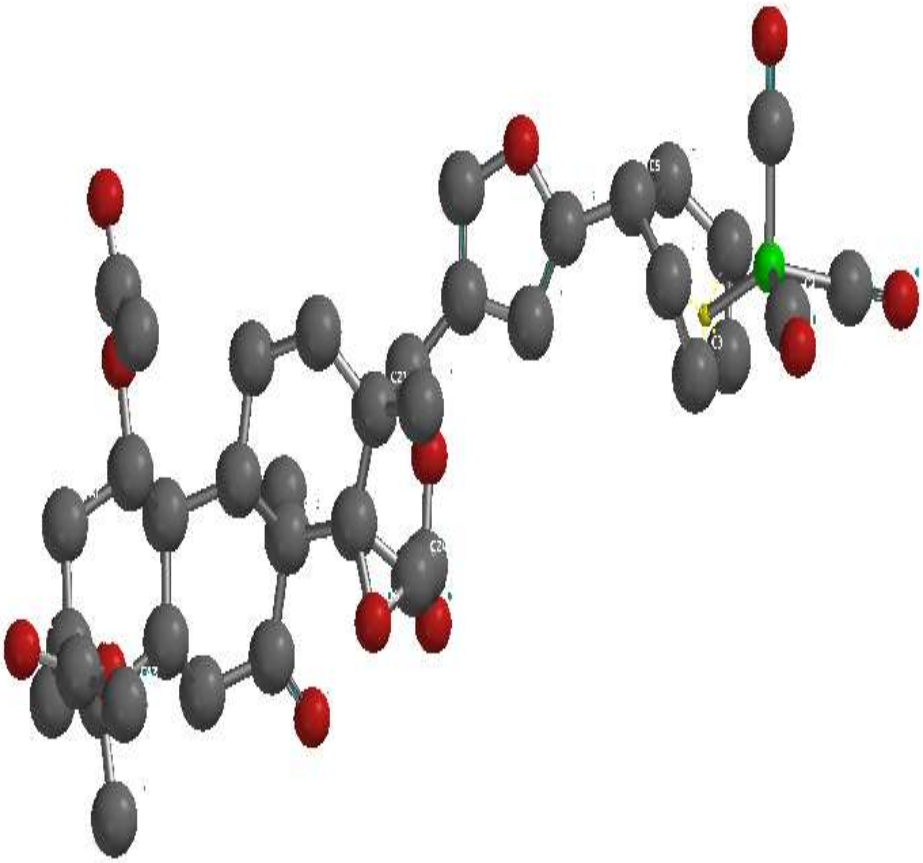

Appendix 43: Computational graphic model of 7-ketokhivorin adduct (tricarbonyl[1-4-η-5-(7-ketokhivorin) cyclohexa-1,3-diene]) iron (21) **showing HOMO**

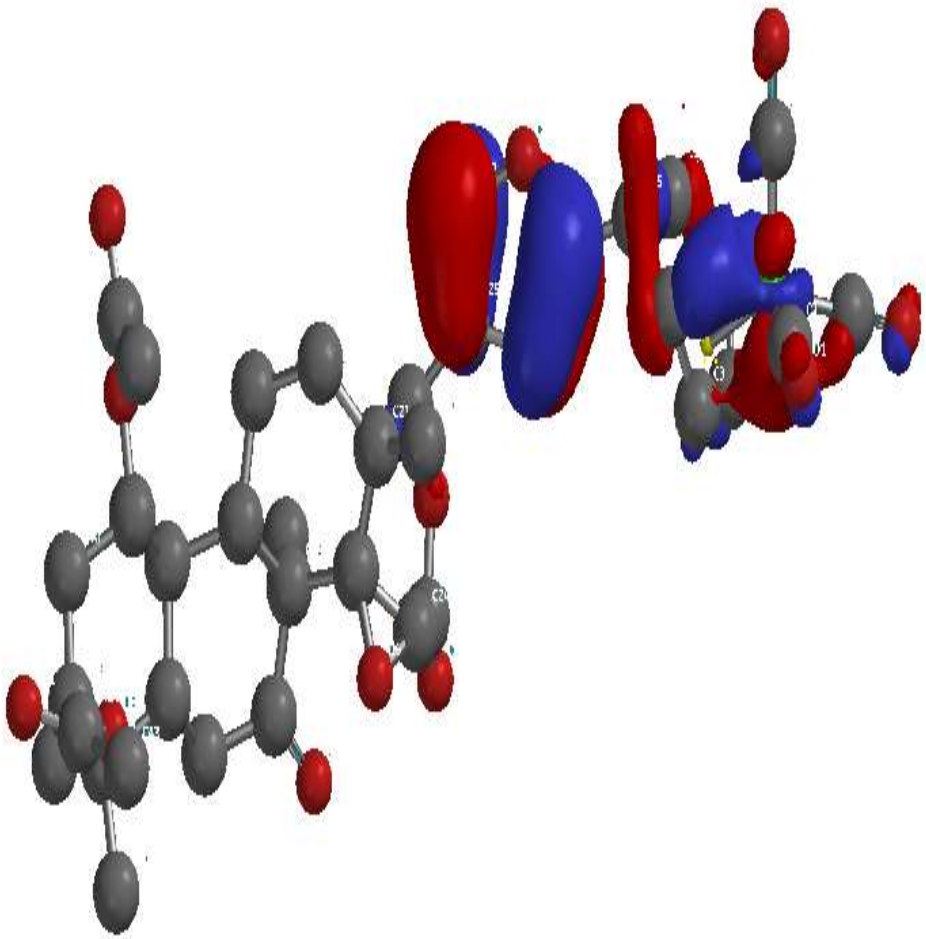

Appendix 44: Computational graphic model of 7-ketokhivorin adduct (tricarbonyl[1-4-η-5-(7-ketokhivorin) cyclohexa-1,3-diene]) iron (21) **showing LUMO**

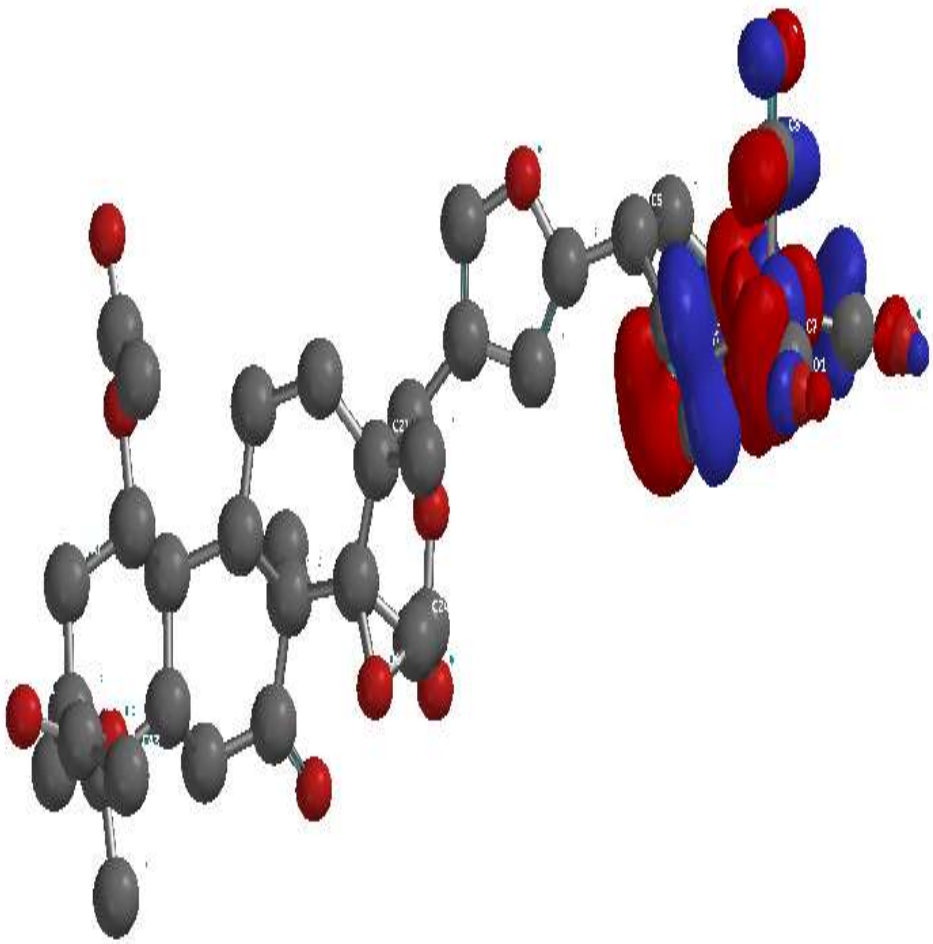

Appendix 45: Computational graphic model of demetallated 7-ketokhivorin (5-exo-(7-ketokhivorino) cyclohexa-1,3-diene) (28)

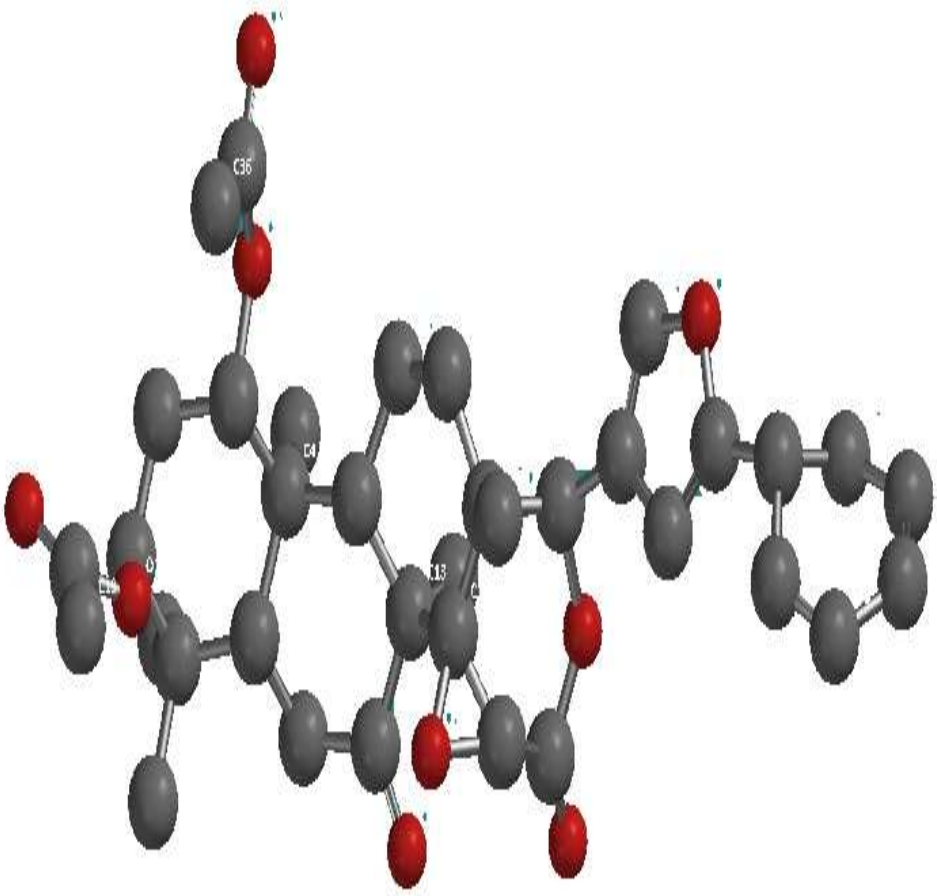

Appendix 46: Computational graphic model of demetallated 7-ketokhivorin (5-exo-(7-ketokhivorino) cyclohexa-1,3-diene) (28) **showing HOMO**

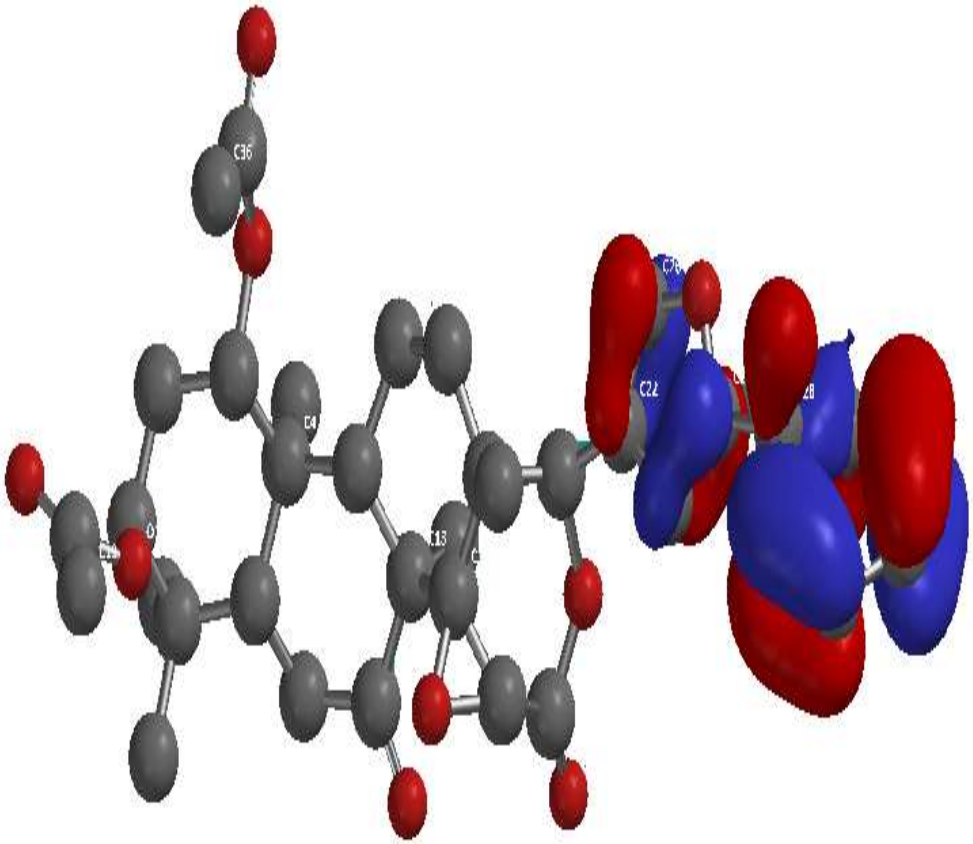

Appendix 47: Computational graphic model of demetallated 7-ketokhivorin (5-exo-(7-ketokhivorino) cyclohexa-1,3-diene) (28) **showing LUMO**

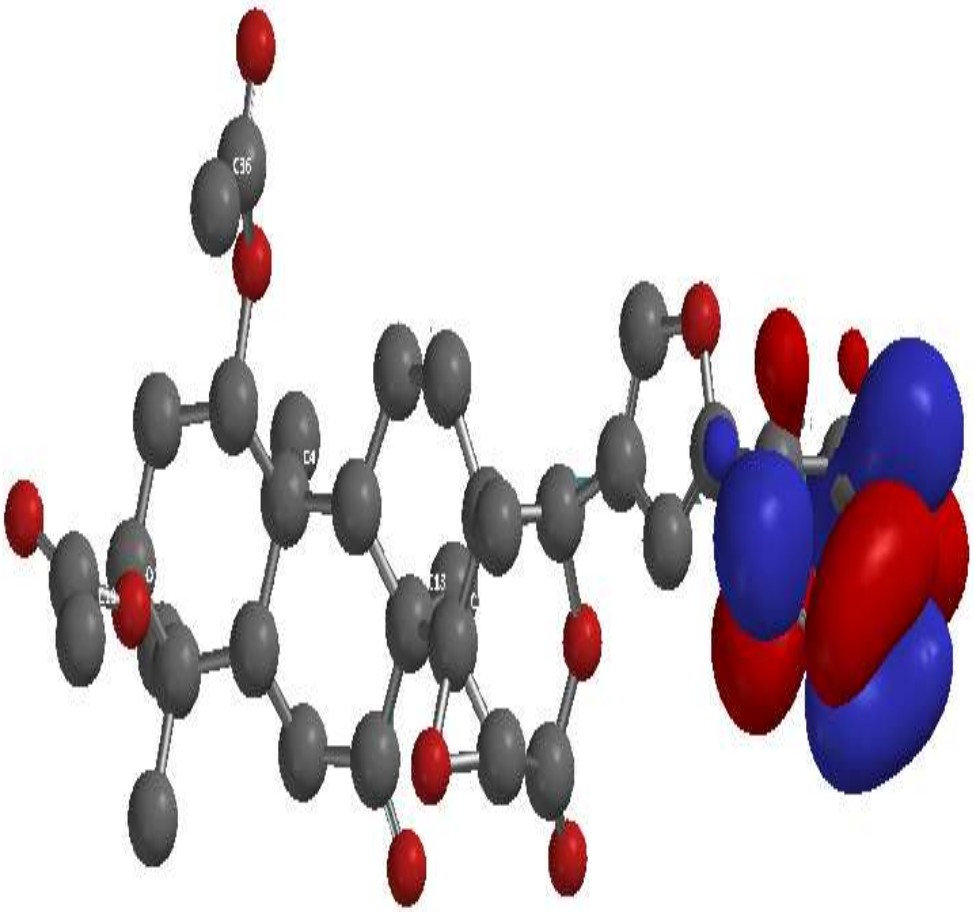

Appendix 48: Computational graphic model of methoxy gedunin adduct (tricarbonyl[1-4-η-2-methoxy-5-(gedunino) cyclohexa-1,3-diene] iron (23) **showing HOMO**

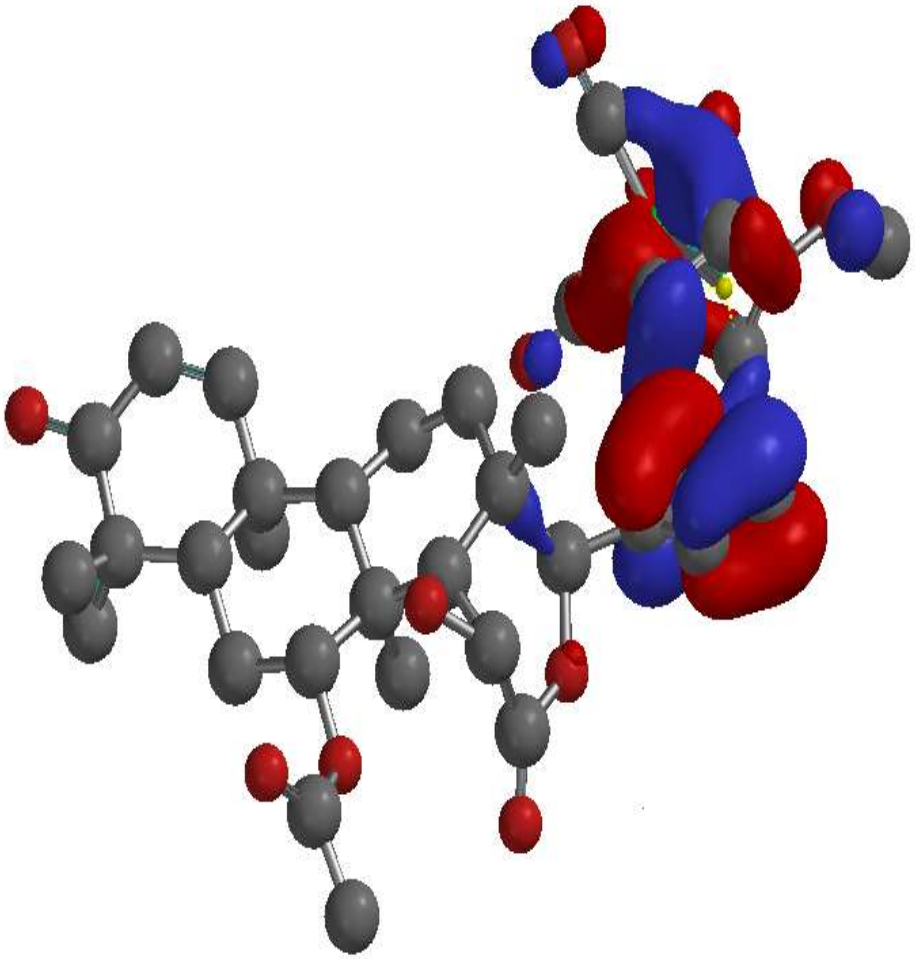

Appendix 49: Computational graphic model of methoxy gedunin adduct (tricarbonyl [1-4-η-2-methoxy-5-(gedunino) cyclohexa-1,3-diene] Iron (23) **showing LUMO**

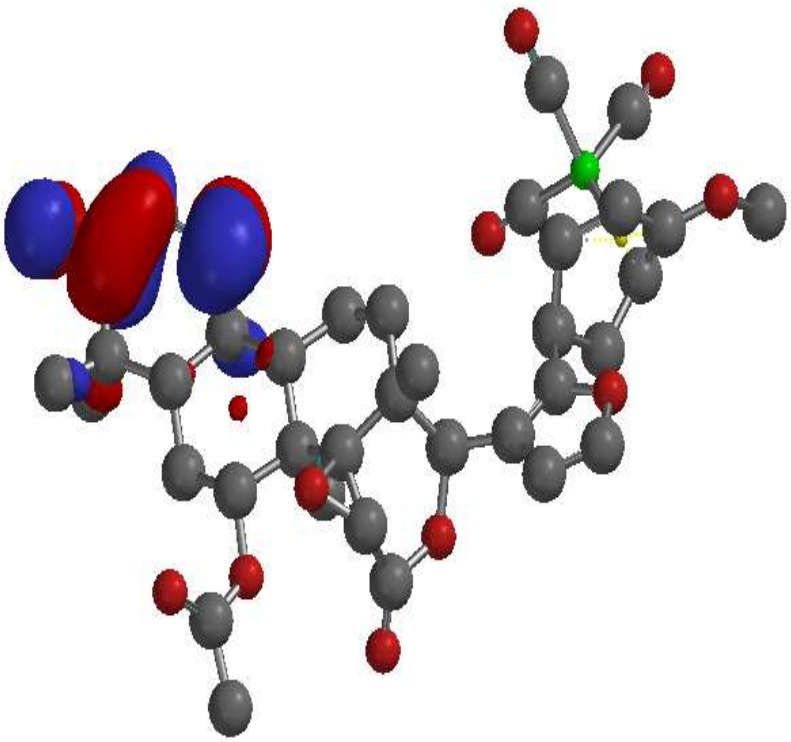

Appendix 50: Computational graphic model of demetallated methoxy gedunin (2-methoxy-5-exo-(gedunino) cyclohexa-1,3-diene) (30)

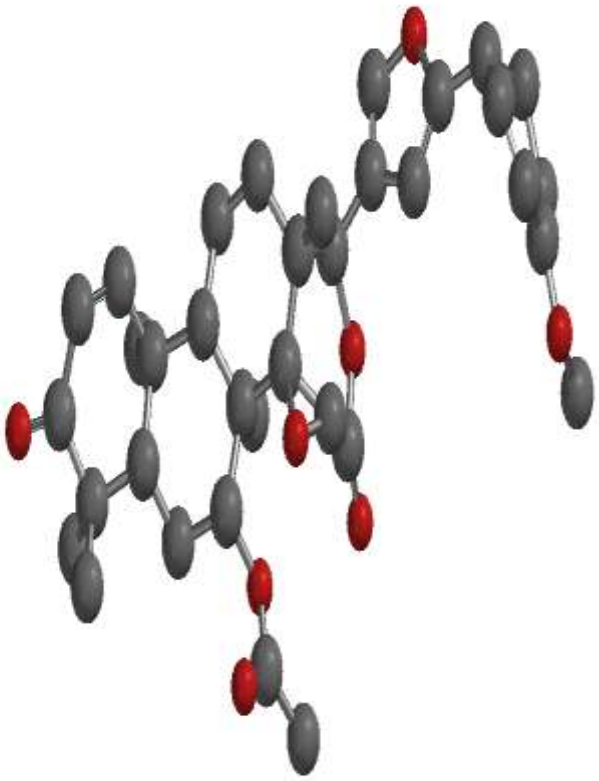

Appendix 51: Computational graphic model of demetallated methoxy gedunin (2-methoxy-5-exo-(gedunino) cyclohexa-1,3-diene) (30) **showing HOMO**

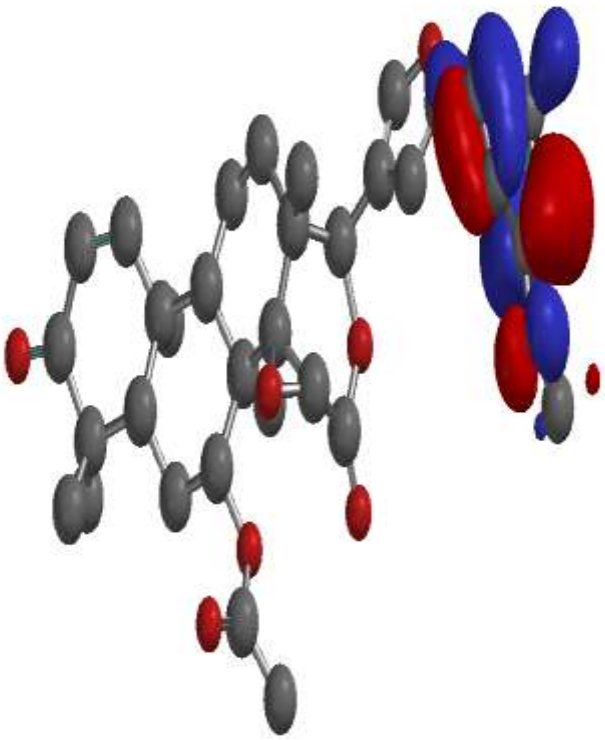

Appendix 52: Computational graphic model of demetallated methoxy gedunin (2-methoxy-5-exo-(gedunino) cyclohexa-1,3-diene) (30) **showing LUMO**